STRATIGRAPHY AND SEDIMENTOLOGY OF THE COVER ROCKS OF THE MAQNA AREA, SAUDI ARABIA

RUSHDI JAMAL TAJ
B. Sc., M. Sc. (JEDDAH, S. A.)

Thesis submitted for the Degree of Doctor of Philosophy in the Department of Geology and Applied Geology, University of Glasgow.

October 1991

ProQuest LLC.
789 East Eisenhower Parkway
P.O. Box 1346
Ann Arbor, MI 48106 – 1346

To my parents, wife, and daughters

Sarah, Saraa, and Hind

DECLARATION

I hereby declare that the following thesis has been composed by me; that the work of which it is a record has been carried out by myself, and that it has not been presented in any previous application for a higher degree.

Rushdi J. Taj

ABSTRACT

The Maqna area, part of the Midyan Peninsula, is characterized by well exposed synrift sediments of Oligocene and Miocene age which can be grouped into four formations: the Sharik, Musayr, Nutaysh and Bad Formations. These mark steps in the geodynamic evolution of the Red Sea associated with sea-floor spreading. The early Sharik Formation consists of fan delta sediments. It covers much of the northern half of the area and deposition was associated with the first movements along the Arabian Wrench Fault which caused the down-faulting of the Midyan peninsula. The Musayr Formation is divided into Lower Gypsum and Upper Limestone members. The Musayr Gypsum is a coastal lagoonal evaporite sequence and has a restricted (L-shaped) distribution along northern and western side of Jabel Tayran. Five lithofacies assemblages are identified in the Limestone sequence. These are: (1) conglomeratic limestone; (2) laminated limestone; (3) oyster limestone; (4) sandstone; and (5) brecciated limestone. The Musayr Limestones are marine sediments (previously known as reefal limestones) deposited in environments ranging from near-shore to slope. Macrofossils present indicate Mediterranean affinities. Two corals, species of *Acanthastrea cf. echinata* and *Lithophyllia michelotti,* are assigned the Burdigalian (Lower Miocene). The Nutaysh Formation is interpreted as a turdidite sequence with proximal coarse grained conglomerate and sandstone sediments concentrated in the northern and western parts of the Maqna area, while towards the southeast, distal fine grained marly sediments are predominant. The capping sequence, the Bad Formation, is a shallow-water deep-basin evaporite. Deposition of the evaporite sequence was followed by the second movement of the Arabian Wrench Fault, post Miocene-Pliocene, which resulted in emergence of the area and local deposition of tufa. The Quaternary coastal limestones and coarse braid delta sediments, a continuation of inland clastic terraces, may reflect tectonic controls related to eustatic falls in sealevel.

The Tertiary formations of the Maqna area contain similar cycles of diagenetic sequences which indicate that burial resulted in similar general diagenetic environments.

ACKNOWLEDGEMENTS

I wish to express my sincere gratitude to my supervisor, Dr. Colin J. R. Braithwaite, Department of Geology and Applied Geology, University of Glasgow, under whose supervision and guidance this work has been prepared. His constructive criticism, unfailing patience and friendly attitude have been invaluable.

I wish also to thank the members of staff, technicians and secretaries of the Department of Geology, University of Dundee and of the Department of Geology and Applied Geology, University of Glasgow for their continuous help and assistance throughout the progress of this research.

I would also like to express my gratitude to Drs. B. Rosen, P. Nuttal and A. Smith, British Museum (Natural History), London, for their considerable assistance in identifying the Tertiary macrofossils.

Thanks are due to the members of staff of the Faculty of Earth Sciences, King Abdulaziz University, Jeddah, for their useful comments and suggestions, to the personnel who have contributed to the success of my two field trips to Maqna area, S. A., and to the drivers and labourers who have helped in the field observation with unlimited patience and cooperation.

Many thanks go to H.R.H. Fahad Bin Sultan, Governor of Tabuk Region, Sheikh Ahmad A. al-Khuraysi, Vice-Governor, and to all those officials for their constant support and kind hospitality with which I was received with my companions during our research in the Maqna area.

Special thanks are due to my parents for their constant support, care and help, and to my wife for her patience, tolerance and sympathy.

CONTENTS

LIST OF TABLES

LIST OF PLATES

APPENDIX

LIST OF FIGURES

CHAPTER I

INTRODUCTION

The purpose of this chapter is to outline the problems which this thesis attempts to examine and to describe the features of the geology of the Red Sea which are relevant to these problems.

In the last two decades, the geology of the Red Sea has been the focal point of a variety of research programs in the geosciences. This has been the result not only of economic interests, but also of its tectonic position. Here we can observe the breakup of the continents, the transition from a continental to an oceanic rift, and the initial steps of sea-floor spreading.

Structurally part of the Red Sea, the Maqna area can be adequately explained by a three stage evolution. Rifting began in the Oligocene (possibly the late Eocene), and was followed by two periods of sea-floor spreading, the first in the late Oligocene to early Miocene (23 to 15 Myr. ago) and the second starting after a spreading hiatus of about 10 Myr. (Girdler & Southern, 1987). Movement still continues as witnessed by elevation of recent coral reefs (Skipwith, 1973 and Zakir, 1982).

1.1 THE AIMS OF THIS STUDY

The Oligocene and Miocene synrift sediments are very thick and well exposed in the Maqna area. The sequences can be grouped into four Formations which have been

named the Sharik, Musayr, Nutaysh and Bad Formations (Clark, 1985). To the east of the Maqna area, these are overlain discordantly by the Pliocene - Pleistocene Ifal Formation.

The present work represents a contribution to the study of the Tertiary and Quaternary sediments of the western coast of Saudi Arabia. The Maqna area was chosen since Oligocene and Miocene sequences are well exposed and easily recognized.

The work includes details of stratigraphic sections measured, and correlation and lateral facies changes within these. Sedimentological investigations were carried out to determine petrographic and diagenetic characters and to investigate burial history. Identification of macrofossils is as far as possible to species level. Finally, results are combined to define depositional environments and to trace the geodynamic history of the area.

1.2 THE MAQNA AREA

1.2.1 LOCATION AND ACCESSABILITY

The Maqna area is located in the extreme northwestern part of Saudi Arabia (Fig. 1.1) between latitudes 28° 14' to 28° 34' N and longitudes 34° 30' to 34° 57' E. Maqna itself is an oasis settlement on the coast of the Gulf of Aqaba.

Several unpaved roads join Maqna and a series of coast-guard posts to a paved road 30 Km. to the east. This in turn links the northwestern part of Saudi Arabia with

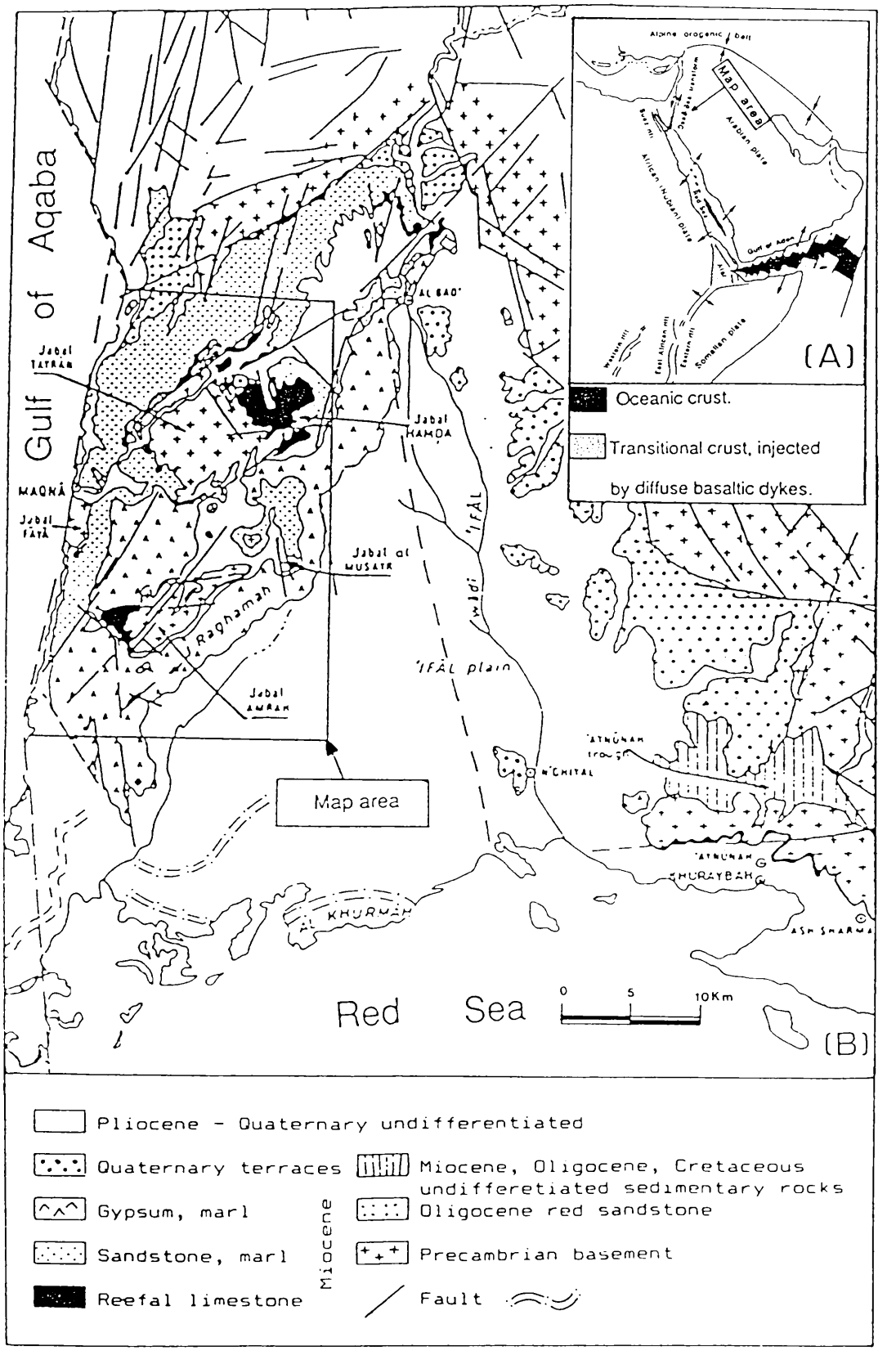

Figure 1.1 Location map (A) regional setting of the Maqna area, and (B) within the BRGM Map (Motti *et al.*, 1982).

areas to the south such as Jeddah, to Haql on the Aqaba Gulf coast, and to Tabuk to the east.The city of Tabuk, about 280 Km. from Maqna is the largest trading center in this part of the Kingdom, and is also the nearest airport, with excellent routes and facilities for domestic flights.

1.2.2 TOPOGRAPHY

The Maqna area is located in the Midyan peninsula between the Red Sea and the Gulf of Aqaba, opposite the Sinai peninsula. It forms a blockfaulted updoming between the Gulf of Aqaba and the young Ifal Basin to the south. Apart from plains to the east and south, the area is mountainous, the highest relief being in the north, with general altitudes between 50 - 300 m. Mountain ridges are rugged and are separated by broad alluvial valleys (wadies) which are, for the most part, accessible. There is a general decrease in elevation southwards towards the Ifal Plain. Along the Gulf of Aqaba, the very steep mountains are either separated from the shore by a narrow littoral fringe or plunge directly into the sea.

Raised Quaternary limestones occur along the coast, sited principally at the mouths of wadies. These range in elevation from several meters to about 20 meters. The wadies themselves are filled with coarse alluvium and are rimmed by discontinuous Quaternary clastic terraces.

1.2.3 CLIMATE

The climate of the area is very arid, and despite the proximity of the sea, the degree of humidity is generally very low (35-40%). Generally the area has rather humid hot

days (35-40°C) and cool nights (15-20°C) in the summer. In winter (January & February) the daytime temperatures are about 20°C but decline to 3°C and it may even freeze at night.

The area is commonly subjected to extremely violent wind driven sand storms with directions variable from the north to southwest, and reaching speeds of more than 100km/h. Rotary dust storms are common, especially within flat areas. At the time of writting , according to local inhabitants, no significant rain has fallen since 1983, apart from a few showers of short duration.

1.2.4 DRAINAGE AND WATER SUPPLIES

The hydrographic network contains no permanent water courses. Wadi Ifal (locations in Fig. 1.1) has a vast basin, extending north-south and then northwest-southeast across the area, and forming the main drainage artery. Wadi Al-Kharaj, extends to the Gulf of Aqaba, and has a small basin. Wadi Al-Hamd rises in a plain to the west of Al-Bad crossing gypsum outcrops obliquely in a northeast - southwest direction. Of these only Wadi Al-Hamd contains sediments which constitute an aquifer of any size.

Other wadies which join the Gulf of Aqaba are all very short, very enclosed and have relatively undeveloped basins from a hydrological point of view.

The primary source of water appears to be underground from fractures in the cover rocks. A relatively shallow source locally emerges as a spring of drinkable water in the Maqna Oasis.

1.2.5 VEGETATION AND WILDLIFE

Wild trees and bushes are sparse in the area and on mountain slopes. Gypsum outcrops discourage vegetation except for some sulphate-tolerant plants. Vegetables and fruits from cultivated lands scattered within oases and wadies are not sufficient to supply local consumers. Jordan is the main source of imported vegetables and fruits. Palm trees are widely distributed and common where there is sufficient water but such areas are sparse. Sheep, goats and camels are common in the area close to habitation. In addition there are desert animals such as foxes, wolves, rabbits, deer and different kinds of lizards (some are edible) and snakes. A number of different kinds of birds and various types of insects are also found.

1.2.6 CULTURE

Maqna is the only village within the map area, and was an ancient maritime port and capital city of the land of Midyan. It was listed by Ptolemy as one of several mediterranean cities in Arabic Felix (Burton, 1878). South of the town beside the oasis, a restricted fenced area contains ancient monumental tombs carved out of the rocks and belonging to Madain Shoaib (city of the prophet Shoaib, Moses' father in law). The bulk of the present population are coast-guards, farmers, government officials and fishermen. The remains of nomad camps have been found in central and northern parts of the area.

1.2.7 PREVIOUS WORK

Among the huge numbers of significant geological papers that have been published on the Red Sea and its margins, as a result of symposia, as collected works centered on specific areas, or as individual research articles, numerous studies on the Maqna area have been made by groups and individuals concerned with both the economic potential of the area and its tectonic position.

The first geologic reconnaissance was carried out by Richter-Bernburg and Schott (1954). They assigned part of the coastal carbonate formation to the Miocene. The name Raghama Formation was proposed by Bramkamp and others (1963) for the rocks of Miocene age in the Midyan area and along the northern Red Sea coastal plain. The type area for these is Jabel (mountain) Ar-Raghama about 16Km south of Maqna. Skipwith (1973) and Bigot & Aladovette (1973), divided the Raghama Formation into three sections separated from each other by unconformities. However, these unconformities have not been recognized by later workers except Zakir (1982). Bokhari (1981) accorded the Tertiary sediments in the Maqna area the status of a Group under the name Raghama Group. This, he suggested, consists of two units, the lower, Tayran Formation (with two informal Members), overlain and separated by an unconformity from the upper, Bad Formation. These are essentially the same three divisions as Skipwith (1973) but Bokhari did not identify any unconformity between the two members of his Tayran Formation. Motti and others (1982) also recognized three major stratigraphic units but noted no unconformity between the lower and middle units and stated quite clearly that the uppermost unit rested conformably on the middle unit. Clark (1985) followed Motti *et al.*, (1982)

descriptions and informally named the Musayr, Nutaysh and Bad Formations in order of decreasing age (Fig. 1.2). Clark suggested that the Tayran Formation of Bokhari (1981) should be abandonned since, as used by him, it included some rocks known to be of Oligocene age. The Oligocene rocks were formally named the Sharik Formation by Clark (1985) after Wadi Sharik just to the north of Al-Bad. Clark's (1985) lithological subdivision is more or less identical with the units given by Dullo and others (1983) but this was apparently not known to Clark.

Vanzques-Lopes & Motti (1981) and Zakir (1982), who carefully studied the geology and tectonics of the Tertiary sediments of the area, both broadly followed the scheme proposed by Skipwith (1973) and, under the name Raghama Formation, divided the succession into three units, lower, middle,and upper. Recently Jado *et al.*, (1989) explained the development of sedimentation along the Saudi Arabian Red Sea coast, including the Maqna area, separating the synrift sediments of the area into four units and, following Clark (1985), assigned ages from Rupelian to Serravalian. Clark's (1985) scheme accords best with the authors observations and is adopted in the present investigation. Table 1.1 shows the different classifications for the Tertiary sediments in the Maqna area suggested by various authors.

The paleoenvironments in the Maqna area have been examined briefly by a number of authors. The lower unit of the basal conglomerate (Oligocene) has been regarded as deltaic and fluviatile by Motti and others (1982), as fluviatile by Dullo *et al.* (1983), as an unspecified continental sequence by Jado *et al.* (1989) and as an

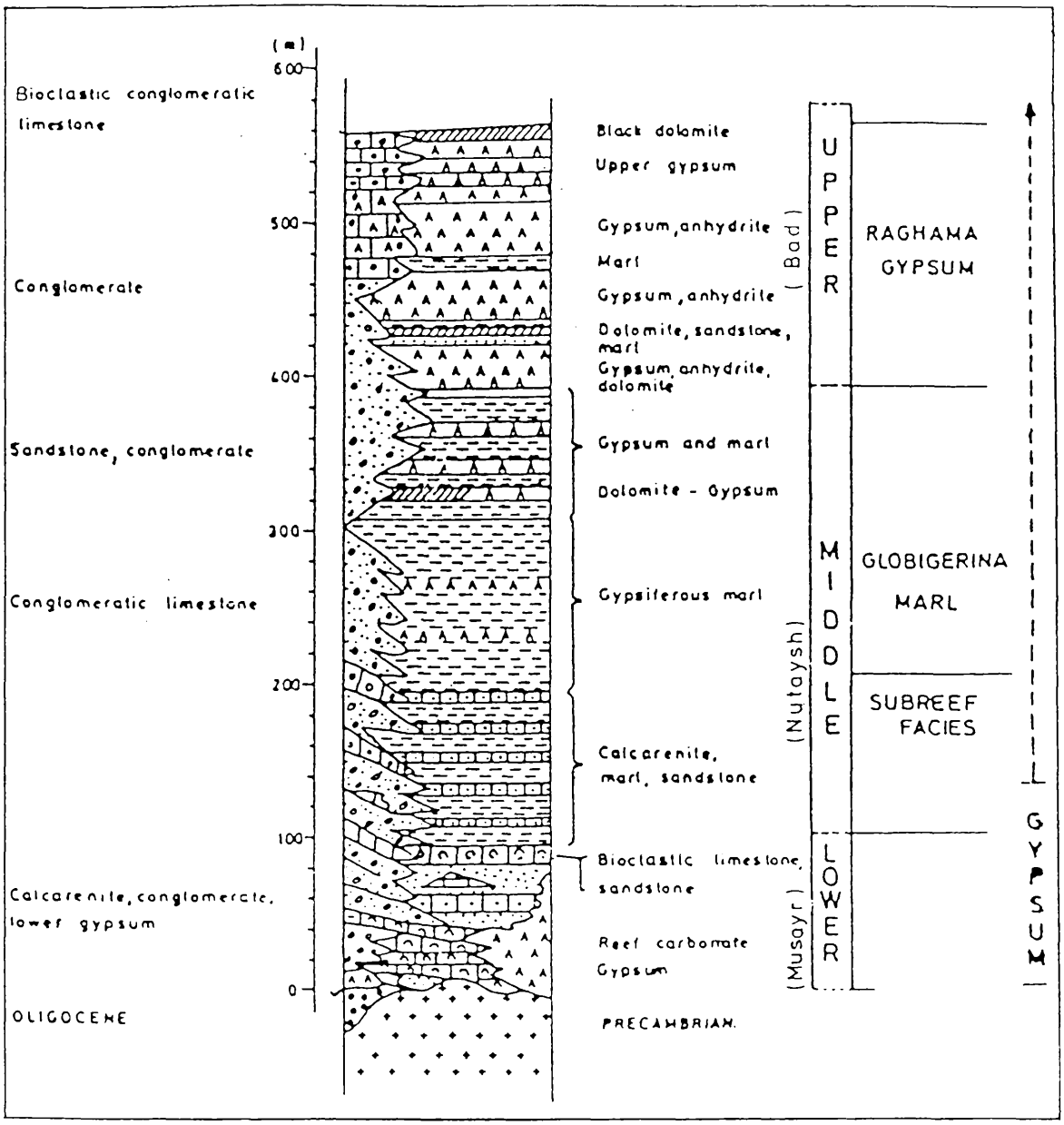

Figure 1.2 Stratigraphic sequence of the Raghama Group in the Maqna massif (from Motti *et al.*, 1982 & Clark, 1985).

Table 1.1 The different nomenclatures suggested for the Tertiary sediments in the Magna area.

Skipwith (1973)		Bokhari (1981)			Motti et al., (1982)		Dullo et al., (1983)		Clark (1985)	
RAGHAMA FORM.	Upper	Al-Bad Form.		RAGHAMA GROUP	MIOCENE	Upper unit	Al-Bad Formation		RAGAAMA GROUP	Al-Bad Formation
	Middle	TAYRAN FM	Upper			Middle unit	TAYRAN FM	W. Telah Member		Nutaysh Formation
	Lower		Lower			Lower unit		W. Al-Kils Member		Musayr Formation
						Oligocene unit		W. Al-Hamd Member		Sharik Formation

alluvial fan sequence by both Zakir (1982) and LeNindre and others (1986). More detailed studies of the Miocene sediments in the area have been made by Zakir (1982) and LeNindre and others (1986) who recognized more or less similar environments, but differed in their interpretations of the depositional environment of the evaporite beds. Zakir (1982) believed that these were of deep marine origin while LeNindre and others (1986) regarded them as continental Sebkha deposits.

1.2.8 STRUCTURAL SETTING

The Red Sea region was covered by marine embayments from time to time during the Jurassic, Cretaceous and Eocene, but the present tectonic pattern first began to evolve in the Oligocene (Ahmed, 1972). Deposition in the Maqna area has taken place in several basins that formed sequentially as a result of faulting, folding and continuous local uplift and subsidence. Movements started with the initiation of rifting in late Oligocene time and continued throughout the geological history of the area (Zakir, 1982).

The Gulf of Aqaba, about 180km long and 15-25km wide, comprises the southern part of the Dead Sea rift. Its floor is up to 1850m deep, about 4km below the neighbouring mountains on land. The Gulf occupies a fault-controlled depression, partly filled by sediments.

The structure of the Gulf of Aqaba is dominated by en-echelon faults of transform type, striking N 20°-25° E (Fig. 1.3). Large numbers of these faults are still active. The rift was formed in the Cenozoic by breakup of the once continuous Afro-

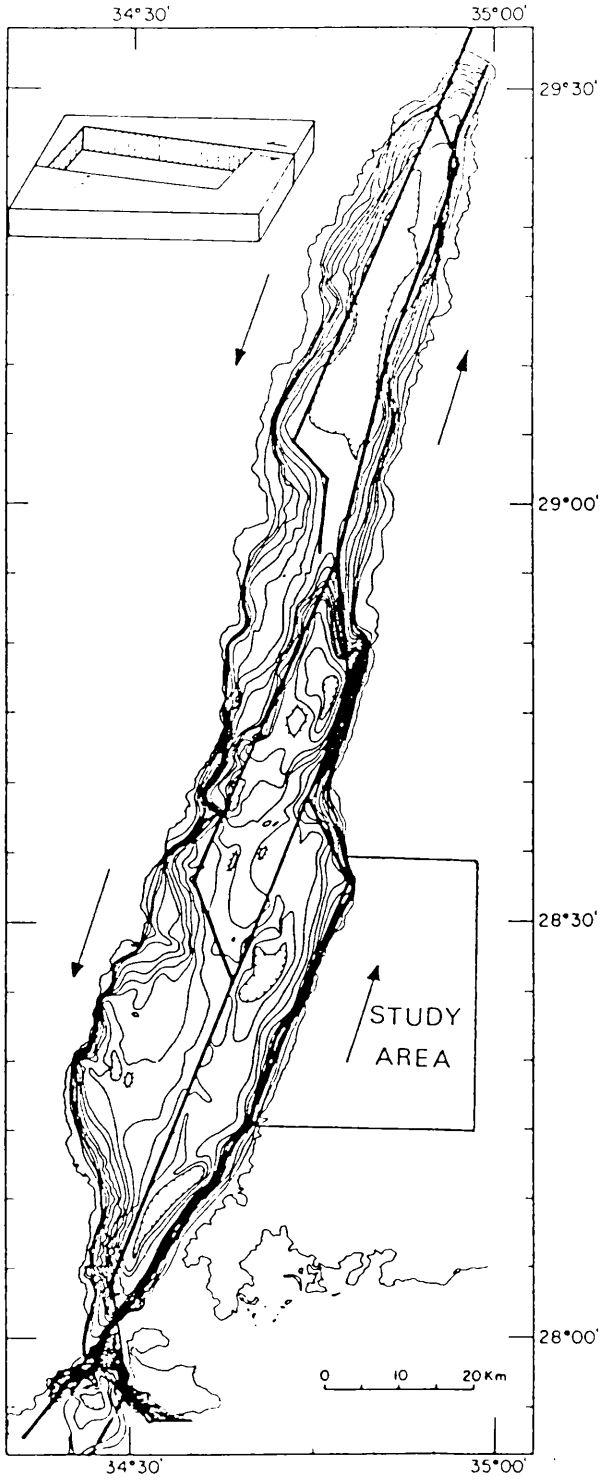

Figure 1.3 Generalised model for structure of Gulf of Aqaba (Elat): the three basins are interpreted as en-echelon rhomb-shaped grabens produced by strike-slip (BenAvraham *et al.*, 1979).

Arabian Plate which had been a tectonically stable area since the end of the Precambrian (Fig. 1.4). The Maqna area is located immediately to the east of the Arabian Wrench Fault, along which the Arabian Plate is drifting away from Africa with a predominantly strike-slip movement. It seems that the present shape of the Aqaba Gulf was acquired during the last stage of movement on the Dead Sea rift, when left lateral slip of about 40-50km took place (BenAvraham *et al.*, 1979)

According to Zakir (1982), the structure of the area is very complicated. There are several sets of both faults and folds present. Stratigraphic evidence indicates two stages of movement occurred along the Arabian Wrench Fault. The first, begining in late Oligocene time, caused down faulting of the Median Peninsula. The second stage, post Miocene-Pliocene, produced northeast trending en-echelon folds and at least six different trends of strike-slip faults. This situation is analogous to the two stage opening of the Red Sea and Gulf of Aden (Ross and Schlee, 1973; Girdler and Styles, 1974).

Motti *et al.*, (1982) suggested that structures in the area are controlled by four main fracture directions and, as will be seen, the role of faults is particulary evident in the evolution of the Miocene Formations.

1.2.9 ECONOMIC POTENTIAL

The earliest investigation concerned with the economic potential of the Maqna area was by Burton (1878), who reported the presence of large amounts of gypsum,

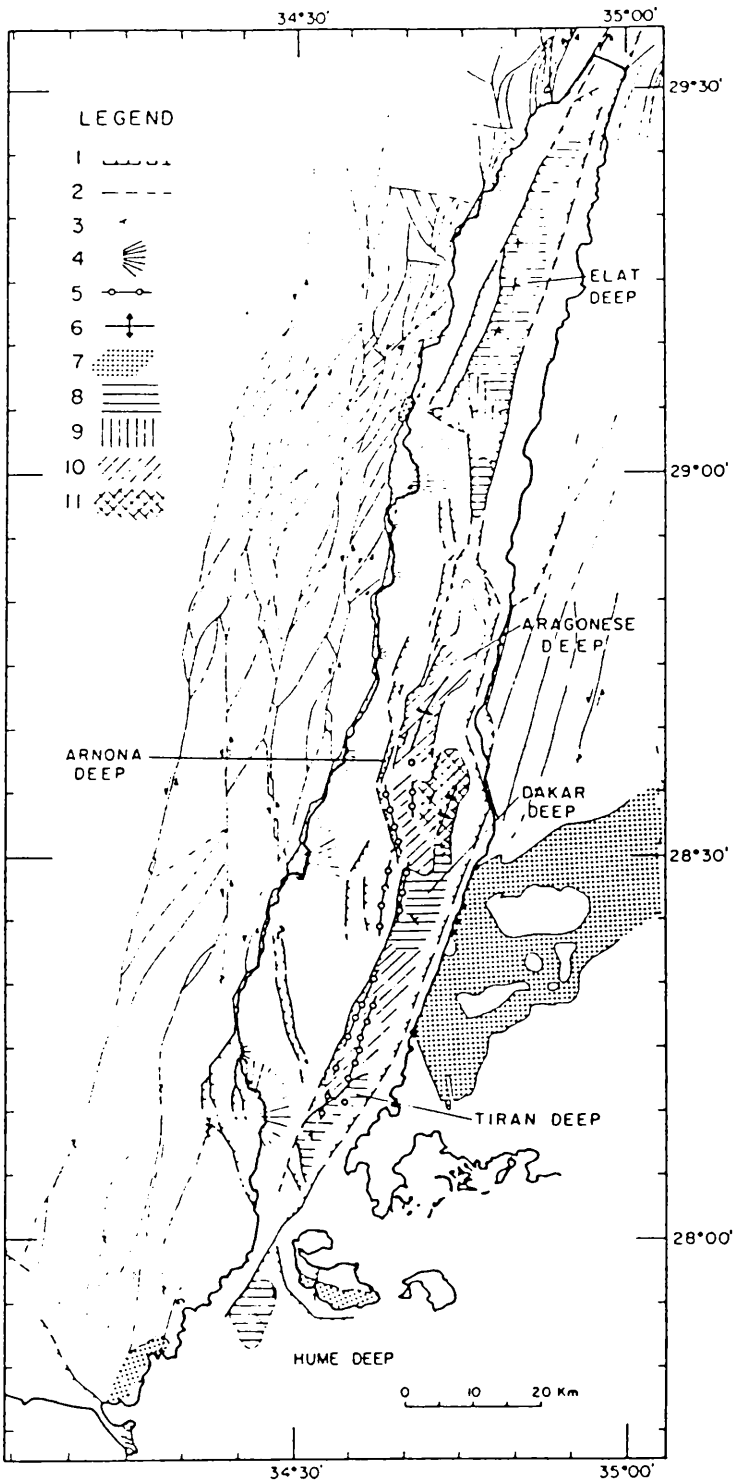

Figure 1.4 Structural elements of the Gulf of Aqaba (Elat). (1) Main active faults; (2) main in active faults of rift margins; (3) dip of basinal sediments; 4) alluvial fan and submarine cones; (5) diapiric folds; (6) main anticlines; (7) outcrops of Neogene sediments; 8) basinal areas with a flat sea floor; (9) disturbed southern part of northern basin; (10) folded and warped basinal areas; (11) uplifted basinal area at sill between central and southern basins (BenAvraham *et al.*, 1979).

sulphur and haematite within Tertiary sediments, and of gold in porphyritic rocks in wadies near Maqna.

Gypsum and dolomitic limestone samples were collected at random by Khaled (1963) from Al-Bad and Umm-Lajj. He reported that the gypsum of these areas is of high grade and suggested that it should be investigated in detail. This view was confirmed by Trent and Johnson (1966) and LeNindre (1981). Hadley *et al.* (1982) summarized the investigations of Tertiary rocks in western Saudi Arabia and indicated that although they have potential for economic mineral resources, prospecting requires further input from basic geology.

Motti and others (1983) investigated numerous occurances of mineralization in the Precambrian basement of the Maqna massif area, in the Precambrian basement (barium, copper, lead and fluorite) and in the Miocene cover (barite, copper, lead and fluorite). They concluded, however that none of these contained sufficient accumulation to make it of economic interest. This is also the situation in relation to phosphates reported by Remond and Teixido (1980).

Ahmed (1972) described the geology and petrolum prospects of the eastern Red Sea and indicated that oil seeps are known in widely separated localities such as the Farasan and Dahlac islands. The chief source and reservoir rock is found in the Lower Miocene Globigerina Bed, and the overlying evaporites equivalent to those in the Maqna area seal the accumulations. He suggested that there is considerable potential and recommended further investigation. However, a number of wells have

been drilled along the Sudanese coast with no productive fields discovered. Recently, Beydoun (1989) described the Arabian side of the Red Sea as the widest and most poorly-explored shelf of the whole region.

1.2.10 METHODS OF INVESTIGATION

Prospecting was carried out in two field trips, the first between February and April 1988, for about six weeks, and the second for five weeks between May and June of 1989. In both periods, a house in Maqna village with water and electricity supply was chosen for residence. Maqna offers a variety of shops and a petrol station covering local needs, in addition to two International public coin telephones.

Since general maps were already available and thought to be reliable, standard methods of sampling, collecting fossils and stratigraphic measurements (logging) were used (Plate 4). Several traverses were made in order to study lateral facies variations, the nature of contacts, and to search for unconformities, as well as to make measurements of all available structural data. Table 1.2 shows the latitudes and the longitudes of the referred locations in the present work. Further mapping was carried out on aerial photographs at a scale of 1:60,000 for the preparation of final maps.

Laboratory work, involved a number of techniques. Petrographic studies used light microscopy, cathodoluminesence and scanning electron microscopy. Mineralogical and chemical analysis by x-ray diffraction and x-ray fluorescence spectroscopy.

Maps were prepared with measured columnar stratigraphic sections. Macrofossils were identified.

The work was begun in the Geology Department of the University of Dundee and completed in the Geology and Applied Geology department at the University of Glasgow. Finally, the Tertiary fauna was identified with the help of the British Museum (Natural History) in London, the acknowledgment of individuals is made in the relavent sections.

1.2.10.1 XRF (X-RAY FLUORESCENCE SPECTROMETRY)

X-ray fluorescence spectrometry was used to determine the trace element compositions of the samples. Analyses were of pressed pellets (Leake *et al.*, 1969), consisting of 6.0gm of 250 mesh rock powder and 1.0gm of thermal binder (phonel formaldehyde). The instrument used was a Phillips PW 1450/20 sequential automatic X-ray spectrometer. the principle behind this technique is that when a sample is bombarded with a high energy X-rays, secondary radiation is emitted, with a wavelength and at intensities dependent on the element present. Measurement of the wavelength(s) of observed emissions serves to identify the laments present, while comparison of the intensities of the characteristic radiation of particular elements gives a value reflecting their concentration in the sample. The emissions from standards (Departmental collection of International standards) are measured first to produce a calibration curve against which the unknown samples can be compared (Appendix 1-A).

1.2.10.2 XRD X-RAY DIFFRACTION)

Qualitative whole rock analyses were preferred for x-ray diffraction. Rock powders of 5-10 microns were mounted in a cavity mount holder in the manner described by Klug & Alexander (1974). The instrument used was a Phillips X-ray Diffractometer, model PW 1450/20 emitting Ni-filtered, Cu Kα radiation (40Kv/25ma, 2Θ and converted to lattice spacing (d-spacing) in angstrom (A°) units, based on Bragg's law: $n\lambda=2d \sin \theta$

Where n= is an integer
d= distance (lattice spacing)
λ= wave length

In fact, prepared tables of 2θ angle versus d-spacing are available for all the common X-ray wave lengths. The diffraction patterns of the unknown mineral phases were compared with a set of Departmental standard patterns of minerals. In addition, some were also compared to index cards which have been compiled by te Joint Committee on Powder Diffraction Standards (JCPDS). Representative X-ray diffractigrams of whole rock analysis are shown in Figure 1.5.

1.2.10.3 SEM (SCANNING ELECTRON MICROSCOPE)

Samples were coated with a gold palladium alloy. The system used was a Cambridge Instruments S360 Scanning Electron Microscope with integrated Link analytical AN 10,000 series EDX system (Fig. 1.6).

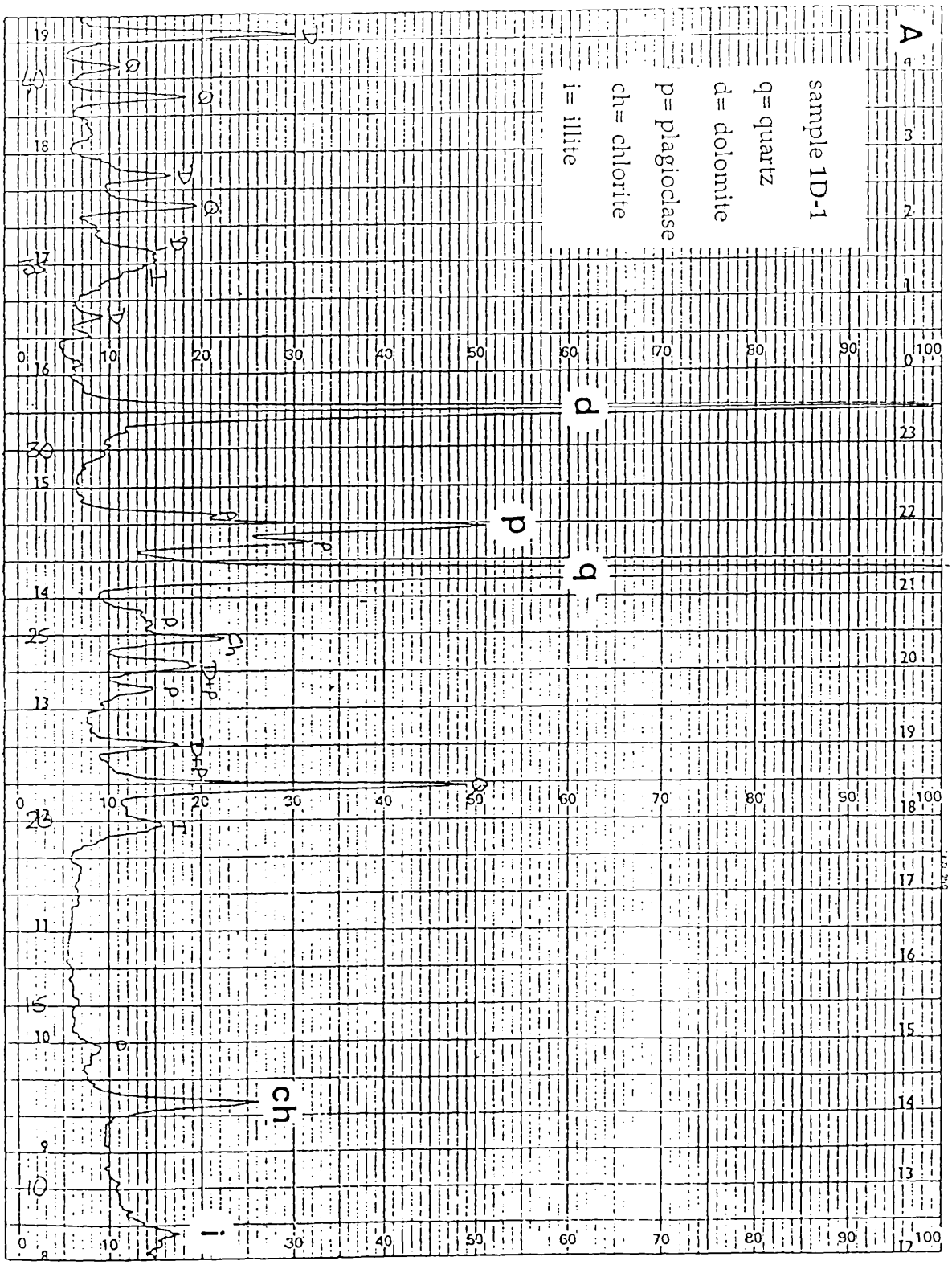

Figure 1.5 Representative x-ray diffractograms of whole rock analyses. Sample are from: A) Lower Nutaysh Formation, B) Upper Nutaysh Formation, and C) Bad Formation.

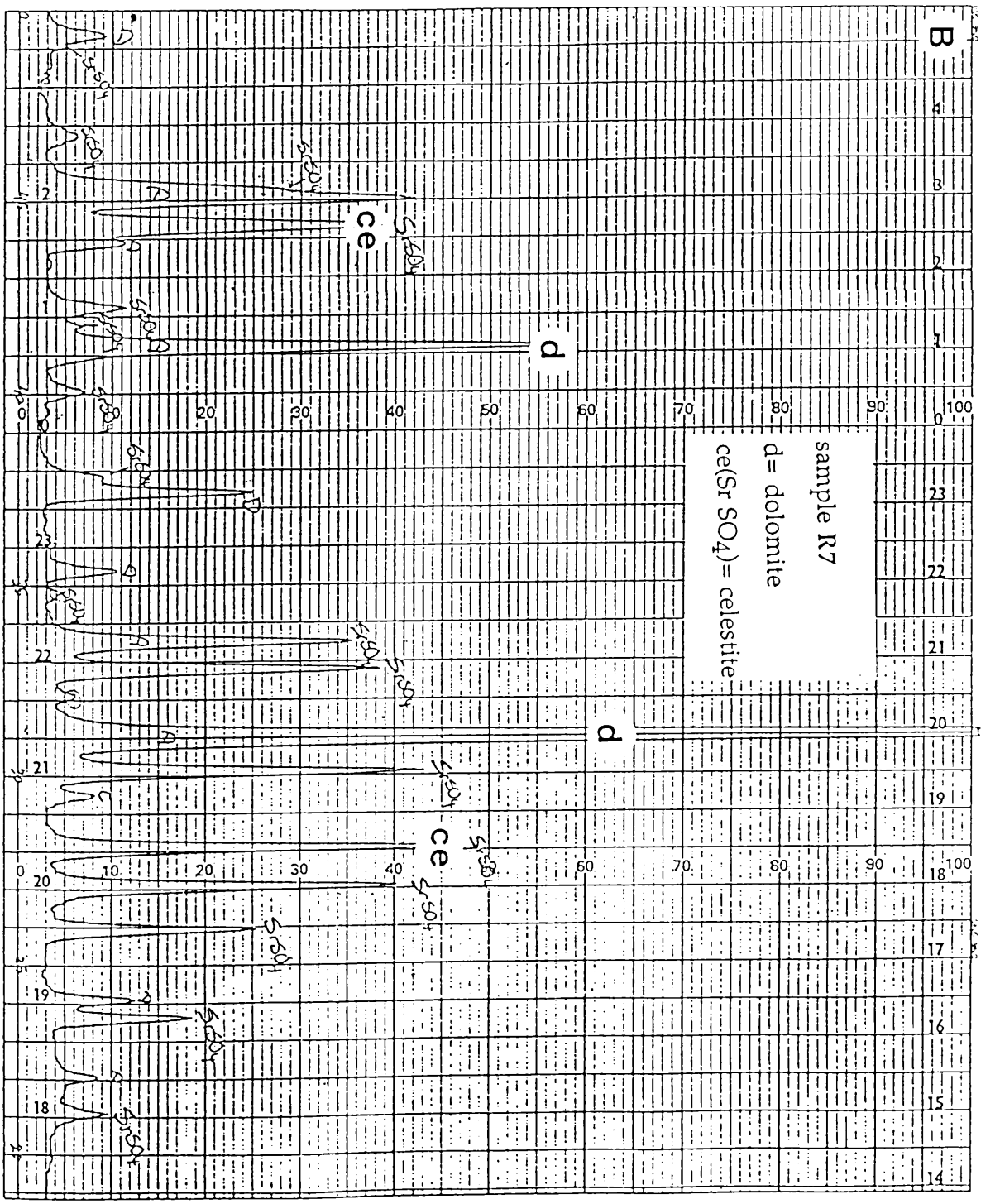
B
sample R7
d= dolomite
ce(Sr SO4)= celestite
d
ce
d
ce

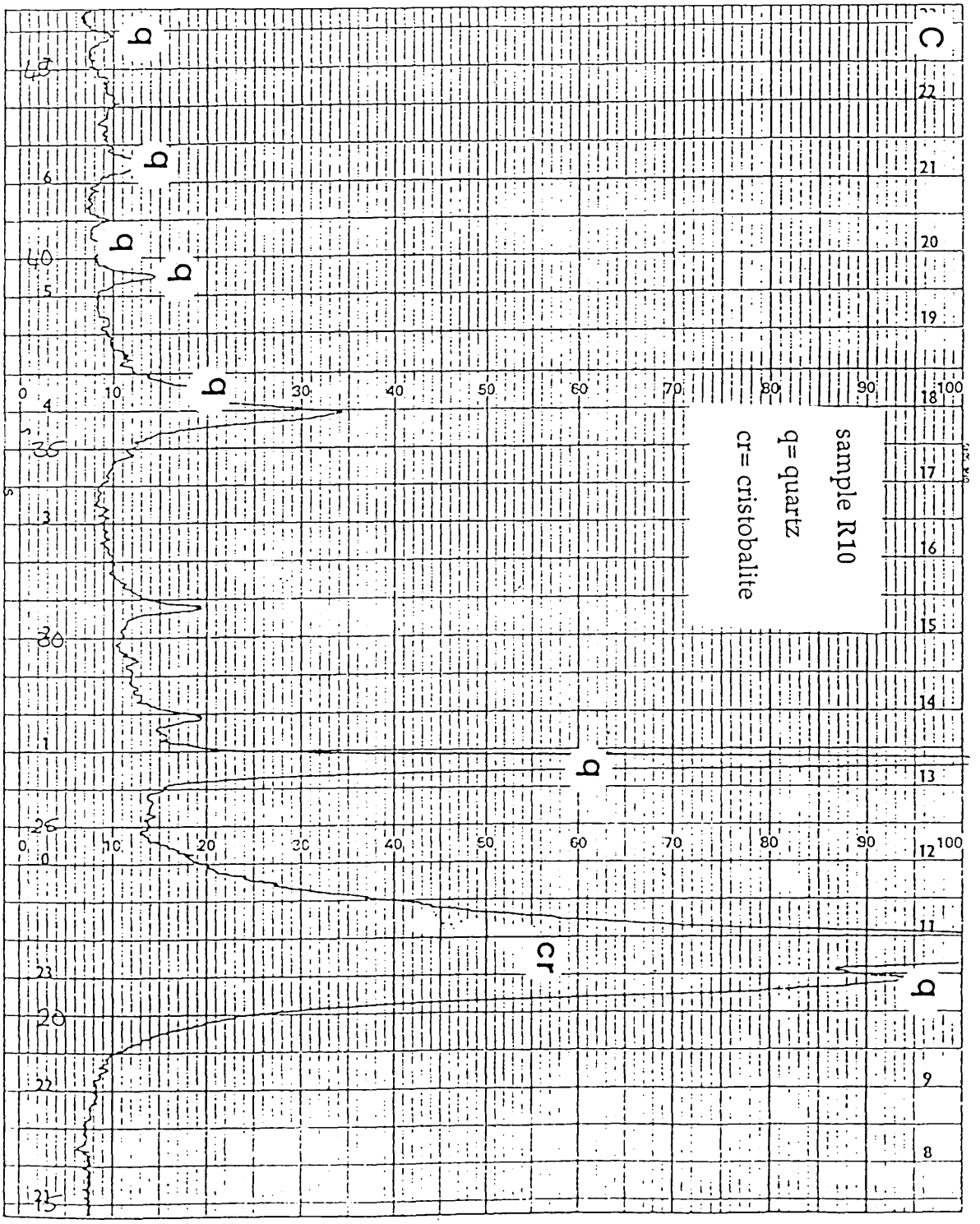
sample R10
q= quartz
cr= cristobalite
q
cr
C

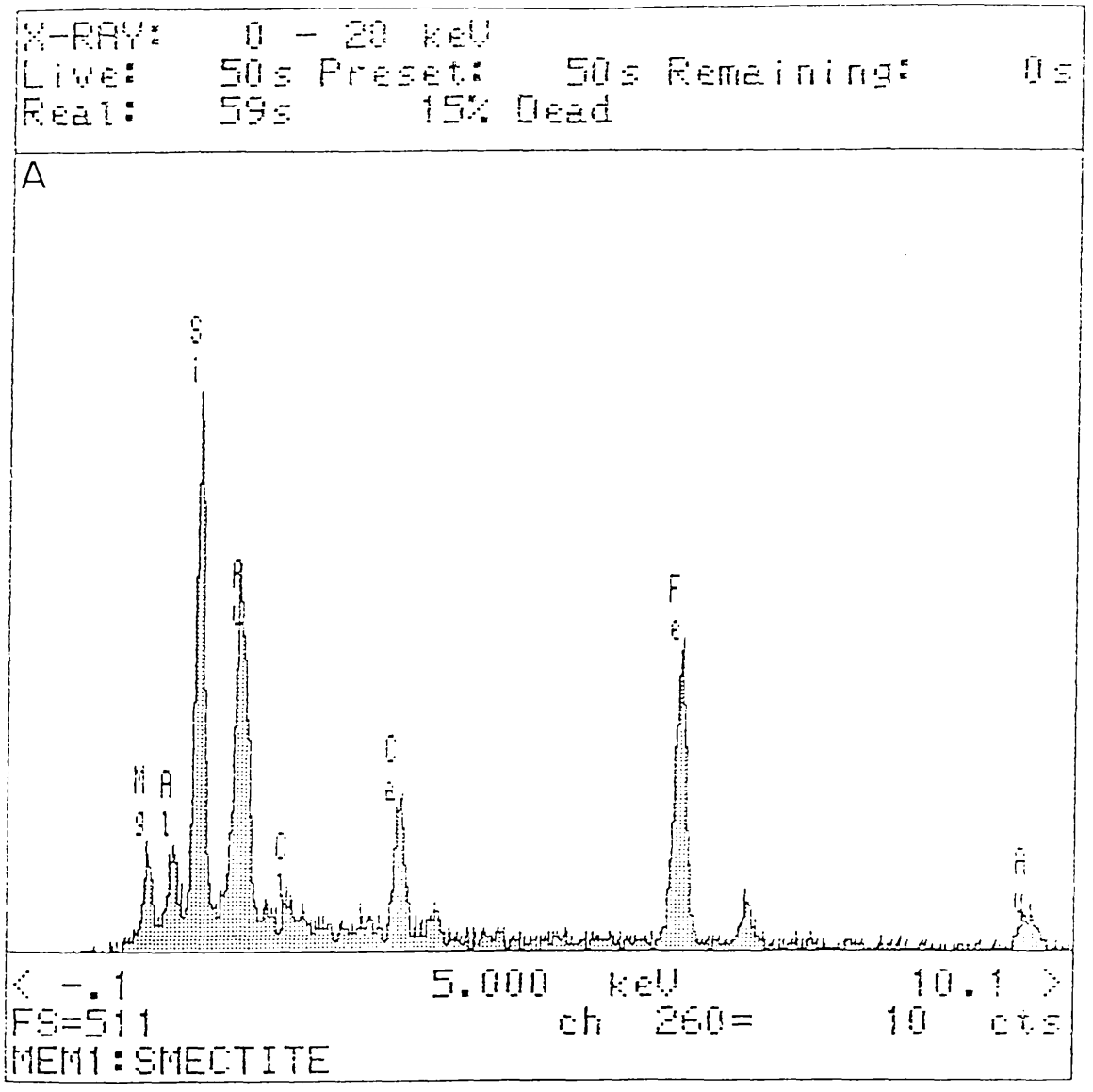

Figure 1.6 SEM energy dispersive spectrum (EDX) showing A) authigenic smectite from sandstone shown in Fig. 3.10-C and B) authigenic illite-smectite mixed layers.

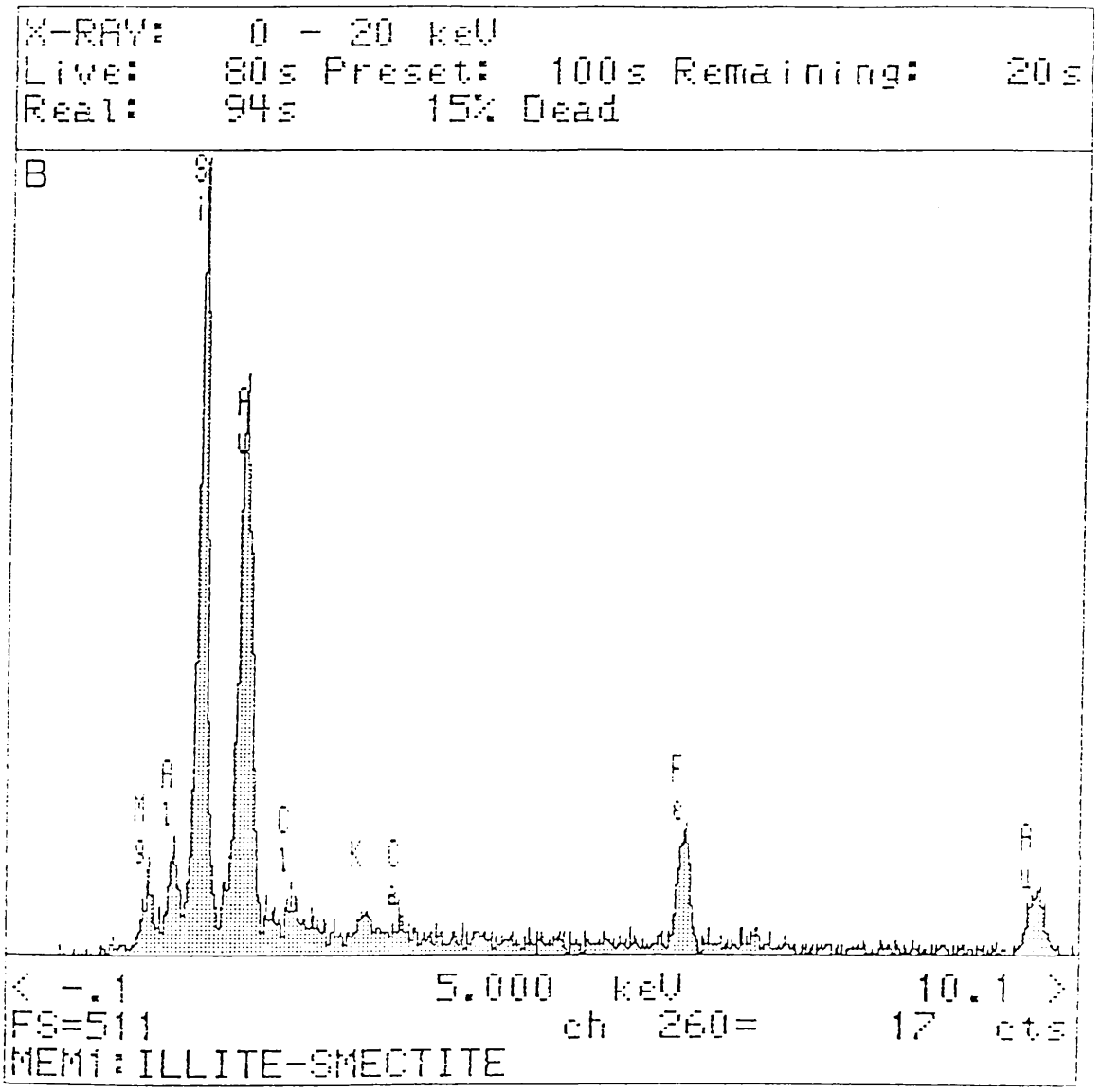
X-RAY: 0 - 20 keV
Live: 80s Preset: 100s Remaining: 20s
Real: 94s 15% Dead
B
< -.1
5.000 keV
10.1 >
FS=511
ch 260= 17 cts
MEM1:ILLITE-SMECTITE

Table 1.2 The latitudes and longitudes for locations referred to in the text (use Plate 1).

loc.	lat. 28°	long. 34°	loc.	lat. 28°	long. 34°
A	24°35′	55°40′	Ms	23°55′	52°20′
AA	17°55′	42°05′	Mu	19°25′	54°10′
B	20°30′	45°40′	N	18°40′	45°10′
C	24°05′	55°40′	P	34°10′	55°10′
D	21°40′	43°55′	1P	34°10′	53°55′
1D	21°45′	44°10′	Q1	23°30′	43°55′
F	23°10′	47°55′	Q2	31°40′	48°20′
G	19°20′	51°15′	Q3	31°10′	40°00′
H	19°40′	53°15′	Q4	30°45′	47°50′
HN	17°20′	47°35′	Q5	26°20′	45°25′
J	28°05′	50°00′	Q6	20°00′	43°00′
1J	28°20′	50°20′	Q7	17°20′	41°40′
2J	29°05′	51°05′	R	20°05′	54°15′
K	26°10′	47°50′	1R	20°15′	54°05′
K1	27°50′	54°05′	Ra	19°30′	48°00′
K2	27°50′	52°10′	S1	23°10′	44°35′
KK	25°40′	48°20′	SA	32°30′	51°20′
KK1	24°35′	48°35′	SA1	32°50′	51°45′
KK2	22°55′	49°05′	SH	27°10′	46°15′
KK3	24°30′	49°00′	SR	21°50′	52°20′
KK4	23°40′	49°10′	T	24°40′	54°05′
L	23°05′	49°55′	Ta	25°50′	55°20′
1L	19°55′	51°50′	Y	29°50′	52°50′
M	29°20′	51°50′	Z	32°20′	54°25′

1.2.10.4 CL (CATHODOLUMINESCENE)

The system used was a Technosyn model 8200 Mk II with Autohold. This was typically run at 25-30 kv with a gun current of 200-250 μA and vacuum of 0.04 Torr.

1.3 THE RED SEA

1.3.1 PHYSIOGRAPHY

The Red Sea, is about 1930Km long between the tip of the Sinai Peninsula in the north, where it bifurcates into the Gulfs of Suez and Aqaba, and the Straits of Bab Al-Mandeb in the south. It forms an elongated trough cutting in a NNW direction across the Afro-Arabian Precambrian shield. It widens from about 175Km in the vicinity of Sinai, to 350Km between Jizan and Massawa, then narrows to 30-40Km in the Straits of Bab Al-Mandeb. The mean depth is 491m, with depths up to 2,200m reached along the central axis (Fig. 1.7). It has an area of 438,000 sq.Km, and a volume of 215,000 cu.Km.

The Red Sea can be divided into two physiographic units which in turn can be subdivided:

(1) The shelf area. This consists of the coastal plain and marginal shelves. The coastal plain varies from less than 1 Km to over 40 Km in width from north to south, and is backed by a prominent 1500-3000m escarpment. Within the coastal plain, the sedimentary rocks exposed on either side of the Red Sea are

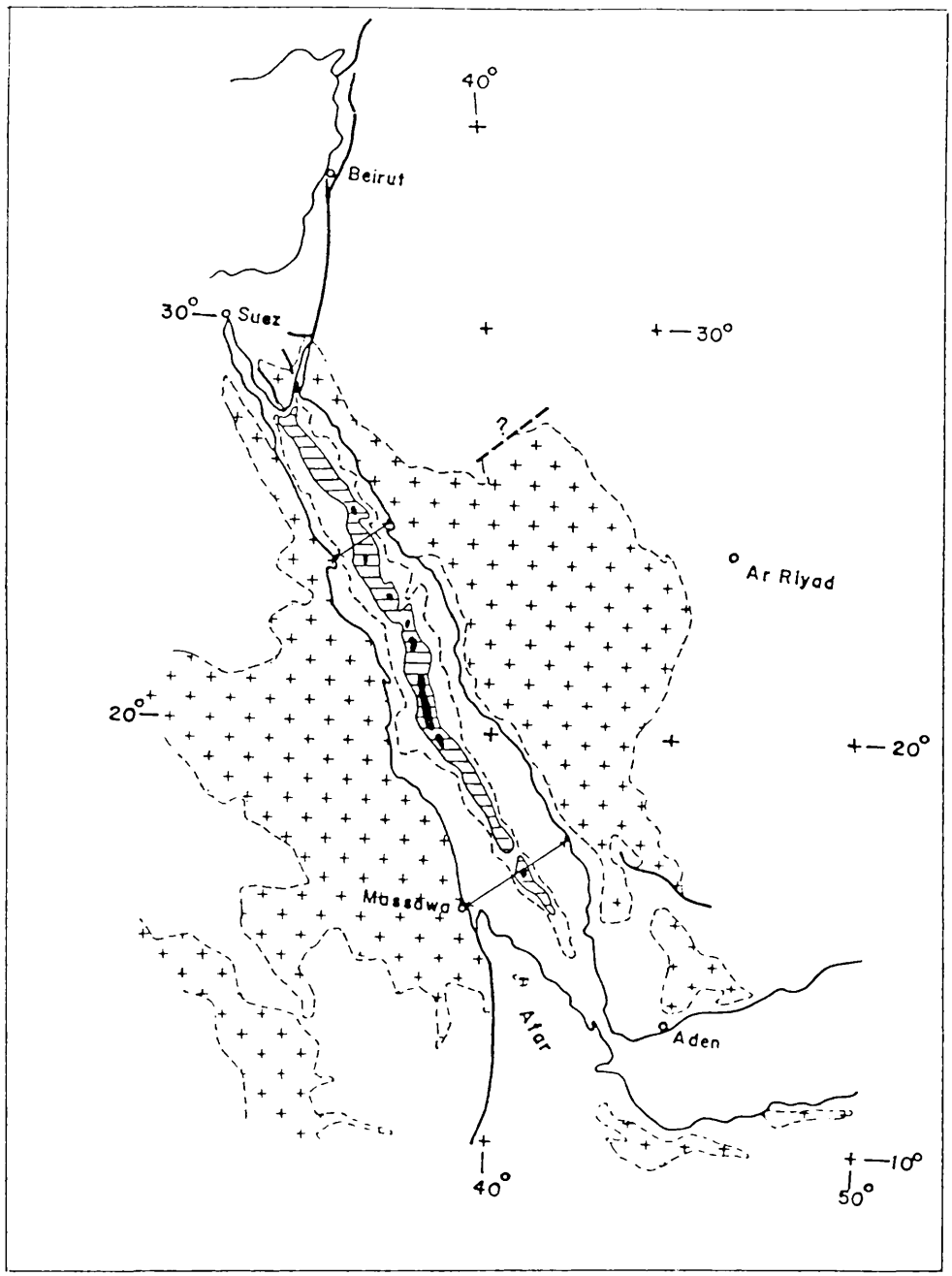

Figure 1.7 The Red Sea cutting through the Precambrian Shield (crosses), the Gulf of Suez; the Gulf of Aqaba-Dead Sea fault and its northern extension. Central trough of the Red Sea: 500m isobath (broken line), 1,000-2,000m isobath (shaded), and in black, depth of more than 2,000m (Dubertret, 1970).

chiefly of Miocene or younger age. Pre-Miocene sedimentary units are scarce and scattered in small areas.

(2) The trough area. This is distinctly demarcated by a steep break-in-slope from 200-300m to 600-1,000m depth at the edge of the marginal shelves. This is wide in the north but narrows progressively until it completely disappears in the Strait of Bab Al-Mandeb.

1.3.2 STRUCTURE

The Red Sea is a part of a regional system of rift depressions which meet at the Afar Triangle and separate the Middle East and Africa into three crustal segments; The Arabian, Nubian and Somaliland segments. The rifts are called, The Red Sea, Gulf of Aden and the East African rift (Gass and Gibson, 1969). Although these three are in different development stages, they all belong to the Tertiary-Recent global sea floor spreading and continental drift episode (LePichon, 1968).

An east-west structural section of the southern part of the Red Sea, shows an anticlinal structure with the Red Sea forming a graben at its crest. The inner margins of the shield have undergone a marked uplift. On the Arabian side the uplifted basement reaches 2000-3000m elevation close to the Red Sea shore. At 100-150Km inland it average 1500m. On the African side the uplift is less pronounced with the basement reaching 1500-2000m elevation along the margin and 1000m or less 100-150 Km inland (Fig. 1.8).

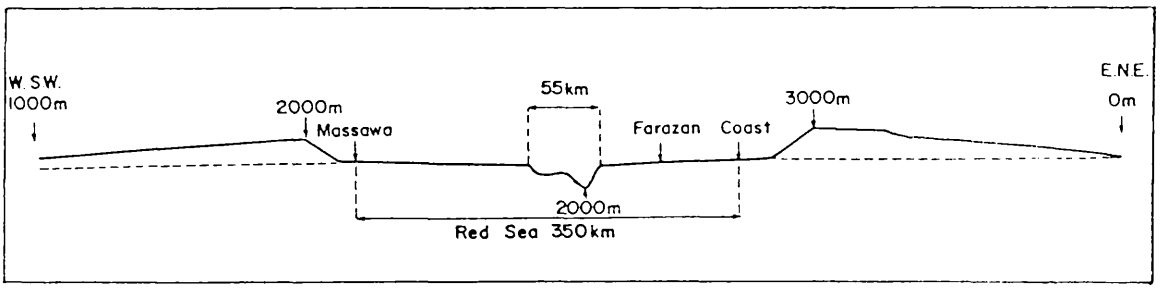

Figure 1.8 Orographic profile across the southern Red Sea, showing the uplift of the adjacent margins of the African and Arabian Precambrian Shields (Dubertret, 1970).

The setting and physiography of the Red Sea is controlled by three major sets of faults:

(1) A NW Erythean trend, parallel to the Gulf of Suez which determined the principal line of weakness and is associated with step faulting.

(2) A NNE, Gulf of Aqaba trend, which is predominantly one of wrench faulting and seems to have determined the direction of crustal separation of Arabia and Africa.

(3) A WNW trend, which is the major fault trend in the Precambrian basement and whose influence can be seen in the sinuousity of the Red Sea coast lines.

There are, in addition, two other fault systems oriented NE-SW and E-W which affect minor trends in coastal morphology (Skipwith, 1973).The two physiographic units, the Shelf and Trough areas of the Red Sea, appear to correspond to two different structural environments. A wide fault zone (1-2Km) lies at the foot of the escarpment on the continent side of the shelf and coastal plain and is concealed by coastal sediments. These faults seem to be high angle and tensional. Seawards of this zone the basement has been modified by step faulting associated with graben rifting. It is possible that block faulting continues into the trough area, but the Red Sea is known from geophysical evidence to be an area of crustal thinning with sea-floor spreading active in the axial trough. The fault zones on the Arabian Plate are still active, as indicated by Recent lava effusions and records of Recent earthquake epicenters in the southern part of Arabia. However, Berry *et al.* (1966) emphasized that the emergent reef deposits show no signs of faulting or warping and suggested

that the constant elevation and sequence of abrasional benches at points along the Sudanese coast indicates tectonic stability in Recent geological time.

1.3.3 TECTONIC HISTORY

The axial trough of the Red Sea is underlain by oceanic crust with well developed magnetic anomalies, as old as anomaly 5, between lats. 16° and 23°N (Cochran, 1983; Roeser, 1975; Yousef and Beckmann, 1981). It is fairly certain that oceanic crust is present for about 80Km on either side of the center of the axial trough at lat. 19°N (Yousef and Beckmann, 1981).

The marine sedimentary record for the Mesozoic provides no strong evidence that the Red Sea depression existed during that time and tectonic activity was generally lacking (GeuKens, 1966; Brown, 1970). The sediments in the Red Sea are up to 5km thick (Drake and Girdler, 1964; Tramontini and Davis, 1969). On the Saudi Arabian shore-line at lat. 17°15' N, a bore-hole penetrated over 3.9Km of chemical, biochemical (limestones and evaporites) and clastic deposits (Ahmed, 1972). Another hole drilled in the Dahlak island region on the west side of the Red Sea penetrated 3.8km without encountering basement (Colman *et al.*, 1972).

The formation of the Red Sea and its surrounding features is the result of many interrelated events. The fact that the Red Sea structures are now an integral part of the world plate-tectonic system has obscured its earlier geologic development. The time of origin is obscure, but all evidence points towards the early Tertiary.

1.3.3.1 SEA-FLOOR SPREADING

Several features along the axial trough support a spreading origin. These include Bouguer gravity maxima greater than 100mgal, indicative of a large basic intrusion, basalts of the mid-oceanic ridge character, high heat-flow, seismicity, refraction velocities indicative of oceanic crust, and symmetrical high-amplitude magnetic anomalies that have been interpreted in terms of sea-floor spreading (Zakir, 1982). Accretion of the oceanic basalt in the Red Sea in the center of the main trough near latitude 18N started 5Ma ago (LePichon and Francheteau, 1978)

Spreading rates have been about 0.9cm/Yr per limb in the western and 1.1cm/Yr per limb in the eastern part of the Gulf of Aden during the past 10 Ma, with crustal separation suggesting a northwards translation of Arabia of 100Km and an anti-clockwise rotation of 7 degrees (Laughton *et al.*, 1970). Mackenzie (1970) suggested that Arabia and Africa have separated by 300km between 15 m.y. ago and the present day, with a spreading rate of 1cm/Yr per limb. More recently, Mart and Hall (1984) have suggested that the spreading rate was 1.2cm/Yr.

Darke and Girdler (1964) interpreted the geophysical data as indicating that the Red Sea formed as a tension feature, the axial trough representing the lateral separation of Arabia and Africa. This interpretation was supported by Abdel Gawad (1970) and Mackenzie (1970) indicated that the pole of rotation of the Arabian Plate relative to the Somalian Plate is at lat. 26°30' N and long. 21°30' E. Allan and Pisani (1966) suggested that tensional forces were restricted to the southern part of the Red Sea

and that, in contrast, the Gulf of the Aqaba might represent the result of compressional forces causing transcurrent faulting.

An essentially continuous zone of sea-floor spreading now extends from latitudes 16°-21°N. From lats. 21°-24°N is a transitional zone where oceanic basaltic accretion is sporadic and occurs in basins separated by attenuated continental crust (Pautot *et al.*, 1984. See Mart & Ross, 1987). In contrast, further north, between lats. 24°-28°N a rift zone is underlain by attenuated continental crust (Uchupi and Ross, 1986).

1.3.3.2 OCEANIC RIFTING

The existance of many down faulted blocks and normal faults striking into the Red Sea axis suggests that it has a rift-in-rift structure (Zakir, 1982). According to Skipwith (1973) the NE-SW tension caused normal step-faulting/rifting of the paar, with associated monoclinal downwarping of the edges during the late Eocene/Oligocene. The most important Oligocene or early Miocene down-faulting is associated with the large Erythean graben marked by the Gulf of Suez and the Red Sea, separating the Arabian and Sinai Peninsulas from the African continent (Picard, 1966). At the turn of the Miocene to Pliocene the Red Sea was connected to the Gulf of Aden through the downfaulted Bab Al-Mandeb Strait. The axial trough of the Red Sea was caused by downfaulting in the Pleistocene (Picard, 1970).

1.3.3.3 RIFTING AND SPREADING

The Red Sea appears to have been formed by a combination of rift-faulting, transcurrent shear movement, and sea-floor spreading. The initial separation was accompanied by much block slumping along the edges, particulary in the northern region of the Red Sea and the Gulf of Suez at the end of the lower Eocene (Swartz and Arden, 1960).

Coleman (1977) suggested that the Red Sea depression developed as a trough between the Arabian and African swells rather than as a downfaulted block. In this view the formation of the axial trough at the beginning of the Pliocene was related to a major rift, a marked departure from the Oligocene and Miocene development of the depression. The physiography of the trough, a steep walled depression with a floor of new basaltic crust, bears out the similarity to other active mid-ocean spreading centers. Gass (1979) reached the same interpretation.

Cochran (1983) proposed that an initial Red Sea rift about 100Km wide was formed by continental rifting in the late Oligocene or early Miocene. This original rift valley widened through a combination of normal faulting and dike injection. The northern Red Sea (north of about 25°N) appears to still be in this stage of evolution. Diffuse extension within the rift resulted in a heterogeneous crustal structure which has been found in seismic experiments both in the Red Sea and along other continental margins (Fig. 1.9). The area between 21°N and 25°N appears to be presently changing from diffuse extension to a sea-floor spreading mode of plate separation.

Mart and Ross (1987) indicated that, in the bathyal zone of the northern Red Sea, dominant elongated evaporite diapirs occur along normal faults associated with the rift and dependent on an extensional tectonic regime. The arcuate configuration of the deeper parts of the bathyal zone changes its trend from NNW-SSE to NNE-SSW, so that the gradual orientational shift from the Red Sea to the Dead Sea trend can be discerned. A new plate boundary, the Dead Sea transform formed along a zone of minimum strength (Steckler & Brink, 1986).

There are a number of groups of views suggesting how the rifting of the Red Sea might have started. Lowell and Genik (1972), and Skipwith (1973) suggested that the regional arching of the continental lithosphere in Oligocene or earlier time initiated the structural evolution of the Red Sea. The continental lithosphere thinned, and stretching was followed by shear on normal faults which caused subsidence in horsts and grabens. In late Miocene/Pliocene times, however, renewed activity caused breaking of the sialic Basement crust and the onset of sea-floor spreading. Ross and Schlee (1973), with similar conclusions, referred the rifting to pre-Miocene, and suggested that during Pliocene time sea-floor spreading caused the evolution of the Red Sea axial trough. This view of doming and uplift during the Oligocene is supported by:

(1) Palaeocurrent trends of the Oligocene red clastic sediments deposited on the eastern and western sides of the trough. These show transport to the NE or NW respectively and thus imply a central high area.

(2) A regional Oligocene unconformity (Dabbagh, 1989) also implies uplift and erosion.

In contrast to this Hotzal *et al.* (1989) and others have suggested that the evolution of the rift started by a gradual stretching of the continental crust following a McKenzie (1978) type model. This led to the formation of a passive margin with accompanying oceanization of the axis.

In the gulf of Suez region, the evidence of emergence during the Oligocene does not conform with the expected response predicted by either the uniform stretching model or the Oligocene crustal thinning proposed by Coleman (1972). This was shown from the study of the facies evolution in the Suez area by Sellwood & Netherwood (1984) who made clear that it is equally difficult to accept that the Red Sea-Suez graben system developed over a major regional arch in the manner proposed in the Lowell & Genik (1972) model. Sellwood and Netherwood (1984) suggested a possible combination of repeated episodes of modest doming and stretching may provide a better explanation in this area.

It is now generally accepted that the Gulf of Aden and the Red Sea depression originated after arching and uplift in the late Eocene. The implications for the Maqna area are discussed in Chpater 7. Subsequent extension, rifting and crustal attenuation in the Oligocene and early Miocene, was followed by the sea-floor spreading which separated Arabia from Africa and rotated it in a counter clockwise direction. This was accompanied by horizontal motion along the Levent Fracture (Dead Sea Transform), and led to the suturing of Arabia with Eurasia and the rise of the Taurus-Zagros fold and thrust belt (Beydoun, 1989).

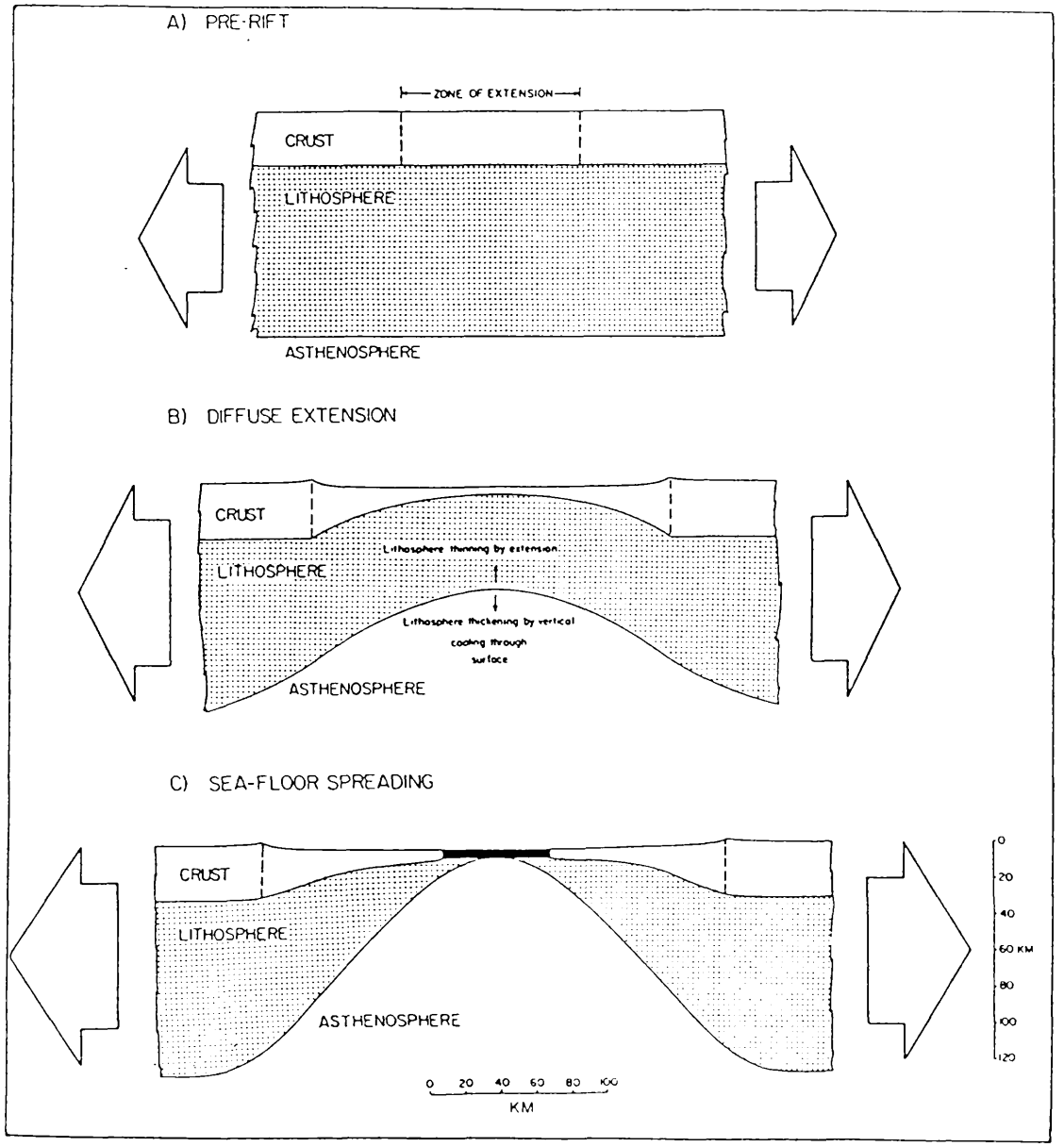

Figure 1.9 Sketch showing development of continental margin and establishment of mid-ocean ridge spreading center (Cochran, 1983).

The precise time of formation of the Red Sea and surrrounding area is not known. During the early Pliocene, it was incorporated into the World Rift system. The magnetic anomaly pattern implies that sea-floor spreading is occurring now and intra-continental and mid-oceanic rift systems are essentially similar.

1.3.4 EASTERN RED SEA COAST STRATA

On the Red Sea coast of Saudi Arabia outcropping sedimentary strata are limited to a thin strip along the outer margins of the coastal plain, except in the north where Tertiary beds occur across the entire width of the plain. The rocks range in age from Eocene to Recent, although they are predominantly of Miocene and Plio-Pleistocence age. Pre-Tertiary beds have been recorded in two areas only. In general, the strata show rapid lateral facies change, as is to be expected in coastal and littoral sediments, and also rapid changes in thickness, as might be expected in an active fault zone. According to Skipwith (1973), there are three locations in Saudi Arabia where the the succession has been described and named:

(1) The Jizan area, in the south, where nonmarine Triassic-Cretaceous beds are overlain unconformably by the basically nonmarine (lagoonal) Baid Formation of Miocene age.

(2) The Jiddah area, where the Usfan Series ranges in age from Maestrichtian to Eocene, and the Shumaysi Formation from Eocene to Oligocene (possibly to Lower Miocene). These strata have both marine and nonmarine associations.

(3) The Maqna area on the Midyan Peninsula, in the north, where the Raghama Formation of nearshore evaporitic deposits ranges from Eocene to Plio-Pleistocene. This is the area considered in the preset investigation.

The general correlation for the Phanerozoic Formations of the Red Sea coast proposed by Beydoun (1989) are shown in Figure 1.10. The correlations of the Tertiary formations in the Maqna area adopted here is shown in Figure 1.11.

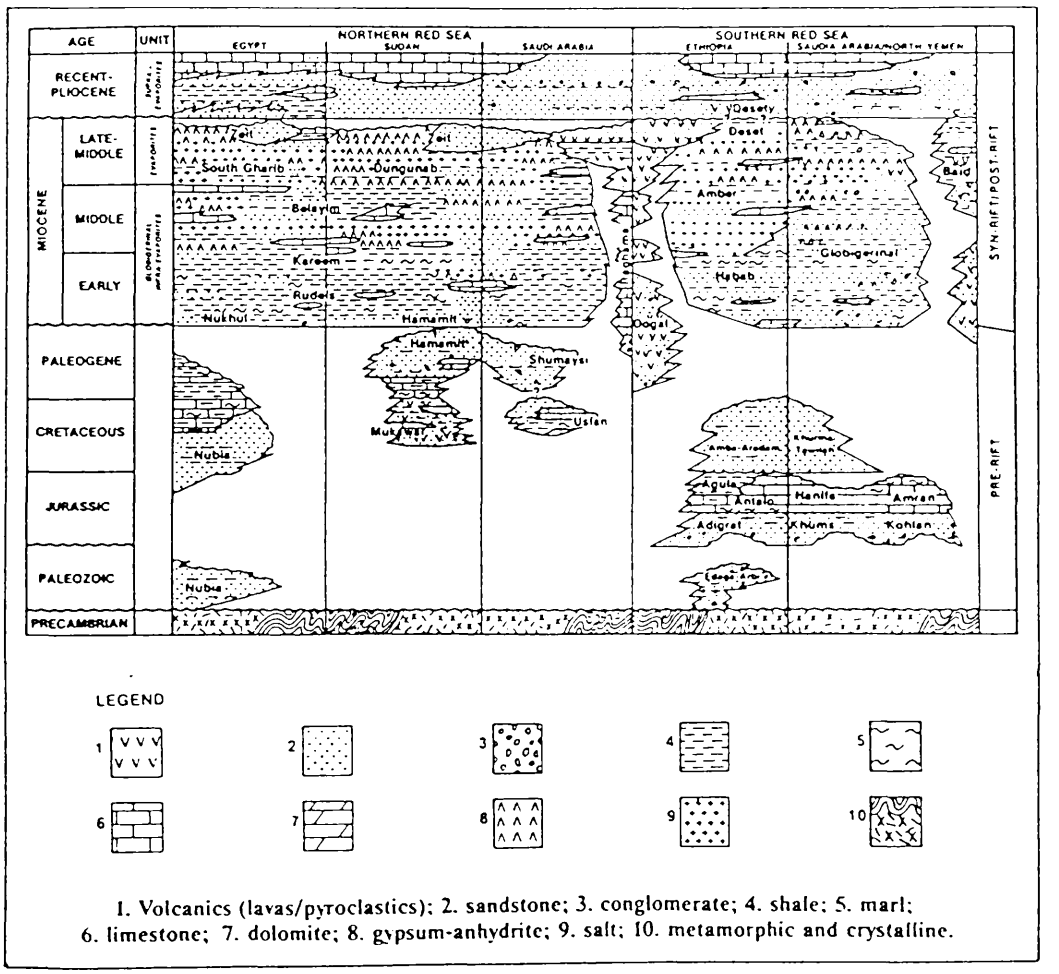

1. Volcanics (lavas/pyroclastics); 2. sandstone; 3. conglomerate; 4. shale; 5. marl; 6. limestone; 7. dolomite; 8. gypsum-anhydrite; 9. salt; 10. metamorphic and crystalline.

Figure 1.10 Red Sea Basin: Phanerozoic formations correlation (Beydoun, 1989).

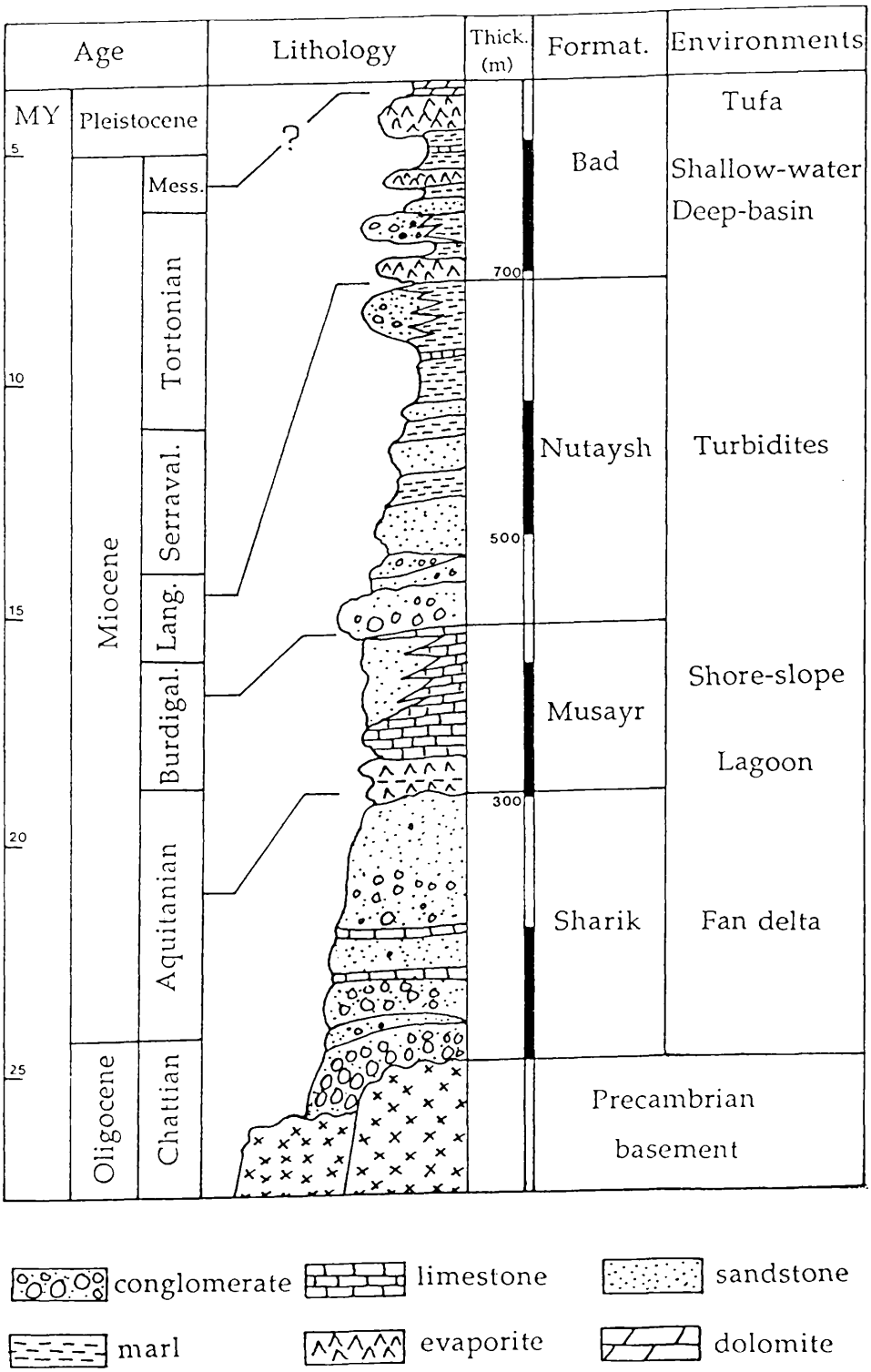

Figure 1.11 Generalized stratigraphic sequence for the Tertiary sediments of the Maqna area.

CHAPTER II

THE SHARIK FORMATION

The synrift sediments of the Maqna area can be divided into four Formations. The Oligocene Sharik Formation is followed by the Miocene Musayr, Nutaysh and Bad Formations (Clark, 1985, see section 1.2.7).

The Sharik Formation was formally named after the Wadi Sharik area just to the north of al Bad. Comparison is made with similar rocks of the Azlam and Jabel Dhaylan basins further south on the Red Sea coast (Motti *et al.*, 1983). The formation forms the base of the sedimentary sequence and rests unconformably on the irregular surface of the Precambrian basement (Fig. 2.1). In the Maqna area, the Sharik Formation is predominantly conglomeratic and varies in thickness. The maximum thickness measured is up to 300 meters, but the unit tends to thin and completely disappear towards the horst structure of the central area.

The Precambrian basement within the Magna area was not remapped and so no major modifications have been made to the boundaries of the facies and units given on the 1:500,000-scale geologic map of Bramkamp and others (1963). The basement is composed mainly of granites intruded by numerous andesite and silicic rhyolite dykes. Small bodies of basic rock with a gabbroic affiliation occur in the central

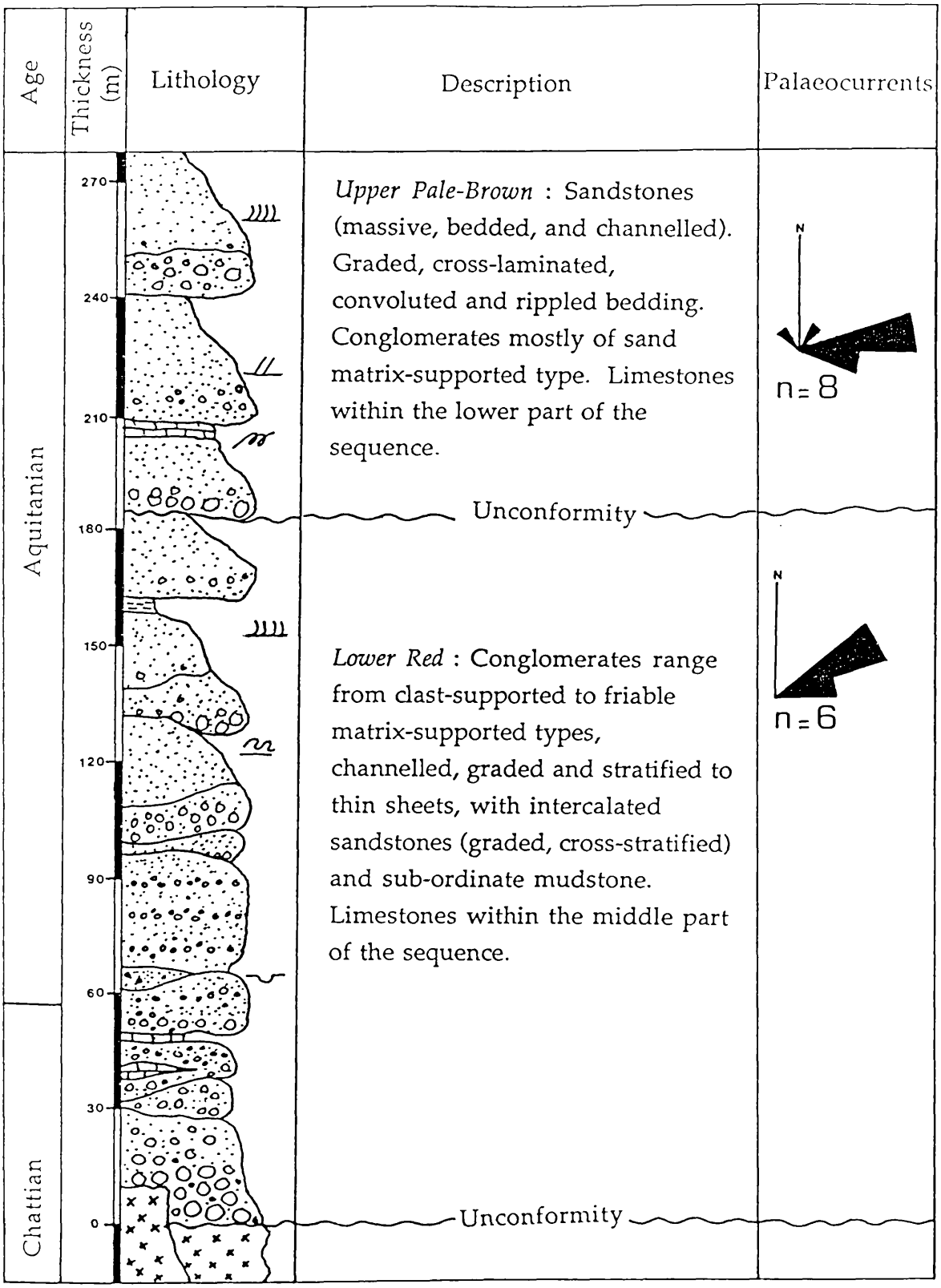

Figure 2.1 Generalized log section for the Sharik formation (see plate 2 for explanation).

part of the area. Volcano-sedimentary rocks are found in the north comprising silicic and basic lavas and tuffs. Outcrops of granodiorite and diorite are present in northwestern areas (Motti and others, 1983).

The boundary with the overlying Sharik Formation is non-conformable, as seen around Jabel Tayran and on the tops of Jabel Amrah and Jabel Musayr. Locally, on the northern and western edges of Jabel Tayran and along Wadi Sek, the contact is faulted. This is clear on aerial photographs (scale 1:60,000) and is confirmed by field observations.

The Sharik Formation can be divided into lower, Red, and upper, Pale Brown, sequences. The distribution of outcrops of the formation is shown in Plate 1.

2.1 THE LOWER RED SEQUENCE

Deposition of the Red beds began with a series of cycles of clast-supported conglomerates representing the initial progradation stages of the deposited sequence. Associated with the conglomerates are arkosic sandstones and subordinate mudstones, derived mainly from the underlying crystalline Precambrian granitic and andesitic rocks. There are also, less frequently, chert fragments which may have come from Eocene cherty beds to the east. Granitic boulders up to 2 meters in diameter are well rounded, but smaller fragments are generally more angular. Notable variations in colour, from red to green, occur mainly along Wadi Sek. These depend partly on the relative percentages of granitic and andesitic rocks. However, there are also distinctive sequence colour changes due to variations in iron

oxides, particularly hematite, which is more common in the lower part of the succession. These conglomerates are extensively exposed in the northern part of the area along Wadi Sek. A maximum thickness of up to 180 meters is found on the north side of Jabel Nutaysh in location SA, and in several smaller outcrops around the granitic mass of Jabel Tayran in the central area, but the unit appears to thin out towards the south. This variation is shown in Plate 2, the changes in thickness are controlled by the underlying Precambrian basement blocks and reflect movements on contemporaneous faults. Examples of these variations are seen in the uplifted faulted block of the central area, where, along Wadi Al-Hamd, the the unit is 50 meters thick in location K and decreases rapidly to the south in localities K1, K2 and KK1, before completely disappearing. In the northern part of the area there is up to 40 meters difference in thickness between localities P and P1 which also indicate uplift of the northern side of the Wadi Sek fault. These changes in thickness are accompanied by facies changes which occur rapidly over short distances.

The conglomerates of the Red unit range from compact clast-supported to friable matrix-supported types. The latter may have a muddy or sandy matrix with a calcareous cement or a friable sandy matrix with a gypsum, calcite or, less frequently, hematite cement (confirmed by petrographic study and XRD analysis). Exposures of this unit along Wadi Sek are eroded into cliff faces and deep gullies. In these there are remarkable high percentages of calcareous cement in clast-supported conglomerates which are most common low in the succession. In location SA1, there are three distinct dolomitized limestones intercalated within the

conglomerates, these are described in more detail below, but are important to the general environmental interpretation.

The sandstones of Red unit are characterized by common planar and trough cross-bedding 0.3-1.5m sets thickness (Fig. 2.5-A), with less frequent large-scale cross-bedding in sets of up to 4 meters thick (location K2 in the upper part of the sequence). Current ripple marks, and thin sheets of conglomerate (Fig. 2.5-B, C) are seen locally. Shallow channels are common, some are tens of meters across (Fig. 2.5-D), and trend between 55°-90°. Palaeocurrents derived from these are of variable direction, but with a major trend towards the East and North East. Analysis of palaeocurrents interpreted from current cross-stratification and cross cutting channel trends around Jabel Tayran shows locally variable directions which imply the presence of a palaeotopography defined by adjacent basement blocks.

The sandstones of the Red unit are dominantly poorly sorted. These are mostly normally graded, but some are inversely graded from fine to very coarse grained. Grains are angular to subrounded and the sandstones are typically porous. Quartz is the most common mineral, forming up to 60% of the sediment, generally as monocrystalline grains, but with some notable polycrystalline fragments reflecting metamorphic and igneous origin (N.B. all grain percentages are based on estimates from comparative charts). Under C.L. quartz grains may be of blue, violet or common dark brown varieties. Some contain fluid inclusions.

Feldspars are dominantly orthoclase and microcline, and may be green or blue under C.L. Some feldspar grains are weathered and in general they are more rounded than associated quartz grains. They may form up to 30% of some arkosic beds. Rock fragments include andesitic, granitic, volcanic tuff and pre-existing sedimentary rocks such as shale, chert and sandstone and form up to 10% of grains. There are small percentages of other minerals such as biotite, rutile and opaques.

Hematite, identifed by XRD, has been formed by oxidation of iron-bearing minerals. (Teodorovich, 1961) noted that hematite is formed during weathering in hot arid climates, due to the rich flow of fresh water. However, Walker (1967) emphasized the importance of iron-bearing detrital grains and noted that weathering occurres long after deposition and may be present in marginal marine as well as subaerial sediments. Generally, there are well developed authigenic silica overgrowths, formed during later stages of diagenesis or epigenesis (Teodorovich, 1961).

SEM examination shows Fe-chlorite (Fig. 2.6-A), smectite, and illite occurring as authigenic cements (confirmed by XRD) as well as authigenic silica overgrowths on quartz grains and authigenic crystals of K-feldspars (Fig. 2.6-B). Grim (1968) suggested that some illite and chlorite form quickly when fresh water muds enter a marine environment. Clay minerals of authigenic origin, have developed subsequent to sediment deposition by precipitation of clay crystals from pore fluids. Smectite forms as a product of hydrolysis of alkali-feldspars (Keller, 1970), but may be transformed into illite during early and deep burial stages of diagenesis (Banat, 1980; Weaver, 1989). It is generally agreed that in mud-shales, but not necessarily in

sandstones diagenetic mixed-layer illite-smectite and illite are formed from smectite. Weaver (1989) believed that the conversion of smectite to illite is gradual, occurring as the sediments settle through the appropriate temperature (50-150C°). Within this temperature zone the proportion of illite in the illite/smectite increases with age. For example, (Weaver, 1989) showed that there is more illite in the Cretaceous than in younger sediments. In the Maqna area, the formation of authigenic illite in the sandstones, and less frequently in the shales is more likely to be as a result of long maturation and higher temperatures than of deep burial. This is clearly indicated from its existence throughout the Tertiary sequence. Further evidence of higher temperatures will be discussed in Chapters 3 & 7.

Locally, in location T, close to the center of the basin and where the effects of overburden pressure might be expected to be greatest, grain boundaries are embayed by pressure dissolution.

In location P, a limestone 1.5 meters thick occurs. This is dolomitized with notable remains of bivalves and coralline algae. The dolomite is of planar-e crystals (40-110μm diameter) and shows homogeneous dull luminescent under CL. It contains a blocky sparry calcite cement (140-220μm diameter) which, under C.L., again shows two generations of growth. However, here an early bright zone which has been partially dissolved and its surface is marked by irregular corroded boundaries (Fig. 2.6.-C). This is overlain by later dark zone, and some with a bright intercalation (subzone).

The limestones intercalated within the Red unit in location SA1 are a maximum of 0.5 meter thickness. They were originally poorly sorted peloidal muddy carbonates, containing bioclasts such as foraminifera, bivalve, echinoderm and gastropod fragments together with lithoclasts and angular to subrounded fine to medium grains of quartz and feldspars. They are now extensively dolomitized with finely crystalline dolomite (<10μm diameter) with non-planar and less frequently planar-s boundaries as described by Sibley and Gregg (1987). Under C.L., the dolomite is of uniform dull luminescence. Some crystals (up to 80μm diameter) are formed as cement within pores and overlain by sparry calcite cement. A few have dark cores and dull outer zones in CL (Fig. 2.6-D). Within moulds of bioclasts, the later blocky sparry calcite cement (crystals 80-150μm diameter) can be divided into two generations under C.L., an early bright and later non-luminescent zones. All dolostones are styolitic and have been extensively fractured. Cements in fractures show an identical zonation.

The dolomite is overlain by the sparry calcite cement which indicates dolomitization during the early burial changes within a shallow marine environment. These dolomitized limestones are all predominantly of marine-derived grains and it is likely that they were in fact marine. They are therefore significant for the interpretation of the unit. The early brightly luminescent sparry calcite cement probably also formed soon after burial in a shallow marine environment while the later non-luminescent zone may reflect deposition in a meteoric environment following later regression.

The boundary between the Red and the overlying Pale Brown unit is disconformable and reflects differences in thickness created by deposition. This can be deduced both from field observation and the summation of stratigraphic columnar sections (Plate 2).

2.2 THE UPPER PALE BROWN SEQUENCE

The Pale Brown beds, sandstones and conglomerates of mostly sandy matrix-supported type with a thickness of up to 80 meters, occur predominantly in the central part of the area (Plate 2). The distribution of the unit was apparently again controlled by faults (horsts) which formed after deposition of the Red unit. The sequence as a whole becomes finer grained upwards as the graben filled.

The base of the Pale Brown sequence in location K2 is formed by laminated fossiliferous grainstones up to 5 meters thick characterized by bioclasts of gastropods, sometimes densely packed and, less frequently, bivalves. These sediments were deposited in a shallow marine environment below the wave-base. Under C.L. three generations of blocky sparry calcite cement are found. An early multiple dull-bright zoned cement (crystals 150-300μm diameter), followed by (80-140μm diameter) bright calcite and a later (crystals 20-70μm diameter) non-luminescence cement (Fig. 2.6-E). The multizoned calcite cement is attributed to changes in porewater chemistry during burial (Tucker & Wright, 1990). Another laminated bed 0.5 meter thick occurs at the base of the Pale Brown unit in locality B. This is composed of several intercalations of gypsum and shale, and was deposited in an isolated lagoonal environment. Where, ordinarily by the time a few

millimeters of gypsum had been precipitated, there would be a new incursion of the sea and the process would be repeated (Adams, 1944). Both of these sequences point to temporary starvation of clastic supply at the beginning of deposition of the unit, allowing either biological productivity or chemical precipitation to predominate.

The remainder of the unit consists largely of sandstones characterized by multiple fining upwards sequences. It includes both simply bedded sequences without structures, and sequences with a wide variety of structures. These include small-scale current-ripple marks, trough and planar cross-stratification up to 2 meters thick, large-scale cross-bedding from 3 to 8 meters thick (Fig. 2.7-A), and lateral wedging on a scale of tens of meters thickness. Current structures indicate variable directions of palaeocurrent (50°-120°), but generally transport was towards Northeast and Southeast. Other features such as convolute bedding ranging from 0.5 to 12 meters amplitude are mainly concentrated on the western side of Jabel Tayran and may be related to local instability (Fig. 2.7-B). Channels, thin sheets of conglomerate, mostly of rounded cobbles of Precambrian rocks, and herring-bone cross-bedding up to 2 meters thick (Fig. 2.7-C) are all common. Herring-bone cross-bedding was noted by Tucker (1989) as a characteristic but not ubiquitous feature of tidal sand deposits. The upper part of this sequence in locations K1 & K2 shows scattered portions of poorly organized branching burrow systems. These features together suggest shallow shelf deposition.

The sandstones of the Pale Brown unit are notably better sorted and finer grained than those in the underlying Red unit. In general they are moderately sorted, fine

to coarse, with angular to rounded grains. Locally, on the western side of Jabel Tayran (locality KK1), conglomerates are still present in the succession with well rounded granitic boulders up to 1 meter in diameter resting in a sandy matrix. These may be locally derived. Generally cobbles and boulders are concentrated along the western side of Jabel Tayran, but a few isolated individuals are scattered throughout. The upper part of the succession varies from sandstones to pebbly sandstones, partially arkosic, with several interclations of well laminated shale.

Quartz forms up to 70% of grains (estimate based on comparative charts). In C.L. it may be brown, blue or violet. Well developed authigenic silica overgrowths are scarce and represented by irregular dull brown rims coating blue grains. A few grains contain fluid inclusions, and so are characteristic of detrital contributions from plutonic igneous and metamorphic rocks (Pettijohn *et al.*, 1973). Feldspars form up to 25% of grains in the Pale Brown unit and include microcline, orthoclase and plagioclase showing characteristic twinning. A few show perthitic intergrowths. Feldspars typically have green or blue luminescense and were probably derived from the same sources as the quartz grains. Some are highly weathered, showing alteration to sericite. There are a few opaque grains and rock fragments including particles of andesite, granite, shale and chert.

The sandstones are mainly cemented by medium grained (80-120μm diameter) blocky sparry calcite. The calcite can be seen under CL to consist of two separate generations, an early bright and later non-luminesent zones of cement. These are followed and overlain by the silica overgrowths refered to above.

In location K, the top of the Pale Brown unit is marked by subaerial weathering. Up to 1.2 meter relief is eroded to form an irregular surface on the sandstones, overlain abruptly by the Musayr gypsum (Fig. 2.7-D). Within these sandstones, SEM examination shows fibrous authigenic gypsum crystals occuring as a cement (Fig. 2.6-F). These could have been derived from fluids present when the overlying gypsum was formed. The gypsum cement is later than either the sparry calcite cement or the silica overgrowths.

West of Jabel Amrah in location N, cerebroid stromatolites are present at the top of the succession associated with a conglomeratic marly limestone and numerous *Ostrea* shells. Here, the Pale-Brown unit 2 meters thick and characterized by common well rounded boulders of chert (5-20cm diameter). Dolomitized cerebroid bodies form individual mounds 30-50cm in diameter (Fig. 2.7-E). Under CL, it shows uniform dull luminescence of planar-s dolomite crystals. In present day environments these are best developed in areas exposed to waves, occuring within a periodically emergent zone, and their morphology may be a biotic response to the physico-chemical stress of drying (Braithwaite *et al.*, 1989).

Dolomitization has taken place during the early burial changes, and overlain by three generations of blocky sparry calcite cement. These are an early multiple-zoned reflects changes in porewater chemistry followed by the bright luminescent, both cements are probably formed soon after burial in a shallow marine environment. The deposition of the later non-luminescent sparry calcite cement after phase of dissolution reflects deposition in a meteoric environment (oxidized).

2.3 INTERPRETATION

The Red unit facies, previously described as an alluvial fan, has the characteristics of a fan delta. According to Coleman & Prior (1982), fan deltas include large-scale cross-bedding which can attain thicknesses of up to 7 meters in braided channels.

Fan deltas are coarse-grained depositional systems developed at the land water interface, where the interaction between an active alluvial fan and the sea or a lake involves a remarkably wide range of sedimentary processes and facies. Nemec and Steel (1988) recognizing the general features of the fan-delta. This shows a prism of sediments delivered by an alluvial fan and deposited mainly or entirely subaqueously, at the interface between the active fan and a standing body of water. There is generally proximity to a Highland area and an association with tectonic escarpments (*i.e.* flanking basin margins which are usually major fault zones). The last are common and important attributes but are not critical. The facies criteria and the evidence of an alluvial fan as the feeder system of the delta are principle features in fan-delta recognition.

Ethridge and Wescott (1984) defined three fan-delta types, shelf, slope and Gilbert types (Fig. 2.2). These are thought to be controlled by basin-margin gradients (tectonic settings). Variations in the structural gradient along the basin margin may produce a spectrum of fan-deltas ranging from low-gradient shelf varieties, through slope-type systems to steep-gradient Gilbert type varieties (Massari and Colella, 1988).

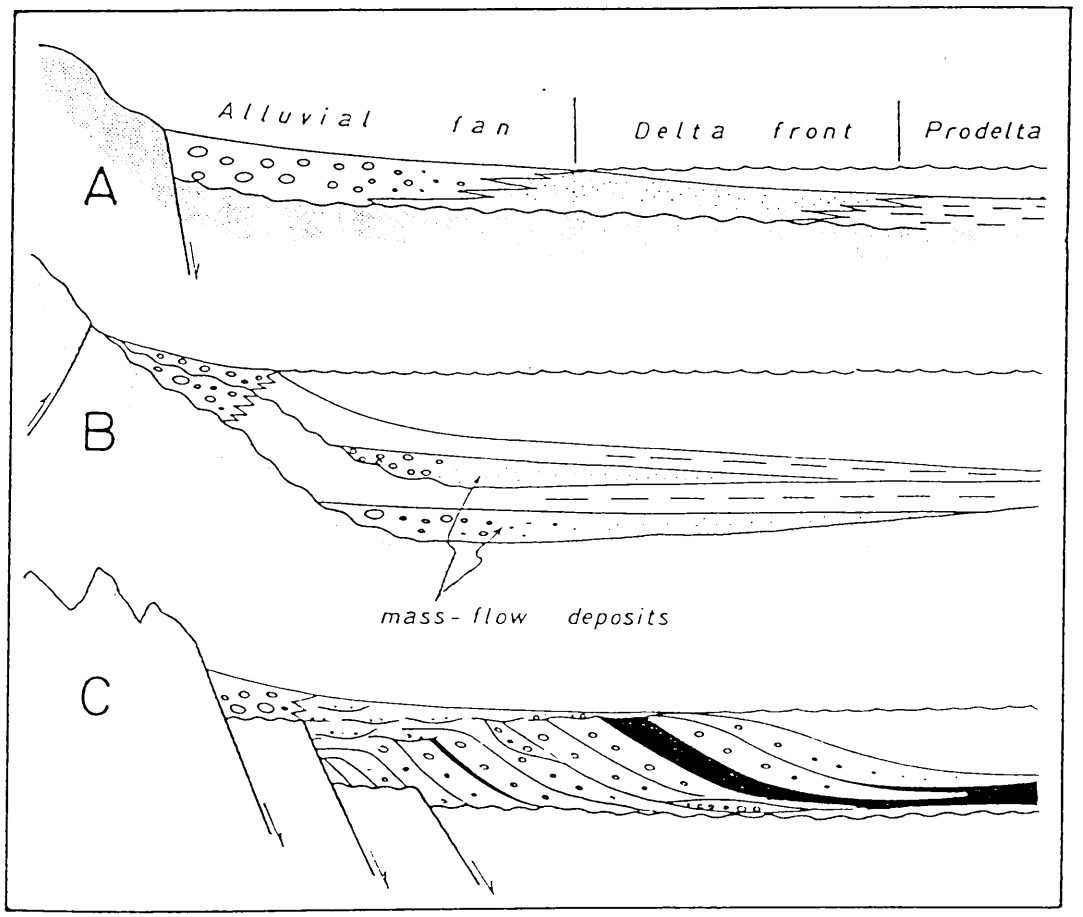

Figure 2.2 Idealized cross-sections showing the three main fan-delta types: A) shelf-type fan delta; 2) slope-type fan delta with a related, slope-onlapping system; and 3) Gilbert-type fan delta (Etheridge & Wescott, 1984).

The limestone beds in the Red unit are important (Fig. 2.5-E). Their intercalation is related to the coarseness of the remaining sediment and the infrequency of terrigenous deposition which allows for the development of carbonates on the fan (Friedman, 1988). Hay *et al.* (1988) suggested that carbonates are deposited where there is no major source of detrital sediments, but this can result simply from temporary starvation as a result of local position on the fan.

The Pale Brown unit is again thought to have been deposited as a fan delta but reflecting more passive deposition than that in the underlying Red unit and a greater degree of re-working by marine processes. Deposition originated by the uplift of the central block horsts following the rifting of the basin margins. The large scale cross-bedding was produced. Similar cross-stratification has been described by Walker (1984) and attributed to deposition in large sand waves.

Large scale crossbedding may be the product of migration of large dunes, either subaqueous or eolian or of lateral migration of large scale channels. The large scale cross-stratification in eolian deposits is characterized by high angle cross lamination, and by slump and sand-flow structures aligned down and cutting foreset beds (Compton, 1985). None of these features are seen in the Maqna area, where large-scale cross-bedding is associated with a sandstone sequence characterized by marine features such as bioturbattion, fossils and herring-bone cross-bedding. These features together indicate that the large scale cross-statification within the Upper Pale-Brown sandstones of the Sharik Formation is likely to be of subaqueous (marine) origin and that they probably represent sand waves.

Sand waves are large-scale, transverse bedforms, generally with straight crests and well defined lee slopes which are most commonly inclined at less than the angle of repose (c.<15°). They usually vary between 3-15m high and with wave lengths between 150-50m. They occur where current velocities are greater than 65cm/s (Johnson and Baldwin, 1980), and represent fluctuating unidirectional flows (Allen, 1980). Levell (1980) suggested that sand waves form in response either to regional transport dominance, to local transport dominance, or to preservation over the long term of master bedding surfaces inclined in one direction. In general, the sand ridges line up, and sand waves are transverse to the long axes of the tidal current ellipses, indicating a tidal control (Walker, 1984).

Allen (1980) proposed six sand wave classes (Fig. 2.3), suggesting that the controlling factors are: 1) the tidal time-velocity pattern, 2) water depth, and 3) bed-material calibre. Classes 1 & 2 represent fluctuating unidirectional flows. Class 3 has a significant still-sand period between critical ebb and flood velocities for sand movement during which time the foresets begin to be bioturbated. Class 4 shows major reactivation surfaces, and classes 5 & 6 show almost symmetrical ebb and flood currents (Fig. 2.3). The sand waves in the Maqna area show: 1) dominantly unidirectional currents, 2) lack of reactivation surfaces and bioturbation, and 3) lack of mud cracks or mud drapes. Accordingly, they are classified under class 1 of Allen. These are thought to be deposited in a strong time-velocity asymmetric, tidal current regime by migration of relatively straight crested large scale sand waves (Allen, 1980).

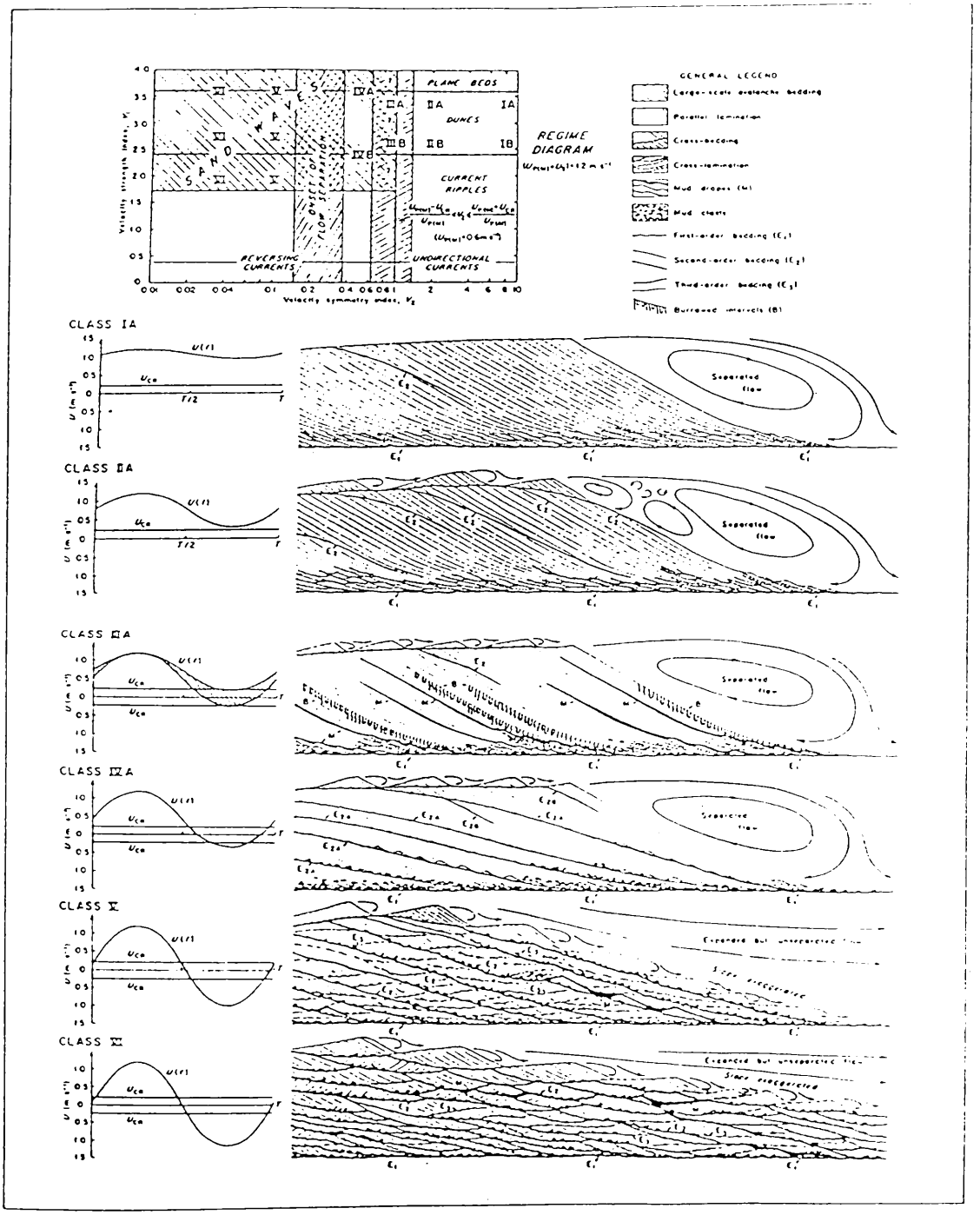

Figure 2.3 Regime diagram, and predicted categories of sand wave and dune internal structure. Note that the six classes are defined by the time/velocity asymmetry (or symmetry), from Allen, 1980.

Ancient and recent examples suggest that tide-dominated shelves are characterized by sand waves and sand ridges (Walker, 1984). Therefore, before the opening of the Gulf of Aqaba, although the Maqna area was located farther south it was probably connected to a sea characterized by strong tides. The connections demonstrated in the Miocene (Chap. 2) are with the Mediterranean rather than the Indian Ocean. However, the recent Mediterranean has only small tides. These features may therefore indicate a time where the Mediterranean and thus the Maqna area had a more open connection with the Atlantic and was swept by strong tidal currents.

The fact that the Pale Brown unit is effectively a fan explains why it wedges out laterally and also why it is so limited in distribution, concentrated in the central part of the area.

The Sharik Formation as a whole represents a shallowing upward sequence. It formed as a result of uplift of marginal blocks, generating coarse grained clastic wedges along the edge of the basin (Ben Avraham, *et al.*, 1979). These wedges are variably dipping but generally facing toward the east. The rocks have generally been tilted to the northeast.

The lower Red unit is thicker in the northern part of the area (180m), where it is dominated by clast-supported conglomerates representing the proximal part of the fan. The unit decreases in thickness and is finer grained towards the south, pointing to the northern Precambrian basement as the main source of the detrital materials.

The upper Pale Brown unit is concentrated in the central part of the area where it is up to 80m thick. The limits in distribution were controlled by the horst structure of the central part of the area and the central Precambrian basement of Jabel Tayran was the main source. Palaeotopograpy and structural inversion also controlled the thickness of the formation (Fig. 2.4)

In the Maqna area, the outcrops of the Sharik Formation comprise a variety of sediments, showing the following features:

(1) A wedge-shaped body of mainly clastic, sediments, that thins to the S & SE (see the cross-section A-A' of plate 1)

(2) Conglomerates occur in composite units up to 10m thick. They are poorly sorted, but generally clast-supported with clast sizes exceeding 1.5m in diameter in some beds.

(3) Channels are common, some found in the Lower Red Sequence are large scale (up to tens of meters) and contain conglomerates.

(4) Poorly sorted calcareous conglomerates are interbedded with dolomitized limestones which contain a fragmental marine fauna.

(5) Several intercalations of dolomitzed limestone contain bioclasts such as foraminifera, bivaves, echinoderms, gastropods and coralline algal fragments. These are predominantly marine-derived gains and it is likely that the sediments were in fact marine.

(6) Sandstones are poorly sorted, and commonly show planar (some large scale), trough cross-bedding, herring-bone cross-bedding, and current ripple marks. Thin sheets of conglomerate are interbedded. These are mostly normally

graded, but some are inversely graded from fine to v. oars sandstones. In addition, some sandstones contain scattered portions of poorly organized branching burrow systems.

(7) There is no evidence of subaerial exposure throughout the sequence.

According to the above characters the Sharik Formation Sequence is likely to be of marine origin, deposited as a fan delta. The sequence in the Maqna area has been compared (plate 2) to similar rift setting fan-deltas and this suggests that the fan-delta reflects an evolution from a Gilbert-type to a shelf-type fan-delta. In the basin-fill succession mainly mass-flow conglomerates are capped by shallow marine fan-delta sediments. The rarity or absence of shelf-marine facies in the lower part of the succession suggests that the basin was bounded by relatively steep slopes, and that the detritus was transported from source areas directly into a deep-marine depositional realm (*c.f.* Massari & Colella, 1988). The large scale channel conglomerates found in the Lower Red Sequence, may have been deposited by floods in high discharge, by fan-head braided streams, or replaced by related mass flow (Ito & masuda, 1988). The conglomerates occur in composite units thought to represent the proximal, upper segment of the succession are interpreted as reflecting the wave-worked deposits of the fan-delta front.

2.4 CONCLUSIONS

In summary, a number of conclusions can be deduced. Some of these (4, 10, 12, and 13) are similar to those of Roberts and Murray (1988):

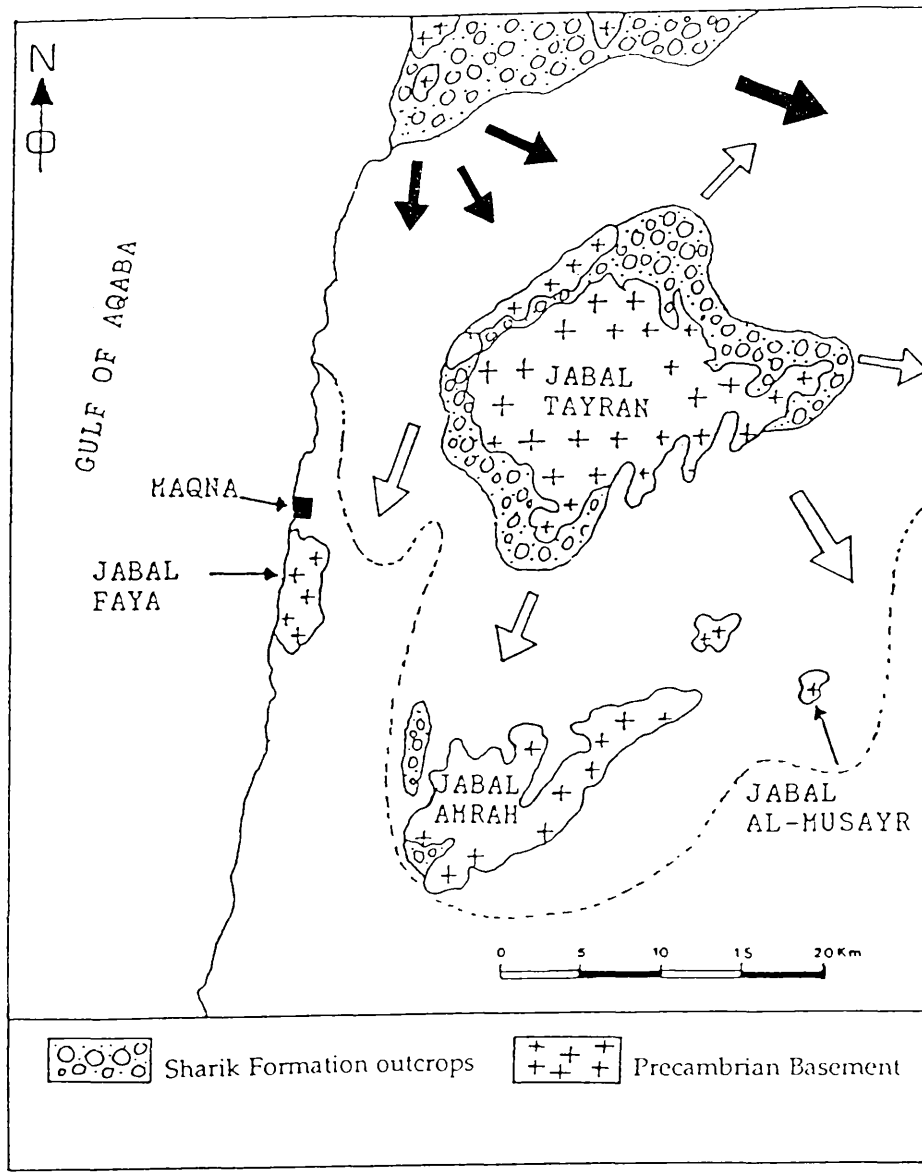

Figure 2.4 Schematic map showing the limit of distribution of the Sharik Formation (dashed line). The source area of the Lower (Red) unit lay to the NW. Transport directions inferred from sediment thickness are indicated by black arrows. Local sources were active during deposition of the Upper (Pale-Brown) unit with measured palaeocurrent directions shown by open arrows.

1. The fan-delta deposits of the Sharik Formation are of Late Oligocene to Early Miocene age, forming a clastic-rich succession which originated after the initial rifting of the Red Sea.

2. The sedimentary succession was deposited along the margin of an active rift, and represents a zone of transition from the uplifted crystalline basement to the subaqueous sedimentary basin.

3. The tectonic setting and the associated active subsidence caused an overall progradation of the Sharik fan-delta system.

4. Tectonic activity controlled the relief on basin flanks and siliciclastic sediment discharge, and also the alternation between carbonate and siliciclast supply.

5. In the Maqna area, the Lower Red Sequence thins rapidly basin wards and merges into scoured, channel-fill conglomerates (locality K), with palaeo-current trends dominantly between 55°-90° (*i.e.* facing NE-E).

6. The deposition of the Upper Pale-Brown sequence followed renewed activity of the basin-boundary faults defining a new topography which influenced the depositional architecture of the fan-delta succession (*c.f.* Wescott, 1988 and Leeder *et al.*, 1988).

7. The palaeocurrent directions are towards the NE & E in the Lower Red unit, and towards the NE & SE in the Upper Pale-Brown unit as a result of movements of the central fault (horsts).

8. The soft-sediment deformation features, such as convolute bedding, found in the Upper Pale-Brown Sequence point to instability resulting from rapid depositional events.

9. The absence of kaolinite which would indicate humid tropical weathering conditions in the source area (Millot, 1970) suggests that deposition occurred in an arid climate.

10. An arid climate promoted sporadic but intensive transport events of dominantly coarse siliciclastic debris. This resulted in the progradation of alluvial fans directly from fault controlled mountain fronts into the marine environment.

11. The conglomerate clasts show an absence of any pre-existing sedimentary cover, all basement rocks are either igneous or metamorphic.

12. Abrupt lateral and vertical facies changes are to be expected in arid tectonic basins.

13. Depositional environments were in general not favourable for the establishment of benthic biota. The speed of accretion during periods of deposition was so rapid that bioclasts, could not accumulate. However, the infrequency of run off to the basin allowed carbonates containing a marine biota to be developed in shoal areas and on the distal parts of the deltas during periods of low discharge.

14. The colour of the sequences is related to the type of detrital materials and the content of iron oxides.

15. The diagenetic sequence suggests that the Red and Pale Brown sequences were subjected to similar diagenetic environments.

16. The subaerial portion of the fan-delta is poorly preserved due to erosion which pre-dated the deposition of the Lower Musayr evaporite sequence.

It is important to note that the emphasis on marine deposition represents a new interpretation of the Sharik Formation which, as noted, has previously been seen as of continental origin.

SHARIK FORMATION

Figure 2.5

A. Low angle trough cross-bedding in the upper sandstone units of the Lower Red sequence in location K2.

B. Current ripple marks on the surface of fine grained sandstone bed close to location K.

C. Sheet flow conglomerates intercalated with coarse grained sandstones in location K.

D. Channels tens of meters across filled with conglomerate occurring at the base of the Lower Red sequence in location K.

E. Limestone intercalated within the Lower Red sequence conglomerates in locality P, north Wadi Sek.

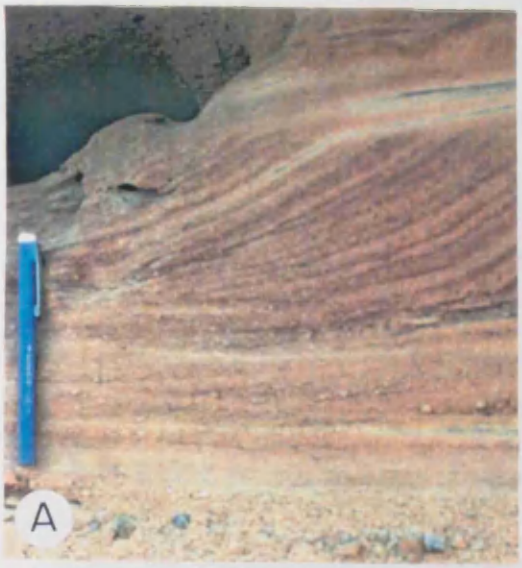
A

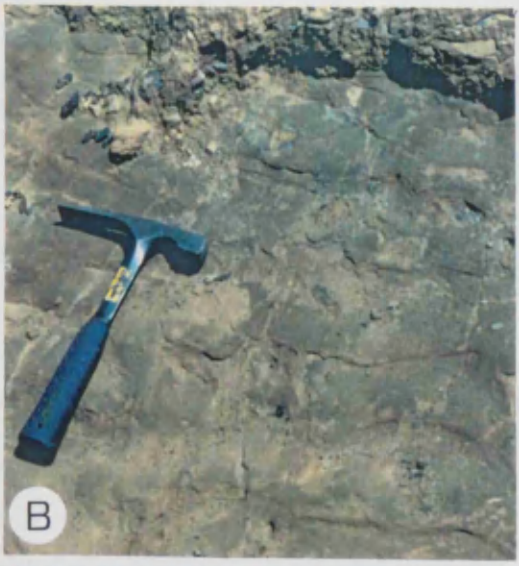
B


C


D


E

Figure 2.6

A. SEM. Authigenic Fe-chlorite crystals (C) within sandstone unit in locality K.

B. SEM. Diagenetic K-feldspar crystals (f), quartz grain (q), with rim of authigenic growth, and overlying authigenic illite crystals (i).

C. Two generations of sparry calcite cement in locality P. Early brightly luminescent, later dark. Thin section, CL. Scale 0.1mm, (arrows point to crystal faces).

D. Planar-e dolomite cement crystals (dull) overlain by sparry calcite cement (bright). Thin section, CL. Scale 0.2mm.

E. Three generations of sparry calcite cement within dissolved bioclast. These are an early multiple-zoned (1) followed by right (2) and later non-luminescent (3) cements. Thin section, CL. Scale 0.2mm.

F. SEM. Gypsum pseudomorphs of fibrous gypsum cement, which partially cements the upper sandstone unit in locality K.

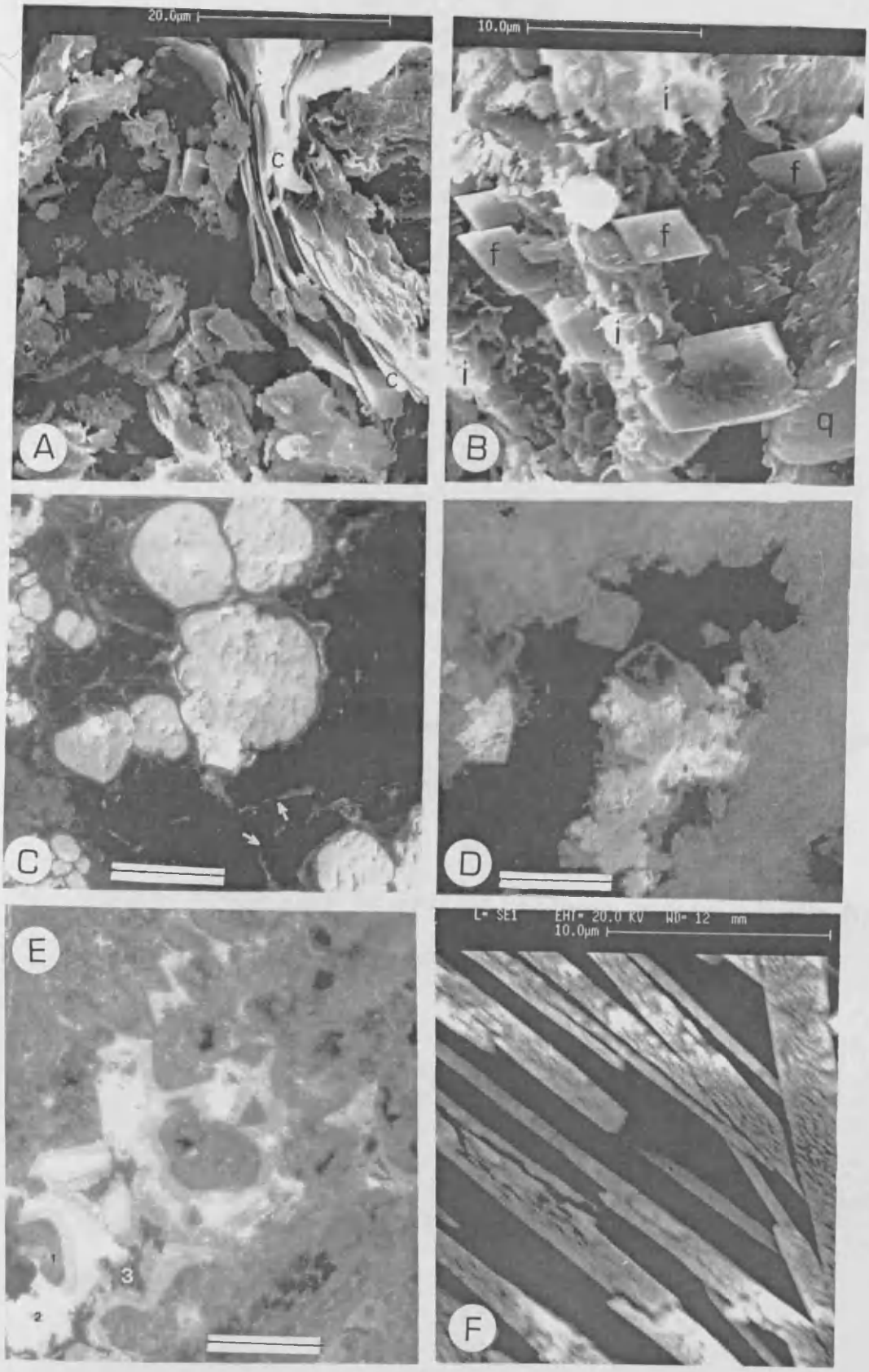
20.0µm
c
c
c
A
10.0µm
i
f
f
f
i
i
q
B
C
D
E
1
2
3
L- SE1 EHT- 20.0 KV WD- 12 mm
10.0µm
F

Figure 2.7

A. Large-scale cross-bedding (set approx. 5m thick) within coarse grained sandstones of the Upper Pale Brown sequence in location K2.

B. Convolute bedding within medium-coarse grained sandstones on the western side of Jabel Tayran.

C. Herring-bone cross-bedding within upper coarse sandstones of the Upper Pale Brown sequence close to location T, on the southern side of Jabel Hamza.

D. Eroded relief of the upper sandstone unit of the Upper Pale-Brown sequence in location K, (arrows point to surface).

E. Cerebroid stromatolites at the top of the Pale-Brown sequence in locality N, on the western side of Jabel Amrah.

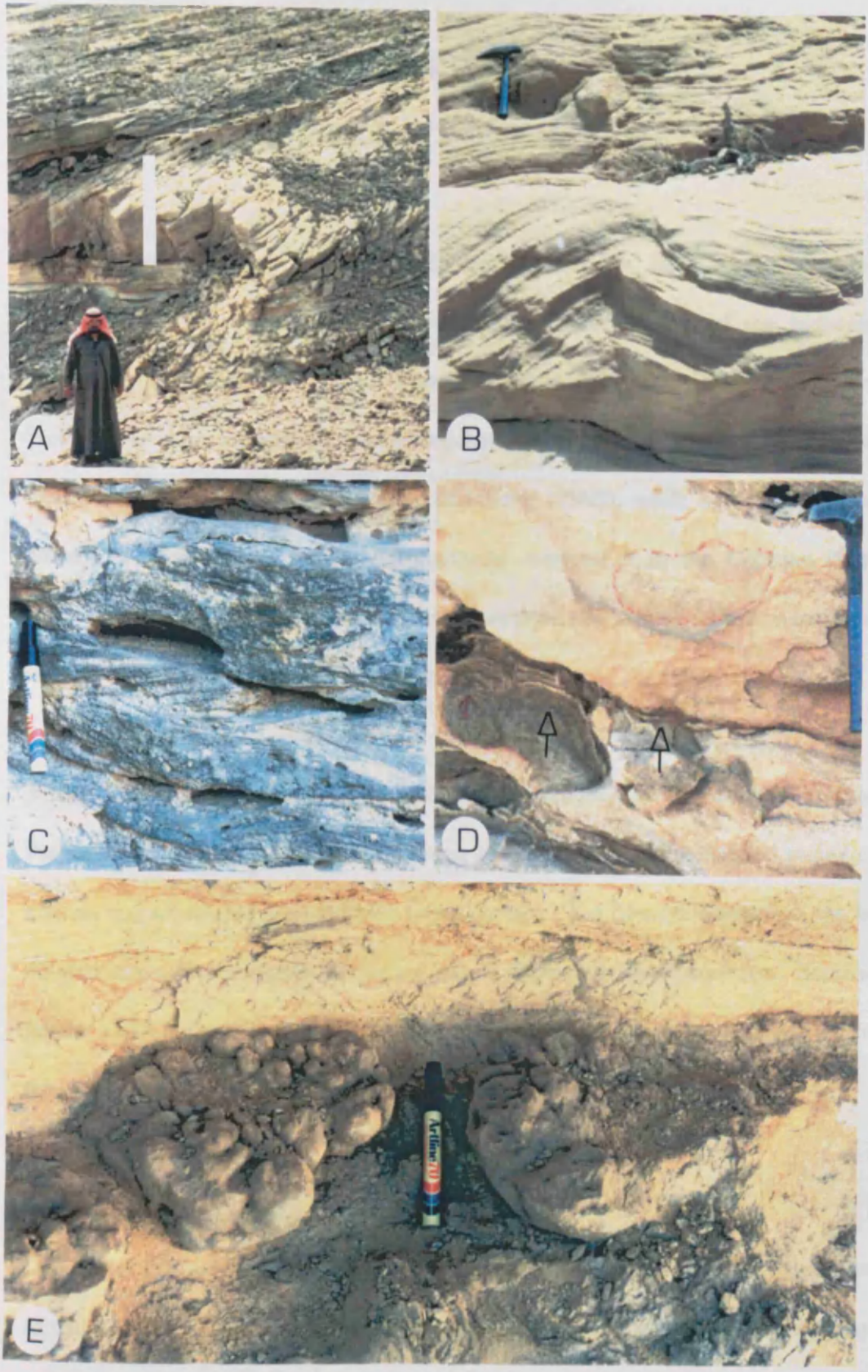
A
B
C
D
E

CHAPTER III

THE MUSAYR FORMATION

The Musayr Formation was informally named after the Jabel Al-Musayr area southeast of Maqna (Plate 1). Motti and others (1983) described the sequence (excluding the gypsum) as Lower Miocene, and as comprising reef and sub-reef facies. The same succession was subsequently recognized by Clark (1985) as the Musayr Formation. However, Purser and Hotzl (1988), while agreeing that the Musayr Formation was marine, provisionally assigned it to the Chattian (Late Oligocene). The present limestone outcrops are generally located on basement highs like Jabel Al-Musayr (the type locality).

The formation (Fig. 3.1) rests unconformably on both the Sharik Formation and the Precambrian. Deposition followed a tilting of about 30° and an extended period of erosion and represents a remarkable facies change. The Musayr Formation can be divided into a lower gypsum sequence and an upper limestone sequence. Because similar thick gypsum (evaporite) deposits also appear higher in the succession, the Musayr gypsum is commonly referred to as the lower gypsum.

3.1 THE MUSAYR GYPSUM

Deposition of the Musayr gypsum probably spans the interval from late Oligocene to early Miocene (Motti *et al.*, 1982). The angular unconformity which forms the

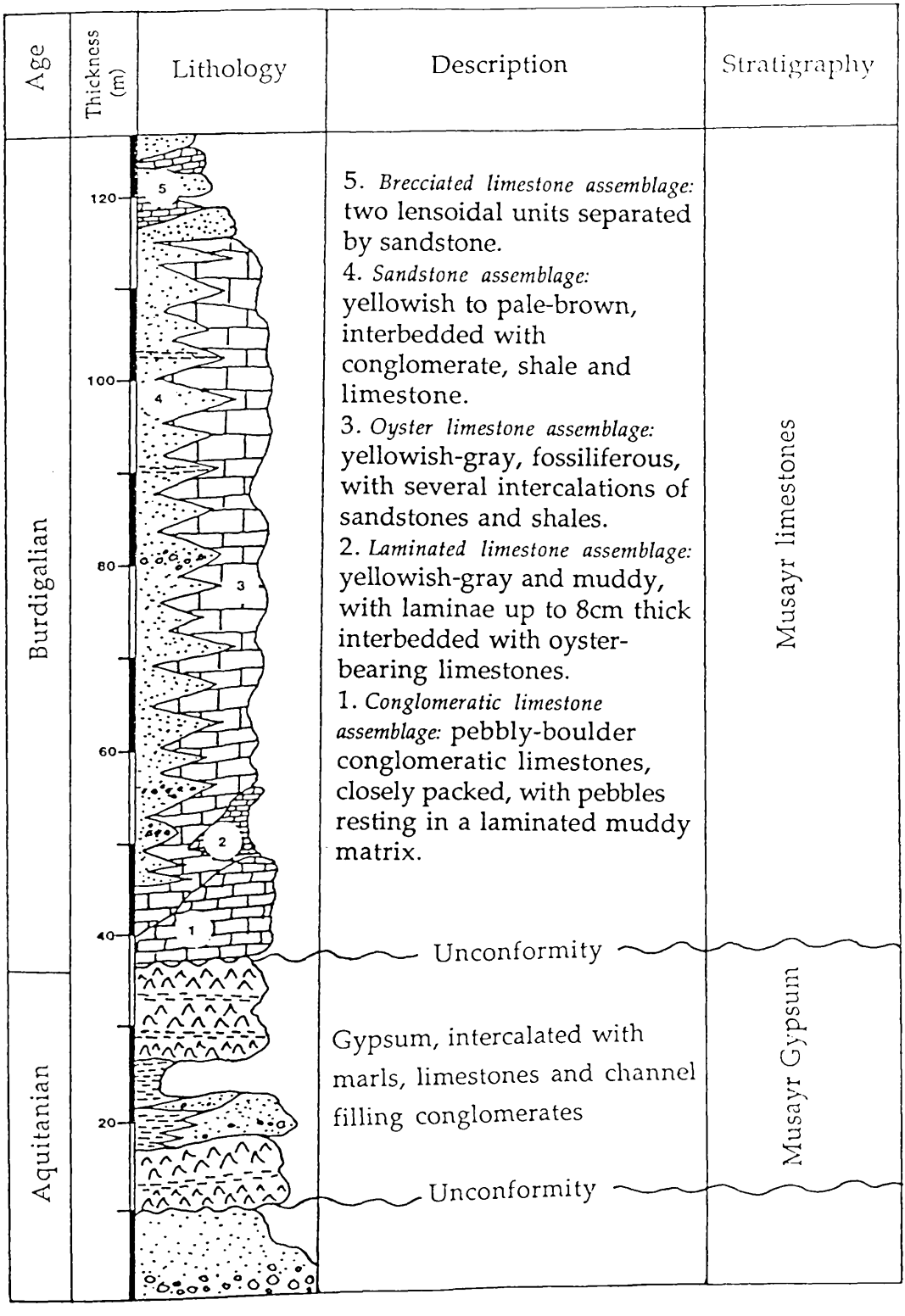

Figure 3.1 Generalized log section for the Musayr Formation (see plate 2 for explanation).

lower boundary is seen in several localites parallel to the northern edge of Jabel Tayran, as in location K (Fig. 3.7-A). The gypsum has been interpreted by Zakir (1982) as having been deposited in a relatively deep-water basin. However, Purser and Hotzl (1988) suggested that it marks a transition between an older, and in their view continental sequence, and a more marine environment. The gypsum may represent beds laterally equivalent to the evaporite diapirs of the northern Red Sea bathyal zone recognized by Mart and Ross (1987).

In the Maqna area, the gypsum unit is distributed as a series of limited outcrops represented by a narrow L- shaped belt north and west of Jabel Tayran. These are more extensive on the northern side of Jabel Tayran (Fig. 3.2). The thickness of the sequence varies from few meters up to a maximum of 40m in locality M in the central part of the area (Plate 2).

The gypsum unit is white and commonly laminated at the base but is apparently coarsely crystalline and massive at the top. In some areas it splits into two or even three subunits (location K). In these locations there may be intercalations of thin beds of greenish-gray marls or aphanitic limestones and laminated calcareous fine sandstones, or, less frequently, massive coarse to pebbly sandstones (localites 1J & KK). However, the bulk of the unit is massive. The upper surface is commonly eroded, probably as a result of subaerial dissolution and the gypsum has been removed from large areas.

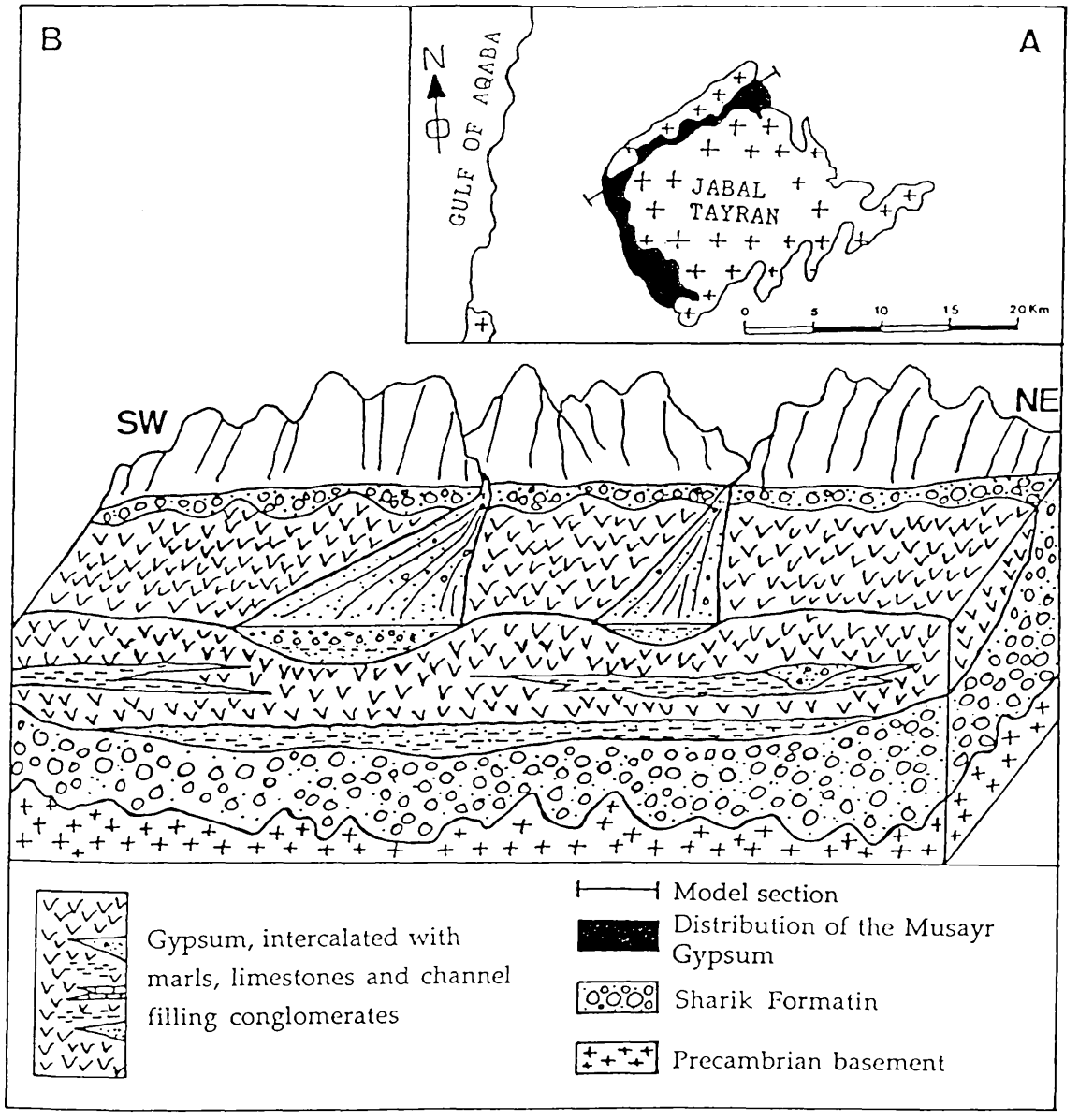

Figure 3.2 Schematic diagram showing: (A) the distribution and limit of the Lower Musayr Gypsum, and (B) a model section along the northern side of Wadi Al-Hamd (NE-SW) indicated on (A).

Thin bedded (5cm) friable shales, greenish-gray to yellowish marls and limestones are intercalated with the gypsum. Shale units like these form in a wide range of environments. The greenish-grey colour may reflect deposition in relatively reducing conditions. These would decrease the Fe^2/Fe^3 ratio, causing a progressive shift in color from red to yellow and finally green (Weaver, 1989). No structures are present but the fine-grained nature of the sediments presumably indicates deposition in a low energy environment. Locally, in location KK, up to 12m of shaley and sandy beds are intercalated with the gypsum.

The sequence in locations 2J & M consists of two gypsum units separated by a marly unit. Locally, the top of the lower gypsum is an eroded surface overlain disconformably by the marl. In location 2J a channel-filling conglomerate, up to 0.5m thick, cuts the top of the marly unit. This consists of well rounded pebbles up to 6cm diameter of limestone and sandstone but also includes angular fragments derived from the marly unit itself. The marl is overlain disconformably by the second gypsum.

3.1.1 PETROGRAPHY

The gypsum is of high quality, and diagenetic gypsum is represented in several patches by pure transparent crystals up to 0.2m diameter, as around location J. Radial crystal growths several centimeters in diameter are recorded at locality 1J (Fig. 3.7-B).

In thin sections the gypsum consists mainly of fine-coarse anhedral crystals 40-180μm diameter forming laminae intercalated with finely crystalline dolomite which is hard to resolve under the normal microscope. Under CL dolomite laminae are seen to be made up to 5μm diameter crystals of planar-s (hypidiotopic) dolomite. These have dull luminescent centers and bright outer zones, reflecting changes in Fe and Mn contents. The dolomite is best described as penecontemporaneous to the evaporites, formation occurring pre-lithification.

Within the gypsum layers, coarse radial crystals contain relics of coarse (120μm diameter) anhedral crystals of anhydrite which indicate neomorphism. The anhydrite typically shows a dull blue luminescence in CL, but the colour is impersistent and fades rapidly. Neomorphism was probably related to the hydration of the anhydrite following penetration by surface waters and release of pressure (Adams, 1944). Fractures and pore spaces are filled by later gypsum cement consisting of anhedral crystals up to 50μm across formed under subaerial conditions. There is a notable absence of dolomite intercalations.

Some of the intercalated limestones are dolomitized. They were deposited as peloidal muddy sediments containing scattered bivalve shells. They include scarce (<1%) fine detrital grains, angular quartz fragments, opaque minerals and phosphatic (bone) fragments. This association of peloidal muddy sediments was referred by Evans (1970) to lagoonal (subtidal to lower intertidal) environments.

Dolomitization of the limestones has produced non-planar crystals 20-50μm diameter. Under CL, these have a relatively uniform dull luminescence with brighter rims. These dully luminescing crystals have higher Fe^{2} and Mn^{2} contents and are thought to have precipitated from reducing pore waters (Barnaby and Rimstidt, 1988; Tucker and Wright, 1990). Some dolomite crystals have bright and dull subzones related to syntaxial overgrowths which are secondary (Fig. 3.8-A). These are of later origin forming in a shallow, burial environment subject to fluctuations in pore water chemistry (Ward and Halley, 1985). In some areas crystal faces are corroded and have been subject to dissolution. The overlying cement is a blocky sparry calcite with crystals 120-200μm diameter. This occurs mainly within pores formed in dissolved bioclasts. It shows early dark and later bright luminescence zones.

Micro-fractures within the limestones reflect shear movements related to the regional faulting system which operated in the area. Many are coated with iron oxides.

3.1.2 DISCUSSION

The Musayr gypsum is characterized by the several intercalations of limestone evaporites and siliciclastic sediments which strongly support a near-shore environment.

3.1.2.1 ORIGIN OF EVAPORITES

Evaporites are rocks composed of minerals that form by precipitation from concentrated brines. The usual source for evaporite deposits is seawater, but saline ground waters are responsible for many smaller evaporites in continental settings.

There are three general environmental settings where evaporites occur, continental, marine marginal (*sabkha*) and subaqueous (Fig. 3.3). The last can be subdivided into shallow and deep basinal models.

(1) CONTINENTAL EVAPORITES

Continental evaporites commonly contain sodium carbonates such as trona, or sodium sulphates (such as miraabilite). such evaporites are associated with alluvial fan and fluvial deposits, aeolian sediments, caliche and lacustrine carbonates (Kendall, 1984) but only make up a small proportion of the total facies assembly. With the exception of lake-deposits, which are commonly laminar continental evaporites typically form within existing sediments and are therefore commonly nodular.

(2) MARINE-MARGINAL EVAPORITES

The marginal marine evaporite deposits form within a granular framework consisting of worked shallow marine sediments, with binding algal mats and, to lesser degrees, continental sediments (Schreiber, 1989). The marine components may include carbonate sands (skeletal remains, ooids, and pellets), carbonate muds, and siliciclastic sands and muds. In addition, there may be a number of organisms associated. These include filamentous algae forming stromatolites and a few species of salt-tolerant bivalves, gastropods, crustacea and insects which occupy the wetter portions of shore areas and tidal channels.

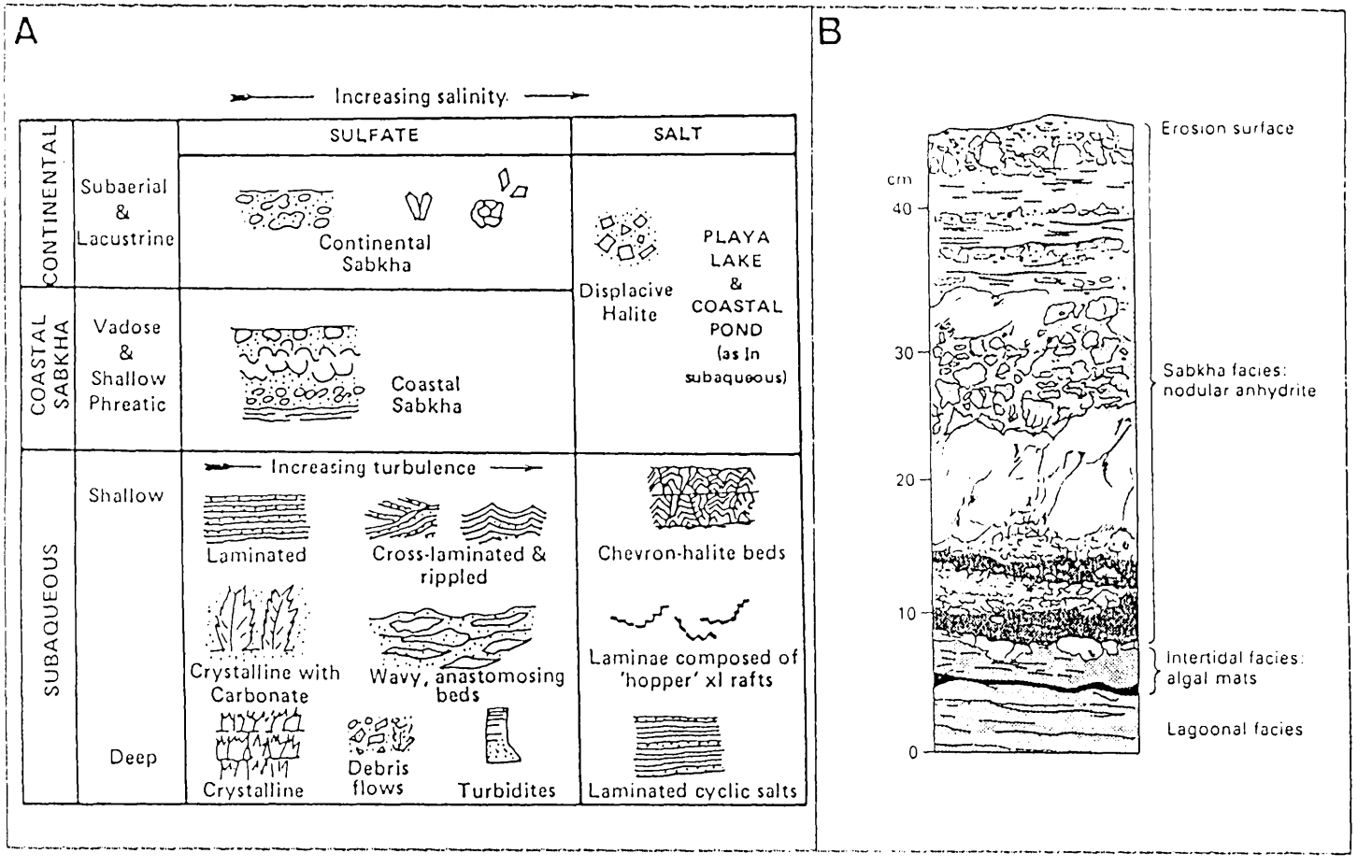

Figure 3.3 A_Summary of the physical environments of evaporite deposition an the main facies present (Schreiber *et al*, 1976&Kendall, 1984).B_ A complete sabkha cycle in the Lower Purbeck beds of the Warlingham borehole (Schreiber *et al*. 1976).

Schreiber (1989) pointed out that most sabkhas form under conditions of marginal to normal or near normal saturation. They must, perforce, pass laterally into marine sediments, often within quite a short distance. Since the sabkha accretes laterally a rise in sea-level will generate a cycle from lagoonal to supratidal deposits. The tops of sabkha cycles are usually truncated by a deflation surface. This may be followed by continental accumulation or revert to the subtidal marine deposits of next transgressive cycle (Shearman, 1978).

Gypsum and halite may form in surficial ponds and in restricted lagoons, and these deposits are then incorporated into the sabkha complex. the gypsum is sporadically converted to anhydrite, commonly resulting in beds of amorphous, nodular anhydrite. Gypsum may also be formed as a through-growing gypsum cement, developed within bottom sediments of rapidly drying pools and blowouts. Such nodular horizons are laterally extensive and may be associated with predominantly laminated sequences correlated with the algal mat stromatolites of the tidal margins. Associated carbonate sediments are commonly dolomitized.

(3) MARINE-SUBAQUEOUS EVAPORITES

Evaporites may develop in saline water bodies of any depth and are interpreted on the basis of their chemical composition and sedimentary structures. Shallow water facies, are chemically nearly identical to those which accumulate in deep-water, but contain very different sedimentary features. The general characteristics of these models are shown in figure (3.4).

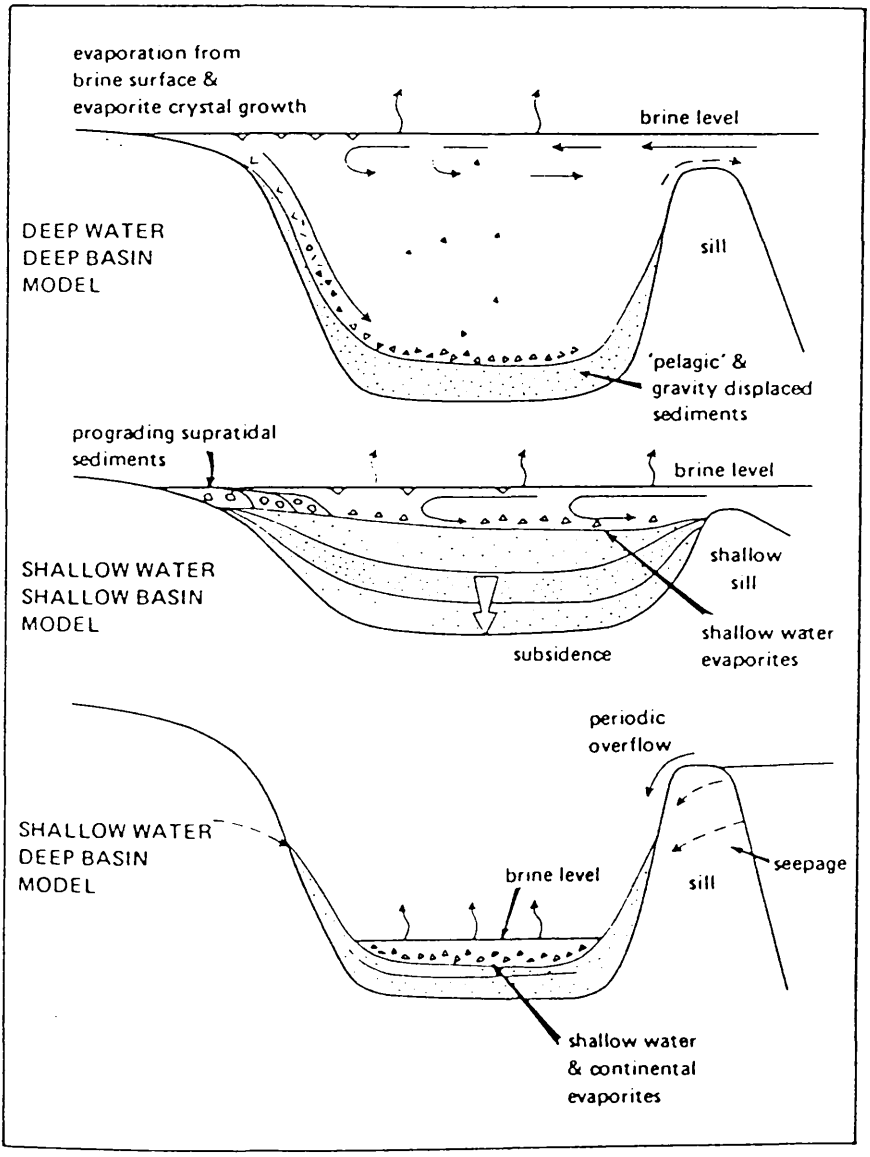

Figure 3.4 Depositional models for subaqueous evaporites (Kendall, 1984).

A. *Shallow water* evaporite facies

Shallow water evaporites have a distinctive suite of sedimentary structures. In shallow, photic-zone water, in situ algal structures (stromatolites) may be present. However, cross-bedding and ripples may occur in sediments which consist almost entirely of sulphates or halites. Erosion surfaces, and channels, together with desiccation surfaces and edgewise conglomerates, suggest lowered water levels and temporary exposure. Fossils may provide evidence of the proximity of open marine conditions. Bedding planes with karst development may indicate uplift and erosion. Examples of shallow water evaporites havebeendescribed from the Miocene of the Mediterranean (Vai & Ricci Lucchi, 1977, and Garrison *et al.*, 1978).

Kendall (1984), suggests a number of characters which he regarded indicating shallow water conditions:

1- Laminated sulphates consisting of current-deposited carbonate micrite and clastic gypsum particles. These may be either reverse or normally-graded laminae.

2- oriented growths of coarsely crystalline, selenite gypsum crystals formed as primary bottom growths, are mostly of very shallow water origin.

3- Halite, occurs in at least three facies, as detrital grains, as crusts, some of which form chevron bottom growths, and as crystals that grow displacively in pre-existing sediments.

B. *Deep water* evaporites facies

The deep-water model was introduced by Shmalz (1969) and assumes the presence of a deep basin, separated from the open sea by a shallow sill in favourable climatic conditions. All ancient, supposed deep water evaporites are characterized by their continuity, both vertical and horizontal. Most deep water deposits are thin-bedded to laminar. The thickness of units varies from tens to hundreds of meters and deposits can typically be correlated over tens to hundreds of kilometres. Resedimented deposits, (turbidites) may be present and these require considerable relief for their development. The sediment in these initially accumulates in the shallow portion of the basin. Clastic evaporite intervals interpreted as slump, mass-flow and turbidity-current deposits (which may include laminae, cross-bedding and ripples) are interbedded with deep water laminate evaporites or with non-evaporite sediments.

Kendall (1984), drew attention to three currently accepted and competing depositional models for basin-centre evaporites, which were originally compared with the deep-water model of Schmalz (1969). These models were described and discussed by Stewart (1963), Hsu (1972), and Kirkland and Evans (1973). The three models are: 1) deep water deep basin, 2) shallow water shallow basin, and 3) shallow water deep basin (Fig. 3.3).

(1) *Deep-Water Deep-Basin* Model

The model is founded upon the evidence that many of the giant evaporite basins of the world were deep topographic depressions. Evidence of this comes from: the comparison of the rate of evaporite deposition to possible rates of basin-floor

subsidence, and from palaeographic reconstructions. An example is the Zechstein (Permian) of Germany (Schmalz, 1969).

(2) *Shallow-Water Shallow-Basin* Model

The shallow water, shallow basin model accounts for the sedimentological and geochemical evidence of shallow water and/or subaerial depositional environments in basin-centre evaporites. An example of this model is seen in the Windsor (Mississippian) evaporites of the Maritime province of Canada which accumulated in a narrow graben (Evans, 1970).

(3) *Shallow-Water Deep-Basin* Model

This model was developed to account for pre-existing deep basins that become filled by evaporites with internal evidence for shallow water and/or subaerial depositional environments. The well known examples of this model are the Miocene Messinian evaporites of the Mediterranean (Hsu *et al.*, 1973). Here, after complete desiccation, the floor of the basin in which the major bodies of evaporite formed must have lain one or more kilometres below sea-level.

3.1.2.2 INTERPRETATION

Introduction

The evaporite outcrops of the Musayr Formation are distributed in a series of limited exposures represented by a narrow L-shaped belt north and west of Jabal Tayran (Plate 1). These show a number of distinctive features:

1. The gypsum is commonly laminated at the base, but is apparently coarsely crystalline and massive towards the top.
2. The intercalated sediments are, marls, peloidal limestones,and sandstones.
3. The associated limestonesaredolomitized but were deposited as peloidal muds. Some contain remains of bioclasts such as bivalves and gastropods.
4. There are scattered patches (up to 0.2m diameter) of pure transparent crystal growths of gypsum (selenite), and radial crystal growths (up to 5cm diameter) within the finely crystalline gypsum.
5. At least two surfaces of erosion are recognized, one at the top of the upper marly unit (locality M) and, the other at the top of the gypsum unit (Locality K).

The Depositional Environment

The Musayr Gypsum outcrops are composed of the following sequences:

1. *Non-evaporite.* Thin beds of greenish-gray marls, aphanitic limestones and laminated calcareous fossiliferous sandstones, or less frequently massive coarse-pebbly sandstones are intercalated with the sulphate deposits (localities IJ & KK). Most of these presumably indicate deposition in low energy environments. However, the sandstones may be interpreted as storm deposits formed when evaporitic tidal flats were flooded by sediment charged water (Kendall, 1984). the lack of algal mats (stromatolites) could be related to the presence of active currents because stromatolities commonly grow in protected, shallow water environments (Kendall, 1984).

2. *Evaporites*. Consist mainly of gypsum, with a laminated base which is likely to have been deposited in a shallow subaqueous environment. This may compared with to the lower part (lagoonal facies) of the Lower Purbeck beds of the Warlingham bore-hole which have been interpreted as a sabkha cycle (Fig. 3.3). Towards the top the growth and accumulation of gypsum crystals is attributed to precipitation in marginal water bodies (Kendall, 1984). Vai and Ricci-Lucchi (1977) describe similar massive gypsum beds (up to 35m thick in the Messinian of the northern Apennines (facies 1-4), and interpreted these facies as having formed in shallow water on the margin of the basin. The abundance of the gypsum rather than other evaporites, may related either to ionic concentration, to a higher temperature or to unlikely presence of a small amounts of dissolved organic components (Cody & Hall, 1980).

3. *Subaerial*. Deposition of the Musayr evaporite was terminated by a relative fall in sea-level. The top surface of the gypsum has been eroded. A channel-filling conglomerate cuts the top of the marly unit intercalated within the evaporite sequence in locality M and the unit has been entirely removed from large areas.

The lower Musayr Gypsum sequence was deposited within a restricted marine coastal inlet formed using movement along the left-lateral Arabian Wrench Fault. These movements produced a rapid fall in sea-level which is indicated by the abrupt facies changes from the fan-delta deposits of the Sharik Formation to the Musayr Formation.

The Musayr evaporite sequence consists of lagoon evaporite facies. It began with the deposition of non-evaporite tidal flat deposits, and continued with a build-up of evaporites from thin-bedded to more massive gypsum deposits which seem to reflect a change to deeper water *i.e.* a shallow lagoon. subsequently exposed to subaerial conditions.

Thus, the deep water evaporite facies suggested by Kendall (984) and the deep-water model of Schmalz (1969) are not applicable to the Musayr gypsum. Once shoreline regression occurs, evaporites are deposited in the upper part of the marine sediment wedge, and dolomitization of associated fine grained carbonate sediments ensues. Dolomitization releases calcium ions which are available for precipitation by the interstitial pore fluids as additional gypsum or anhydrite (Kinsman, 1969). Dolomitisation by marine or hypersaline waters, was followed by recrystallization and then selective dissolution in meteoric or hydrothermal fluids (cf. Conglio *et al.*, 1988). The last may have resulted from the involvement of hydrothermal solutions associated with the rifting which formed the Red Sea.

The abrupt facies change from the fan-delta deposits of the Sharik Formation to the gypsum-depositing shallow water lagoons of the Musayr Formation, together with the local unconformities within the gypsum unit, are indicators of rapid relative falls in sea-level. The gypsum sequence was deposited within a restricted marine coastal inlet formed during uplift movements along the left-lateral Arabian Wrench fault. These movements produced a rapid fall in sea-level which brought shallower water and the deposition of shallow lagoonal sediments with the subsequent formation of

gypsum. In arid and semi-arid areas, high evaporation produces hypersaline conditions, but salinity may fluctuate dramatically as a result of increased input of freshwater during wet periods or of marine waters during storms (Elliott, 1989). It is thought that the erosion of the gypsum was a result of events of this kind rather than sea-level change or uplift.

3.2 THE MUSAYR LIMESTONES

The Musayr limestones are represented in the Maqna area by a variety of carbonate rocks and intercalated calcareous sandstones. All are typically light colored, yellowish to gray, and reflect shallow marine (shelf) environments. The limestone sequence unconformably overlies the Musayr gypsum sequence, overlapping to rest on the Sharik Formation and locally lying directly on the Precambrian basement, as reported by Clark (1985). It clearly reflects an important marine transgression.

Purser and Hotzl (1988), noted that the Oligocene transgression in the Maqna area covered only the axial part of the graben while erosion or coarse clastic sedimentation took place along the margins. This general distribution of facies was repeated during the Miocene.

Outcrops of the Musayr limestones are concentrated in the central part of the area where they form the cap of Jabel Hamza. Here the most complete profile is exposed, with a thickness of 80 meters in location T, considered as the type section (Plate 2). Outcrops are distributed in several other localites within the study area, and variable thicknesses, sometimes of only a few meters, are associated with abrupt

lateral passage to sandstones and conglomerates. The base is clearly defined above the lower gypsum, but where this is absent and the unit overlies the Sharik Formation, siliciclastic materials gradually change to the Musayr limestone facies and the boundary is not always apparent.

Several lithofacies assemblages are represented, and the Musayr limestone sequence as a whole is characterized by lateral variations in thickness and lithology. The boundaries between lithofacies assemblages are commonly gradational.

3.2.1 STRATIGRAPHY AND PETROGRAPHY

Five lithofacies assemblages are distinguished within the Musayr Limestone sequence. These are:

1. Conglomeratic limestone
2. Laminated limestone
3. Oyster limestone
4. Sandstone
5. Brecciated limestone

They overlie the eroded surface of the Musayr gypsum, overlapping to rest unconformably on the Upper Pale-Brown unit of the Sharik Formation in locations K1, K2 and Y, and the Precambrian basement in location H. Rapid vertical and lateral facies changes are related to a pre-existing topography defined by faulting (Fig. 3.5). The distribution of the lithofacies assemblage units is shown in Plate 2.

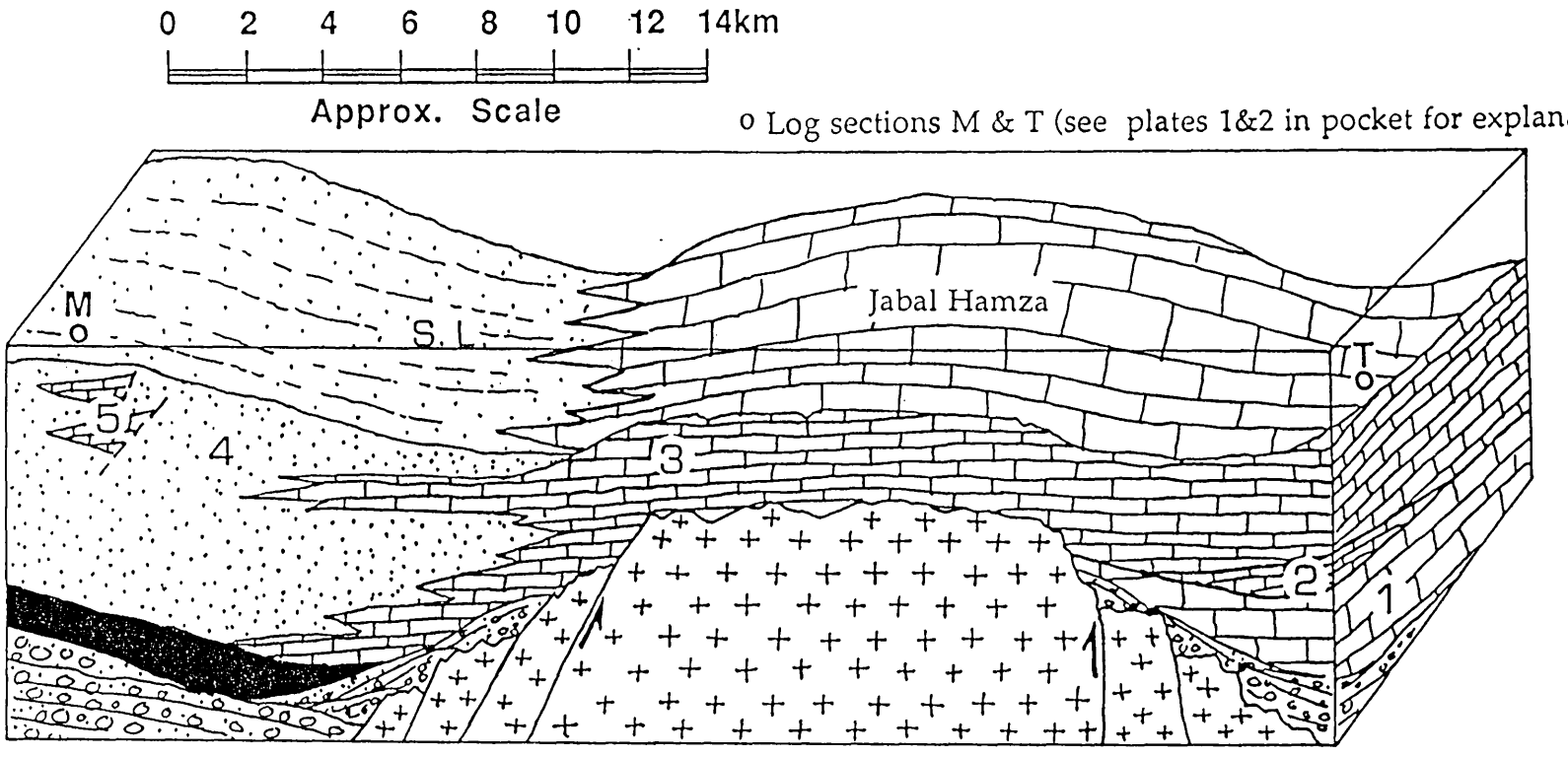

Figure 3.5 Diagrammatic model showing the relationship between the Musayr limestone assemblages: 1) Conglomeratic Lst, 2) Laminated Lst, 3) Oyster Lst, 4) Sandstone, and 5) brecciated Lst.

3.2.1.1 CONGLOMERATIC LIMESTONE ASSEMBLAGE

This is a sequence 1-20m thick, of pebbly-boulder conglomeratic limestone, showing a lateral gradational relationship with the oyster limestone assemblage. In general the thickness decreases from south to north, where Wadi Al-Hamd represents the final limit of the facies. The distribution of the conglmerate is controlled by the raised structures (horsts) of the central area.

In Jabel Al-Musayr, the type locality of the Musayr Formation, the 20m of limestone strata exposed consist entirely of this sequence. Jabel Al-Musayr is defined by west-northwest, north- northeast, and east-west faults which were doubtless responsible for its up-lift as a horst (Vial, 1978). A north-northwest fault splits the conglomeratic limestone into eastern and western outcrops and is thus relatively young. There is an unconformable contact with the basement in the eastern outcrop (Fig. 3.7-C). While to the west there is simply a discordant contact with a conglomeratic sandstone bed (pebbles 20cm max. diameter) 0.5m thick provisionally assigned to the Sharik Formation. This is important in placing some fault movements as later than the Sharik and earliar than the Musayr Formations.

The base of the assemblage, is formed by a laminated bed up to 1 meter thick of finely crystalline dolomite. Above this, the conglomeratic limestone includes boulders up to 1m maximum diameter, closely packed but resting within a muddy laminated matrix. These are also dolomitised but were originally of muddy peloidal limestone with scarce angular detrital quartz grains <0.25mm diameter. Dolomite crystals in the boulders are <1μm diameter. Those in the matrix consist of planar-s

crystals 10-30μm diameter but both are characterized by a uniform dull luminescence in CL, suggesting that they were dolomitized at the same time. Other dolomite crystals, forming a cement lining fenestral vugs in the matrix, consist mainly of planar-e crystals of 60-110μm diameter which under CL show dull centers but bright outer zones. Dissolution has affected these and etched surfaces are coated with iron oxides. Overlying them a sparry calcite cement consists of equant crystals 70-120μm diameter. These show two distinct generations under CL, an early dull, and the later non-luminescent with bright rims. The matrix in addition, shows mineralization, with replacement by rhodochrosite, forming euhedral fibrous pinkish crystals, by barite forming white bladed crystals, and enrichment with iron and manganese oxides. The barite and rhodochrosite probably formed after the calcite spars were deposited but no direct relationship has been seen. The oxides are almost black and scoriaceous and occur as an impregnation of crystalline dolomite and as fracture fillings. The most recent cement consists of gypsum, forming coarse anhedral (120μm diameter) crystals filling secondary pores.

On the southern side of Jabel Tayran, in location Ms, conglomeratic limestone assemblage is represented by only 8m of conglomeratic limestone. This rests unconformably on the Upper Sharik Formation and shows a gradational transition to oyster bearing limestone (oyster limestone assemblage) towards the top. The boulders are 1.5m maximum diameter and are again packed in mutual support. They have similar characters to those of Jabel Al-Musayr, but rest in a fossiliferous muddy matrix (Fig. 3.7-D) a slightly bioturbated bioclastic packstone. This contains fossils such as foraminifera, coralline algae and molluscs including the dominant oyster

bioclasts. Some bioclasts have dissolved and two types of sparry calcite cement are visible under CL within the resulting pores. These are, an early dull fibrous cement, with crystals 50um long & 10um wide, and a later non-luminescent fibrous cement (crystals 80um long & 20um wide). Both are overlain by colloform silica and mega-quartz cements (Fig. 3.8-B).

In location T, 3Km to the east of location Ms, the conglomeratic limestone is only 3 meters thick. Here, the boulders are completely dolomitised, and are predominantly derived corals (*Porites*). These are 40cm maximum diameter and show extensive borings, including sponge and *Lithophaga* borings, on their outer surfaces (Fig. 3.9-A). The matrix in which they rest is a bioturbated packstone. Within it notable micrite cement could be of originally marine, coated walls of bioclasts with dull luminescence in CL. A spar cement of equant 150-280μm diameter calcite crystals occurs filling vuggy porosity. Under CL, this shows three generations, an early bright zone followed by multiple subzones (4 dark-bright cycles), and a later non-luminescent zone which overlies a prominant dissolution surface.

On top of Jabel Amrah, in locality N (southwest of locations T & Ms), conglomeratic limestone assemblage is at least 20 meters thick. Here, the base of the sequence is formed by a laminated calcareous sandstone 1.5m thick. The upper half of this is convoluted. It is overlain by 0.3m of pebbly conglomeratic limestone (pebbles 3cm max. diameter) which forms the base of the overlying limestone conglomerate.

The boulders here are up to 0.8m maximum diameter and are also dolomitized. They were probably originally of fossiliferous wackestone, including bivalves and foraminifera. The dominantly dissolved bivalve clasts are filled with a later calcite cement. Scarce detrital grains (quartz & feldspar) and bone fragments are present in the matrix which is largely dolomitic. In some areas dolomite crystals are calcitised, indicated in thin section by the presence of relic rhombs, outlined by staining of the former crystals by iron oxides within coarse calcite. A blocky sparry calcite cement with crystals (70-180μm diameter) overlying the calcitized dolomite has occluded the pores. Under CL this shows two generations, an early phase of multiple growth zones (up to 5 dull-bright cycles) with two separated nuclei. This was partially dissolved before deposition of a non-luminescent cement.

The enclosing sediment is largely dolomite, consisting of non- planar crystals <3μm in diameter. These show a uniform dull luminescence under CL, but has bright equant sparry calcite cement crystals up to 50μm diameter filling intercrystalline pores (Fig. 3.8-C). Some dolomite crystals float within the micrite matrix suggesting replacive growth which could be related to subaerial exposure (Esteban and Klappa, 1983). Large fibrous crystals (1.2 x 0.3 cm) of rhodochrosite are present as a late vein filling. These are non-luminescent under CL. A late gypsum cement partially fills residual pores with anhedral crystals up to 80μm across. As a result of increased compaction a number of stylolites are present.

In addition to these minerals visible microscopically XRD analysis of the muddy matrix indicates the presence of illite and halite. Illite forms authigenically under

a wide variety of conditions, and diagenetic illite is formed over a large range of depths (Lee *et al.*, 1985). The main requirements for formation appear to be a source of K, which is commonly external, and an elevated temperature, 96 to 136C (Weaver, 1989). Weathering of the Precambrian basement could provide a potassium source here.

The halite may form a cement may precipitated as a result of recent surface weathering.

Along the western edge of Jabel Tayran the conglomeratic limestone assemblage is absent in locality KK but increases in thickness towards the south in localities KK1, KK2, KK3 & KK4. In these localities thicknesses are from 2 to 10 meters, and the facies is characterized by gradational interclations to calcareous sandstone, fossiliferous grainstone and oyster-bearing limestone. The oyster limestones form beds up to 20cm thick and fill fissures up to 0.5m wide cutting the matrix enclosing the boulders (Fig. 3.9-B). The fissure fillings could be early, synsedimentary, remobilisation structures formed close to the paleo sediment-water interface. They express periodic instability which is best explained by repeated earthquake shocks associated with Red Sea rifting (cf. Plaziat *et al.*, 1990).

The boulders in this locality were originally a bioclastic packstone and some have their outer surfaces bored by *Lithophaga*. Bioclasts within the boulders include bivalves, gastropods, coralline algae and benthic forams. Other allochems include pellets, ooliths and intraclasts. The matrix contains burrows filled with pelloidal

carbonate mud, and scarce sand size subangular detrital quartz and feldspar grains. Vuggy and mouldic porosity occurs within the boulders mainly as a result of dissolution of the bioclasts. The sparry calcite cement formed within this includes two separate generations recognized under CL. These consist by two blocky crystals 60-130μm diameter comprise an early bright and a later non-luminescent zone, and affected by separate phases of dissolution. Overlying the calcite, quartz occurs as colloform chalcedony and as mega-quartz which, according to Milliken (1979), develops at a temperature of <40C in fluids derived from meteoric water.

The matrix surrounding the boulders is a bioturbated fossiliferous packstone. The burrows resemble *Chondrites*. Bioclasts are similar to those within the matrix of the boulders themselves, but some are again broken as a result of mechanical compaction. Other grains include scattered honey-yellow grains of glauconite and monocrystalline quartz, mostly in fine-medium angular grains. Algal coatings (oncoids) on fossil fragments may indicate that deposition was slow and that the sediment remained on the surface of the sea floor for a long time. According to Gall (1983), oncolites form above wave base in a high energy environment where fine-grained particles are winnowed out. Their presence in a muddy matrix suggests that they have been derived. The calcite cement present within matrix bioclasts shows three separate generations under CL. An early dull micrite cement, followed by two blocky calcite 80-170μm diameter crystals as first bright which were subjected to dissolution during subaerial diagenesis and the later non-luminescent cements.

3.2.1.2 LAMINATED LIMESTONE ASSEMBLAGE

This assemblage is represented by laminated limestones scattered around Jabel Hamza. These are yellowish-grey and fine grained with laminae up to 0.8cm thick. The total thickness of the unit is up to 5.5m in locality T where it consists of two laminated limestone sequences with an intercalated oyster-bearing limestone.

In locality T the base of the 2m thick lower laminated sequence is bioturbated. Above the laminated sequence 1.5m of oyster bearing limestone includes 10cm of finely crystalline dolomite. At the top this has a 20cm band of concentrated oyster shells. The upper laminated limestone above is also bioturbated at the base but is cut by a channel 20cm deep filled with oligomictic conglomerate. This has a sandy calcareous matrix and includes fragments 4cm across of granite, chert and reworked oysters.

In thin section the laminated limestones are fossiliferous wackestones. The muddy matrix contains scattered angular detrital quartz grains and the fossils are bivalves and gastropods, some of which have been dissolved. A sparry calcite cement has occluded pore spaces within them. Under CL, this comprises a dull fibrous zone, with crystals 200μm long, followed by four separate generations of blocky 70-250μm crystals. The first of these is bright, the second non-luminescent, the third a multiple-zone with 4 cycles of bright and dark sub-zones, reflecting rapid changes in pore-water chemistry, and the last zone non-luminescent (Fig. 3.8-D). Inter-phase dissolution occured between the first and second blocky zones. Scattered idiotopic

dolomite crystals <5μm diameter occur within the micrite matrix and replacing bioclasts. These have a uniform dull luminescence under CL.

On the northern edge of Jabel Hamza, in locality K1, 2m of laminated limestones occur at the top of the Musayr succession. These are bioclastic packstones, characterized by large (up to 5mm long axis) foraminifera (*Nummulites*) and oyster shells, the last mainly concentrated in the upper 0.5m of the unit. The larger foraminifera characterize rock strata formed during a maximum marine invasion, being most abundant in shallow water marine deposits, and absent in brackish-water near-shore sediments or in evaporites (Moore *et al.*, 1952).

3.2.1.3 OYSTER LIMESTONE ASSEMBLAGE

The oyster limestones are thickest in the central area south of Wadi Al-Hamd, where they reach 70 meters in location T, but gradually decline elswhere. The limestones are dominantly yellowish to gray with several intercalations of sandstone and shale. The sequence is commonly of fossiliferous packstones characterized by the abundance of large oyster shells. Many of these retain both valves and it is likely that most were deposited in situ. Shells vary in size, but are large and some valves are up to 15cm diameter and 3cm thick. A high proportion are extensively bored by sponges and algae. The sequence is partially dolomitised and styolitic. Micro-structures in the form of broken bioclasts and fractured coralline algae with shear displacement occur within the dolomitised beds. These features reflect the later stages of mechanical compaction (Tucker and Wright, 1990).

On the southern edge of Jabel Hamza, in locality T, the oyster sequence consists of several beds ranging from 1 to 3.5 meters in thickness (Fig. 3.9-C). The dominant oyster shells are up to 15cm diameter, but the base of the succession shows a concentration of small shells of only 3cm diameter. Thin intercalations of bioturbated finely crystalline dolomite are concentrated in the lower 2m of the sequence and a conglomeratic limestone 4m thick occurs towards the top. The conglomerate consists of boulders of limestone, a few of 20cm maximum diameter, bored by *Lithophaga*. Generally, the oyster shells are scattered within a yellowish-white muddy matrix. They are associated in places with other bivalves, gastropods, corals, coralline algae, foraminifera, echinoderms and, less frequently bryozoa. Scarce subangular quartz and feldspar grains of variable sizes occur together with grains of glauconite, pyrite, iron oxide coated grains and opaques.

The micrite matrix of the oyster limestones is partially dolomitised. It is replaced by non-planar crystals of dolomite 20-40μm diameter. In CL these have dull or non-luminescent cores and bright rims. Vuggy, and less commonly mouldic, porosity is mainly related to the dissolution of shell fragments. An equant sparry calcite cement with crystals 30-70μm diameter has occluded these pore spaces and shows two luminescence generations under CL, an early bright zone, with a prominant dissolution surface forming its outer margin, is followed by a later non-luminescent zone.

Some corals collected from the unit near location T consist of sparry calcite with patchy replacement by non-planar dolomite crystals <20μm in diameter (Fig. 3.8-E).

The calcite is a cement, filling pores formed by the dissolution of the original aragonite of the corals. It is a blocky spar with crystals 40-120μm diameter. Under CL it shows an early dull zone with bright subzones terminated by a dissolution surface, overlain by a late non-luminescent zone. The dolomite crystals show non-luminescent cores and bright yellow-orange outer zones under CL.

On the western side of Jabel Tayran, in localities 1KK, 3KK & 4KK, the oyster limestone sequence is up to 5m thick. Here it contains abundant foraminifera, dominantly *Nummulites* and *Textulariina*. In location 3KK the base of the sequence is a fossiliferous pelsparite (bioclastic calcarenite) 0.5m thick which shows a gradual vertical increase in oyster shells. The increase in both abundance and diversity of benthic foraminifera indicates a shallow marine environment (Poag, 1981). There is a lack of dolomitisation within the sequence in this area.

In this central area south of Wadi Al-Hamd, a collection of corals from locality K1 were identified as: *Favites neugeboreni*, *Montastrea* sp., *Acanthastrea* sp., *Acanthastrea* cf. *echinata*, *Montastrea schweinfurthi* and *Lithophyllia michelotti*. This assemblage is clearly of Mediterranean origin and contrasts with the Indo-Pacific affinities of present day Red Sea faunas (B. R. Rosen, pers. commn. in 1989). The dominant forms are characteristic of lagoonal or intermediate depths rather than reef crest environments. A lagoonal or shallow shelf environment is more likely as they do not form any constructional coral frame.

Thin sections of corals selected from this collection indicate that, while some are wholly calcite, they are dominantly dolomitised. Some corals contain micrite trapped within their calyces and this contains benthic foraminifera and bone fragments and shows aggrading neomorphism (Fig. 3.8-F). Rare detrital grains (<1%), occur within surface depressions. These are mostly angular grains of quartz up to 0.15mm in diameter which have a blue luminescence under CL.

Spaces formerly occupied by coral septa have been filled by blocky crystals of slightly ferroan sparry calcite cement consisting of crystals 60-250μm in diameter. It is quite common to find that the late stage void-filling sparry calcite within former aragonite moulds is iron-rich (Scoffin, 1987). Under CL, two generations are recognizable, an early bright zone, truncated by a dissolution surface and a later non-luminescent zone. The terminal crystal faces have also been partially dissolved and are coated with iron oxides. Dolomite of planar-s cystals (40-90μm diameter), commonly replaced the trabecular aragonite walls of the corals. Under CL, these dolomite crystals have dull cores and bright rims. Euhedral dolomite crystals occur as void fillings. Some are up to 550μm diameter (Fig. 3.10-A), with multi-zoned syntaxial overgrowths which have been partially dissolved in the way which would be expected in the mixing zone where strata were subjected to subaerial conditions (Ward and Halley, 1985).

The sandstones which are commonly intercalated in the central area (locations K1, K2 and T) include low angle trough cross-bedding indicating current flow towards the east. They are often extensively burrowed, particularly towards their upper

margins, and some burrows resemble *Chondrites* (Fig. 3.9-D). In general, sandstones are medium grained, up to 1.5m thick, and gradually become more laminated and finer grained upwards. Notable patches of concentrated shelly debris occur within some which probably represent isolated winnowed accumulations.

3.2.1.4 SANDSTONE ASSEMBLAGE

This assemblage is well exposed along Wadi Al-Hamd where it reaches a thickness of 85m in locality K. It shows intercalations of conglomerate, shale and, less frequently, limestone. The sandstones represent the lateral shoreward counterpart of the oyster limestone sequence. The sandstone sequence includes channel-filling conglomerates but gradually fines upwards to siltstone and/or shale. Sandstones are yellowish to pale-brown in colour.

To the north of Wadi Al-Hamd, and mainly in the area to the east of locality M, a number of limestones near the top of the Musayr sequence are associated with pale-brown sandstones. The limestones are typically fine grained, dense and porcellanous but vary rapidly in thickness over short distances so that they form distinctive mounds several meters high. Among these, are mound-like structures packed with stick-like fragments which resemble the stags-horn varieties of *Acropora*. The surfaces of some of these appear to have been bored but do not have the calcareous algal encrustations which might be expected. These mounds are 1-2m high and extend laterally for 10 meters.

In the central part of the area, north of Wadi Al-Hamd, the sequence unconformably overlies the lower gypsum. Faulting and erosion of the gypsum occured before deposition of sandstones so that they locally rest on the basement. One fault, trending 240, which acted in this way lies east of location K. The sedimentological characteristics of different localities will be briefly described to simplify the overall view of this assemblage.

In locality Ra, on the northern side of Jabel Amrah, a series of small scattered outcrops consist of massive medium-coarse calcareous sandstones 4m thick and including thin layers of oyster shells, corals and stromatolites. The stromatolites, which occur at the top of the sandstone, are domical, cerebroid and branching shapes (Fig. 3.11-A), which point to deposition in an intertidal or shore-face environment (Gall, 1983). All of the stromatolites are partially or wholly dolomitized.

The dolomite crystals are of non-planar type (<3μm diameter) and show homogeneous dull luminescence in CL. The domical stromatolites have multi stage surface cavities filled with laminated micrite which shows areas of neomorphism to sparry calcite.

Several bands (<20cm thick) of fossiliferous packstone are intercalated in this sandstone outcrops. These contain bivalves, mainly oysters 2-4cm across, brachiopods, gastropods, ooliths (0.2-0.3mm diameter), intraclasts up to 1mm diameter, oncolites and fragments of encrusting coralline algae (*Lithothamnium*), *Halimeda* and a few benthic foraminifera, glauconite grains and bone fragments.

Detrital grains of quartz and feldspar (<3%) are also present. These are fine-medium grained (0.1-0.5mm diameter) and their angular to sub-angular shapes suggest a relatively short distance of transportation (Fuchtbauer and Elord, 1971). The quartz is mono-crystalline and the feldspar is dominantly microcline and plagioclase. XRD indicates that the packstones are dominantly calcite but also shows some replacement by dolomite.

Within these packstones a sparry calcite cement, consisting of blocky crystals (80-200μm diameter), has occluded vuggy and less frequent mouldic pores. Under CL, three generations of cement are recognizable. An early dull dolomitized fibrous cement is followed by two blocky cements, one bright and the other non-luminescent (Fig. 3.10-B). The bright blocky cement shows 5 cycles of dark and bright growth zones reflecting subtle changes in pore water chemistry during growth (Tucker and Wright, 1990).

In the northern part of the area, in Wadi Sek, in locations SA and 1P, sandstone assemblage is represented by a pale-brown sandy dolomitized unit up to 12m thick. Some of the dolomites contain sparse bioclasts which are dominantly of coralline algae, bivalves and echinoderms, but *Ostrea* and an external mould of *Pecten* have also been found in location SA. Detrital grains form <15% and include quartz, feldspar and rock fragments derived from sandstone, chert and aphanitic limestone. These vary in size with a maximium diameter of 1.5mm. The quartz grains are mono-crystalline, and commonly of subrounded shape. They are either of blue or dark-brown luminescence under CL, some showing authigenetic overgrowths.

Feldspar grains are of medium size and are of microcline, plagioclase, and perthite. Under CL detrital feldspar grains are typically blue or green while authigenetic overgrowths are brown. SEM (EDX) analysis shows some authigenetic K-feldspar crystals also formed within pore fillings.

The dolomite appears to have originally been a muddy peloidal sediment. It now consists of planar-s crystals 20-50μm in diameter showing uniform dull luminescence in CL, but crystals are sometimes partially calcitised. A blocky sparry calcite cement occurs within intercrystalline pores and mouldic pores representing dissolved bivalve shells. Crystals in this are 80-50μm diameter and under CL show two luminescence zones, an early bright and a later dark zone. SEM examination indicates that an authigenic smectite cement post-dates this blocky calcite (Fig. 3.10-C) and authigenic K-feldspar probably also formed relatively late.

In location K north Wadi Al-Hamd, the lower part of the sandstone unit consists of up to 20 meters of bioturbated friable sandstones, including medium to pebbly grains. The sandstones are poorly to moderately sorted, with the whole sequence fining upwards to siltstones which tend to be more resistant and are separated from overlying clastic sediments by 1.5m of limestone. The middle part of the sequence, shows at least six interclations of near-shore (coastal) channel filling conglomerates. These are each up to 2m thick and consist of well rounded pebbles (20cm max. diameter) of andesite, granite and aphanitic limestone. Less common are intercalated thin sheets of conglomerate but these are not more than 30cm thick. The unit

includes a prominant sandstone bed 0.5m thick showing low angle trough cross-bedding laminae dipping at 15, indicating flow towards the east.

The upper part of the sandstone assemblage in location K, has three intercalated limestones, with individual units up to 3m thick. The limestones are yellowish-grey bioclastic wackestones. They have relatively shaley bases which are commonly micro-styolitic as a result of late burial compaction. They are intensively biotubated in their upper parts. Bioclasts include bivalves, coralline algae, gastropods, corals and echinoderms. To the east, towards location M, the wackestones become matrix poor packstones. Thses contain up to 10% detrital grains. Quartz is dominant and subangular grains are 0.6-2mm maximum diameter. Feldspar grains are scarce, and are mainly angular orthoclase (simple twinning), and are of medium sand size, 0.8-1.2mm max. diameter. Small numbers of honey yellow glauconite grains are also present. These are probably the result of the alteration of detrital biotite (Kerr, 1977), because glauconite does not usually precipitate from introduced fluids (McDonald, 1979).

The limestones are dolomitised. The dolomite consists of planar-s crystals <20μm in diameter with a uniform dull luminescence in CL. Equant sparry calcite crystals 30-70μm diameter, occur as a pore lining cement after the dolomite. Under CL these show early bright and later dark luminescence zones.

Corals collected from the lowest two limestones include *Montastrea Tarbellastrea, Favites, Porites* and *Favia*. All of these are low hydraulic energy, sand-dwelling

species typical of shallow shelf environments and again demonstrate Mediterranean rather than Indo-Pacific affinites (B. R. Rosen, pers. commn. in 1989).

Selected corals have been examined as a guide to the petrography of the unit. Within the corals, large areas are dolomitised with planar-s crystals of 30-80μm maximum diameter (Fig. 3.10-D). These have a homogeneous composition with uniform dull luminescence in CL. Iron oxides are present as opaque granules lining pores, and staining the dolomite crystal surfaces. Within the vuggy pores, the sparry calcite cement consists of blocky crystals of 70-180μm maximum diameter. Under CL these show two separate generations, an early bright zone followed by a non-luminescent zone. These calcite cement generations were subjected to inter-phases of dissolution.

In location M, north of Wadi Al-Hamd, sandstone assemblage is 30m thick. It consists of laminated to thinly bedded sandstones which commonly show trough cross-bedding. Small spheroidal calcareous concretions (up to 4cm diameter) are concentrated within the top part of the sandstone units (Fig. 3.11-B). The sandstones contain echinoderms, large numders of bivalves, crabs and silicified wood fragments. Generally, the sandstones are characterized by intercalations up to 1m thick of bioclastic wackestones and/or grainstones. The bioclasts in these limestones include bivalves, dominantly oysters and pectenids, various gastropods, echinoderms, corals and larger foraminifera (*Nummulites* up to 2mm long axis). Calcareous algal colonies are common, and a few stromatoporoids (0.5 x 1.5m) are recorded near location 2J.

In the central area north of Wadi Al-Hamd, in localities K & M, the sandstones are partly arkosic, and consist of angular to subrounded, medium to coarse, poorly to moderately sorted grains. Up to 60% of the grains are colourless quartz. Most are mono-crystalline and some contain fluid inclusions. A few show authigenetic overgrowths. Some quartz grains are poly-crystalline with sutured boundaries and these were probably derived from metamorphic rocks (Adams *et al.*, 1984). Under CL the quartz grains dominantly show blue or dark-brown and less frequent pink luminescence. Twinned feldspars form up to 30% of grains and are brownish and partially weathered, with some alteration to sericite. Under CL they show lime green, dark-brown, or blue luminescence. Some grains with blue luminescence have dark-brown authigenetic overgrowths. Accessory grains include biotite and opaque grains, mainly iron oxides. Lithic fragments include volcanic rocks containing phenocrysts of plagioclase, and fragments of claystone and chert. Contacts between grains are sutured and corrosion of grain boundaries as a result of burial compaction and subsequant pressure-dissolution (Adams *et al.*, 1984; Hird & Tucker, 1988) is common.

Echinoderm and molluscan fossils were collected in location M, from both the basal and the uppermost sandstones within this unit. The echinoderms are of three main species; *Echinodiscus* cf. *desori*, *Brissopsis* cf. *latidunensus* and *Clypeaster latiratris*. These are similar to Miocene species from the Arabian peninsula, India and the Mediterranian. Only *Clypeaster* has a world wide distribution (A. Smith, pers. commn. in 1989).

The molluscan shells include bivalves and gastropods. The bivalves are well-preserved fossils of *Pecten* and Oysters, and less well preserved (represented by moulds) members of various Veneracea such as *Cardiniacea, Dosinia*, a pectinid and a Tellinid. The guide fossils are *Pecten fraasi*, and the oyster which belongs to a variable and extremely wide-spread species *Hyotissa virleti* and is a member of the family *Pycnodontidae* (P. Nuttal, pers. commn. in 1989). Gastropods are poorly preserved, mainly as external moulds and are dominantly turrited forms, varieties of genera identified as *Strombus, Rapana, Cypraea, Conus* and *Turritella*. Other relatively large gastropods belong to Tonnacea, *Cassidaria* and *Cypracassis*.

The limestone beds in location M are dolomitised in a similar way to those in location K, but the dolomite crystals are <5μm in diameter. However, under CL they have three generations of sparry calcite cement. These are, an early dolomitized marine fibrous dull zone overlain by blocky calcite crystals (60-150μm diameter) bright and finally non-luminescent zones (Fig. 3.10-E). A well defined dissolution surface occurs between the penultimate bright and non-luminescent zones and probably reflects transient undersaturated conditions. A dolomite cement consisting of prominantly zoned planar-e crystals of 200-300μm maximum diameter, occupies pore residual cavities. The cores of these crystals are ferroan and non-luminescent while rims are less-ferroan and dull (Fig. 3.10-F).

South of Wadi Al-Karaj, in location B, an isolated elongated outcrop dips towards the east as a result of what look-like step faults becoming more horst-like on the southern edge of the outcrop. Here, the sandstones are slightly different. They are

about 60 meters thick and are characterized by gypsum veins attributed to present arid surface conditions. They are friable, commonly coarse, sandstones grading upwards to laminated siltstones. They consist mainly of angular grains and are moderately-well sorted. Most are slightly bioturbated. The sandstones are intercalated with reddish-brown channel filling conglomerates up to 1.5m thick which contain pebbles of 8cm maximum diameter. These are commonly quartz with a minority of fragments of andesite, rhyolite and limestone, and are supported by a sandy matrix with a calcareous cement.

The earliest cement is a blocky sparry calcite with crystals 80-220μm maximum diameter, which is completely non-luminescenct in CL. This is overlain by an Fe-dolomite cement of planar-e crystals 50-140μm diameter. These show corroded dull cores and bright yellow luminescent rims. The leaching of Fe-dolomite (ankerite?) cores was probably a result of freshening mixing zone waters (cf. Conglio *et al.*, 1988). Iron oxides occur on dissolution seams (styolites) as an insoluble residue. SEM examination shows that some clay cements post-dated calcite spar and dolomite precipitation. These include an early kaolinite, followed by illite and by later illite-smectite mixed layer clay.

In location B, sandstones are characterized by several lensoidal intercalations of fossiliferous packstones. These are up to 12m thick and extend over a few hundred meters. The XRD indicates that they are dolomitized but this is not obvious in the field. Coralline algae are predominant among the bioclasts, less frequent are bivalves, corals, gastropods, fish bones and benthic forams (commonly *Textularia*).

Scarce angular to subrounded detrital grains (<1mm) include quartz, feldspar and opaque grains. The dolomite consists of a finely crystalline (<3μm diameter) replacement of an originally peloidal muddy matrix. Under CL crystals show a homogeneous dull yellow-orange luminescence. Yellow luminescence is caused by an increased percentage of divalent manganese (Osiko & Maksimova, 1960).

A later dolomite cement lines residual pores. This consist of planar-e crystals 80-150μm diameter, which under CL have multiple alternating zones of dull and bright luminescence. The dolomite crystals are coated with notable iron oxides which also form rims in secondary pores. They are overlain by a blocky sparry calcite cement (crystals 120-200μm diameter) which is non-luminescent under CL.

The palaeontological and sedimentological characteristics of the sandstones are those of shallow neritic environments receiving terrigenous sedimentation. The thickest sequences are expected along the margins, as on the northern side of Wadi Al-Hamd. However, one moves progressively off-shore from northwest to southeast.

3.2.1.5 BRECCIATED LIMESTONE ASSEMBLAGE

This assemblage occurs only on the northern side of Wadi Al-Hamd, concentrated in and around location M. It forms a lensoidal unit consisting of two brecciated limestones separated by a sandstone.

The lower limestone is 1.5m thick, while the upper is up to 3m. Both are characterized by angular clasts of fossiliferous wackestone of 3cm maximum

diameter. These lithoclasts occur within a pelloidal wackestone matrix associated with foraminifera, oysters, and fragments of echinoderms and coralline algae. The foraminifera include both benthonic and planktonic genera such as *Nummulites* and *Globigerina*. Scarce angular detrital monocrystalline quartz grains are also present.

The dissolution of shells has left mouldic or vuggy porosity. A blocky sparry calcite cement with crystals 80-180μm diameter and tooth like crystal terminations has formed within this. Under CL, this includes three generations. The initial phase was dull, the second bright with dull luminescent subzones. This was subjected to dissolution before precipitation of the last non-luminescent zone. Planar-s dolomite crystals (10-20μm diameter) occur within the micrite matrix. In CL these have non-luminescent cores and bright rims. Styolitic seams occur within the dolomitized matrix as a result of later compaction.

The associated sandstone, 3 meters thick, it is pale-brown, medium grained, and calcareous. Most of this unit is thinly bedded but the upper 2 meters are convoluted, indicating liquefaction as a result of dewatering associated with rapid deposition (Lindholm, 1987). In thin section, the sandstone consists of poorly sorted grains from 0.1 to 1mm diameter. Monocrystalline quartz grains form up to 60% of the sediment, showing blue and dull-brown luminescence in CL. Feldspars form up to 20% of grains and are dominantly microcline. Other grains include scarce biotite and bioclasts such as oyster fragments and foraminifera. An equant sparry calcite cement with crystals <10μm diameter fills intergranular pores. Under CL this is generally non-luminescence but a few crystals have thin bright overgrowths.

3.2.2 INTERPRETATIONS

The Musayr limestones have previously been described by a number of authors as reefal limestones (eg. LeNindre *et al.*, 1986) or even sub-reefal limestone (Skipwith, 1973). They have been described more precisely as a patch-reef within a back reef environment (Dullo *et al.*, 1983) or as reefs which accumulated preferentially on structural highs (Purser & Hotzl, 1988). These interpretations are not borne out by the present observations.

The Musayr limestones are characterized by five lithofacies assemblages reflecting a range of depositional environments ranging from slope to near shore. There are rapid lateral facies changes and boundaries between these are commonly gradational. The limestones were deposited during a transgressive phase of the Mediterranean in the early Miocene (Burdigalian).

3.2.2.1 CONGLOMERATIC LIMESTONE ASSEMBLAGE

The boulders were derived from limestones and include coral blocks presumably derived from living coral associations. The distribution of the unit indicates that the dominant direction of transportation was towards the southwest. The boulder deposit is a calcidebrite (Stow, 1989), which travelled over the gentle slopes of the carbonate ramp. Boulders were derived from the upper part of the ramp or from a shelf which lay within the central area and which has now been completely eroded. The well rounded boulders have extensively bored outer surfaces, as in location T, and indicate long-term exposure in shallow water and with low rates of deposition before submarine mass transport. After mass movement with back ground deposits of the

poorly laminated wackestone matrix, they formed a series of lobate mounds which thin rapidly when traced laterally.

3.2.2.2 LAMINATED LIMESTONE ASSEMBLAGE

The laminated bioclastic wackestone unit includes a channel filled with siliciclastic sediment, an association typical of low energy tidal flats (Barwis, 1978). It contains larger foraminifera interpreted as most abundant in shallow marine deposits. The unit overlies conglomeratic limestone, the debris flows (as in location T), with a gradational contact suggesting that deposition occured in a period of relatively shallow water depth.

3.2.2.3 OYSTER LIMESTONE AND SANDSTONE ASSEMBLAGE

The oyster limestones are concentrated in the central area, capping structural highs such as Jabel Hamza as a result of pre-rift fault movements (Fig. 3.11-C). The oyster limestone association indicates a rapid vertical accretion of the platforms at a rate higher than the rate of eustatic sea-level rise (cf. Vail *et al.*, 1977). The facies grades laterally to north and west, towards the continent, into the sandstones assemblages bearing a similar faunal assemblage.

The huge thickness of the oyster limestones in the central area is thought to reflect deposition in a shallow marine environment over a topographic high. In places, the unit contains pure coquinas consisting dominantly of oysters with thick shells, often bored and with associated sediments bioturbated. The fossil assemblage includes echinoderms such as *Clypeaster* and provides strong evidence of water depth and/or

shore distance at the time of depositon (Boggild and Rose, 1984). They suggest a depth of about 4m (Wilson, 1975).

The fauna and flora found in the upper sandstone of locality M, in addition to the dominant trough cross-bedding, indicate a near-shore shallow marine environment. The low-angle trough cross-bedding is interpreted as reflecting accretion by a storm beach prograding over a sand flat (compare Purser and Evans, 1973).

3.2.2.4 BRECCIATED LIMESTONE ASSEMBLAGE

The brecciated limestone is the upper-most assemblage of the Musayr limestones. Scattered similar brecciated sediments were found along fracture zones around location M, the breccias probably resulting from seismic instability during deposition (cf. Plaziat *et al.*, 1990). The brecciated limestone is intercalated with convoluted sandstones, which increase the possibility of tectonic influence. Such localized influence would help to explain the lensoidal shape of the units.

The Musayr limestone sequences were deposited on and around pre-existing structural highs (horsts) formed by vertical movements along normal faults. Generally, oyster limestone and sandstone assemblages reflected normal conditions during their deposition and indicated a transition from slope to shallow, and finally to near-shore environments.

3.2.3 HYDROTHERMAL DEPOSITS

Skipwith (1973), referred to the occurrence of lead, zinc and copper mineralization in Tertiary rocks of the coastal plain of Saudi Arabia between Yanbi (300km N. of jeddah) and the gulf of Aqaba. These deposits lie close to and over fault zones associated with Red Sea rifting and it is likely that their generating solutions were similar to those of the brine deeps described by Hendrick *et al.* (1969). This is indicated by the comparison between isotope analyses of lead from mineral veins which occur east of Al Wabigh (120km N. of Jeddah), and those of lead from the hot brines (Skipwith, 1973). Since faulting is common in the Maqna are selected samples from the Tertiary formations were analysed for trace element compositions. It was considered that if faults had been important as pathways for diagenetic fluids flowing into the Tertiary sediments, then the sediments might also carry this distinctive metallic signature. The analyses reveal the presence of Pb, Zn, ...etc, which are unlikely to have been derived from the sedimentary cover and this suggest that some proportion of the diagenetic fluids were derived from the basement of deeper (Appendix 1-B), and, also by comparison with the present day hydrothermal emissions, that the waters were relatively warm (>50C°). Both rhodochrosite and barite are regarded as replacement minerals related to hydrothermal solutions.

3.2.4 THE DIAGENETIC ENVIRONMENT

The Musayr limestone sequences were subjected to a series of different diagenetic environments. The variations in the diagenetic sequence within the five lithofacies assemblages of the Musayr limestones is shown in Figure (3.6). However, not all diagenetic products are found in one sequence. The initial cement is fibrous and dull

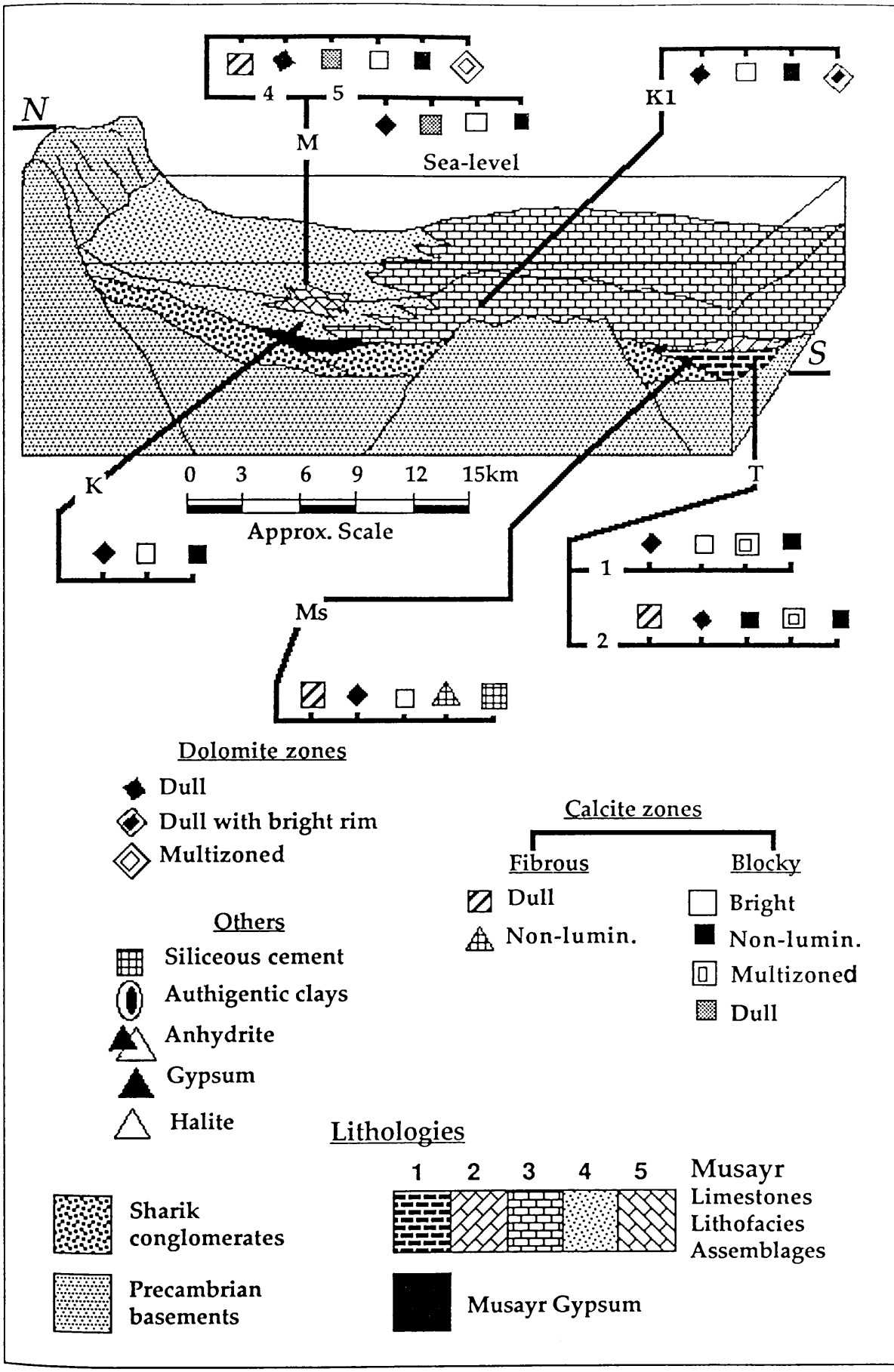

Figure 3.6 Lateral distribution of the diagenetic sequence in the Musayr Formation. The Lst. lithofacies assemblages are numbered systematically as described in the text. The diagrammatic model shows the relationship between the Musayr Lst. lithofacies assemblages and the underlying rocks. (see Plate 2 & 4 for the log locations referred to here).

and probably formed in a marine environment, takes place on or just below the seafloor. This is overlain by blocky sparry brightly luminescent calcite. Dissolution of this indicates a major change, probably to an active meteroic environment. The later two sparry calcite generations are a blocky multizoned cement, which was also dissolved, and a blocky non-luminescent cement with bright overgrowth rims. The multizoned sparry calcite cements are dominant in elevated limestone units which could reflects shallow burial subjected to repeated changes in porewater chemistry. The last (non-luminescent cement) probably precipitated under phreatic conditions following burial. The common interphase dissolution within the sparry calcite cements, and the well developed moldic porosity, are features taken by many workers as evidence of subaerial diagenesis (Allen & Matthews, 1982).

Dolomites have a relatively uniform dull luminescence and bright zones are probably of late syntaxial overgrowths. The dolomite was formed by marine (hyper-saline) to burial dolomitization. Some are neomorphosed by meteoric or hydrothermal fluids and were then subject to selective dissolution. The dolomite cements are coarse grained, and zoned as a result of an increase in the amount of freshwater in the mixing-zone (Tucker & Wright, 1990).

The diagenetic environments of the Musayr limestones of Maqna include:

(1) Marine near-surface: (dull fibrous sparry calcite cement dolomitization).

(2) Shallow burial [blocky sparry calcite (bright, multizoned) cement, formation of clay minerals, barite and rhodochrosite, dolomitization].

(3) Mixing zone to meteoric phreatic (deposition of multizoned dolomite cement, and multizoned blocky sparry calcite cement).

(4) Meteoric vadose (deposition of non-luminescent calcite with bright calcite overgrowth), and the halite and gypsum form the final cements. The non-luminescent fibrous calcite cement and the overlying siliceous cement as colloform chalcedony and as mega quartz within the boulders of the conglomeratic limestone are also attributed to early meteoric environment during their lithification.

3.2.5 AGE ASSIGNMENT

The fossil assemblage including corals, echinoderms and bivalves suggests that the Musayr limestones were deposited during the Miocene.

Corals include *Acanthastrea* cf. *echinata* and *Lithophyllia michelotti* which are assigned to the Burdigalian (Lower Miocene). The echinoderms are Miocene Clypeastroids and Spatangoids including, *Echinodiscus* cf. *desori*, *Clypeaster latirostris* and *Brissus* cf. *latidunensus*. *Brissopsis* sp. is exceptional because of its long time range (Eocene - Recent). Finally, the bivalve assemblage includes *Pecten fraasi* which is identical to that from the Miocene of Egypt. The oysters are provisionally identified as *Ostrea digitata*, a species occuring in the Miocene of the Sinai area, and Hyotissa virleti, which is known from the Miocene of east Africa, the Arabian region and the Arabian (Persian) Gulf. These macrofossils are important

because they have not previously been described in any detail.[1] They suggest a slightly younger age for the formation than that assigned by Dullo *et al.* (1983) on the basis of the microfauna.

3.2.6 COMPARISON WITH NEIGHBORING AREAS

A number of authors have shown that the Neogene stratigraphy of the Red Sea is almost identical to that of the Gulf of Suez (Beydoun, 1989).

3.2.6.1 SAUDI ARABIA

Several limestone outcrops along the Saudi Red Sea coast (north of latitude 24°N) are Miocene. These are described as massive bioclastic reef limestones but so also was the Musayr limestone in the Maqna area. It is therefore not clear whether these are similar to the Maqna area limestones or of some quite different lithofacies assembalges. As much as 40m thickness of limestone outcrop intermittently along the flanks of the coastal hills and are referred to the Lower Raghama Formation (Davies and Grainger, 1985), known here as the Musayr limestone. Towards the south, there is no Musayr limestone equivalent in the vicinity of Yanbu Al-Bahr (south of latitude 24°N), hence there is no link with the Miocene Baid Formation, which forms the cap rocks of the Jizan salt-dome (Prinz, 1983).

[1] The Tertiary fossils, corals, molluscs and echinoderms were identified early in 1989 at the British Museum (Natural History) in London with the kind assistance of Drs. B. Rosen, P. Nuttal and A. Smith.

3.2.6.2 EGYPT

Along the Egyptian border of the Red Sea, recent sedimentological research has demonstrated that the structural horst relief developed progressively during sedimentation (Plaziat *et al.*, 1990). Thus, as reported by Sellwood and Netherwood (1984) for the Gulf of Suez area, the area studied has not undergone significant pre-rift doming.

In the Gulf of Suez, Miocene carbonates are well exposed along the western side of the Gulf. In Jabel Abu Shaar a Miocene reef-platform was developed on basement horsts, this graded gently westward into a sand gravel plain formed by alluvium derived from the Red Sea hills. The platform is undeformed and the present topography is close to the original depositional morphology (Aissaoui *et al.*, 1986). All of the Abu Shaar carbonates are dolomites, the rapid vertical and lateral facies changes are related to pre-existing topography (Haddad *et al.*, 1984). Three lithofaces are present described as platform interior, platform edge, and talus slope. Compared to the Musayr limestone assemblages, only the platform interior has analogues and is similar to sandstone assemblage which consists of mixed bioclastic carbonates and siliciclastics.

On the northern Egyptian Red Sea coast, in the Quseir region, a mixed siliciclastic-carbonate series is present showing marked facies changes closely related to the pre-existing morphology. The sequence begins with a relatively thick (100m) series of conglomeratic fan-delta deposits which compare with the Sharik Formation and are currently also interpreted as fan-delta deposits (Purser & Hotzl, 1988). The

overlying marine sediments contain a Burdigalian microfauna and are considered to be the transgressive equivalents of those in the Maqna area represented by the Musayr limestone sequences. The main components of the lower part of the succession in the Quseir region include well sorted marine siliciclastic sands and sandy dolomites with molluscs, red algae and other normal marine elements similar to sandstone assemblage of the Musayr limestone. However, the upper part of the sequence consists of sediments described as barrier reef deposits which are certainly not represented in the Maqna area.

Pre-rift, two dominant fault trends, a Clysmic (NW-SE) trend and an Aqaba (NE-SW) trend, have cut the crystalline basement and pre-Neogene cover. Their existence during the Miocene has profoundly influenced Neogene sedimentation and diagenesis (Burollet *et al.*, 1985, in Aissaoui, *et al.*, 1986). The Musayr limestones were deposited in an isolated tectonic basin. The Maqna area formed part of the Midyan region which was situated close to the axis before it subsequently migrated along the Aqaba fault. Sequences therefore differ lithologically from those more peripheral sequences outcropping along the Egyptian coast (Purser and Hotzl, 1988).

MUSAYR FORMATION

Figure 3.7

A. Angular-unconformity between the Sharik Conglomerates (S) and the Musayr Gypsum (G) in locality K. Scale approx. 15m.

B. Radial growth of gypsum crystals in Musayr Gypsum.

C. Conglomeratic limestone overlying the Precambrian basement, eastern outcrop capping Jabel Al-Musayr.

D. Boulder conglomeratic limestone unit in locality Ms. Some boulders (B) are up to 1.5m diameter.

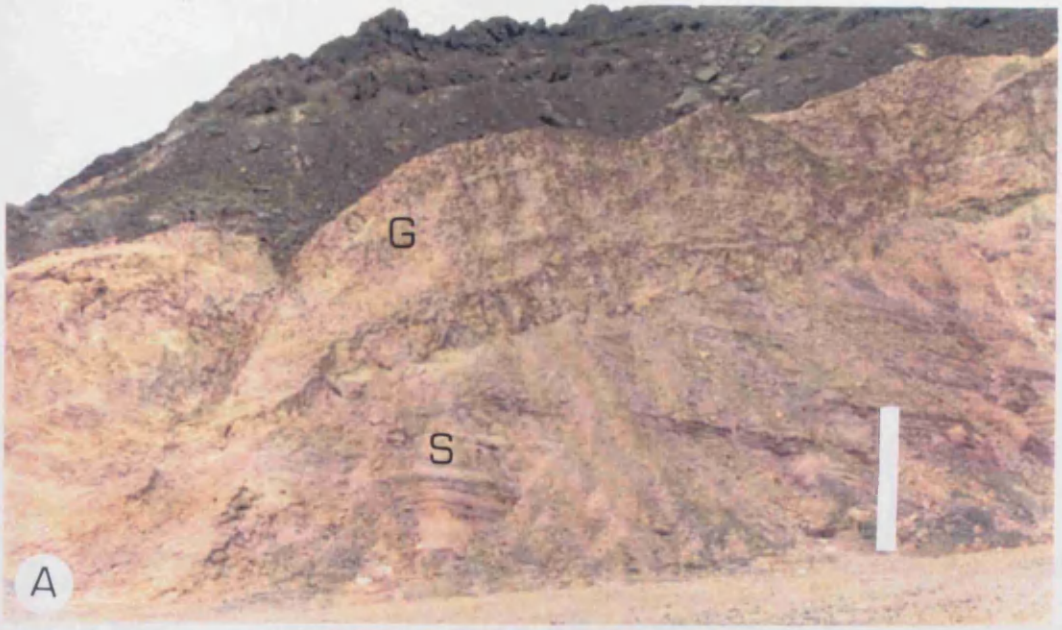
G
S
A

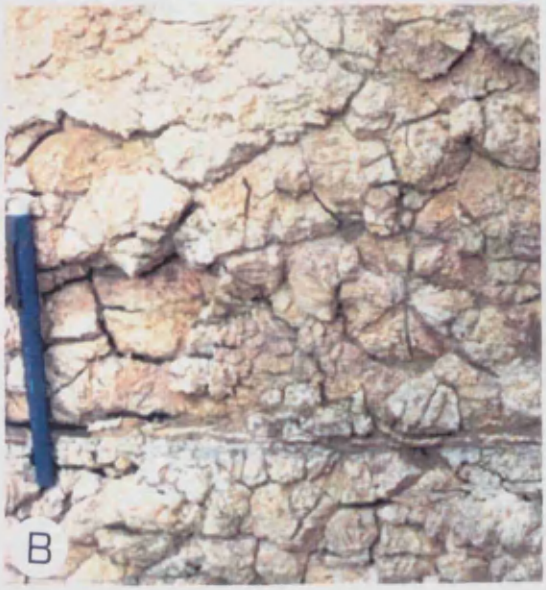
B

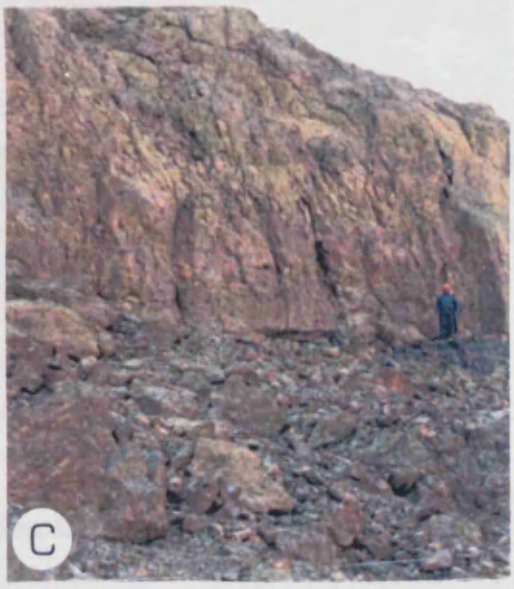
C


B
D

Figure 3.8

A. Dolomite crystals, some have bright and dull subzones. Thin section, CL. Scale 0.2mm.

B. Colloform fibrous silica within dissolved bioclasts. Thin section, Ppl. Scale 0.2mm.

C. Finely crystalline dolomite (D) with styolites (S) formed as a result of compaction. The dolomite is replaced by rhodochrosite (R) and overlain by sparry calcite cement (C). Thin section, CL. Scale 0.4mm.

D. Sparry calcite cemnet sequence. An early fibrous cement (F) is overlain by a zoned blocky cement (C). Thin section, CL. Scale 0.4mm.

E. Neomorphic dolomite (D) replacing calcite (C). Thin section, CL. Scale 0.2mm.

F. Benthic foraminifera within dolomitized micrite trapped in the coral clyces. Thin section, CL. Scale 0.2mm.

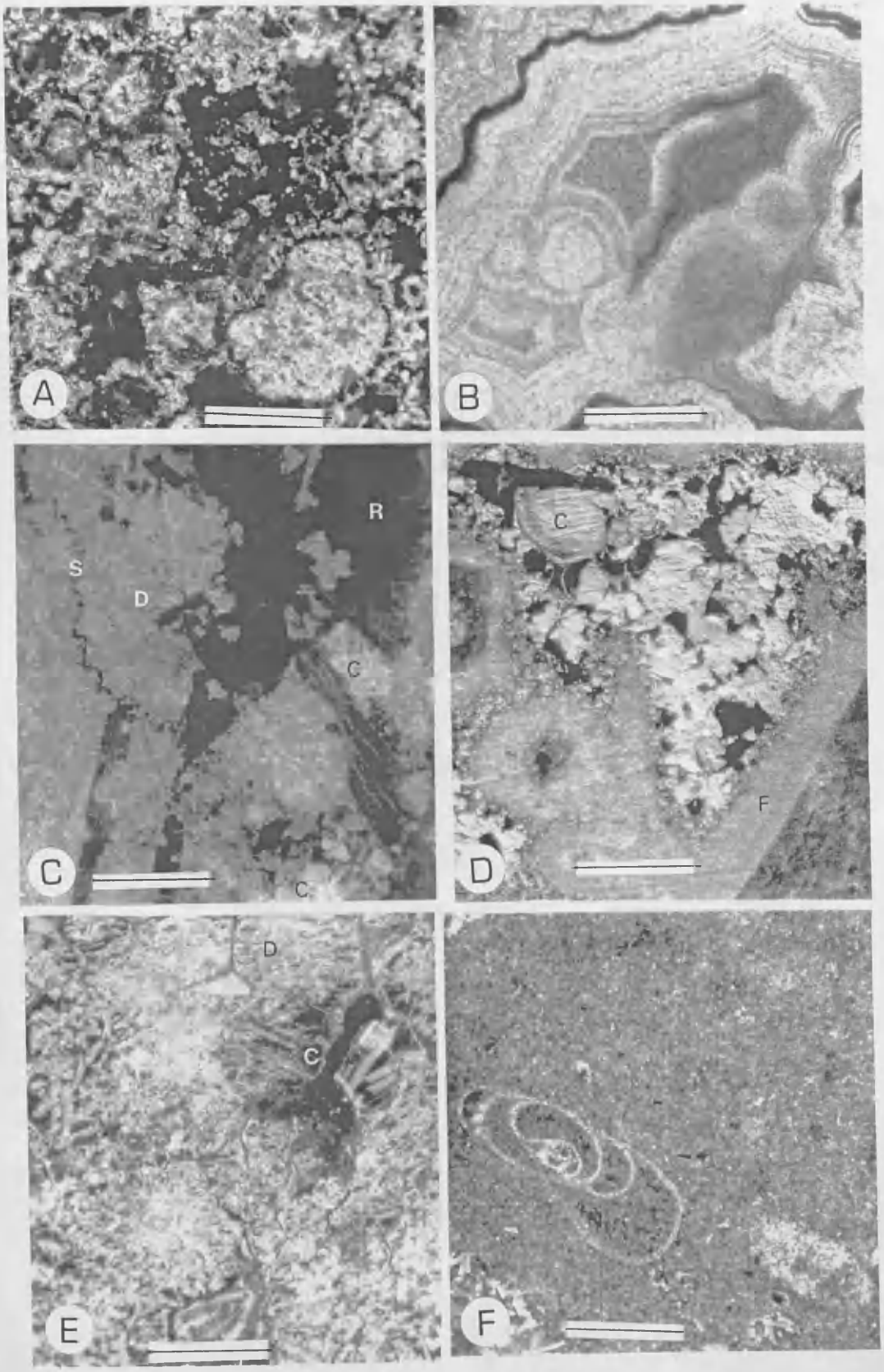
A
B
R
S
D
C
C
C
D
C
F
D
C
E
F

Figure 3.9

A. Boulders of derived corals have extensive borings on their outer surfaces in locality T.

B. The oyster-bearing limestone (O) filling fissures cutting the boulder conglomerate limestone unit (G) in locality KK2 on the western side of Jabel Tayran.

C. Close view of oyster limestone in locality T.

D. Extensively burrowed sandstone unit in locality K2.


A

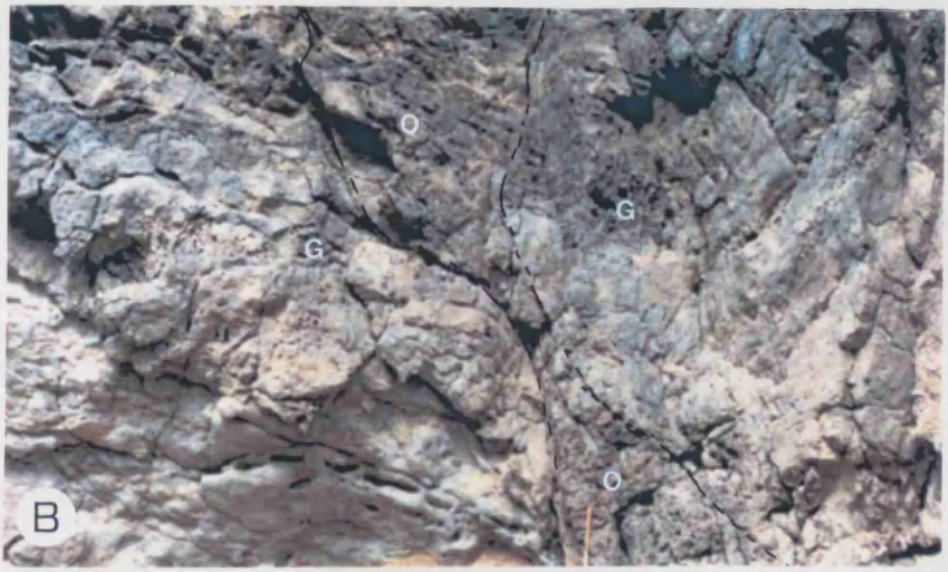
O
G
G
O
B


YASHICA
C


D

Figure 3.10

A. Dolomite cement, multi-zoned crystals have been partially dissolved and pores filled by later bright calcite cement. Thin section, CL. Scale 0.2mm.

B. Sparry calcite cement, crystals of an early, dolomitized, fibrous cement (F) are followed by blocky cement. Thin section, CL. Scale 0.4mm.

C. SEM. Authigenic smectite cement (S) overlying blocky sparry calcite cement (C).

D. Dolomitization of corals (dull). Sparry calcite cement (C) occurs as a pore filling. Thin section, CL. Scale 0.2mm.

E. Sparry calcite cement. An early dolmitized fibrous cement (F) is overlain by blocky crystals. Thin section, CL. Scale 0.2mm.

F. Dolomite cement, planar-e crystals have ferroan dark cores. Thin section, CL. Scale 0.2mm.

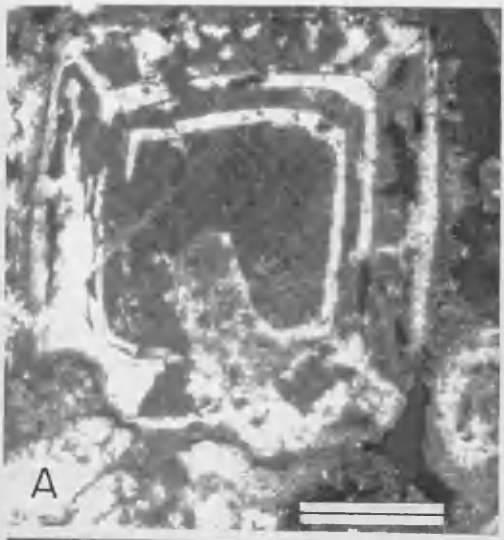
A

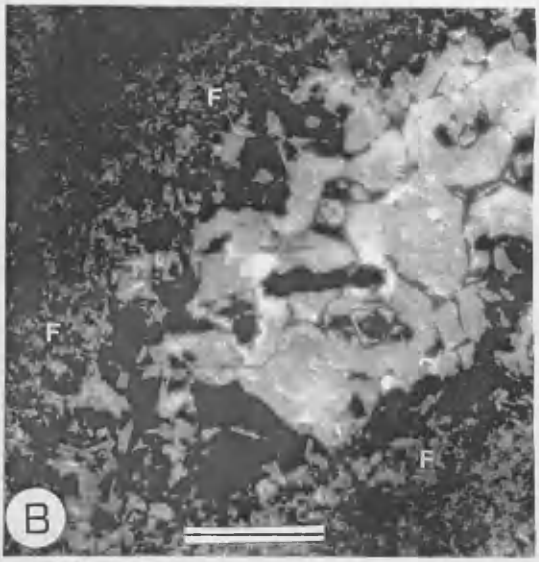
F
F
F
B

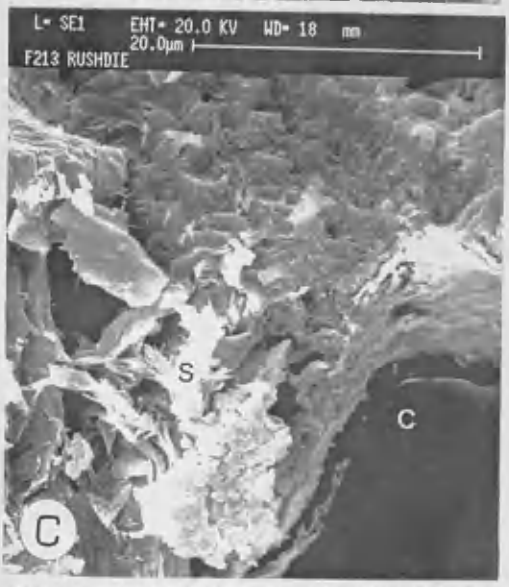
L= SE1 EHT= 20.0 KV WD= 18 mm
20.0µm
F213 RUSHDIE
S
C
C

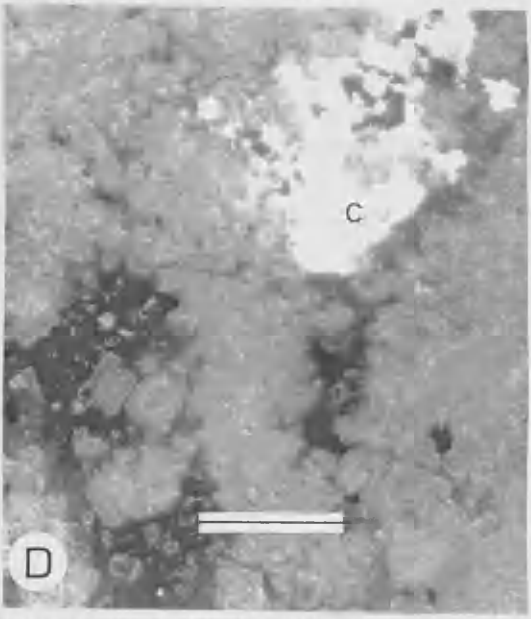
C
D

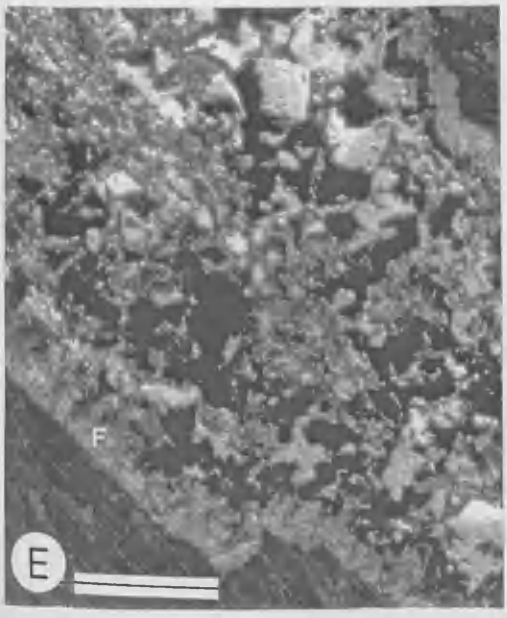
F
E

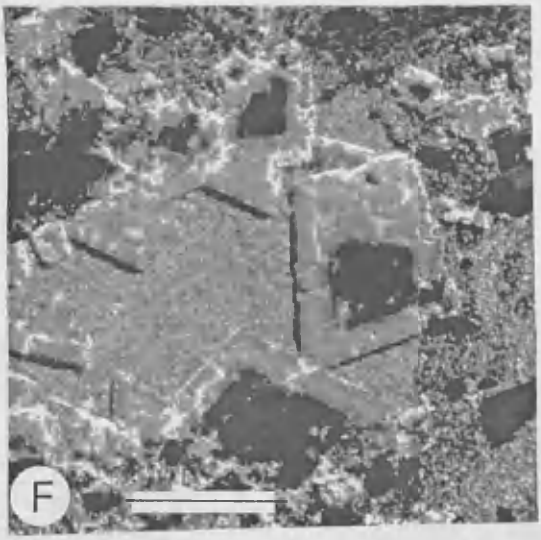
F

Figure 3.11

A. Cerebroid stromatolites at the top of the sandstone sequence in locality Ra.

B. Small spheroidal calcareous concretions within the upper sandstone unit in locality M.

C. Panoramic view (looking SE), showing the oyster limestones (O) capping Jabel Hamza (H), and their counterpart sandstones (S) across Wadi Al-Hamd (W).

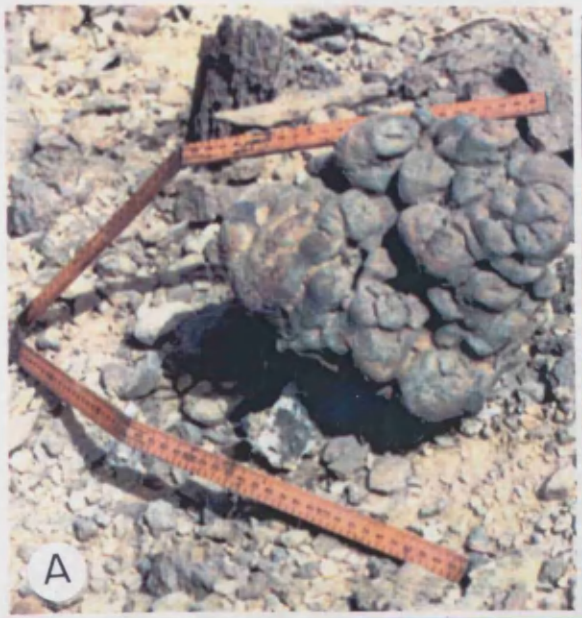
A


B


O
H
O
S
W
C

CHAPTER IV

THE NUTAYSH FORMATION

The Nutaysh Formation was informally named after the Jabel Al-Nutaysh area to the north of Maqna (Clark, 1985). This name replaced the Wadi Telah Member, a part of the Tayran Formation proposed by Dullo *et al.* (1983) and was subsequently accepted by Purser & Hotzl (1988).

The formation is represented by a sequence of abrupt facies changes. The formation generally dips towards the east, and has a thickness of at least 280 meters (Fig. 4.1). The angular unconformity with the underlying Musayr Formation is clearly seen on the eastern side of Jabel Hamza. In location S1 to the east of Jabel Faya the Nutaysh Formation rests unconformably on the basement, indicating prolonged erosion before deposition.

In the Maqna area, the relationships and distribution of the Nutaysh sediments are shown in Plates 1 and 3.

4.1 THE LOWER NUTAYSH FORMATION

This unit, totalling up to 180m thickness, is thickest in the northwest, and thins towards the Southeast. It was deposited within a graben-like basin as a result

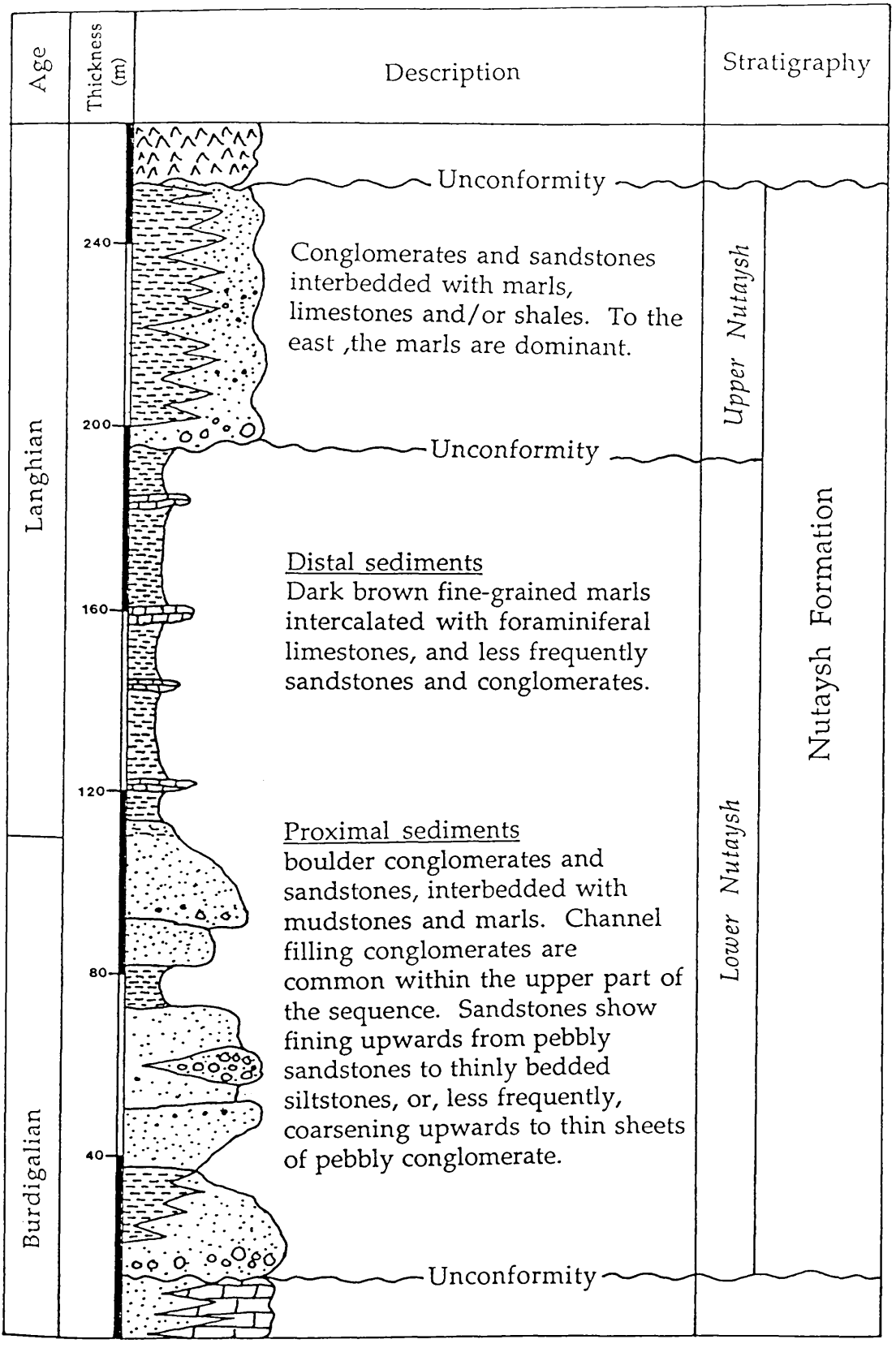

Figure 4.1 Genralized log section for the Nutaysh formation (see plates 2 & 3 for explanation).

of vertical movements of normal faults. It consists of proximal coarse clastic sediments along the fault margins which thin laterally towards the basin. Their, distal finer grained sediments, commonly carbonates (marls), form a rhythmic sequence of beds intercalated with sandstones and partially dolomitized limestones.

4.1.1 THE PROXIMAL CLASTIC ASSEMBLAGE

This part of the sequence covers the northern and western areas. Boulder conglomerates up to 5m thick occur in north-western outcrops and these, and sandstones, are interbedded with mudstones and greyish-green marls. In northern exposures close to Jabel Al-Nutaysh (location SH), the succession is relatively thin (50m) but consists almost entirely of conglomerates with only a few thin (<10cm) marly beds interclated at the base. In contrast, marls are common in western areas and some are up to 14 meters thick, as in location S1. A much thicker clastic sequence is seen further south, south of Jabel Faya (near the coast). Here, in location 1D (Plate 3), sediments vary from pebble-grade conglomerates to pebbly sandstones and fine sandstones with individual unit thicknesses up to 13.5 meters. Conglomerates contain boulders up to 8cm diameter of dominantly granitic and andesitic rocks. The upper part of the succession is almost entirely channel- filling conglomerates (Fig. 4.6-A). Channels trend mainly east-west. Subangular to well rounded boulders up to 2.2m diameter in the upper unit are derived from the Pre-cambrian basement, but are mainly granitic. A few consist of irregular blocks of greyish-green shale. The angular shapes and presumed lack of mechanical strength of these suggest that they can only have been transported short distances (Fig. 4.6-B).

Sandstones in locality 1D, are yellowish-brown and commonly show normal grading upward from pebbly sandstones to thinly bedded siltstones. Some of these sandstones are coarsing upwards to thin sheets of pebbly conglomerate (Fig. 4.6-C). Most consist of angular grains and they are generally poorly sorted and immature; many are arkosic. Some have a calcareous cement but others are friable. Bioturbation is common with *Chondrites* burrows with individual tubes up to 0.4cm across. Scattered transported blocks of coral (1m max. diameter) occur within two sandstone beds.

Marls are dominantly greyish-green to dark-brown and vary from 5cm to 8m thick, interclated between sandstones. They vary in the total volume of carbonate they contain and their degree of cementation. With increasing carbonate they range from laminated shale to aphanitic limestone or even dolomite.

Within the sandstones, quartz grains are commonly mono-crystalline. A few are polycrystalline and contain fluid inclusions or minerals such as muscovite, suggesting that they may be of metamorphic origin. Under CL coarse quartz grains have a dominantly dark-brown or blue luminescence with less common red or pink grains. By contrast, fine grains (0.1-0.3mm diameter) have a predominantly blue luminescence. This suggests that there are may be at least two sources for these materials and that different sizes are transported selectively. The percentage of quartz within the sandstones varies and may reach 60% in coarse grained sandstones. Some fractured quartz grains have sutured contacts as a result of early compaction and pressure dissolution. However, others bear authigenic overgrowths.

Feldspars form up to 30% of detrital grains and are characterized by various types of twinning but are dominantly microcline. Composite grains showing feldspar related textures such as graphic, myrmekitic and perthite intergrowths are also present. Under CL feldspars show blue, green, red or brown luminescence.

Accessory minerals include flakes of biotite and opaque grains, mainly of iron oxides. In addition to these the bulk rocks have a slightly ferruginous appearance which is related to later seepage by iron rich solutions and in situ weathering of iron rich minerals.

A sparse sparry calcite cement is developed within the sandstones, represented by scattered fine (<5μm) equant crystals characterized by bright luminescence in CL. These are overlain by dolomite which forms the bulk of the cement in the form of planar-s crystals (Sibley & Gregg, 1987) of <10μm diameter. These have uniform dull under CL. SEM examination shows angular grains of quartz and feldspar cemented by finely crystalline dolomite (Fig. 4.7-A). It also indicates that dolomite crystals show dissolution of faces with the production of micro-channel porosity.

Sandstones in location 1D contain dolomitized derived blocks of corals. Within these dolomite crystals up to 20μm diameter form a hypidiotopic mosaic. Under CL, these generally show a homogeneous dull luminescence but a few have bright rims. Surface cavities in the corals have a thin ferruginous surface stain and are filled by angular detrital quartz and feldspar grains, ranging from fine to medium sand size. Intraskeletal cavities in the corals are occluded by the later blocky sparry calcite

cement crystals of 70-120μm diameter. These are generally non-luminescent but scattered samples have brightly luminescent overgrowths zones.

Authigenic clay minerals present as cements have been identified by XRD as illite, chlorite and dickite (Fig. 4.7-B). Dicktite usually forms by hydrothermal action and occurs as a replacement of quartz in quartzite (Kerr, 1977). It most commonly occurs in sandstones as a pore filling, and forms in the temperature range of 70° to 90°C (Weaver, 1989). Dicktite may form from kaolinite during burial through the stage of mixed-layer growths (Shutov *et al.*, 1970). Gypsum forms a later cement and occurs as anhedral crystals up to 50μm diameter overlying clays.

In location S1, the clastic sequence shows similar characters to those in location 1D, but lacks bioturbation. Intercalations of Globigerinid marls which up to 14 meters thick are generally dolomitized. They have a sucrosic texture with dolomite crystals 10-30μm diameter and show a uniform dull luminescence under CL. The marly beds contain detrital grains, mainly angular fine to medium grains of quartz (40-170μm diameter) which form up to 3% of the rock. The quartz grains are mainly of blue luminescence although there are less frequent brown grains. Notable fragments of algal oncolites are locally present. Laminae in these show alternating dull and non-luminescent zones under CL, apparently related to selective replacement.

Moldic pores formed by dissolution of Globigerinids and other bioclasts are occluded by calcite cement in the form of blocky crystals 80-130μm diameter. Under CL, these shows two generations, an early bright and a late non-luminescent. The blocky

calcite contains numerous brown inclusions of iron oxides which may have formed in oxidizing water. Adams *et al.* (1984) suggested that under such conditions ferrous iron oxidizes to produce iron oxide granules and is not incorporated into ferroan calcite.

Location SR in the central hilly area, represents the final eastward extension of the lower coarse clastic sediments in the Maqna area. The clastic sequence here is characterised by the presence of normal graded bedding in fining upward units of either pebbly conglomerates or coarse sandstones to siltstones and/or marls. Individual clastic units are up to 10 meters thickness. The dolomitized marls intercalated within the clastic sequence include two lensoidal dense dolomite beds (0.8m thick) which have compeletly obliterated the original marly texture. The dolomite crystals are esentially the same as those described for location S1.

4.1.2 THE DISTAL CARBONATE ASSEMBLAGE

This unit represents a lateral facies equivalent of the proximal conglomerate and sandstone sediments, and forms the dominant outcrops in the eastern half of the area. It is characterized by dark-brown fine grained sediments, occuring in a series of outcrops which have clearly been affected by the later tectonic activity of the area. They take the form of step fault blocks, generally with trends perpendicular to the Gulf of Aqaba. The unit dips mainly to the east, with a thickness up to 120m in Location 1R.

In northern localites, north of Wadi Al-Hamd in location Z, the sequence is represented by greyish-green marls intercalated with several beds of poorly sorted graded sandstones and conglomerates, the last with boulders up to 20cm diameter. Again, the marly beds are not strictly marls, they include well laminated, partially fissile calareous shales and limestones. They are sometimes lensoidal, ranging from 0.3 to 1 meter thick and dying-out over tens of meters laterally. The limestone units (bioclastic wackestones) are individually up to 6 meters thick, consisting of partially packed bioclasts, including abundant Globigerinid forams up to 0.3mm diameter, together with benthic foraminifera including a large, (2.5mm long axis), agglutinated biserial Textularids. Other abundant micro-bioclasts include fragments of bivalves and gastropods, but the maximum sizes of these is only 4mm. The micrite matrix is slightly ferroan and under CL shows a uniform dull luminescence.

The limestones include scarce detrital quartz grains which are mainly fine sand size, of 100um average diameter, and show blue luminescence in CL. Scarce bone fragments (fish) have an elongated shape, and are nearly isotropic, some showing parallel extinction. Mouldic pores formed within dissolved bivalve clasts are occluded by sparry calcite cement. This consists of blocky crystals (100-180μm diameter) which are characterized by iron oxide inclusions. Under CL three generations are recognized. An early blocky calcite containing dusty inclusions is non-luminescent. This is overlain by a new nucleation of brightly luminescent cement packed with iron oxide inclusions. This has undergone a localized selective dissolution but is overlain in turn by larger crystals which are predominantly non-luminescent but have bright rims (Fig. 4.7-C).

To the south, in location A, there is a progressive decrease in siliciclastic content and an increase fine grained marly beds. There are no conglomerate intercalations, and sandstones, representing only 15% of the sequence, are dominantly fine-medium grained (0.1-0.4mm diameter). The marly beds are mainly bioclastic packstones, and XRD analysis indicates the abundance of calcite.

The packstones contain <2% fine angular detrital grains, mainly quartz and feldspar. Under CL the quartz is mostly blue with less frequent brown grains. Some grains have a non-luminescent rim of authigenic quartz overgrowth. The feldspars have blue or lemon-green luminescence under CL. Scarce phosphate fragments (fish bones) are present.

The planktonic foram *Globigerina* (1mm max. diameter), is the dominant bioclast and internal cavities are full of sparry calcite cement or mud from the micrite matrix. Under CL, the micrite shows a homogeneous dull luminescence. The calcite cement can be divided into an early fibrous dull phase, and a later blocky (70-110μm diameter crystals) phase with bright luminescence. Scattered anhedral neomorphic crystals of dolomite (<20μm diameter) show dull luminescence under CL. Partial dolomitization of the micrite matrix has caused vuggy porosity to develope locally.

Marly beds at the base of the unit are gypsiferous, while the upper beds are free of gypsum. The gypsum is of secondary origin and occurs fillings fractures and veins.

The intercalated sandstone beds are arkosic and poorly sorted with a range of angular grains (0.1-3mm diameter). They contain bioclasts of foraminifera and bivalves. The forams are mainly *Nummulites* up to 1.2mm in diameter (Fig. 4.7-D). The detrital grains are dominantly quartz (50-60%), mainly consisting of mono-crystalline grains which under CL show violet-blue or brown luminescence. The feldspar grains (20-30%), are alkali-feldspar, characterized by simple and cross-hatched twinning and textures such as perthite and graphic intergrowths. Under CL they luminesce blue and yellow-green. Other detrital grains include a few pellet-like grains of glauconite, and fragments of sandstone, chert and volcanic rock. A spar cement consisting of blocky calcite crystals 80-120μm diameter occurs mainly within intergranular porosity. It shows uniform bright luminescence under CL.

On the eastern side of Jabel Al-Musayr in location 1R, the Nutaysh sediments are represented by 110 meters of fine grained carbonates (marls). These include foraminiferal limestones, predominantly packstones and less commonly grainstones, and mudstones, showing rhythmic alternation. Near the base of the succession, a coarse fossiliferous limestone occurs as a lensoidal bed 1m thick within the marly unit. Fossil fragments in this include corals (25cm max. diameter), echinoderms, bivalves, and coralline algae and these are accompanied by lithoclasts up to 1cm diameter dominantly of foraminiferal packstone (Fig. 4.7-E). These clasts are of shallow water origin and have been transported by turbidity currents. It is notable in such cases that clasts and sediment are often of different ages (Gall, 1983).

The marly units are generally ferroan, as indicated by dark blue staining with Alizarin Red S and potassium ferricyanide. They are of variable thickness, ranging from 0.2 up to 1 meter thick, and crowded with Globigerinids (2mm max. diameter) and *Nummulites* (3mm max diameter). Other forams are less abundant but include benthonic forms such as *Elphidium, Dentalina, Quinqueloculina* and the agglutinated *Textularia* (Fig. 4.7-F). The limestones contain fragments of echinoderms, bivalves (mainly oysters), corals, an agglutinated tubes of worms (Fig. 4.8-A), coralline algae and cadiaceae algae including *Halimeda*. Algae are essentially restricted to the zone of penetration of light (the photic zone) and most living species are found in depths of less than 25m, although they are known from water as deep as 200m (Horowitz and Potter, 1971). The limestones contain up to 10% of detrital grains, mostly fine grained and angular. Quartz is the dominant mineral and most grains show blue luminescence under CL. Other grains include feldspars, glauconite, bone fragments and opaque minerals. Diagenetic pyrite is also present.

Broken algal fragments and bioclasts indicate pre-cementation compaction. Primary pores and secondary cavities formed by the dissolution of bioclasts are filled with a sparry calcite cement. There are three generations visible within this under CL, an early fibrous dull phase followed by two blocky (60-130μm diameter crystals) cements, the earlier bright and the last non-luminesent. Two similar generations of blocky cement are present in a coral sample (*Montastrea* sp.). The micrite walls of some bioclasts have been replaced by sparry calcite crystals (neomorphism). The micrite matrix shows replacement by dolomite, with scattered mostly subhedral crystals (<20μm diameter) showing dark cores and bright rims in CL.

There is also a siliceous cement (cristobalite) occuring as a cavity filling in secondary pores (dissolved *Globigerina*). Cristobalite either occurs as a result of penetration by hydrothermal solutions, or by the re-precipitation of dissolved biogenic opal such as that derived from radiolaria, diatoms or sponges (Scoffin, 1987), but there is no additional evidence of the presence of any of these here.

Some friable marls (10-60cm thick) intercalated within the limestones are shown by XRD analysis to be composed of calcite, quartz, plagioclase, chlorite, illite and halite. The origin both chlorite and illite is suggested to be as neoformed clays, which are built entirely from solution during the deep burial stages of diagenesis.

In location 1R, the lower part of the sequence contains a unit of poorly sorted sandstone 15m thick. This contains several beds (10-30cm thick) which grade upwards to siltstone or mudstone. This indicate the final stages of distribution of the distal sediments. Sandstones are immature with abundant fine angular grains (0.1-0.5mm diameter). They contain foraminifera such as *Globigerina, Nummulites* and *Textularia*. A number of lithoclasts are present, mainly fragments of re-worked packstone containing forams. Grains of quartz form up to 50% of the sediment. They show dominantly blue luminescence under CL, and dark-brown or red luminescence is less frequent. Feldspar grains form up to 20% of grains and are dominantly plagioclase, partially alterated to sericite. They are of blue or yellow-green luminescence in CL. Other grains include elongated biotite flakes, opaques and fragments of volcanic rock. Mechanical and chemical compaction has resulted in an absence of intergranular porosity. Pores formed where bioclasts have dissolved

are occluded by micrite or later sparry calcite cement. Under CL, two generations of spar cement are present. An early equant (<30μm diameter crystals) dull cement and a later blocky bright cement (50-70μm diameter crystals).

4.2 THE UPPER NUTAYSH FORMATION

The upper Nutaysh sequence in the Maqna area is mostly overlain by the evaporite cap beds of the Bad Formation and is thus poorly exposed. A few scattered outcrops occur in the central hilly area to the west of Jabel Ar-Raghamah.

In the western areas, as in locations D and F, where the marginal proximal sediments are to be expected, the maximum thickness is 20 meters. Laterally to the east, towards the center of the basin, there is a gradual increase in thickness, up to 95 meters south-east of Jabel Al-Musayr in location Mu. Here, the Lower Nutaysh sediments are unconformably overlain by dominantly finer grained sediments as a result of continued subsidence of the basin. The angular contact can be seen on the western side of Jabel Ar-Raghamah in locations 1R and R.

4.2.1 THE WESTERN OUTCROPS

In location D, the sequence consists of 20 meters of coarse sediments represented by four clastic units. At the base, a massive pebbly conglomerates 4m thick contains scattered subrounded pebbles up to 3cm diameter. These are commonly granitic and were presumably derived from the Precambrian basement. Above this the bulk of the sequence consists of three graded pebbly sandstones each fining upwards to siltstones. These units are interbedded with thin (0.3-0.5m thick) beds of greyish-

brown calcareous shale. Thickness varies irregular as a result of differential compaction. At the base of the lowest sandstone in the sequence, the sand has been injected downwards and forms sandstone dykes within the underlying shale (Fig. 4.6-D). Pettijohn *et al.* (1973), indicate that under some conditions sands become quick, that is, they have such a loose structure and contain so much water under pressure that they are capable of injection into fissures which may form as a result of repeated earthquake shocks (Plaziat *et al.*, 1990).

To the south in location AA, at the base a red-brown clastic unit 10 meters thick occurs and reversely grading. Upwards transition from poorly laminated mudstone through sandstone to a massive boulder conglomerate. The same unit is overlain by pale-brown unit 4 meters thick which also coarsens upward from coarse sandstone to conglomerate, and reflected local lateral shift of the channel currents. Notable channel filling conglomerates with boulders up to 20cm max. diameter occur cutting through the sandstone unit. Channel axes trend east-west (Fig. 4.9-A). The rest of sequence in location AA, is characterized by fine grained distalturbidite sediments which are commonly marls.

In the central area, in location F, the marly units are well laminated, and partially fissile. They consist of alternating laminae of foraminiferal packstones, some of which are nodular (Fig. 4.9-B), and calcareous shales. The nodular texture is thought to be due to local diagenetic concentration of CaC03 within the marly sediments.

The base of the sequence is formed by 17m thick of calcareous shales. These are brownish and commonly gypsiferous. The gypsum filling later fractures up to 1cm wide. XRD indicates that the shales consist, in order of relative abundance, of calcite, quartz, gypsum, illite, chlorite, plagioclase and halite.

The middle part of the sequence is of greyish-green foraminiferal packstone unit up to 5m thick which are generally nodular. Bioclasts are mainly micro-fossils including abundant Globigerinid forams with less frequent benthic forams such as *Nummulites* and *Textularia*. Siliceous micro-fossils have also been found here including the radiolarian *Actinomma* which is pelagic and lives mainly in surface waters (Moore *et al.*, 1952), and diatoms (Fig. 4.8-B). Detrital grains form <1% of the sediment and are mainly fine angular grains of quartz, and phosphate fragments (fish bones). Cavities formed by dissolution of bioclasts are filled by cements consisting of either cristobalite and/or calcite. Under CL, the calcite can be seen to consist of three generations, an early fibrous dull zone, which may originally have been aragonite, followed by a blocky (40-90μm diameter) bright zone the surface of which has been partially dissolved and, finally by blocky 120-180μm diameter non-luminescent crystals. The cristobalite is quite localized and it is predated the blocky sparry calcite cement.

Dolomite occurs as scattered fine (10-30μm diameter) euhedral to subhedral crystals within the micrite matrix. Under CL these have dull cores and bright rims. However, there are a few coarser crystals with non-luminescent cores and bright rims, reflected an origin later during burial (Fig. 4.8-C).

The upper part of the sequence consists of 8 meters thick of sandstones which include a wedge shaped disorganized bed of conglomerate tapering from 1.5m thick. This dies-out within a few tens of meters. It consists mainly of rounded boulders, 20cm max. diameter, derived from the basement but also contains notable blocks of marl (40cm x 10cm diameter) as intra-formational clasts concentrated at the base. In general it is slightly coarser at the top than at the base. The top of the sequence is formed by 3m unit consisting of coarse sandstone grading upward to laminated siltstone, becoming gypsiferous in the top 15cm. This is overlain by the first evaporite of the Bad Formation.

The sandstones are poorly sorted, consisting of medium to coarse (0.2-1.5mm diameter) angular grains. Quartz forms up to 50% of grains. Most are monocrystalline, but some poly-crystalline grains (the boundaries between the crystals are sutured) could have been derived from metamorphic rocks. About 20% of quartz grains contain opaque or fluid inclusions. The quartz grains are of blue or, less commonly dark-brown luminescence under CL. Feldspars form up to 30% of grains, they are mainly microcline, orthoclase and plagioclase partially altered to sericite. Some K-feldspar are of diagenic origin (Fig. 4.8-D). Under CL, they are commonly of blue and less frequently yellow-green luminescence. Other detrital fragments occurring in low percentages are opaque minerals, glauconite and volcanic rock fragments.

The cement is a blocky sparry calcite 40-70μm diameter crystals (Fig. 4.8-E) with bright luminescence under CL. Sparse euhedral dolomite crystals (30-50μm

diameter) are scattered within cement. These have dull cores and bright rims under CL. SEM examination shows that some dolomite crystals have dissolved cores (Fig. 4.8-F). Similar extensive incongruent dissolution of dolomite crystals was attributed by Machel and Mountjoy (1986) to mixing zones that were either not saturated with respect to dolomite or had not been in place for a long enough period of time. As the dolomite solution, initially oversaturated with respect to dolomite, approaches saturation with both dolomite and calcite, the cores of the dolomite crystals which are more soluble than the clear dolomite rims are dissolved and replaced by calcite (Theriault & Hutcheon, 1987).

4.2.2 THE EASTERN OUTCROPS

Outcrops along Jabel Ar-Raghamah in locations R, Mu and HN, are characterized by the accumulation of fine grained distal sediments with a maximum thickness of 95 meters. These are foraminiferal limestones which are partly dolomitized to planar-e crystals (20-50μm diameter) scattered within the micrite matrix. These have multiple-zoned bright and dull luminescence under CL (Fig. 4.10-A).

The foraminiferal limestones are mainly Globigerinid packstones to grainstones, dominantly of a greyish-green colour, and are well laminated. Foraminifera include abundant *Globigerina* up to 1mm across and, less commonly, other forams such as *Nummulites* and *Textularia*. The rocks also contain scarce fragments of echinoderms, bivalves, bryzoans and what could be fish bones (Fig. 4.10-B). Detrital grains, which are <0.3mm in diameter, form <1% of the sediments. They are generally angular and are commonly quartz.

A cristobalite cement lines some *Globigerina* cavities, partially overlain by the dominant blocky sparry calcite cement (Fig. 4.10-C). Under CL, the calcite shows three generations. An early fibrous dull cement, is followed by a blocky dull cement (50-110μm diameter crystals) with a bright subzone but has been partially dissolved. The final blocky cement (100-280μm diameter crystals) is non-luminescent.

The last stages of mineral precipitation within secondary fenestral pores are of radiating crystals of anhydrite up to 100μm in length, which may formed as a primary phase or by dehydration of gypsum, either by heating or by saturation in a very saline fluid, it commonly reflects deeper burial (Scoffin, 1987). Finally, gypsum occurs as an abundant secondary fracture-filling.

The limestones are intercalated with calcareous shales forming rhythmic bedding (Fig. 4.9-C). XRD indicates that the shales consist of quartz, plagioclase, chlorite, illite, calcite, strontian apatite and anhydrite.

The upper part of the sequence includes a dolomitized mudstone 3m thick. The base of this has moved downward as a result of differential liquefaction, load structures were formed accompanied by upwards injection of the underlying laminated marly bed and the formation of flame structures (Fig. 4.9-D). The dolomite has a sucrosic texture of planar-e crystals 10-30μm diameter with vuggy porosity. Under CL, most dolomite crystals have dull cores and bright rims, but some have dull cores with three bright, dull and finally bright outer zones (Fig. 4.10-D). XRD indicates that the dolomite consists of up to 20% of celestite (SrSO4). This can form within

sabkha sediments from strontium released during dolomitization of aragonite and also during the secondary gypsification of anhydrite (Tucker & Wright, 1990). The celestite therefore indicates that the top of the sequence had an evaporative concentration of seawater. However, the XRF indicates higher concentrations of Sr within the marls, these are up to 1203ppm as recorded in location R.

4.3 INTERPRETATION

4.3.1 INTRODUCTION

The Nutaysh Formation has been studied and described by a number of authors in the last decade in attemps to unravel the geodynamic history of the Maqna area in relation to the opening of the Red Sea.

Dullo and others (1983) described the Nutaysh Formation, under the name Telah Member, as a sequence of alternating sandstones, siltstones and marls. They interpreted it as deposited during the lower Miocene in a near shore shallow marine environment where planktonic foraminifera occur frequently.

In 1985 Clark introduced the name Nutaysh Formation for the same sequence and described it as conformable on the Musayr Formation. His descriptions indicate that the unit is characterized by abrupt, mainly dischronous lateral facies changes, from conglomerate to sandstone to shale or marl. He also regarded the sequence as deposited in a shallow water to emergent enviroment.

The same sequence was described by LeNindre *et al.* (1986) as deposited during the late early Miocene along the northern border of the basin. They suggested that it consists dominantly of green marl passing laterally into thin accumulations of conglomerate and sandstone which they regarded as generated in a deeper open marine environment.

Purser and Hotzl (1988) described the Nutaysh Formation as an essentially clastic sequence ranging in age from Aquitanian to Burdigalian. They noted that it seems to reflect increased tectonic activity associated with additional uplift of the flanks and stronger subsidence of the basin. They noted that it consists of sandstones which thin towards the centre of the basin where marls and siltstones prevail and also noted fringing reefs intercalated within the sandstones developed around islands and on marginal fault steps. None of these views is supported by the present observations.

4.3.2 DISCUSSION

Along the northwestern side of the area, clastic sediments, conglomerates and sandstones, formed submarine fans in front of the marginal fault escarpment. They are related to rapid subsidence of the basin as a result of synsedimentary block faulting accentuating the graben and horst pattern. The unstable accumulations from the margin were carried down the fan and finally onto the basin floor (Fig. 4.2).

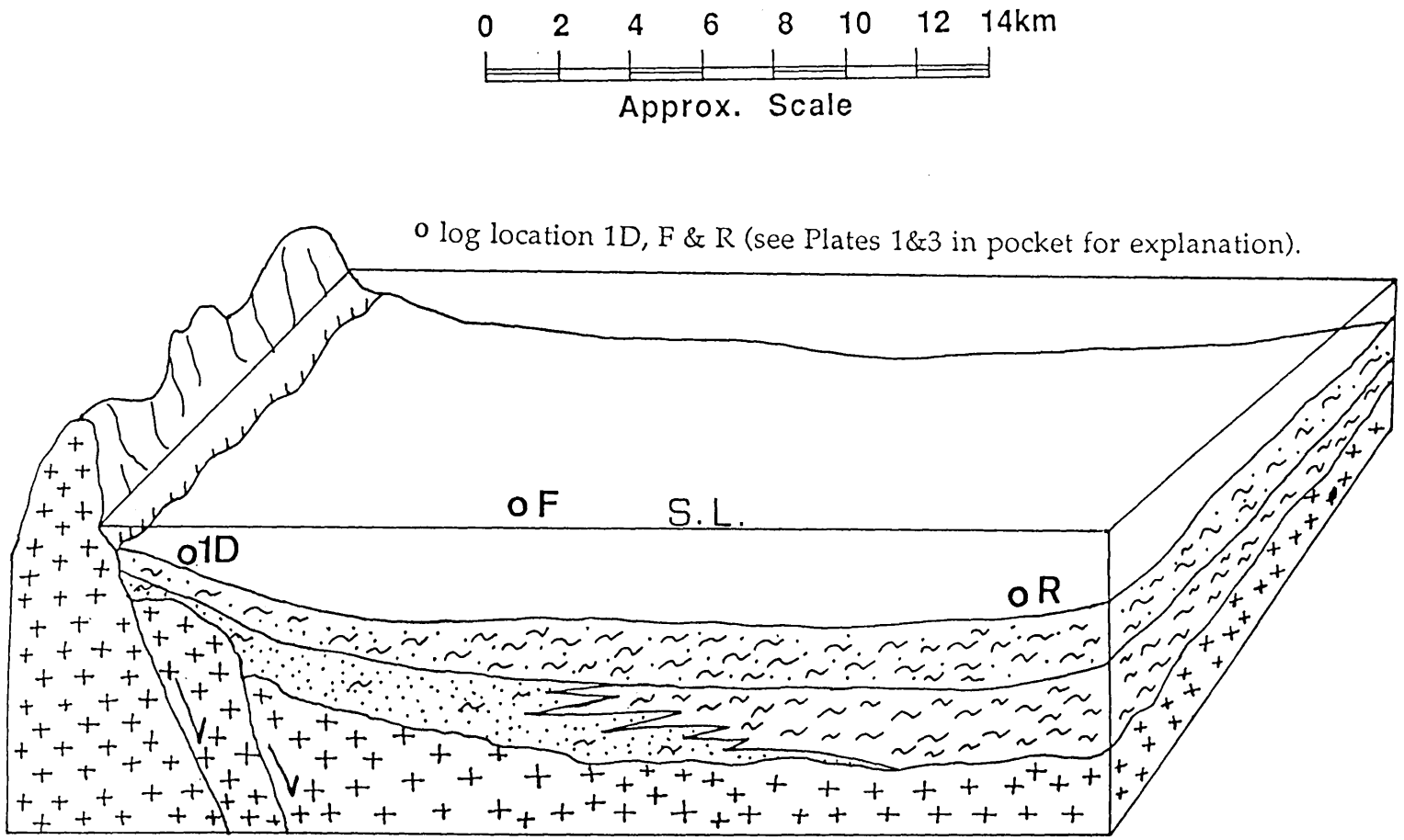

Figure 4.2 Diagrammatic model showing the sequence of depositional environments of the Nutaysh tubidite sediments.

4.3.2.1 INTRODUCTION

The general characteristic of the Nutaysh Formation suggest two possible interpretation, as turbidites, or as storm sediments. The features of each of these systems will be examined in turn.

A-TURBIDITES

Turbidity currents and turbidites

Density currents flow-downslope to basin floors, driven by the density difference between the fluid within the current and the surrounding sea water. This density contrasts could be due to colder temperatures, higher salinities, or to suspended sediment in the current. When the density is due to suspended sediment, the flow is termed a turbidity current. A turbidite is defined as the deposit of a turbidity current.

The concept of turbidites has been used to account for graded sandstone beds that lack evidence of shallow water reworking, and also to explain the transport of shallow water organisms within sandstones which are interbedded with shales containing a bathyal, abyssal or pelagic fauna (Walker, 1984).

Turbidites in the geological record

There are a number of features which can be taken as a set of descriptors for *Classical* turbidites (Walker, 1984):

1. Sandstones and shales are monotonously interbedded through many tens or hundreds of meters of stratigraphic sections.

2. Sandstone beds have sharp, abrupt bases, but tend to grade upwards into finer sand, silt or mud.

3. The undersurface of the sandstones carry abundant markings, now classified into three types; a) *tool marks*, carved into underlying mud by rigid objects (sticks, stones) carried in the turbidity current; b) *scour marks* cut into the underlying muds by fluid scour; and, c) *organic markings* representing trails and burrows filled by deposition from the turbidity currents.

4. Within the sandstone beds, combinations of parallel lamination, ripple cross lamination, climbing ripple cross lamination, convolute lamination and graded bedding occur

An ideal, or generalized sequence of those last features was proposed by Arnold Bouma in 1962, and what is now called the Bouma sequence can be regarded as an excellent facies model for *Classical* turbidites (Fig. 4.4). This model has acted as a general basis for hydrodynamic interpretation.

Facies Classifications

Since Bouma's work, a wider variety of resedimented deposits has been added to the turbidite association. This has been divided by Walker (1978) into a series of facies groups:

(1) Classical turbidites (discussed above).

(2) Massive sandstones. This facies consists of thick sandstones with thin or no interbedded shales. Individual sandstone beds range from about 50cm to many meters thick, and the only Bouma division normally present is division A. A

typical sequence of beds would be measured as A.a.A.a. using the Bouma model. Channelling is frequent, but the one sedimentary structure commonly found in the massive sandstones is the dish strucutre, indicating abundant fluid escape during deposition (Lowe, 1975).

(3) Pebbly sandstones. This facies cannot be described using the Bouma model,nor does it have much in common with the massive sandstone facies. Pebbly sandstones tend to be well graded and stratification is fairly abundant. The facies could easily be confused with a coarse fluvial facies, but the safest way to approach the interpretation is to examine their context, where pebbly sandstones are associate with or interbedded with classical turbidites, their resedimented origin is clear.

(4) Conglomerates are an important facies in deep water environments. Walker (1975a) proposed a sequence of four models for resedimented (deep water) conglomerates, recognized by combinations of structures. They are probably intergradational, their character relating to relative positions down-flow (Fig. 4.3).

(5) Slumps, slides,debris flows and other exotic facies. These facies include diverse group of rocks which are generally poorly to unstratified, and which are commonly poorly sorted. Blocks and boulders which may be many meters in diameter rest in a fine grained matrix, which may show evidence of sedimentary deformation.

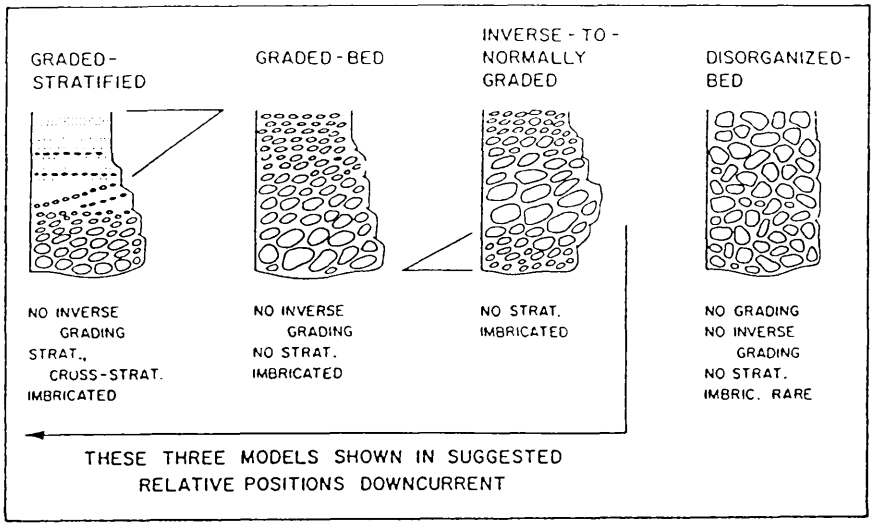

Figure 4.3 Four models for resedimented (deep water) conglomerates, shown in their inferred downcurrent relative positions (Walker, 1975a).

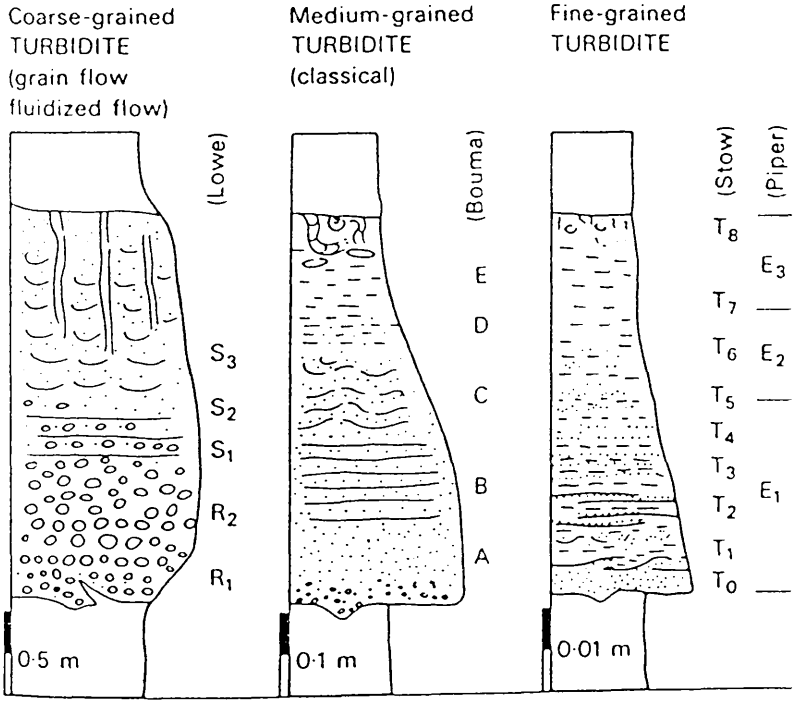

Figure 4.4 Clastic facies models for turbidites (Stow, 1985).

B- STROM DEPOSITS

Storm deposits are characterized by laterally persistent commonly graded, sandstones (and/or conglomerates) interbedded with biotrubated mudstone. Such sandstones commonly have sharp and/or erosive bases, and average 5-100cm thickness. Current-ripple cross-lamination, and medium scale angle-of-repose, crossbeding tend to be rare or absent,and the characteristic sedimentary structure is hummocky cross-stratification (Johnson & Baldwin, 1989).

There are three main associations of storm deposits (Johnon & Baldwin, 1989):

(1) *Shoreline storm sands.* These comprise an amalgamated sequence of erosively bounded storm deposits, with individual beds 5-130cm thick, and without intervening shale layers.

(2) *Proximal storm sands.* These comprise beds between 5 and 100 mm thick which commonly preserve singly waning flow depositional sequences. Each complete sequence consists of (bottom to top): 1) an erosional base, 2) a graded sand layer, 3) a shell layer with a mixed fauna, 4) parallel to low-angle lamination with minor internal discordances (=hummocky cross-stratification), 5) wave ripples, and 6) a mud layer.

(3) *Distal storm sands.* These are finer grained and are generally less than 50 mm thick. Layers may display the following: 1) erosive or non-erosive bases, 2) internal flat lamination, 3) rare grading or cross-lamination, and 4) parautochthonous shell layers, mainly winnowed and only slightly transported.

A major problem in identifying storm layers is their association with bioturbation. this can completely obliterate individual storm sand layers in off shore/outer shelf settings (Howard and Nelson, 1982). Individual storm sandstone beds are probably deposited rapidly, possibly over a period of a few hours to several days, and represent single waning flow events, which frequently possess a strong oscillatory flow component. Superficially some storm beds resemble turbidites, but they are distinguished by the presence of wave-formed sedimentary structures or shallow marine faunas in the intercalated shale layers. Thickness, geometry, and composition, are influenced particularly by the magnitude and duration of the storm, the nature and proximity of the sediment source area, and relative position of deposition along the storm transport path, beds pass downcurrent into thinner, more distal units.

4.3.2.2 INTERPRETATION

Introduction

In the Maqna area, the Nutaysh formation is represented by a sequence of siliciclastic sediments which show abrupt facies changes from what are presumably proximal coarse conglomerates and sandstones to fine grained marls which thought to be the distal sediments of deeper water. The formation has a thickness of at least 250 meters.

A number of features are recognized throughout the Maqna area:

(1) The sandstones are immature and poorly sorted and commonly contain angular to subsangular gains. Channels are common, and contain subangular to well

rounded boulders up to about 2m diameter, mainly of granite but with a few irregular blocks of shale.

(2) Sandstone beds are typically graded, passing upwards into finer sands, silts and muds. Many are arkosic. Some contain a shallow water transported faunal assemblage.

(3) Sandstones and marls form monotonously interbedded rhythmic sequences through several tens of meters. Individual beds have flat tops and bottoms and are laterally persistent..

(4) Marls are laminated and contained a bathyal or abyssal fauna as a result of hemipelagic deposition. Generally, the marly beds are not strictly marls, they include well laminated, partially fissile calcareous shales and limestones which may be partly or wholly dolomitized. Bioclasts are micro-fossils including abundant Globigerinid forams with less frequent benthic forams such as *Nummulites* and *Textularia*. Siliceous micro-fossils hace also been found including the pelagic radiolarian *Actionomma* and diatoms.

(5) Pebbly sandstone beds commonly fill channels and are laterally discontinuous, they are rarely interbedded with shales.

(6) Conglomerates (Boulders up to 8cm), are graded, normal grading being more common than inverse, and in places they are stratified into thin sheets.

Aigner and Reineck (1982) described a number of features to differentiate storm sediments from turbidites. These are: 1) wave ripple cross-lamination, 2) wave rippled top surfaces, 3) in situ shallow marine shelf faunas within distal shelf muds, 4) a marked increase in the bioturbation of storm sand layers from proximal to distal

settings, and 5) an association with shallow water facies. The Nutaysh Formation sequences show none of the above features, and in addition, the characters of both conglomerates and channel-filling conglomerates cannot be produced by storm deposits.

The Depositional Environment

Along the northern edge of the Maqna area, clastic sediments, conglomerates, sandstones and marls, formed submarine fans in the front of the marginal fault escarpment. their deposition was related to rapid subsidence of the basin as a result of the synsedimentary block faulting accentuating the existing graben and horst pattern. The unstable accumulations from the margin were carried down the fan by turbidity currents and finally onto the basin floor.

The sequence of the Nutaysh Formation, represents a composite cycle from coarse, medium and fine turbidites. The proximal clastic sediments include polymict conglomerates and immature sandstones which commonly show graded bedding. The sandstones are poorly sorted with angular grains and sometimes contain irregular blocks of shale. the upper part of the unit is characterized by channels filled with conglomerate. To the SW, towards the center of the basin, finer grained sediments reflect more distal turbidity currents. These are relatively free of terrigenous grains. Immature sandstone intercalations contain sparse bioclasts of shallow water organisms. Vertically, the rhythmic bedding, mainly of carbonates, together with the siliceous micro-fauna and planktonic forams all indicate a quieter deeper marine environment.

Stow (1989), recognized three turbidite models (Fig. 4.4). These include:

1. *Coarse-grained turbidites* (Lowe, 1982). The lower part of the sequence can comprise gravel, pebbly sand or sand, overlying a sharp, scoured base. Characteristic structures include, negatively-graded lower division (R_1), graded-stratified (S_2) and pipe structure(S_3) divisions. The top is commonly sharp and flat.

2. *Medium-grained turbidites* (Bouma, 1962). Five structural divisions are present overlying a sharp, erosive or loaded base, massive to graded sand (T_a), parallel-laminated sand (T_b), cross-laminated and convolute sand (T_c), parallel-laminated fine sand and silt (T_d), and massive to bioturbated mud (T_e).

3. *Fine-grained turbidites*. A graded silt-laminated mud division (E_1) passes upward into a graded mud (E_2) and nongraded mud (E_3) described by Piper (1979). Stow (1985) suggested that the grade laminated unit (E_1) can be further subdivided into a thick, often lenticular, basal laminate silt with fading ripples at the top (T_0), a relatively thick mud layer with convolute silt laminae (T_1), low amplitude ripples (T_2), parallel distinct laminae (T_3), parallel indistinct laminae (T_4) and wispy siltlaminae(T_5). These are overlain by graded mud (T_6), nongraded mud (T_7) and a thin micro-bioturbated zone (T_8) Stow (1989) suggested that complete sequences are rarely deposited and partial sequences are the rule (top-absent, base-absent, mid-absent, etc.).

The turbidite sequence of the Nutaysh Formation in the Maqna area includes: *coarse* R_2 & S_2 (Lowe, 1982), *medium* A, B, D & E (Bouma, 1962), and *fine* E_1 & E_3

(Piper, 1979) turbidites (Fig. 4.4). However, part of the sequence includes B, D & E units of Bouma (1962) which are common in turbidites (Walker, 1984).

4.3.3 THE DIAGENETIC ENVIRONMENT

The early burial changes were characterized by the prcipitation of near surface marine fibrous sparry calcite cement, originally of aragonite. Microcrystalline dolomite was formed during the early stage of diagenesis. This stage corresponds to the transformation of aragonite into microcrystalline dolomite; the Sr^{+2} released from aragonite reacts with $SO4^{-2}$ to form celestite (Kinsman, 1969). The aragonite was partially dissolved and replaced by cristobalite cement which may have formed from hydrothermal solutions released by axial rifting. The authigenetic clays in the sandstones and in the shales formed as a result of later diagenetic changes over a long time and/or following deep burial (Pettijohn *et al.*, 1973). Finally, the evaporite cements include gypsum and halite. These were products of surface weathering under subaerial conditions as the rocks returned to the telegenetic zone. Figure (4.5) shows the lateral distribution of the digenetic sequence in the Nutaysh Formation.

In the Maqna area, the sparry calcite cement sequence reflects the burial history. The marginal siliciclastic turbidite sequence contains three generations of calcite cement. An early equant (dull) calcite of marine phreatic origin was followed by a blocky bright cement with dull subzones formed in the mixing zone (high content of iron oxides) and then later precipitation of blocky non-luminescent cement under subaerial conditions. In cotrasts, in the center of the basin, the fine grained turbidites contain four generations of calcite cement. An early fibrous (dull)

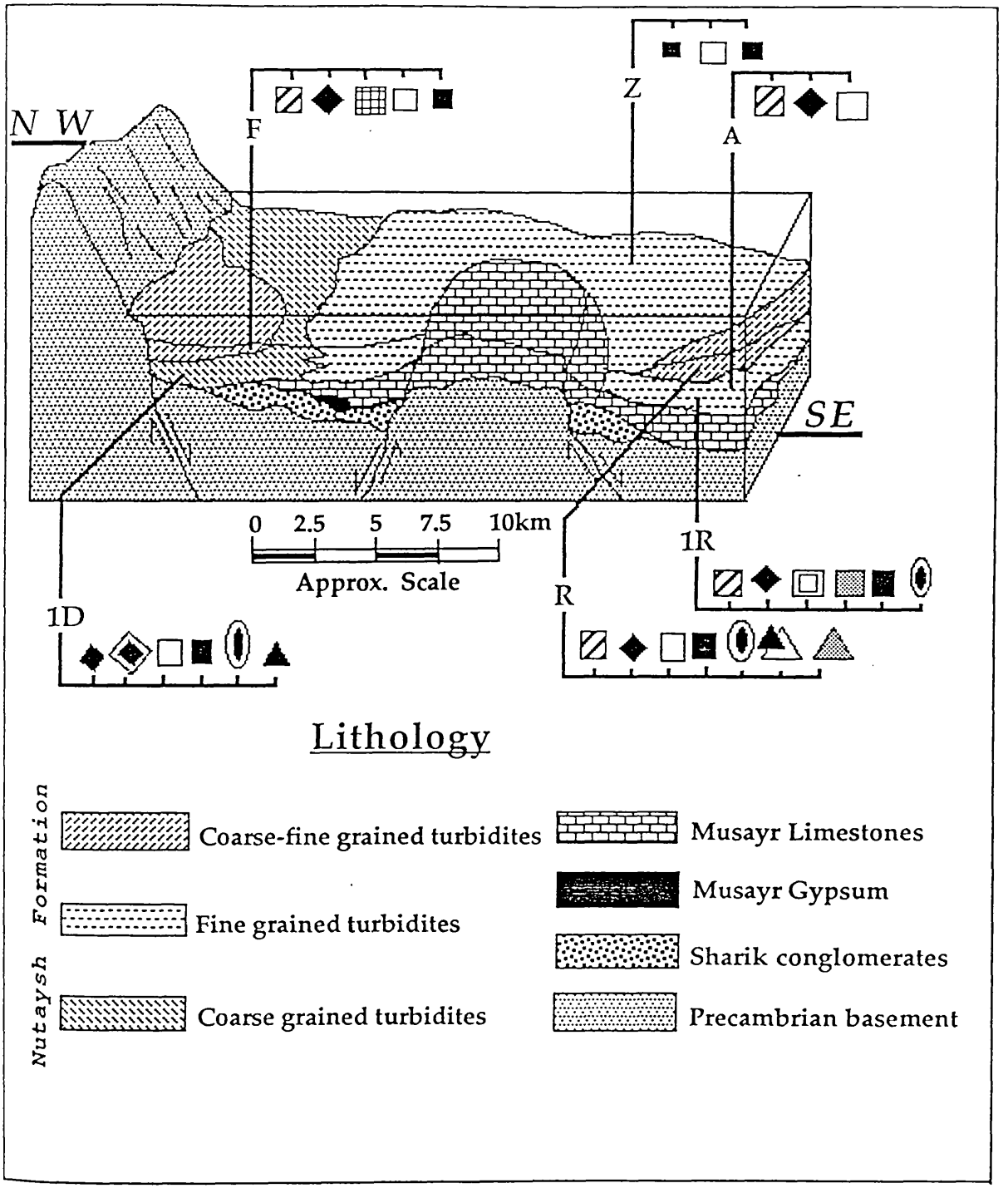

Figure 4.5 Lateral distribution of the diagenetic sequence in the Nutaysh Formation. The diagrammatic model shows the relationship between the Tertiary sediments excluding the Bad evaporite sediments (see Fig. 3.6 for the explanation and Plates 3 & 4 for the log locations referred to here).

originally marine aragonite, is followed by blocky bright marine phreatic and blocky dull cements formed in the mixing zone. The final blocky non-luminescent cement formed under subaerial conditions. In both calcite cement sequences, dissolution occured before precipitation of the late non-luminescent phase. The difference between the two sparry calcite sequences is attributed to their structural positions during diagenesis. The margins of the basin are structural higher, increasing the possibility for the early fibrous sparry calcite cement to have been dissolved.

The cement sequences of the Nutaysh turbidites in the Maqna area indicate a gradual fall in sea-level. The diagenetic environment of the sediments changed from marine to mixing zone and finally to subaerial conditions.

4.3.4 COMPARISON WITH OTHER AREAS

The Nutaysh Fomation may be compared with the sequence decribed by Said (1962) from the Gulf of Suez Region including the basal Miocene beds and the lower *Globigerina* Marl (Lower Miocene). In marginal areas of the Gulf of Suez basin, as well as on certain isolated highs, sediments include limestones with abundant *Pecten* and oyster shells, while in deeper parts of the trough the *Globigerina* Marl beds (greenish-grey to brown) accumulated (Said, 1962). However, in the Maqna area, Said's suggestion is not acceptable, as it indicates a contemporaneous deposition for the Musayr and the Nutaysh Formations.

According to Said (1962), the *Globigerina* Marl follows the basal Miocene beds or rests on older rocks in different parts of the Gulf of Suez. The basal Miocene is a

series of sandstones and polymictic conglomerates composed of a great variety of rocks of both extra- and intraformationl origin. These are similar to the Nutaysh clastic sediments, but their environment was not defined.

Recent studies (Purser & Hotzel, 1988; Purser *et al.*, 1990), suggest that the Midyan Region represents a different siliciclastic-carbonate association from that in Egypt. The marine transgression probably affected the axial parts of the basin in the Midyan region before reaching its periphery on the Egyptian coast.

NUTAYSH FORMATION

Figure 4.6

A. Part of the channel-filling conglomerate in locality 1D. The boulders derived from the Precambrian basement and are mainly granitic.

B. Channel containing irregular blocks of greyish-green shale in locality 1D.

C. Reverse current grading. Sandstone coarsening upwards to pebbly conglomerate in locality 1D.

D. Sandstone dykes cutting underlying shales in locality D.

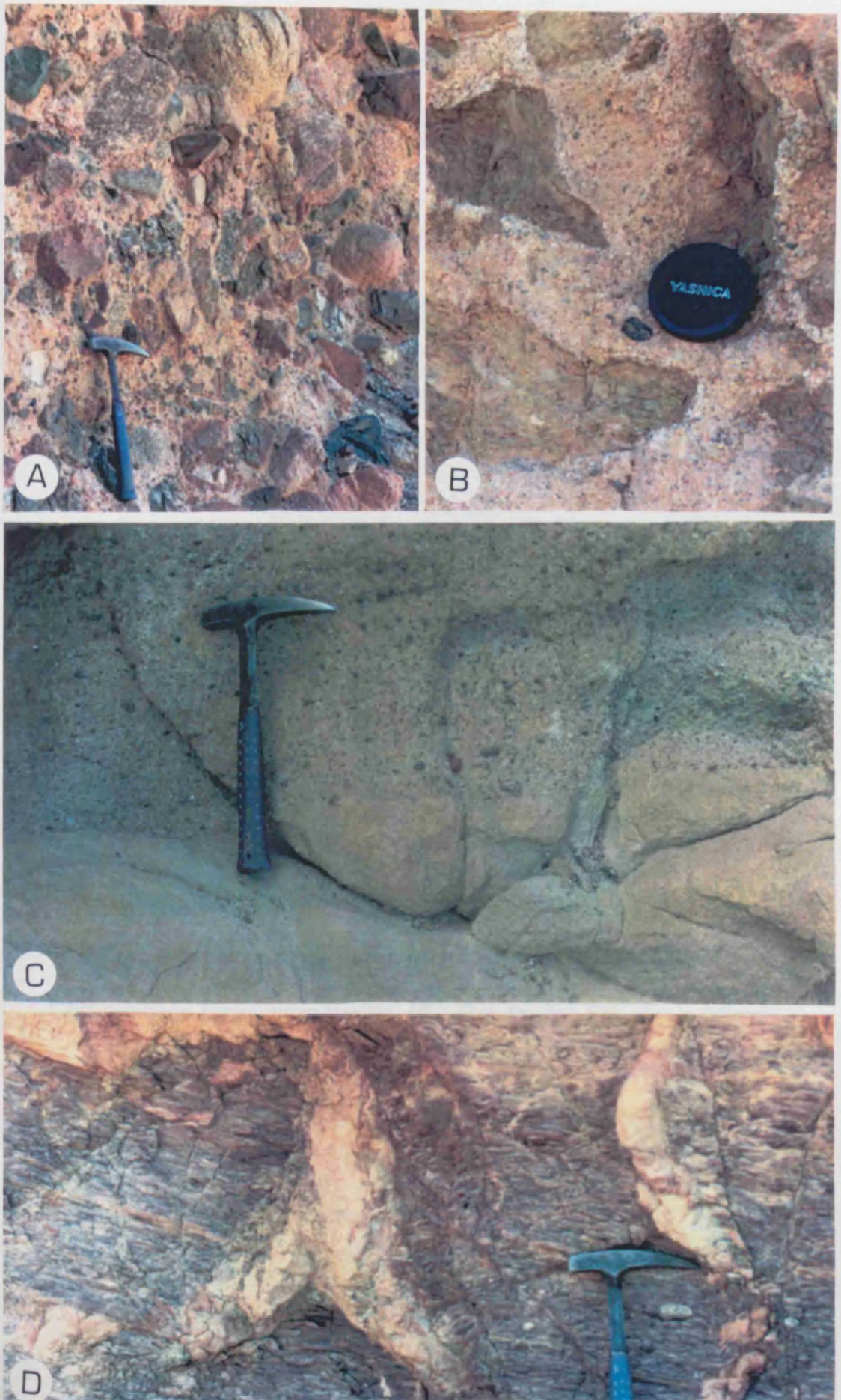
A
B
YASHICA
C
D

Figure 4.7

A. SEM shows angular grains of quartz (Q) and K-feldspar (F) cemented by finely crystalline dolomite (D).

B. SEM, shows authigenic illite crystals (i) cementing the detrital quartz grains (Q).

C. Three generations of blocky sparry calcite cement within dissolved bivalve bioclasts. These are dark, bright and, finally dark with bright rims. Thin section, CL. Scale 0.2mm.

D. Nummulites (N) enclosed within turbidite sandstone in locality A. Thin section, CL. Scale 0.4mm.

E. Shallow-water bioclasts including oyster (O) and coralline algae (C) within foraminiferal limestone in locality 1R. Thin section, Ppl. Scale 0.8mm.

F. An agglutinated Textularid within foraminiferal limestone in locality 1R. Thin section, Xpl. Scale 0.2mm.

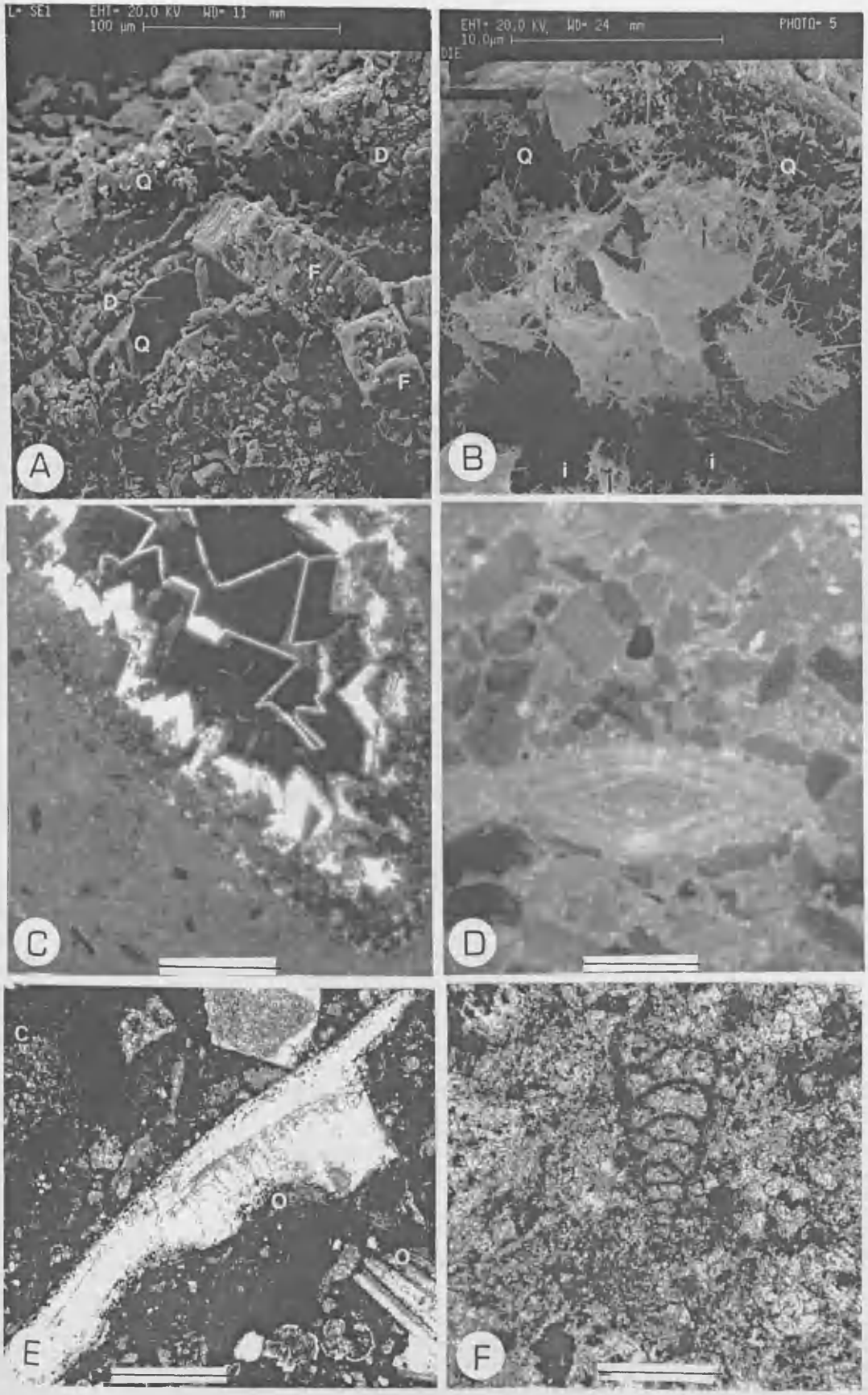
L* SE1 EHT= 20.0 KV WD= 11 mm
100 µm
D
Q
F
D
Q
F
A
EHT= 20.0 KV WD= 24 mm PHOTO= 5
10.0µm
DIE
Q
Q
B
i
i
C
D
C
O
O
E
F

Figure 4.8

A. Agglutinated worm tubes filled by micrite matrix within foraminiferal limestone in locality 1R. Thin section, CL. Scale 0.4mm.

B. The radiolarian *Actinomma* (R) within foraminiferal limestone in locality F. Thin section, CL. Scale 0.1mm.

C. Dolomite crystals scattered within the micrite matrix of the foraminiferal limestone in locality F. Thin section, CL. Scale 0.2mm.

D. SEM. Diagenetic crystals of K-feldspar (F) within sandstone in locality F.

E. SEM, shows blocky sparry calcite cementing the detrital grains of sandstone in locality F.

F. SEM. Dolomite crystal (D) with dissolved core overlain by calcite cement (C) within sandstone in locality F.

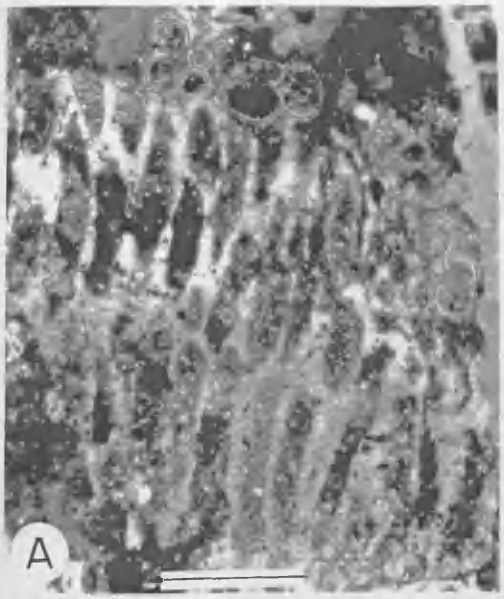
A

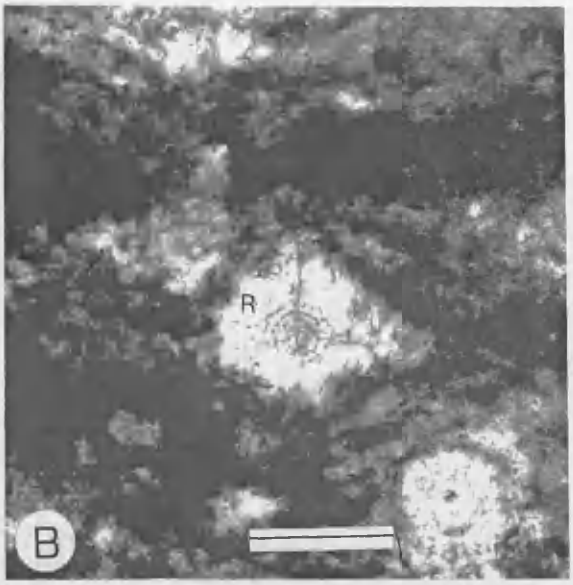
R
B

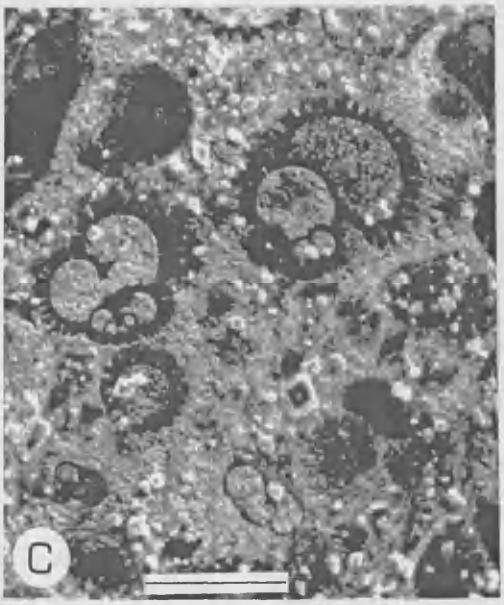
C

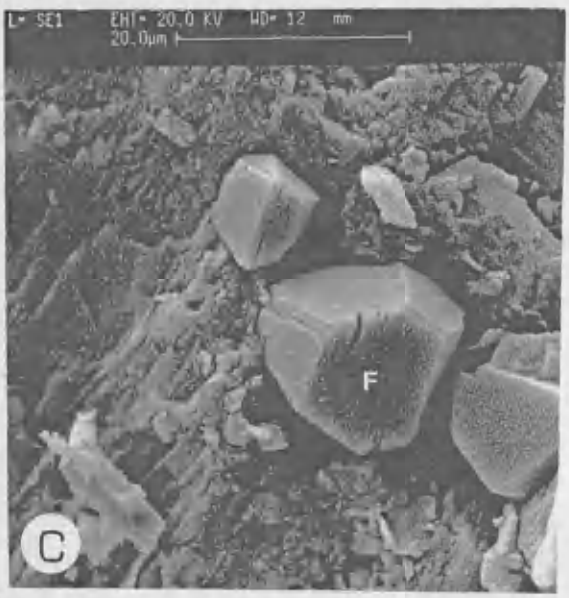
L- SE1 EHT- 20.0 KV WD- 12 mm
20.0µm
F
C

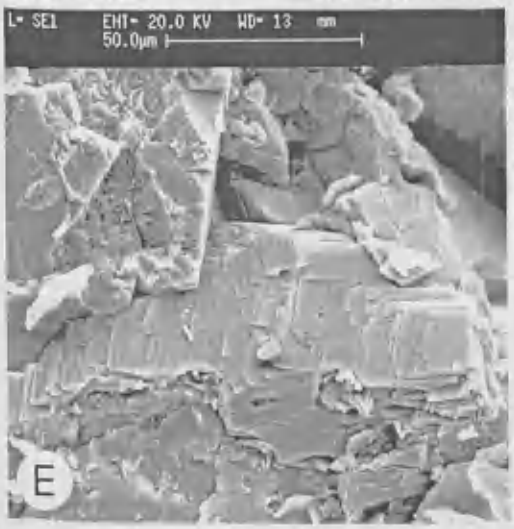
L- SE1 EHT- 20.0 KV WD- 13 mm
50.0µm
E

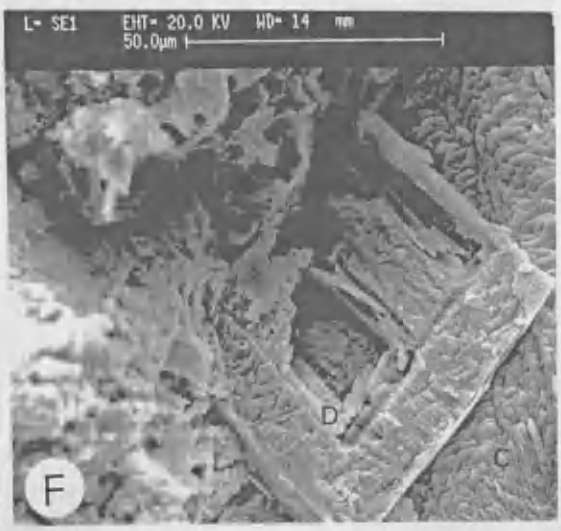
L- SE1 EHT- 20.0 KV WD- 14 mm
50.0µm
D
C
F

Figure 4.9

A. Upwards transition from poorly laminated mudstone through channel sandstone to boulder conglomerate in locality AA. Channel-filling conglomerate (C) cutting through the sandstone unit.

B. Marly units in locality F. These are well laminated and partially fissile, some are nodular.

C. Rhythmic bedding formed by foraminiferal limestones intercalated with calcareous shales in locality R.

D. Load structures, in the upper part of the marly sequence of locality R.


c
A


B

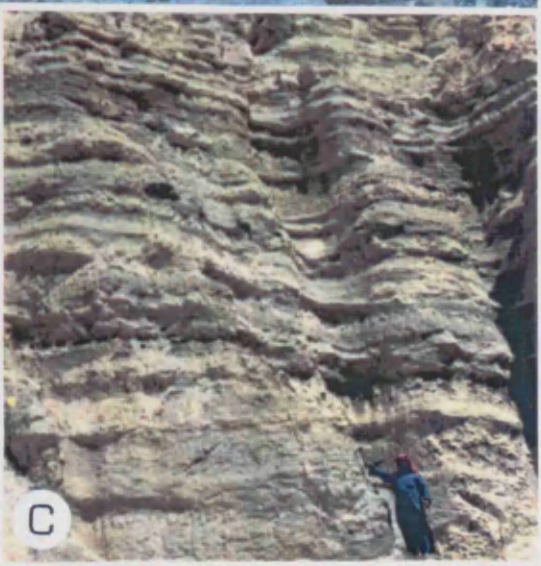
C


D

Figure 4.10

A. Dolomite crystals scattered within micrite matrix of foraminiferal limestone in locality R. Thin section, CL. Scale 0.2mm.

B. Fragments (B) of what could be fish bones. Thin section, CL. Scale 0.2mm.

C. Cristobalite cement occluding *Globigerina* cavity. Thin section, Xpl. Scale 0.1mm.

D. Multi-zoned planar-s dolomite crystals in locality R. Thin section, CL. Scale 0.2mm.

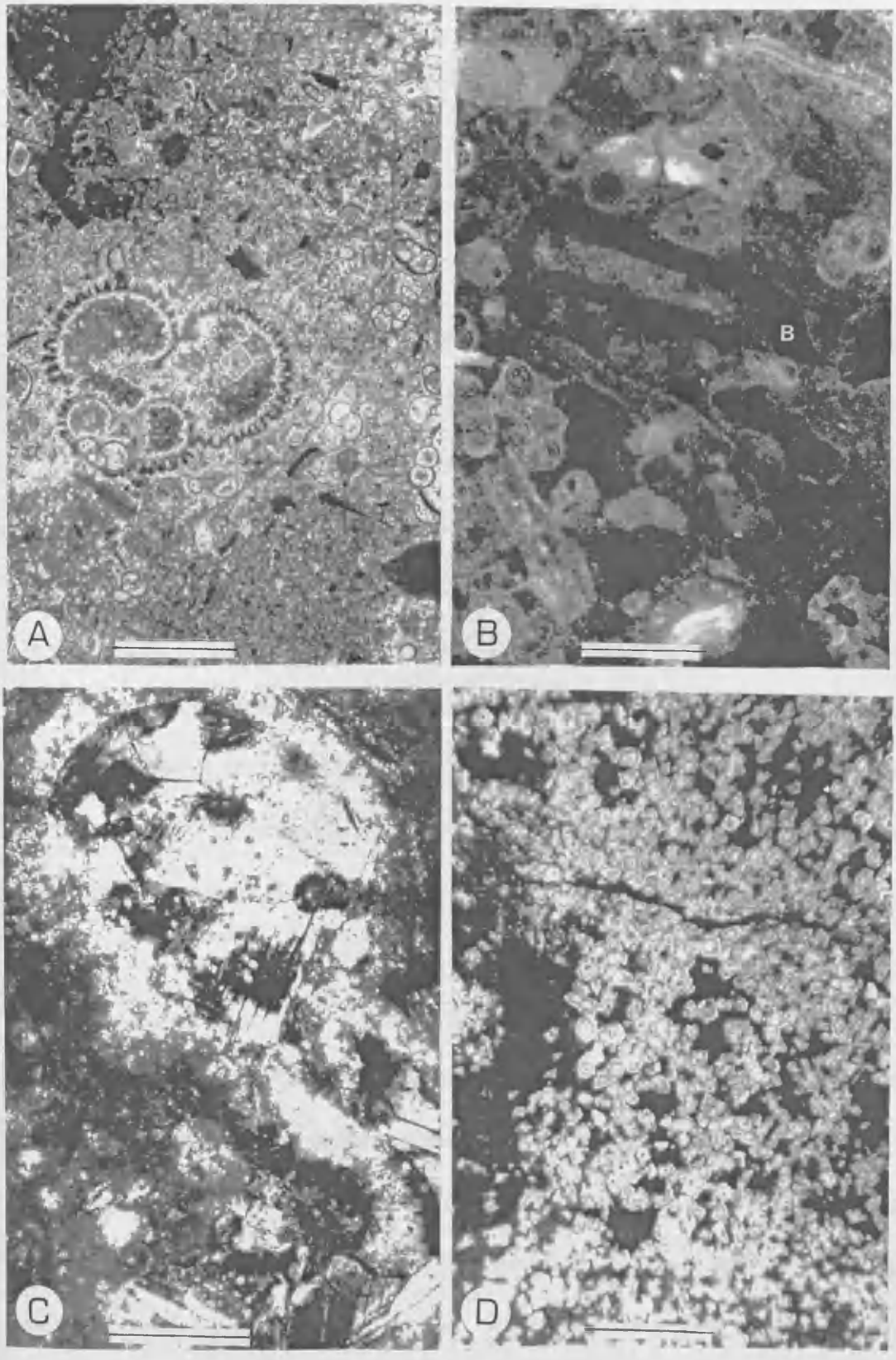
A
B
B
C
D

CHAPTER V

THE BAD FORMATION

The Bad Formation was informally named by Bokhari (1981) after the town of Al-Bad, a large oasis settlement located 35Km to the east of Maqna. Outcrops of the Bad Formation are characterized by the occurence of evaporites, seen capping mountains throughout the area. The true thickness of the unit is often masked as a result of weathering and erosion of these evaporite beds. In places the whole surface is covered by a coat of evaporite blocks within a white evaporite soil, completely obscuring the underlying rocks. For this reason there are wide variations in the thickness of the Bad Formation suggested by different workers, ranging from 130m (LeNindre, 1981) up to 1,500m (Bokhari, 1981). In the present work the thickness of the Bad Formation is regarded as 120 meters, recorded west of Jabel Tayran in location F.

In the Maqna area, the Bad Formation unconformably overlies the Nutaysh Formation. The relatively uniform character of the formation strata do not allow it to be separated into different members (Fig. 5.1). In general, beds dip to the east, forming the steep faces of cuestas, but they are clearly folded to form broad domes and there are a number of normal faults. Agocs and Kahr (1962), noted that the evaporite outcrops form broad domal structures and later Bigot and Aladouvette

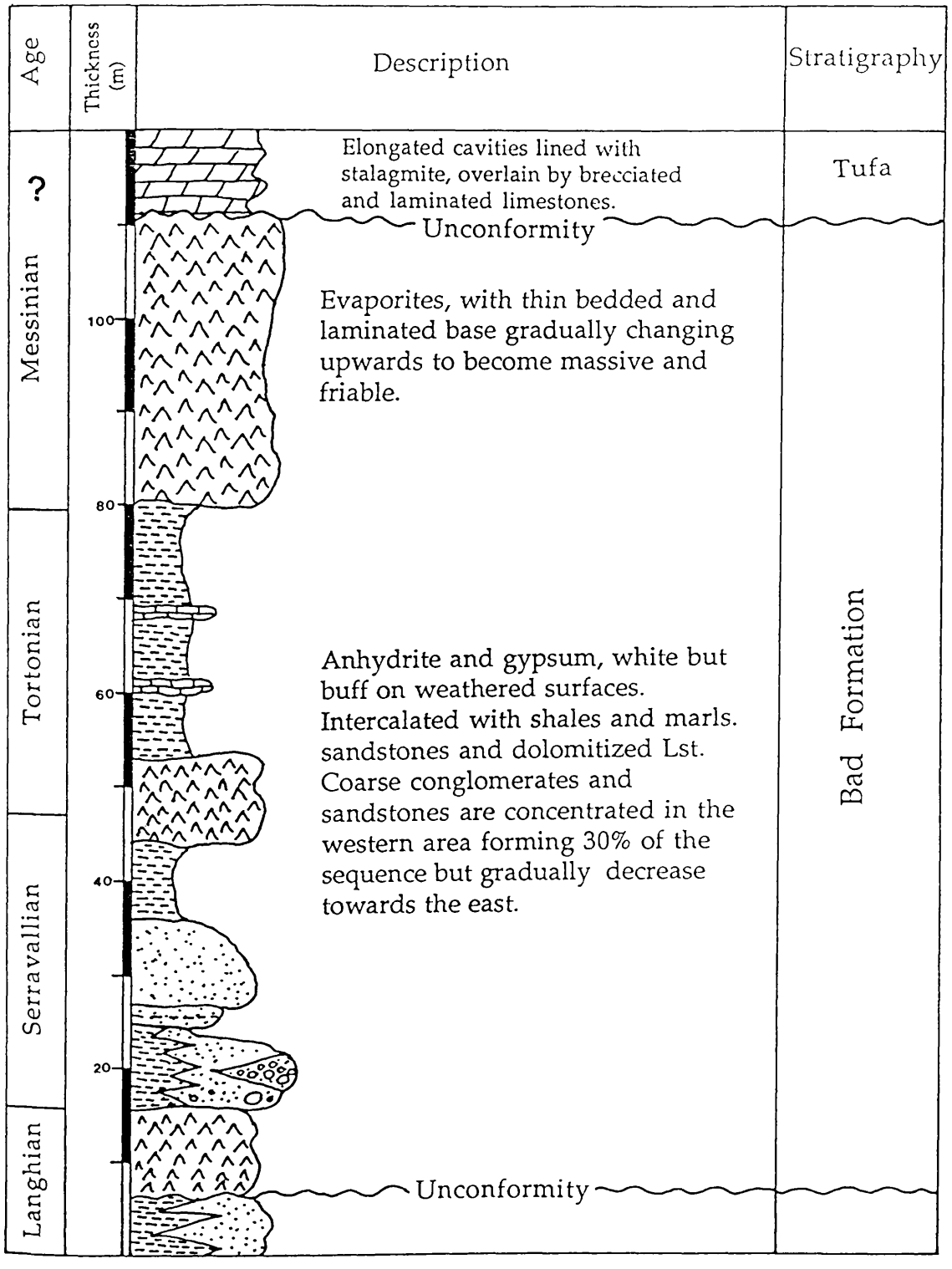

Figure 5.1 Generalized log section for the Bad Formation (see Plates 2 & 3 for explanation).

(1973) suggested that these were probably salt domes. Motti *et al.*, (1982) also suggested that open fold structures in the Maqna area may have resulted from plastic diapiric movements of some deeper underlying salt but no thick salt deposits have been identified in this area.

Outcrops of the Bad Formation are mainly concentrated in the southern and eastern parts of the Maqna area. They are extensive and their total surface area in the Midyan peninsula (including the Maqna area) is estimated at 175Km/sq (Spencer, 1985).

Spencer (1985) suggested that the evaporite body as a whole is mostly anhydrite, and that all the gypsum present lies in the upper 15-20m. In his view the anhydrite is secondary and anhydritisation was probably the result of a period of burial. The subsequent transformation of anhydrite into gypsum was probably caused by surficial circulation of fresh water folloing exposure (LeNindre *et al.*, 1986).

The strata of the Bad Formation are thought to have been deposited during the Middle Miocene but there is a lack of macro-fossil content. However, the foraminiferal fauna of carbonates within the formation suggests a Middle Miocene (Langhian) age, as assigned by Purser and Hotzl (1988). Van der Ploeg (1953) suggested that during the Middle Miocene (Helventian) a submarine sill formed to the north of Suez, perhaps as a result of intensive tectonic activity. This may have continued during the Burdigalian (Swartz and Arden, 1960) and could reflect the beginnings of basin restriction which led eventually to regional evaporite deposition.

However, evaporites are found from Suez southward to Farasan and beyond (Swartz and Arden, 1960), and it is not yet clear whether these separate occurences represent parts of a single basin.

5.1 SEDIMENTOLOGY AND PETROGRAPHY

As indicated, the Bad Formation is characterized by evaporites, beds of anhydrite and gypsum known by earlier workers as the Maqna Massif Evaporites. The sequence is represented by several evaporite units of variable thickness from 2m up to the 40m recorded in Jabel Ar-Raghama in location R. The evaporite units are white when fresh but buff on weathered surfaces. The evaporite beds are mainly intercalated with shales, sandstones and carbonates (dominantly dolomite). Coarse detrital materials are concentrated in western parts of the area. Around location F coarse detritus forms up to 30% of the sequence, gradually increasing towards the northwest.

5.1.1 WESTERN OUTCROPS

The western outcrops of the Bad Formation are represented by locations D and F (Plate 3).

In location D south of Jabel Faya, the Formation is represented by evaporites up to 4m thick, generally dipping to the east. There are no clastics in this area. The evaporites unconformably overlie the brownish gypsiferous shales of the Nutaysh Formation. At the base about one meter is thin bedded and laminated. This gradually changes upwards to become massive and friable (Fig. 5.3-A). XRD

analyses indicate that the laminated part of the unit is composed of anhydrite with a little dolomite while the rest is pure anhydrite.

In thin section the laminated anhydrite consists of layers of needle-fibrous crystals of anhydrite (500μm max. length) and discontinuous lamellar interclations of dolomitised carbonate mud, made up of non-planar dolomite crystals up to 10μm diameter. Under CL the dolomite generally has a homogeneous dull luminescence but some crystals have bright rims.

To the east, in location F, south of Jabel Tayran, the sequence of the Bad Formation is up to 120m thick and includes three evaporite units, each up to 4.5 meters thickness. The XRD analyses indicate that these evaporites are predominantly anhydrite and no dolomite is present in this area, although there is some halite. Interclated with the evaporites are shales, sandstones and conglomerates. The sequence again rests unconformably on the greyish-green shales of the Nutaysh Formation. Beds generally dip to the southeast and are massive and friable and commonly contain veins filled with gypsum.

In location F, the base of the succession is marked by 3 meters of thinly bedded evaporites. Overlying these is a well laminated greyish-green marl which is in part gypsiferous. This contains several thin white beds (6cm max. thickness) of fine grained calcareous sandstones and siltstones with prominent veins of gypsum. A second 2m thick evaporite is followed by about 6m of marls similar to those below.

The middle part of the sequence, 30 meters thick, is predominantly of coarse clastic sediments. These begin with sandstones 3m thick, grading from pebbly-coarse to medium grained with a reddish-brown muddy matrix. The sandstones fill the floor of a large channel and contain blocks of greyish-green shale up to 30cm long and 8cm wide forming large scale rip-up clasts (Fig. 5.3-B).

The overlying sequence consists of about 25m of interbedded sandstones and mudstones (marls). The sandstones are 10-50cm thick but are grouped into packets of several meters which increase in thickness upwards. These sandstones are graded, fining upwards into laminated siltstones, but lack any other structures. Above them, about 15m of sandstones include two prominantly graded conglomerates. The conglomerates contain subrounded to well-rounded boulders, up to 20cm diameter, mainly of igneous rocks such as andesite and rhyolite. The upper part of the unit is formed by two cycles of channel filling up to 1.5m thick. Elongated blocks of marl rest parallel to the channel floor within the lower cycle (Fig. 5.3-C).

In location F the upper part of the Bad Formation consists of 40m of laminated greyish-green gypsiferous marl, weathered brown. Two units of thin bedded white calcareous fine sandstones and siltstones up to 6m thick and lacking structures are included within these marls.

The marly units are dolomitised of originally fossiliferous wackestone. The XRD analyses indicate the presence of quartz, cristobalite and halite. Dolomite crystals are non-planar grains <10μm diameter, they are mostly ferroan with non-luminescent

or dull cores and bright rims. Detrital quartz grains are scarce (<1%) most are fine grained <80μm diameter and angular with blue luminescence under CL. The cavities produced in dissolved foraminiferal shells are occluded by a cristobalite cement consisting of dominantly anhedral crystals 120um X 50um. Iron oxides occur intermittently, staining the surfaces of fractures and dissolution seams. Intercalated black laminae, most obvious in thin section, may represent stromatolitic algal mat films and thus growth in the photic zone (Schreiber & Friedman, 1976). The lower marly beds include notable burrows of 500μm diameter crossing the lamination.

The marly sequence is intercalated by several shalely units, which are friable gypsiferous and containing foraminiferal bioclasts. The XRD analyses indicate the presence in these of dolomite, illite, kaolinite, plagioclase quartz and gypsum. They also contain elongated phosphate fragments (fish bones) deposited mainly parallel to lamination. The last suggest a period of relatively slow deposition under open marine infuence. A gypsum cement with anhedral crystals <20μm diameter occurrs as fructure fillings.

The sequence is capped by 4.5m of friable jointed evaporites with blocks dispersed on the mountain slope. These are thin bedded at the base, intercalated with thin carbonate muds, but are massive and unbedded at the top (Fig. 5.3-D). They consists predominantly of fine crystalline anhydrite with notable cavities filled with coarse polygonal crystals (600um X 200um) of anhydrite cement. The associated carbonate muds include fenestral porosity but are commonly compacted as a result of displacive growth of evaporites (cf. Walker, 1984). Under CL, the mud is dull

while pores contain a non-luminescent blocky spar cement (crystals 60-100μm diameter). Notable non-planar dolomite crystals (<10μm diameter) with dull cores and brighter rims occur scattered within the carbonate muds.

To the south, on the south side of the western entrance of Wadi Al-Karaj, only the upper-most part of the sequence is exposed. The upper evaporite unit is dominanly well bedded and is here interclated with greyish-green marls and fine sandstones 15-20cm thick. Within the sandstones convolute bedding and climbing ripple lamination are present. Climbing ripples suggests rapid deposition from suspension while convolute bedding suggests liquefacation as a result of dewatering associated with rapid deposition (Lindholm, 1987).

5.1.2 EASTERN OUTCROPS

The eastern outcrops are represented by locations R and Mu on Jabel Ar-Raghama, close to Jabel Al-Musayr. In contrast to the area to the west, the Bad Formation in location R is represented largely by marls. There are no conglomerates and almost no sandstones, suggesting that this may have been a deeper part of the basin or further from the source. Four units of evaporites ranging from 1-40 meters thick are present. Most are thinly bedded but only the basal 2 meters of the upper-most evaporite is laminated, becoming more massive upwards and forming the steep faces of cuestas facing west. Interclated within the second evaporite are discontinuous lenses of marls 30cm maximum thickness.

The third evaporite consists almost entirely of equant crystals (20μm max. diameter) of anhydrite with fibrous crystals (up to 300μm length) of anhydrite occuring as a later fracture filling. Non-planar (15μm max. diameter) dolomite crystals are scattered within the anhydrite, and under CL, show dull ferroan cores and bright rims, while the anhydrite shows transient blue luminescence. However, XRD analysis indicates that halite is also present. The sequence is capped by the upper evaporite, 40 meters thick, the thickest evaporitic unit in the Maqna area (Plate 3).

The interclated marly units vary in thickness. The thickest, 28 meters, occurs below the upper evaporite bed. In general the marls beneath evaporites are slightly bioturbated and more gypsiferous as a result of recent dissolution of the overlying evaporite layer. They are well laminated and mainly greyish-green in colour, while interclated layers of calcareous mudstone are yellowish-green or brownish.

Within the three marl sequences quartz and feldspar grains are generally scarce. Grains are mainly angular <40μm diameter and under CL show blue luminescence for quartz and lemon-green for feldspar. Elongated bone fragments occur mainly within bands parallel to the laminations. A cement of dominantly cristobalite (confirmed by XRD) fills cavities and partially replaces fibrous anhydrite crystals. Neomorphic spotted dolomite crystals up to 30μm diameter with corroded edges occur within the matrix which is generally fine grained calcite (micrite). These have dull cores and bright outer zones of luminescence under CL (Fig. 5.4-A). They probably indicate dolomitization by marine or hypersaline-water, followed by neomorphism in meteoric or hydrothermal fluids, and then selective dissolution

(Conglio *et al.*, 1988). Only one bed 0.5 meter thick, overlying the third anhydrite, is completely dolomitised. This is characterized by a fine grained texture (crystals <3μm diameter) and a rounded vuggy porosity. Crystals in this show a homogeneous dull luminescence under CL (Fig. 5.4-B). Fine grained dolomite associated with evaporites is usually of early diagenetic, near-surface, origin and indicate an arid climate (Lumsden & Chimahusky, 1980). However,such dolomite would not be expected to show bright luminescence and these must therefore be of later origin or have been neomorphsed during burial.

To the south of location R, in location Mu, the entire sequence of the Bad formation is represented by only 15 meters of massive and fractured sulphate conformably overlying the *Globigerina* Marl of the Nutaysh Formation.

5.1.3 SOUTHERN OUTCROPS

The sequence of the Bad Formation in southern outcrops can be illustrated by the stratigraphic log of location HN north of Wadi Al-Karaj. This shows two evaporite units separated by a dolomitised marly unit.

The lower evaporite is 3 meters thick, laminated, and becomes fractured and less laminated towards the top. The overlying marly unit is 20 meters thick, greyish-green and well laminated. These are slightly gypsiferous and include a number of thin (3-10cm thick) dolomite beds. The base of the marly unit includes a greyish hard bed 0.3m thick of finely crystalline dolomite which weathers to dark brown. This dolomite bed consists of sucrosic planar-s crystals (10-40μm diameter), with

early calcite and later gypsum cements filling pores formed after dissolution of the dolomite. Under CL the dolomite crystals generally show bright luminescence but some have dull ferroan cores (Fig. 5.4-C). The equant calcite spar cement (crystals <20μm diameter) has a dull luminescence.

The upper evaporite, 6 meters thick, is massive and fractured. Laterally over distances of hundreds of meters it seems to be split into three or even four separate beds. Scattered ellipsoidal blocks of greyish anhydrite (0.8m max. diameter) occur embedded within the upper evaporite and on its surface. These may be residual masses following hydration. The anhydrite blocks consists of coarse radial crystals with local patches of polygonal crystals of the original gypsum. Up to 20% dolomite is present consisting of non-planar crystals (5-30μm diameter) which have a generally bright luminescence under CL; scarce crystals have dull ferroan cores (Fig. 5.4-D). Anhydrite can form by the dehydration of gypsum, either by heating or by immersing it in a very saline environment (Kendall, 1984). Increased salinity has the effect of increasing the pore-fluid Mg/Ca ratio (Lumsden & Chimahusky, 1980). However, the reactions are reversible and as anhydrite is brought within the influnence of meteoric water it rapidly hydrates and forms gypsum.

5.2 DISCUSSION AND INTERPRETATION

In the Maqna area, regression initiated at the end of the *Globgerina* Marl (Nutaysh Formation) episode was associated with movements of faults in the pre-existing graben and horst system (sea chap. 3). These controlled the development of the sedimentary basin and led to the accumulation of evaporites in different areas (Plate

1). It is of interest to note that the evaporites of the Esh-Mellaha area in Egypt are of the same age and were probably deposited under similar conditions, although they accumulated in grabens below raised reefal deposits (Rochy *et al.*, 1983).

5.2.1 INTRODUCTION

The Middle-Upper Miocene evaporites in the Midyan Peninsula are extensive and their total surface area (including the Maqna area) is estimated at 175Km/sq (Spencer, 1985). The evaporite sequence of the Bad Formation is up to 120m thick, characterized by several units of anhydrite and gypsum 2-40m thick intercalated with shales, sandstones and carbonates (dominantly dolomite).

Intercalations of coarse detrital materials are concentrated in the western parts of the area (locality F), and include: 1) poorly sorted sandstones up 3m thick, grading from pebbly-coarse to medium grained with a reddish-brown muddy matrix, 2) sandstones which fill the floor of a large channel and contain blocks of greyish-green shale up to 30cm long and 8cm wide forming large scale rip-up clasts, 3) conglomerates which contain surrounded to well rounded boulders up to 20cm diameter, mainly of igneous rocks, and 4) channel filling conglomerates up to 1.5m thick which contain elongated blocks of marl (up to 35 X 8 cm) resting parallel to the channel floor. At the western entrance of Wadi Al-Karaj, the upper part of the evaporite sequence is dominantly well bedded and intercalated with greyish-green marls and fine sandstones 15--20cm thick. Within the sandstones convolute bedding and climbing ripple lamination are present.

In contrast, in areas to the east, the vaporites in Location R are mainly thin-bedded, and largely intercalated with marls. There are no conglomerates and almost no sandstones, suggesting that this may have been a deeper part of the basin or further from the source.

The evaporite sequence of the Bad Formation has been compared to the general environmental setting of evaporites discussed in Chapter 3.

5.2.1.1 SHALLOW-WATER DEEP-BASIN EVAPORITES

The shallow water, deep basin model was developed to account for pre-existing dep basins that became filled by evaporites with internal evidence of shallow water and/or subaerial depositional environments. It was developed largely to account for two major evaporite deposits--the Middle Devonian Elk Point evaporites of western Canada and the Miocene Messinian evaporites of the mediterranean. However, most support for the shallow-water deep basin model, cam from the DSDP program in the Mediterranean (Hsu *et al.*, 1978). During eh Late Miocene the Mediterranean basins were covered by deep marine waters when evaporites were not being formed. Nevertheless, there is abundant evidence that the evaporites were deposited in shallow water, on brine-flats, or subaerially on the floor of the basin, thousands of meters below sea-level. hsu (in Hsu *et al.*, 1978) calculated that h Mediterranean would have reached saturation with respect to evaporites while still more that a thousand meters deep. However, upon complete desiccation, the floor of the basin in which the major bodies of evaporite formed must have lain one or more kilometres below sea-level. Such a large depression would provide the high

temperature (perhaps exceeding 60C°, the brine temperature would be even higher, 80°C or more) and humidifies would be very low because of the extreme continental isolation of the basin floor and because of reduced vapour pressure, caused by the high temperature. Such conditions should markedly influence the type of evaporite minerals formed and it is possible that primary subaqueous anhydrite might have been able to form during the extreme desiccation stages of the Mediterranean (Kendal, 1984). Deep basins must intersect the goundwater pattern of neighbouring areas and, if deep enough, would constitute a major sink for groundwater flow. Much shallow water, deep basin evaporite may thus be derived from ground water (Kendall, 1984).

5.2.2 THE DEPOSITIONAL ENVIRONMENT

In the Maqna area, regression initiated at the end of the *Globigerina Marl* (Nutaysh Formation) episode was associated with the movements of faults in the pre-existing graben and horst system (see Chap. 3). These controlled the development of the sedimentary basin and led to the accumulation of evaporites in different areas (plate 1). The sedimentary basin of the Maqna area was described by Skipwith (1973) as a local embayment tending NE-SW and separated from a WNW-ESE tending basin off-shore by a basement ridge lying at <1,000 meters below sealevel. During the Middle Miocene, the Maqna area remained attached to the axial part of the Red Sea (Purser & Hotzl, 1988). Accordingly, the evaporites of the Bad Formation are likely to have been deposited within a shallow water deep basin similar to that described by Kendall (1984) (see chap. 2).

The sequence of evaporites in the Maqna area (Plate 3), represents a lateral facies change from a shallow basin shelf sequence to a shallow water deep basin sequence (Fig. 5.2). Consequently evaporite successions may not fall simply into one or other depositional model and may have elements of several. On the margin of the basin, along the north-western side of the Maqna area, the evaporite sequence is intercalated with marls which contain algal mats. Numerous channels are present but there is no evidence of desiccation features or of any substantial erosion surface since the evaporites are subaqueous deposits. To the east, where the evaporites formed in the centre of the basin, sequences are thin-bedded (localities R & HN) and parts of them display considerable lateral continuity. Intercalations of marls contain planktonic forams indicting relatively deeper water sediments.

5.2.3 THE DIAGENETIC SEQUENCES

The evaporites are mostly composed of anhydrite. The anhydrite was formed either by dehydration of gypsum or by immersing it in a very saline environment during extreme desiccation stages as described by Kendall (1984) for the Mediterranean. No evidence indicated the present of marine sparry calcite cement (fibrous) could be as a result of complete dissolution of it and subsequently replaced by the cristobalite and/or halite. Sparry calcite cements show dull or non-luminescent zone probably reflect later meteoric origin.

The dolomite (crystals up to 40μm diameter) with homogeneous dull luminescence and some have corroded edges probably indicate dolomitization associated with evaporites by marine or hypersaline-water followed by recrystallization in meteoric

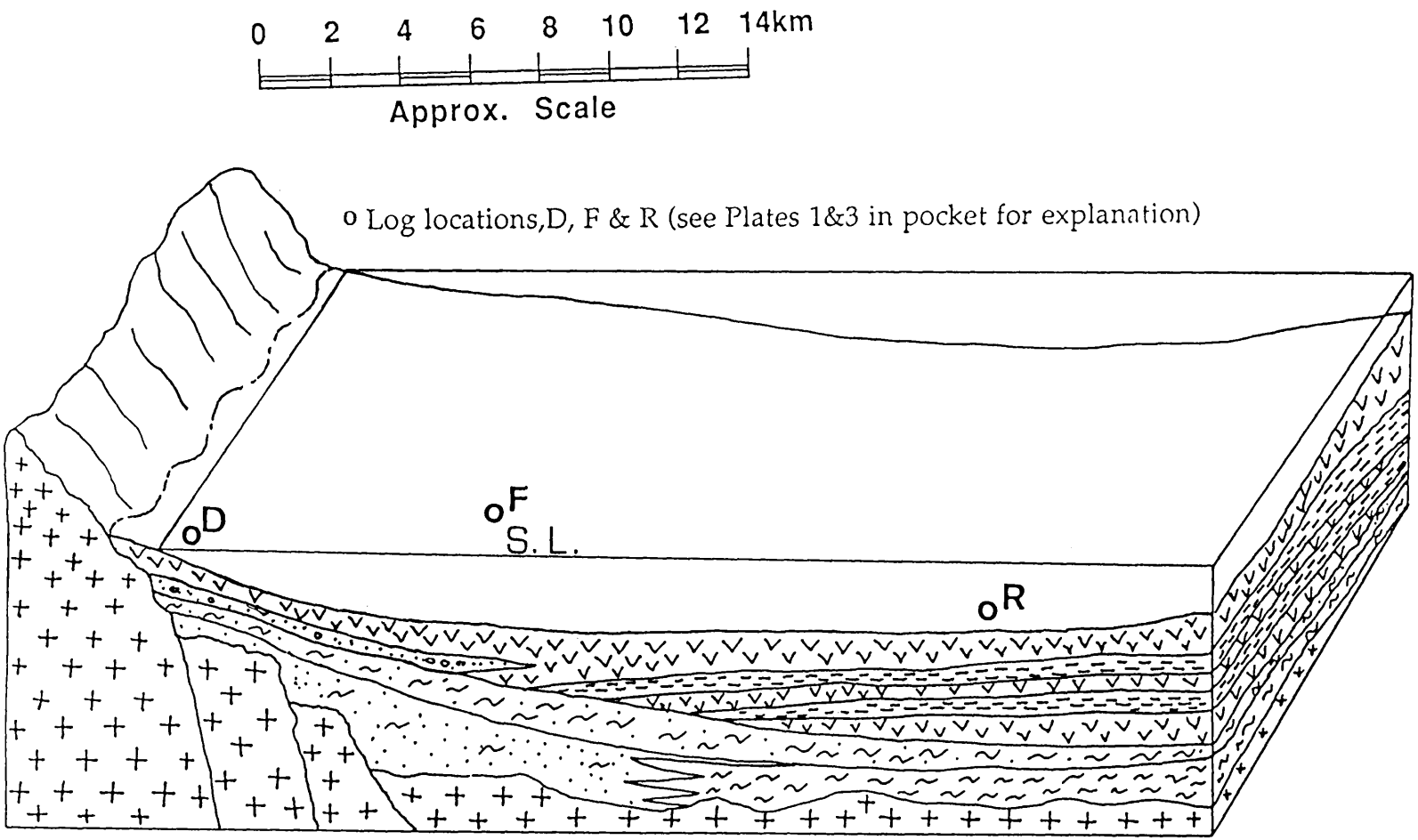

Figure 5.2 Diagrammatic model showing the sequence of depositional environments of the Bad evaporite sediments.

or hydrothermal fluids and then selective dissolution. Dolomite crystals of later origin or neomorphosed during late burial changes have bright luminescence in CL.

Finally, the iron oxides produced staining of the surface of fractures and dissolution seams. The gypsum cement occurred as a result of the recent dissolution of evaporites under subaerial conditions.

5.2.4 COMPARISON WITH OTHER AREAS

In the Gulf of Suez and the eastern desert of Egypt, a similar evaporite series was deposited in the middle Miocene. A promontary at Suez was elevated causing the Gulf embayment to be converted into a lagoon or a series of lagoons with a hydrographic setup that produced a continuous but limited influx of sea water (Said, 1962). Sadek, 1959 (in: Said, 1962) described the evaporite series of Jabel Hammam Faraun which attains a thickness of 595m and contains intercalated fossiliferous marls and two massive beds (180m & 170m thickness) of anhydrite. Only the upper part of the evaporite series is represented by gypsum beds with interbeds of calcareous marls (70m thick) which are similar to the evaporite facies in the Maqna area.

The evaporites of the Kareem Formation (Rhami Member) in the Gulf of Suez assigned to the Mid-Miocene (Langhian-Serravalian) are also mainly anhydrite. Core studies reveal a series of well developed sabkha-type evaporite cycles indicating very shallow to emergent conditions in the basin, but it is difficult to determine whether

sedimentation patterns are a response to global sea level change, rift tectonics, or a combination of both (Richardson & Arthur, 1988).

The Messinian evaporite sequence of the Zeit Formation in the Gulf of Suez, consists of thin (0.01-1 meter) alternating beds of shale and anhydrite with occasional beds of halite. In the Maqna area, these are similar to Bad evaporites and tentatively correlated with the top of the Messinian evaporites in the Mediterranean basin (Haq *et al.*, 1987).

5.3 TUFA DEPOSITS

Tufa deposits are recognized in several places in the Maqna area. In location F tufa rests unconformably on dolomites above the upper evaporites bed and in scattered outcrops west of Jabal Al-Musayr is also found in dolomites unconformably overlying the basement rocks (see Plate 1, the cover rocks). This is the first time that the tufa deposits have been recorded in the Maqna area. The tufa is probably older than the Pliocene Ifal Formation and was possibly deposited during the upper Miocene.

In location F, the Tufa deposit is a maximum of 5 meters thick filling an elongated cavity (Fig. 5.5-A). The host rock is a browish dolomite, dense and highly resistant to weathering. The walls of the cavity are lined with a layer of stalagmite several centimetres thick. Overlying this is a sequence of brecciated limestone, laminated limestone 1.5m thick, a few centimetres of intraformational conglomerate and finally laminated limestone having the same dip as the host rock (Fig. 5.5-B).

The stalagmite coating is characterized by large elongated radial calcite crystals (Fig. 5.4-E). These are mainly dull in CL but a few are non-luminescent. They are partially dolomitised. The dolomite crystals are generally non-planar and <5μm diameter with dull cores and bright rims under CL.

The lower laminated muddy carbonate is completely dolomitised and in thin sections it is seen to contain scarce angular detrital quartz grains, of 0.1-1.5mm diameter, showing blue or dark-brown luminescence in CL. The dolomite is of non-planar crystals (<3μm diameter) which generally show homogeneous dull luminescence under CL. Dolomite cement crystals up to 60μm diameter which occur as a pore lining have dissolved cores occluded by the later dull blocky sparry calcite cement (Fig. 5.4-F). The SEM shows the development of small scale channel porosity and the growth of calcite cement after the partial dissolution of the rhomb dolomite crystals (Fig. 5.6-A).

The cavity filling brecciated limestone is probably of fresh water origin. This is indicated by association of the growth of radial calcite stalagmite crystals between blocks. A sparry calcite cement formed filling pores. Under CL this blocky cement (60-200μm diameter crystals) generally shows a uniform dull luminescence but some crystals have non-luminescent syntaxial overgrowths. Crystals faces have been corroded, further evidence supporting a meteoric origin. The sparry calcite cement was also partially dissolved and a later non-luminescent sparry calcite cement deposited (Fig. 5.6-B). Notable precipitation of iron oxide coated the sparry calcite

cement crystals. Neomorphic planar-s dolomite crystals (<1μm diameter) are distributed within the muddy matrix.

Similar tufa deposits lie to the west of Jabel Al-Musayr. Several isolated outcrops of up to 4 meters diameter of cavity filling occur within a dolomitised limestone (Fig. 5.6-C). A fibrous stalagmite coating is overlain by two cycles of brecciated limestone and laminated limestone. No samples were taken from this location but it is important to record that it exists.

5.3.1 INTERPRETATION

Purser and Hotzl (1988) noted that neither Tortonian nor Messinian faunas have been recorded in Egypt or Saudi Arabia and there therefore appears to be a major stratigraphic break following evaporite sedimentation.

The accumulation of the tufa deposits parallel to the pre-existing sediments could reflect deposition before the rapid vertical movement which caused the Upper Miocene sediments to be eroded. The tufa deposits are dolomitized. They are formed as a result of carbonate dissolution, evaporation and subsequent calcite precipitation under near-surface conditions (cf. James & Choquette, 1984).

The evaporite sequence of the Middle Miocene Bad Formation (location R) contains dolomitized carbonates which show diagenetic evidence that they were uplifted and eroded by subaerial dissolution before deposition of the tufa. Accordingly, the Maqna Tufa is thought to have been deposited either during the Upper Miocene and

uplifted erosion of the Miocene evaporites, or to be younger and to have formed during deposition of the early fluviatile sediments of the Pliocene Ifal Formation.

BAD FORMATION

Figure 5.3

A. The unconformable contact between the Nutaysh Formation sequence (N) and the overlying evaporites of the Bad Formation (B) in locality D. The evaporites have a thin bedded base, but upwards become massive and friable.

B. Large scale rip-up clasts of greyish-green shale within sandstone intercalated with evaporites in locality F.

C. Elongated blocks of marl resting parallel to channel floor in locality F.

D. The cap of evaporites in locality F. Broken blocks and debris are dispersed on the mountain slope.


B
N
A
B
C
D

Figure 5.4

A. Dolomite crystals with coroded cores and edges. Thin section, CL. Scale 0.2mm.

B. Finely crystalline dolomite with a uniform dull luminescence replacing foraminiferal wackestone. Thin section, CL. Scale 0.2mm.

C. Dolomite with sparry calcite cement (C) filling pores formed after phase of dissolution in locality HN. Thin section, CL. Scale 0.2mm.

D. Dolomite crystals (brightly luminescent) formed within anhydrite (dull) blocks scattered on the top of the upper evaporite unit in locality HN. Thin section, CL. Scale 0.2mm.

E. Stalagmite of large elongated radial calcite crystals. Thin Section, CL. Scale 0.2mm.

F. Dolomite cement crystals with dissolved cores (arrow) occluded by sparry calcite cement. Thin section, CL. Scale 0.2mm.

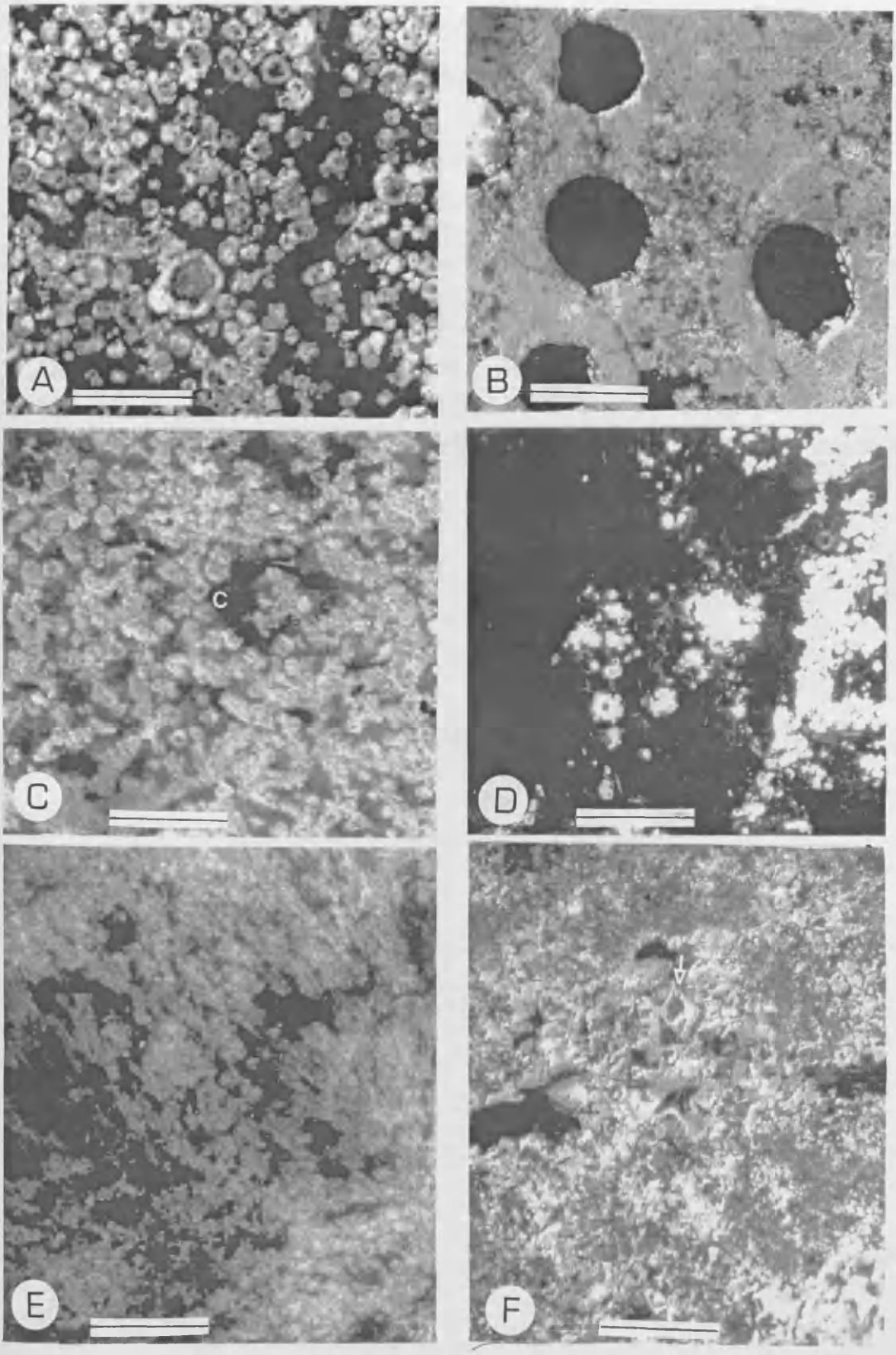
A
B
C
c
D
E
F

Figure 5.5

A. Tufa deposits filling an elongated cavity. The upper part of tufa is represented by laminated limestone (L). Scale (Mohammed) indicated by arrow.

B. Stalagmite (S) coating the brecciated limestone (B) overlying laminated limestone (L) filling residual hole. Scale 0.75m.

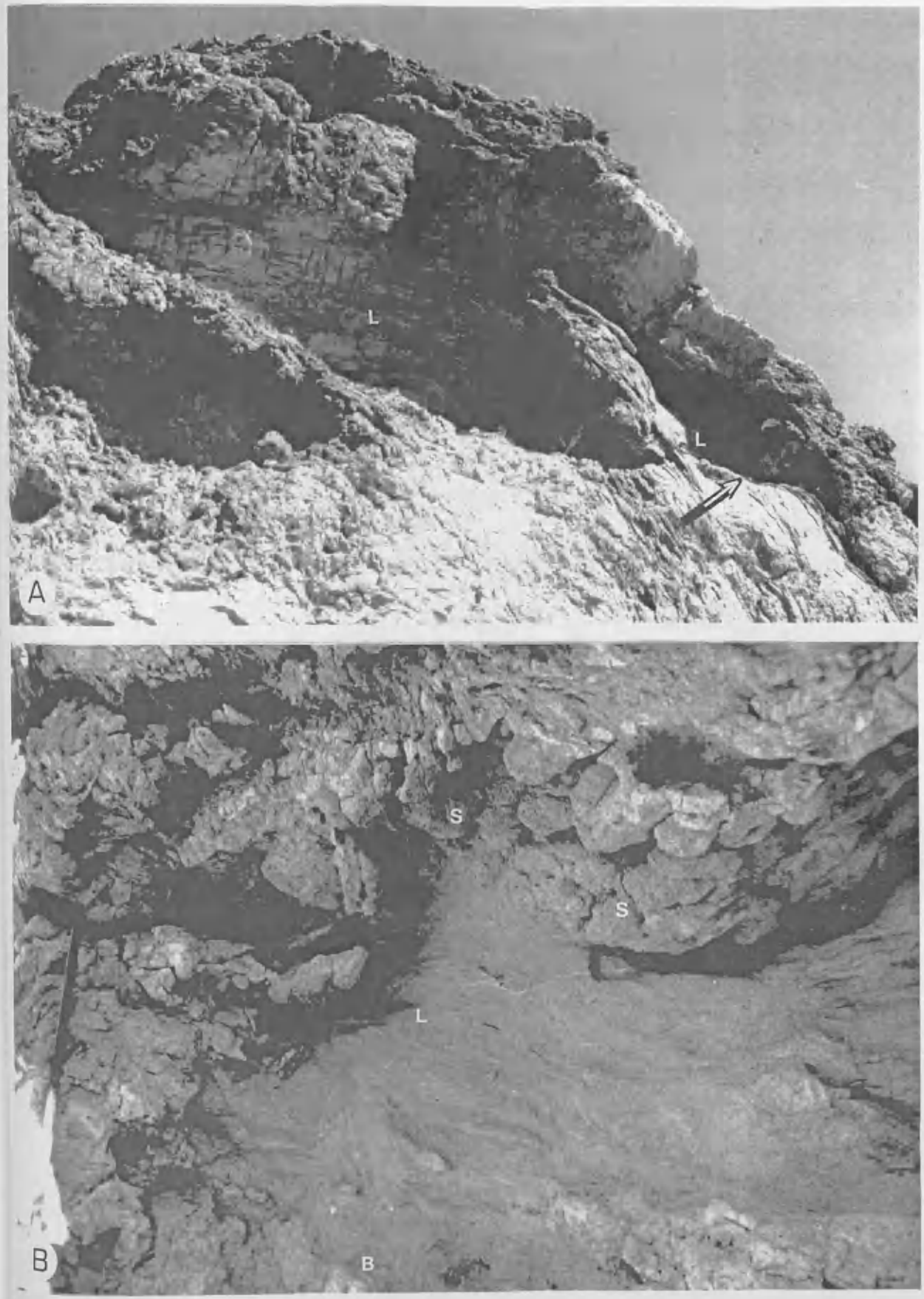
L
L
A
S
S
L
B
B

Figure 5.6

A. SEM. Micro channel porosity occluded by sparry calcite cement (C) after partial dissolution of the rhombic dolomite cement crystals (D).

B. Blocky sparry calcite cement (dull) with non-luminescent syntaxial overgrowths. Thin section, CL and Xpl. Scale 0.2mm.

C. Several isolated outcrops of tufa deposits (T) to the west of Jabel Al-Musayr.

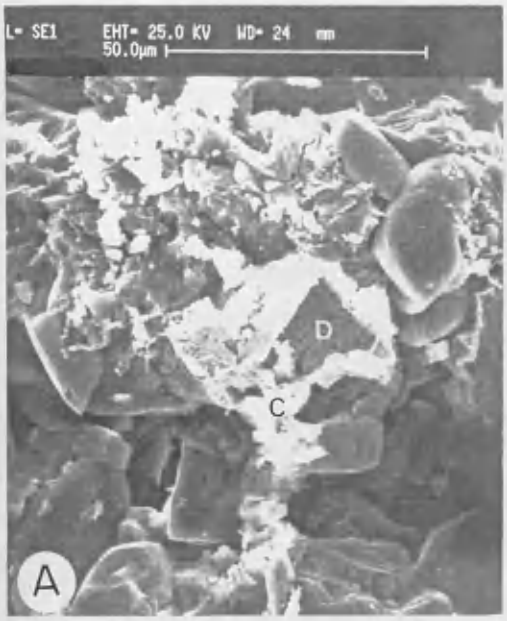
L= SE1 EHT= 25.0 KV WD= 24 mm
50.0µm
D
C
A

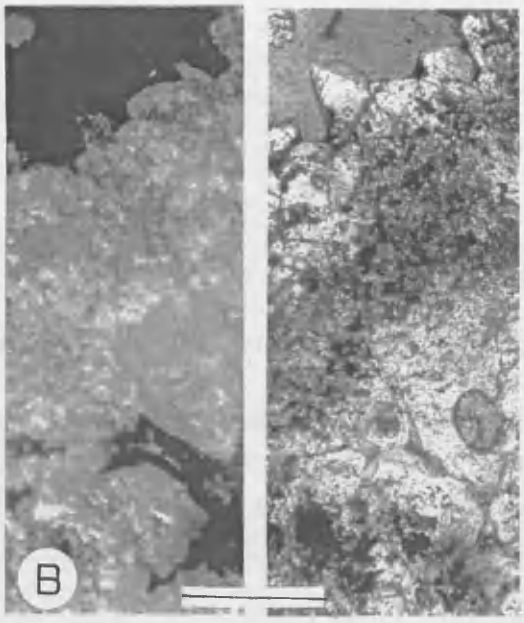
B


T
T
T
T
C

CHAPTER VI

THE QUATERNARY DEPOSITS

The Quaternary sediments of the Maqna area form a narrow coastal strip varying from a few meters to several tens of meters wide, and extending inland filling wadies. In these, larger areas, which are presumably underlain by Quaternary sediments, are thinly covered by more recent deposits.

The sequences include sediments of marine and continental origin and can be divided into Pleistocene and Holocene deposits (see Plate 1, the cover rocks).

6.1 THE PLEISTOCENE SEDIMENTS

The Pleistocene deposits include raised coastal limestone terraces and fluviatile deposits.

The fluviatile deposits in the Maqna area are believed to indicate continuity of tectonic activity, documented by the basin-ward tilting of terraces and by the vertical displacement of even the youngest terraces along the coast of the gulf of Aqaba. The basin-ward tilting is a consequence of further opening of the Red Sea and indicates that the area was active during and following Pliocene sedimentation (Purser & Hotzl, 1988).

In the Gulf of Aqaba, to the north of the Maqna area, Gvirtzman and Buchbinder (1978) recognized three main periods of coral limestone development, at 10-140ka, 200-250ka and > 250ka (B.P.). A fourth (younger) unit seems to underlie the present day reef but has not been accurately dated. The four cycles formed as a result of at least four sea-level changes resulting in repetition of onlap sequences during the last glacial sea-level low (Gvirtzman, *et al.*, 1977). A fall in sea-level would restrict the inflow of Indian Ocean waters cutting them off completely if it fell below the sill in the straits of Bab Al-Mandab, which is about 100 meters below present sea-level (Braithwaite, 1982).

6.1.1 THE LIMESTONES

Pleistocene limestones, mainly fossiliferous packstones and less frequently fossiliferous grainstones, are exposed along the coast in the form of discontinuous lenses up to 20 meters thick interclated with alluvial fan sediments. In places they occupy positions up to 25 meters above present sea-level, as on the western side of Jabal Faya. They have formed overlying the Pre-cambrian basement and the Tertiary Nutaysh Formation. The limestones are nearly horizontal but incline to dip slightly to the west (seawards) as a result of their formation on the tops of fan deltas.

South of Wadi Qsarah, in location Q2, Quaternary sediments are 20m thick, and include two limestones intercalated with alluvial fan deposits eroded from the adjacent mountains. The base is a conglomerate 12 meters thick, becoming thicker to the east towards the source area. This consists mainly of sub-rounded basement fragments (up to 15cm diameter) with a calcareous cement. Above this, the

limestones, the lower 3m and the upper 2m are lensoidal beds separated by 3m of conglomerate and extending laterally for several hundreds of meters. Both are dominanted by in situ growths of *Porites* (Fig. 6.1-A).

In general, the alluvial sediments are correlated with periods of higher rain-fall (pluvial periods) and lower sea-level (Braithwaite, 1982).

Further south, in location Q3, limestones are up to 8m thick and the *Porites* colonies up to 1.5m high and 3m in diameter. The base of the succcession is again a calcareous pebbly conglomerate but in this area it is 6m thick and contains scattered in situ coral colonies. Growth of these may be related to the rapid consolidation of the clastics or simply reflect pauses in conglomerate deposition (Fig. 6.1-B).

In location Q4 further to the south, limestone up to 10m thick forms the base of the succession and is covered by 1m of conglomerate. In situ growths of *Acropora* are common here and these are probably related to deeper a position or temporary rise in sea-level (Fig. 6.1-C).

Further south, in location Q5, Pleistocene deposits rest unconformably on the Miocene Nutaysh Formation. The base consists of 2.5 meters of limestone with derived blocks of coral, overlain by a pebbly conglomerate 1m thick with patches of coral in growth position which are mainly *Porites*. The derived corals were transported as a result of currents sweeping shallow areas and carrying them into deeper water. A second bed of derived corals (0.5m thick) follows above, overlain

by 1.5 meters of conglomerate containing abundant coral fragments. The sequence is capped by 10m of limestone consisting dominantly of *Porites*; colonies are in growth position in the last meter of the unit. This may imply a gradual shallowing.

In location Q1, further to the south along the western side of Jabel Faya, the Precambrian basement is overlain by 1.5m of conglomerate containing rounded boulders (80cm diameter) of mainly andesitic and granitic rocks. This is followed by 2m of limestone which extends laterally up to 100m, and contains dominantly derived Porites which are extensively bored. Further south, within the same limestone unit, notable in situ *Porites* colonies are present. These have flat tops and borings are much deeper (Fig. 6.1-D). The limestone is truncated by an irregular erosion surface (Fig. 6.1-E). The sequence is capped by 3 meters of conglomerate, fining upwards to pebbly conglomerate and characterized by prominent coatings of calcareous algae on fragments (Fig. 6.2-F).

To the south, in location Q6, 2.5m of limestone rests unconformably on the irregular surface of the Miocene Nutaysh Formation. This contains mainly derived *Porites*.

Finally, north of Sharm Dabbah in location Q7, the coastal Quaternary terraces consist of a conglomerate 16m thick with a calcareous sandy matrix, overlain by 1.5m of conglomerate containing abundant coral debris, followed in turn by a lensoidal limestone unit 5m thick containing derived corals and extending laterally at least 300m. Only the lower part of the unit contains scattered in situ corals, and includes a 20cm thick calcareous conglomerate.

6.1.1.1 FOSSIL ASSEMBLAGES OF THE PLEISTOCENE LIMESTONES

Corals, gastropods and bivalves were collected from the northern limestones in locations Q2, Q3 and Q4 between Wadi Sek and Maqna. Corals were identified as far as possible to species level.

(A) The coral assemblage includes: *Acropora formosa* (Dana), *Acropora hebes* (Dana), *Acropora implicata* (Dana), *Acropora teres* (Verrill), *Acropora* sp, *Alveopora ocellata* (Wells), *Balanophyllia* cf. *irrortata* (Conrad), *Diploria* sp, *Favia speciosa* (Dana), *Favia* sp, *Favites obdita* (Ellis and Solander), *Favites* sp. *Fungia fungites haimei* (Verrill), *Heteroastrea haimei* (Duncan), *Hydnophora excesa* (Pallas), *Goniastrea pectinata* (Ehrenberg), *Indophyllia* sp, *Pavona clavus* (Dana), *Pavona varians* (Verrill), *Pavona* sp, *Platygyra* cf. *lamellina* (Ehernberg), *Plesiastrea versipora* (Lamarck), *Porites* sp, *Porites andrewsi* (Vaughan), *Porites lutea* (Milne *et al.*), *Pocillopora damicornis caespitosa* (Dana), *Stylophora* cf. *suevica* (Becker) and *Stylophora* sp.

(B) The gastropod assemblage includes: *Athleta* sp, *Buccinulum* sp, *Calliostoma* sp, *Conus* sp, *Colubraria* sp, *Cypraea* sp, *Cymatium* sp, *Globularia* sp, *Murex* sp, *Latirus* sp, *Nerita* sp, *Nassarius* sp, *Sigatica* sp, *Soleniscus* sp, *Strombus* sp, *Trochus* sp, and *Turbo* sp.

(C) The bivalve assemblage includes: *Arca* sp, *Barbatia* sp, *Cerastoderma* sp, *Chama* sp, *Macoma* sp, *Magilus* sp, *Micromeris* sp, *Lucinoma* sp, *Spondylus* sp, *Tridacna* sp and *Venus* sp.

Finally, spines of at least six different echinoderm types have been recorded in Locations Q3 and Q4. These were seen in other places but were not collected.

6.1.1.2 PETROGRAPHY AND DIAGENESIS

The lenses of limestones are mainly of sandy fossiliferous packstones containing blocks of coral. These are mostly derived. Bioclasts include bivalves, gastropods, echinoderms, coralline algae, foraminifera, dominantly *Nummulites* and *Globigerina*, and a few bryzoa. Detrital grains form up to 20% and are angular, consisting of quartz, feldspar, and rock fragments up to 3mm in diameter.

The detrital fragments and forams have a thin muddy carbonate coating which represents an early micrite cement (Fig. 6.2-A). Two generations of blocky sparry calcite cement (crystals 100-250μm diameter) are present within dissolved intraclasts. Under CL, these are seen to be an early bright cement and a later non-luminescent cement. The bright cement was partly dissolved before precipitation of the later cement, suggesting that the limestones were exposed to sub-aerial conditions (Fig. 6.2-B). The absence of an aragonite cement may reflect alteration to calcite since aragonite is common in the reef limestones of the coastal plain of northwestern Saudi Arabia (Dullo *et al.*, 1983). The limestone terraces of the coastal plain of the Gulf of Aqaba are of several ages but there are contrasting views on their diagenesis. Al-Sayari and others (1984) suggeste that they show more or less the same degree of diagenetic alteration in different facies as a result of the aggressive (subaerial) diagenetic environment. On the other hand, Dullo (1986) describes wide variations within and between the limestones.

6.1.2 THE TERRIGENOUS TERRACES

Fluviatile wadi deposits are widely scattered in the Maqna area. They are correlated generally with periods of higher rainfall (pluvial periods). The thicknesses of these terrace deposits range from a few meters on the western side of Jabel Faya and along secondary wadis in the southern part of the area, up to more than 20m in Wadi Sek. Sediments are mainly derived locally from adjacent mountain ridges and the overall colours of the terraces reflect the main sources of the fragments.

East of Maqna, at the mouth of Wadi Al-Hamd, several siliciclastic terraces form nearly horizontal units overlying the inclined Miocene Nutaysh Formation. These form a layered sequence up to 8m thick. The terraces are alluvial fans as indicated by the dominance of boulders, notable trough cross-bedding, thin sheet-flow conglomerates and fining-up graded bedding within the distal sandy parts of the sequence. A number of channel filling conglomerates contain rounded boulders up to 1.5m diameter. These are mainly granitic derived from the underlying Precambrian rocks but less frequently include carbonate and evaporite fragments. The deposits are moderately sorted, gypsiferous in parts and are typically unconsolidated.

In Wadi Sek, terrace deposits are derived either from the Precambrian basement or from the Oligocene Sharik Formation. The source rocks strongly influence the colour of the terrace sediments which are locally dominated either by andesitic fragments derived from the Precambrian (Fig. 6.2-C), or by a mixture of rock fragments from the Sharik Formation (Fig. 6.4-D).

6.1.3 THE GYPSIFEROUS TERRACES

These terraces occur in a narrow wadi south of location B. The deposits are about 3m thick with high percentages gypsum fragments derived from the surrounding evaporite beds of the Bad Formation. Sheet flow (Fig. 6.2-E), and crossbedding structures are common and indicate that the sediments are of fluviatile origin (Fig. 6.2-F).

6.2 HOLOCENE AND RECENT SEDIMENTS

6.2.1 THE FRINGING REEFS

The present fringing reefs are believed to have formed during the last 7,000 yrs (Gvirtzman *et al.*, 1977). In the Maqna area, they are covered by water from 0.5m up 2m deep and extend along the coast as a strip from a few meters up to 200m wide. In places, such as south of Maqna along the western side of Jabel Faya, reefs are discontinuous and broken by alluvial fan conglomerates derived from the adjacent mountain ridges and locally spreading as braided streams onto the reef flats. In places shallow furrows cross the reef flat and in one location, Sharm Dabbah, a deep channel or sharm cuts completly through the reef.

The Holocene of the northern Red Sea has been described by Behairy (1983) and Dullo (1986). The carbonate sediments include skeletal debris similar to that recorded in the Maqna Pleistocene limestones. In this the cement in the intraskeletal pores of the corals consists of aragonite, either needle-shaped or less commonly spherular crystals, and blocky magnesium calcite containing 17 mol% $MgCO_3$ (Behairy & El-Sayed, 1984).

6.2.2 TUFA DEPOSIT

Quaternary tufa has been recorded in only one area (location Ta), on the southern slope of Jabel Hamza. In the main occurrence the tufa sequence consists of a brecciated limestone boulder bed overlain by laminated fine grained limestones and capped by recent detrital sediments including plant remains. The tufa sequence forms a cone 6m high and 5m wide but has already been partly eroded. It probably formed by monsoon rains during the last few thousand years. It formed at water falls and cascades by precipitation of carbonate derived from limestones on the hillsides above.

6.2.3 RECENT DETRITAL SEDIMENTS

Recent alluvial fans are concentrated on mountain slopes and at the debouchment of wadis. Recent sediments have accumulated along the wadi drainage and coastal sheets are formed by the coalescence of coastal plain sands and gravels derived from wadies. Wind-blown sand dunes are rare in the area but those present are dominantly transported from the northwest.

Sabkha deposits are not seen within the mapped area but are common on the coastal plain to the south. They are represented by halite, red calcareous clay and very fine sand (Zakir, 1982).

6.3 INTERPRETATION

During the last glacial period, sea-level fell by at least 120-130m. In the previous ice-age it stood perhaps as much as 20m above the present position. Similar positive

and negative changes have occured several times in the recent past and explain the multi-generations of Pleistocene coastal terraces in the area. The relatively low thicknesses of Pleistocene limestones in the Maqna area may be related both to fluctuations in sea-level during the last glacial period (cf. Gvirtzman, *et al.*, 1977) and to relative frequency of siliciclastic run off to the basin (cf. Roberts & Murray, 1988). Both control the opportunites for limestones to form.

In the Maqna area, the limestones are lensoidal. This indicates that their deposition was patchily distributed and was not continuous. Pleistocene reefs were not formed. Eustatic changes in sea-level during the Pleistocene led to enormous retrograde erosion as a result of increased gradients. This locally resulted in the complete erosion and removal of early reef limestones (>200ka) along the Red Sea coast and the Gulf of Aqaba.

The emerged coastal terraces of the Maqna area can be referred to the younger transgression, during the last interglacial high sea level (10-140ka), in comparison with the Mediterranean stages of Pleistocene stratigraphy. An unaltered *Tridacna* shell from the Pleistocene limestone dated by radiocarbon methods has given an age older than 35ka (Al-Sayari *et al.*, 1984). However, such dates are regarded as unreliable. Comparison with the Sudanese coast (Berry *et al.*, 1966) and Sinai (Gvirtzman & Friedman, 1977) where dating depended on Th/U dates, suggests that an age of 90-110ka is more likely for the Pleistocene coastal terraces in the Maqna area. This agrees broadly with the ages adapted by Dullo (1986), Red Sea localities south of Maqna.

Comparison of the Pleistocene coral assemblage with that described by Davies *et al.*, (1971), suggests that it formed in a shallow marine environment. However, in the Maqna area the truncated tops and borings in *Porites* colonies indicate that water was commonly only about a meter deep. The fossil assemblages are consistent with depths of only a few meters.

QUATERNARY AND RECENT

Figure 6.1

A. Pleistocene limestones in location Q2, contains large in situ growths of *Porites*.

B. The conglomerates intercalated with limestones in location Q3, contain scattered in situ coral colonies.

C. The limestones in location Q4, where in situ growths of *Acropora* are common.

D. In situ *Porites* colonies in location Q1. These have flat tops with deep borings.

E. The limestone in location Q1, truncated by an irregular erosion surface and overlain by a sheet flow conglomerate.

F. Calcareous algae within conglomerate in location Q1. The conglomerate is fining upwards to pebbly conglomerate.

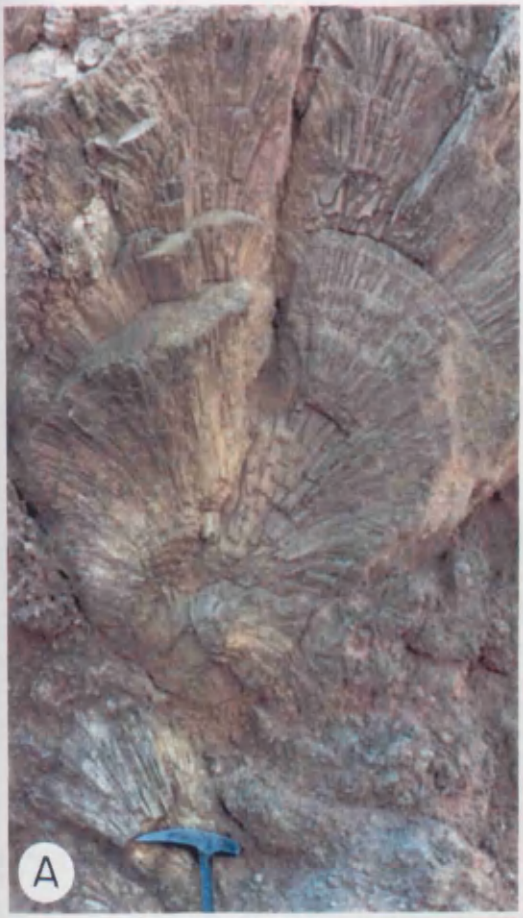
A


B


D

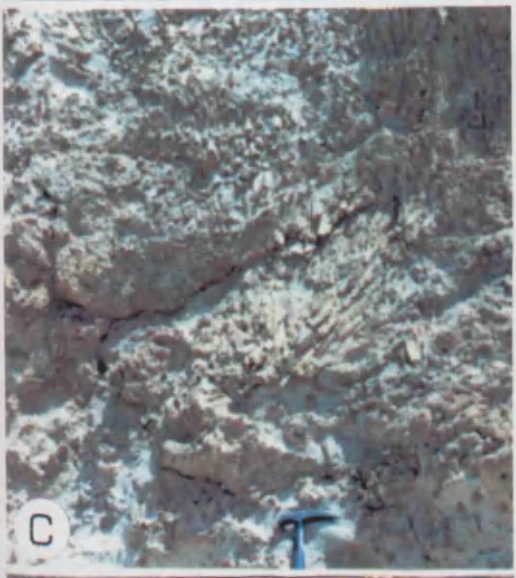
C


E


F

Figure 6.2

A. The micrite cement and the detrital fragments and forams. Thin section, Ppl. Scale 0.5mm.

B. Two generations of sparry calcite, an early bright and later non-luminescent cements. Thin section, CL. Scale 0.2mm.

C. Pleistocene siliciclastic terrace north of Wadi Sek. The Precambrian basement is commonly of andesite and represents the main source of rock fragments.

D. Same as above. But, south of Wadi Sek. Here the fragments are derived from the Oligocene Sharik Formation.

E. Pleistocene gypsiferous terrace south of location B, shows sheet flow structures formed by detrital gypsum fragments derived from the cap of evaporites (Bad Formation) on surrounding mountains.

F. Same as above. But, showing sets of low-angle cross-bedding.

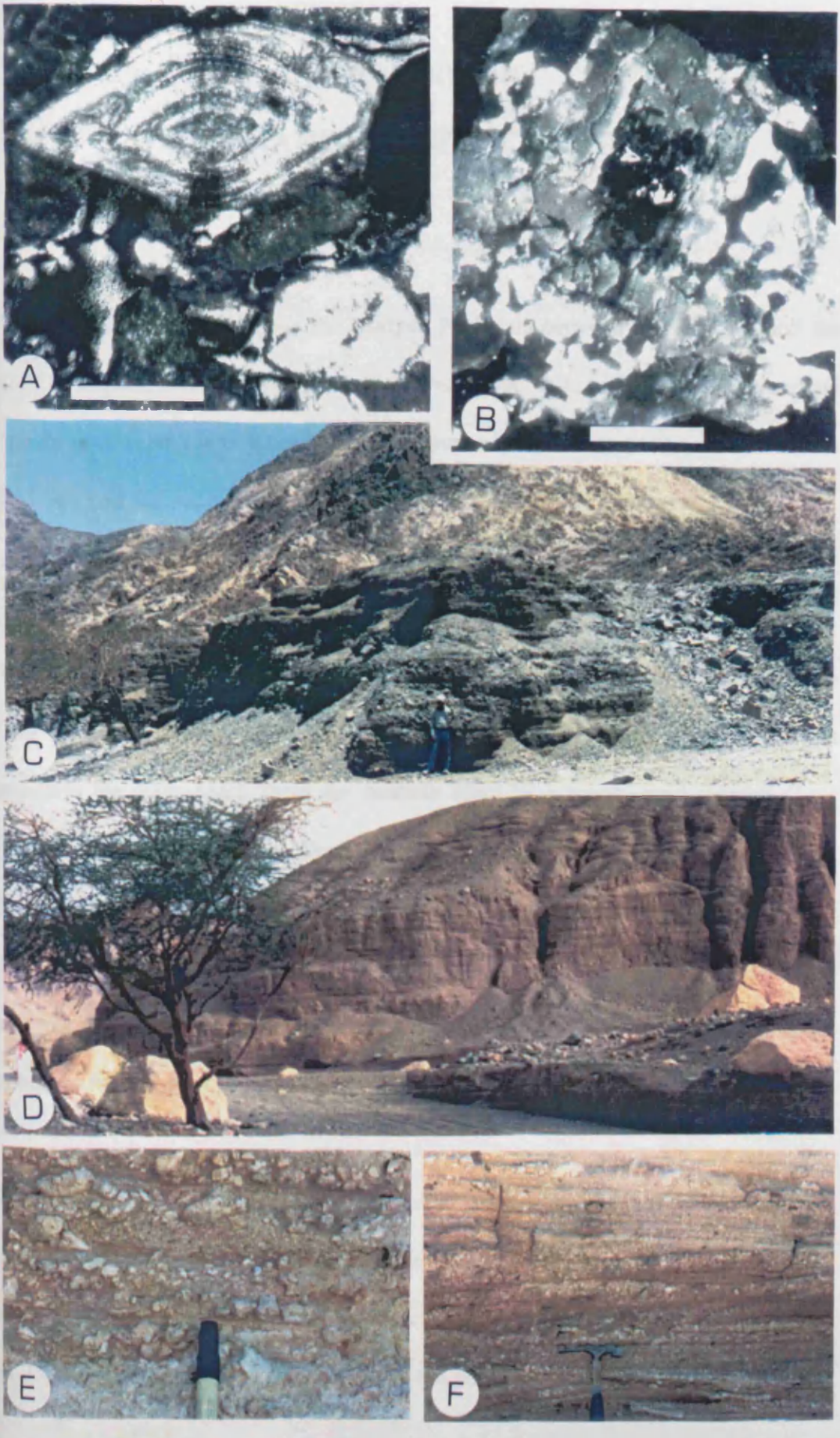
A
B
C
D
E
F

CHAPTER VII

SUMMARY AND CONCLUSIONS

The Maqna area is located on the Midyan Peninsula between the Red Sea and the Gulf of Aqaba, and opposite to the Sinai Peninsula. It is located in the immediate area of overlapping two decisive tectonic structures for the northwestern Arabia: the Red Sea and the Aqaba-Dead Sea (Arabian Wrench Fault) systems.

7.1 STRUCTURE

The Oligocene and Miocene synrift sediments are very thick and well exposed. The Gulf of Aqaba-Dead Sea rift is a NE-SW striking transcurrent fault system that separates the Sinai block from the Arabian Plate by a pronounced sinistral shear movement along the Aqaba- Dead Sea fault system. The lateral shear caused a further extension of the rearranged graben structure, with the opening of rhombically defined en-echelon parts of the graben. In the Gulf of Aqaba, this movement includes 60km of shear in what today is the sea, and a further of movement 50km in highly faulted shear belts on either side of the Gulf.

The geological evidence indicates that, during the earliest phase of rifting, the Red Sea propagated NNW towards the Mediterranean Sea, creating the Gulf of Suez. Subsequently, most of the relative movement between the plates shifted eastward to the Dead Sea transform. The increase in the strength of the lithosphere across the

Mediterranean continental margin acted as a barrier to the propagation of the rift. A new plate boundary, the Dead Sea transform formed along a zone of minimum strength.

In the Maqna area, the stratigraphic evidence from the Tertiary sediments, which began with the fan delta deposits of the Sharik Formation (see Chap. 2), supports the notion that the rift formed in the Red Sea prior the late Oligocene (Chattian). Rifting occurred after a prolonged phase of exposure which is indicted by the complete erosion of pre-existing sedimentary rocks in the area. Here, rifting apparently commenced with subsidence rather than shallowing and emergence and this supports the view of stretching rate than doming for the initial movements. It is clear (as is well seen in Chaps 2, 3, 4 & 5) that block faulting, and rifting, accompanied subsidence and continued to influence deposition throughout the Tertiary. The sequences are grouped into four formations which have been named the Sharik, Musayr, Nutaysh and Bad Formations.

The Neogene stratigraphies of the Red Sea, Gulf of Suez and Gulf of Aqaba are almost identical, with the Miocene successions containing Mediterranean faunas. These contrast with the Gulf of Aden Miocene fauna which is of Indian Ocean affinity.

The Upper Oligocene Sharik Formation is a clastic succession which originated after initial rifting of the Red Sea as a fan-delta. The sediments are predominantly conglomerates and are divided into Lower Red and Upper Pale-Brown sequences.

The Lower Red covering the northern half of the area while the Upper Pale-Brown mainly concentrated in central area. The Pale-Brown unit is generally sandier, reflecting more passive deposition than that in the underlying sequence, and contains a wider variety of structures (sand waves etc.) which suggest a greater degree of reworking by marine processes.

The Musayr Formation includes a Lower Gypsum and an Upper Limestone sequence. The Musayr Gypsum probably spans the interval from late Oligocene to Lower Miocene. The gypsum was deposited within a resticted marine coastal inlet, formed during uplift. This movement produced a rapid fall in sea-level and brought shallower water and the deposition of shallow lagoon sediments with the subsequent formation of gypsum. The overlying Musayr Limestones reflect an important marine transgression. The sequence is divided into five lithofaces assemblages identified as 1 conglomeratic limestones, 2 laminated limestones, 3 oyster limestone, 4 sandstones, and 5 brecciated limestones. These represent a range of depositional environments from slope to near shore. The present investigation suggestes that the term reefal limestone previously applied to the Musayr Limestones is inoppropriate.

For the first time macrofossils reflecting Mediterranean affinities have been identified from the Musayr Limestones. The echinoderms, bivalves and corals indicate that deposition has taken place during the Miocene. However, two corals, species of *Acanthastrea* cf. *echinata* and *Lithophyllia michelotti*, are assigned the Burdigalian (Lower Miocene).

The Nutaysh Formation is a turbidite sequence. Sediments reflect increased tectonic activity associated with additional uplift of the flanks and stronger subsidence of the floor of the basin. The formation is represented by facies changes from dominantly proximal clastic turbidites along the northwestern part of the area to fine grained distal sediments in the center of the basin towards the southeast.

The Bad Formation is characterized by further evaporites, predominantly anhyrite. The Bad sediments are interpreted as shallow water deep basin evaporites. In the western outcrops they are intercalated with marginal shore clastic sediments. The sequence was deposited during a quiescence in subsidence in which a lowered global sea-level resulted in the deposition of a series of evaporites which expand from the Middle to Upper Miocene.

Tufa deposits, have been recorded for the first time in the Maqna area. The Maqna tufa is thought to have been deposited either during the Upper Miocene, or during deposition of the early fluviatile sediments of the Pliocene Ifal Formation.

A rapid global sea-level rise concomitant with a pulse of increased tectonic activity in the earliest Pliocene returned the Maqna area to dominantly marine conditions by a break through to the south that connected the Red Sea rift with the Indian Ocean via the Gulf of Aden. In the Maqna area the Cenozoic sedimentary sequence reflects both eustatic and isostatic sea-level changes (Fig. 7.1).

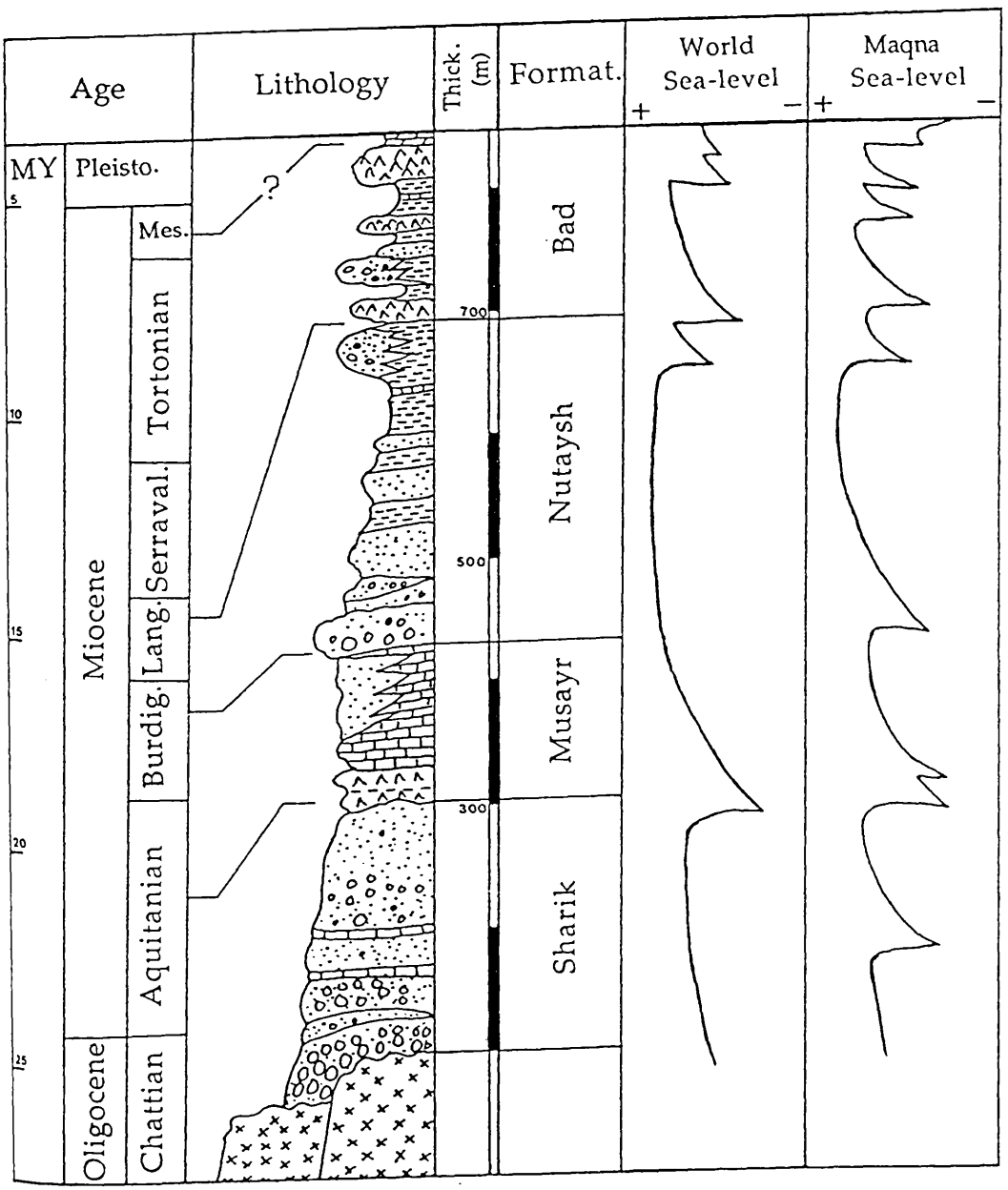

Figure 7.1 Sea-level changes in the Maqna area, compared with the Global cycles of relative changes during the Cenozoic suggesed by Vail *et al.* (1977).

The Pleistocene terraces along the Gulf of Aqaba coast within the Maqna area include important carbonate-clastic transitions. The limestones are lensoidal which indicates that their deposition was patchily distributed and not continuous. Pleistocene reefs are not found. An age of 90-110ka is considered likely for the Pleistocene coastal terraces. The Quaternary sediments as a series of both fan delta and fluviatile terraces may reflect tectonic effects together with the influence of eustatic changes in sea-level and varing climate.

7.2 DIAGENETIC SEQUENCE

The Tertiary formations in the Maqna area contain similar cycles of diagenetic sequences which indicate that they formed under similar diagenetic environment (Fig. 7.2). The sequence can be divided into six stages as below, arranged in ascending order according to their time of formation;

1. Fibrous sparry calcite. Dull and less frequently with bright luminescence under CL, this fibrous cement is common in the Musayr and Nutaysh Formations within the central part of the basin (locations T, KK, Ms, A, 1R, R & F), but is not generally found towards the supposed basin margins. It is thought to be marine, formed during early burial. In addition, a non-luminescent fibrous cement is found within the limestone boulders of conglomeratic limestones of the Musayr limestones. Because this represents a highly oxidized environment it is interpreted as reflecting early exposure to meteoric conditions. These non-luminescent cements are overlain by the luminescent (marine) cement formed after transport of the boulders. Parts of the fibrous cements are altered to finely crystalline dolomite which commonly preserves primary textures.

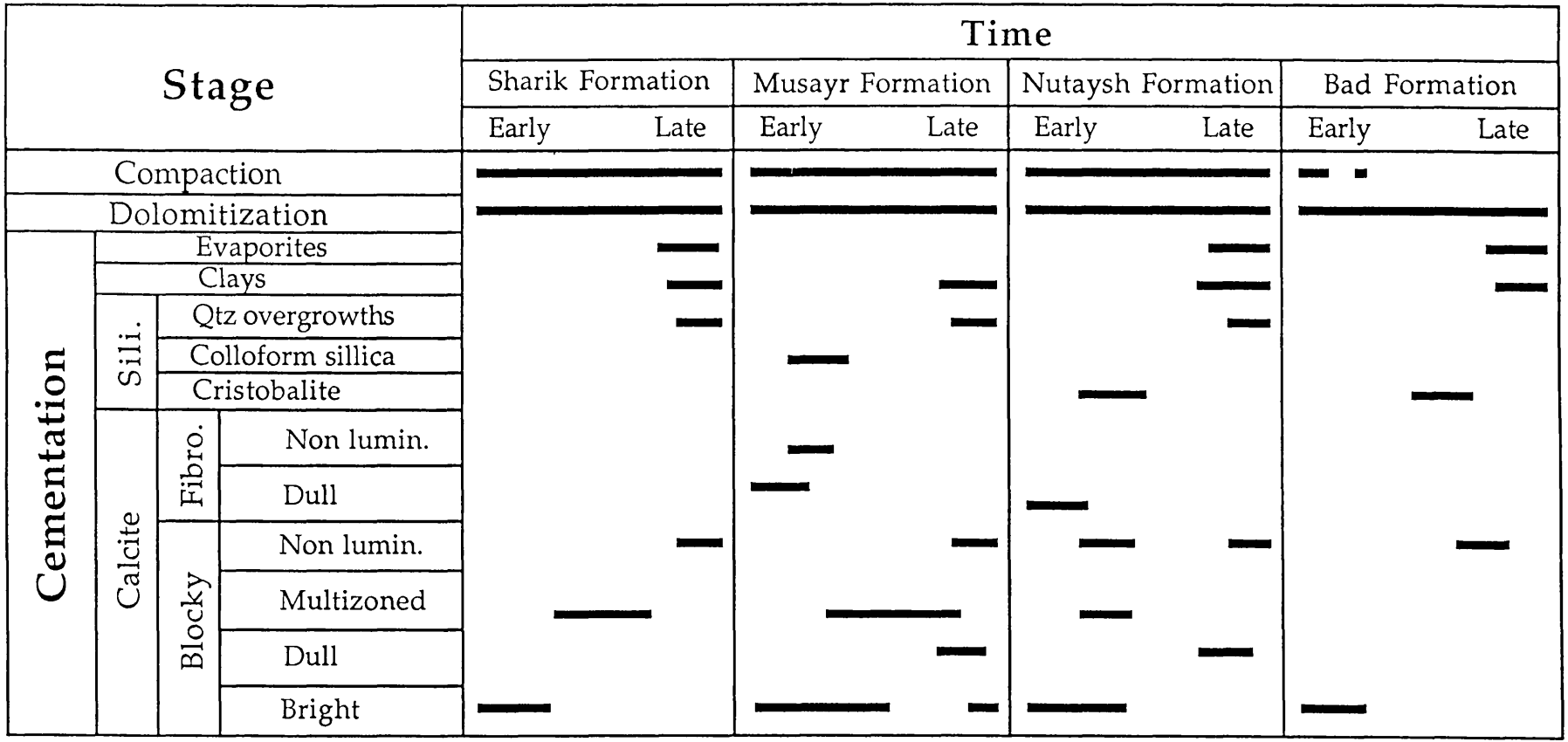

Figure 7.2 The diagenetic sequence of the Tertiary sediments in the Maqna area.

2. Dolomite. Planar-s crystals of dolomite of various sizes but commonly fine grained (<10um) may selectively or non-selectively replace calcite. These show a uniform dull luminescence under CL. Dolomite cement crystals formed during burial are euhedral and coarse (>30um). Under CL, these show multiple luminescence zones reflecting chemical variation of pore fluids during crystal growth. The dolomites are attributed to downwards percolation of marine hypersaline waters formed as a result of deposition of the capping shallow-water deep basin evaporites. There is no obvious petrographic difference between dolomites from the Bad Formation and those from the Sharik Formation which may be as much as 600m below. Dolomites in the Sharik Formation might have been formed by waters derived from the Musayr evaporites. However, they occur in locations SA1 and P in the north of the area where there are no Musayr evaporites. Therefore, either evaporites were present and have been eroded (the Musayr evaporites are truncated by an erosion surface) or waters were indeed derived from the Bad Formation.

3. Siliceous cements. Siliceous cements occur in the form of banded colloform fibrous chalcedony growths, as mega quartz (locations Ms & KK) and as cristobalite (locations R, 1R & F). The colloform growths are found in the Musayr Formation (location Ms) within derived boulders, overlying fibrous non-luminescent calcite cements. This suggest that they formed before transport. Milliken (1979), has suggested an association between colloform silica cements and meteoric conditions, underlining the possible meteoric origin of the fibrous calcite beneath. Cristobalite is rare and occurs only in the supposed turbidite

sediments of the Nutaysh Formation. Scattered radiolaria are seen within this unit and these seem the most likely source of the cristobalite, but since this is a rift area the possibility of hydrothermal solutions cannot be ruled out.

4. Blocky sparry calcite cement. Under CL, blocky calcite cements may be bright, dull, multiple-zoned or non-luminescent. Bright luminescent cements are widespread and seen throughout the Sharik, Musayr, and Nutaysh Formations but are absent from the Bad Formation. In the Musayr Formation, in marginal sandstones in locations Ra, SA & M they seem to be absent and their place is taken by dull crystals. These probably reflect the approach of more oxidized waters. Dull cements are also seen in the Bad Formation in locality HN. The multiple-zoned crystals are less frequent and are found in structurally high locations, in the Sharik Formation in location K2, and in the Musayr Formation in locations T, Ra, K & Ms. They are absent from the Nutaysh and Bad Formations. The reasons for this distribution are not clear. The multiple zones point to fluctuations in the pore-water chemistry during crystal growth and thus in turn suggest near-surface conditions. However, there is no obvious emergent surface within the sequence other than that overlying the Musayr evaporites which are below the Musayr limestones. Both the Nutaysh and Bad Formations are predominantly fine grained and it may be that there are few suitable pores for these cements to develope. The only alternative seems to be that they represent an interface zone of waters derived from the Bad Formation or, possibly, the overlying Ifal Formation. The non-luminescent crystals are in the Sharik, Musayr & Nutaysh Formations but are absent from the Bad. They

commonly overlie a dissolution surface on earlier cements. They also imply increasing influence of more oxidizing waters and suggest penetration of waters from above.

5. Diagenetic clays. These are predominantly intrastratal weathering products, formed only within sequences rich Al-silicates. Clays have been found in four locations K, Sa, R and 1D. Chlorite, illite and smectite postdate the blocky sparry calcite cement (SEM analyses) and are known to form under shallow burial conditions. Dickite has been found in only one location, 1D. It is a relatively unusual mineral and may imply hydrothermal influence.

6. Evaporites. These are represented by gypsum, anhydrite and halite. These are scarce as a result of dissolution, and are found within sequences in areas underlying the capping evaporites, their presence depending on the penetration depth of the surface waters. They are seen in the Bad Formation (locations D, F & R), and in location R extending down into the Nutaysh Formation.

In conclusion:

1. The Sharik Formation is a fan delta sequence and indicates the Oligocene to early Miocene begining of the Red Sea graben. Subsidence produced a series of prograding, siliciclastic fan-deltas at the rift margins. The marine influence in the upper unit indicates that the marine ingression in the graben took place before the Miocene.

2. Gulf of Aqaba sedimentation intially occurred in series of isolated sub-basins. The earlist episode of vertical uplift is recorded by the transition from the Sharik fan-delta to the Musayr shallow marine sediments.

3. The structural horst relief was developed progressively during sedimentation, and the Musayr Limestones were deposited on and around pre-existing structural highs. Two coral species are assigned to the Burdigalian for the Musayr Limestones.

4. During the early and Middle Miocene, subsidence was rapid along and across the entire rift basin. This is reflected by in Nutaysh turbidite sediments which occurred within the Maqna basin.

5. Following a lowered global sea-level, the Bad evaporites were deposited within a shallow water deep basin, which extended from Middle to latest Miocene when a second episode of vertical uplift occurreded.

6. The continuous left lateral displacement of the Maqna area along the Arabian Wrench fault, beginning from the Upper Oligocene is reflected by the presence of angular unconformity between the Sharik conglomerates and the overlying Lower Musayr gypsum.

7. The Oligocene and Miocene synrift sediments within the Maqna area indicate that the marine transgression was almost from the south, suggesting a coast along the eastern side of Sinai Peninsula.

8. Tufa was deposited either during the Upper Miocene, or during the early Pliocene indicating a period of meteoric conditions.

9. The Pleistocene sediments post-date the latest episode of vertical uplift. These formed both fan delta and fluviatile terraces. Only a few terraces are gypsiferous.

10. Holocene and Recent sediments are mostly alluvial, aeolian, tufa and fringing reefs.

11. The Tertiary formations in the Maqna area contain similar cycles of diagenetic sequences which indicate that they formed under the similar diagenetic environments. This may reflecting a fall in sealevel during the upper Miocene and the continuous lateral movement of the area (2nd movement) along the eastern side of the Aqaba Dead Sea fault as the area was finally uplifted and exposed.

12. The relatively high concentrations of heavy metal elements (e.g. Pb 134ppm, Zr 425ppm, Zn 257ppm, Ni 46ppm and Cu 14pmm) increase the possibility of the sediments having been influenced by hydrothermal fluids originating from

the Red Sea rift. This could be reflected on the presence of neomorphosed minerals such as cristobalite, barite and rhodochrosite.

The results from the present work sugges several futher projects:

1. Sedimentological study of individual Maqna formations in order to fully understand the relation between sedimentation and tectonic events, in comparison to surrounding Red Sea areas.

2. Further studies on of geochemistry and paleontological aspects of Maqna formations in relation to Red Sea rifting and Mediterranean faunas.

3. A new exploration of tufa deposits should be made to provide more details on their distribution and stratigraphic order with essential dating.

4. The Pleistocene coastal raised terraces require both dating and detailed sedimentological study to understand their possible classification, and to facilitate comparison with the Red Sea and Gulf of Suez.

Finally, the present work represents the first detailed study in the Maqna area concerned with the sedimentology and stratigraphy of the Tertiary and Quternary sediments. The writer believes that the sedimentary environments of the synrift

sediments and the geodynamic evolution of the area have been satisfactorily established.

REFERENCES

Abdel-Gawad, M., 1969. Geological structures of the Red Sea area inferred from sattelite pictures. In: Hot Brines and Recent Heavy Metal Deposits in the Red Sea (Ed. by E. T. Degens and D. A. Ross) pp. 25-38. Springer-Verlag, New York.

Adams, J. E., 1944. Upper Permian Ochoa Series of Delaware Basin, west Texas and southern New Mexico. Amer. Ass. Petrol. Geol. Bull., 28: 1596- 1625.

Adams, A. E., Mackenzie, W. S. & Guilford, C., 1984. Atlas of sedimentary rocks under the microscope. Longmans London. 104 p.

Agocs, W. B. & Kahr, V. P., 1962. Results of geological-gravimeter investigation of Al-Lisan Basin area. DGMR open-file report, No. 140, Jeddah, Kingdom of Saudi Arabia.

Ahmed, S. S., 1972. Geology and petroleum prospects in the eastern Red Sea. Amer. Ass. Petrol. Geol. Bull., 56: 707-719.

Aigner, T and Reineck, H., E., 1982. Proximality trends in modern storm sands from the Helegoland Bight (North Sea) and their implications for basin analysis. Senckenbergiana marit., 14: 183-215.

Aissaoui, D. M., Coniglio, M., James, N. P. & Purser, B. H., 1986. Diagenesis of a Miocene Reef-Platform; Jebel Abu Shaar, Gulf of Suez, Egypt. In: Reef Diagenesis, Ed. by J. H. Schroeder & B. H. Purser, pp. 112-131. Spring-Verlag, Berlin, Heidelberg.

Al-Sayari, S. S., Dullo, C., Hotzl, H., Jado, A. R. & Zotal, J. G., 1984. The Quaternary along the coast of the Gulf of Aqaba. In: Quaternary period in Saudi Arabia (Ed. by A. R. Jado and J. G. Zotal) pp. 32-46. Springer-Verlag, Wien, New York.

Allen, T. D. & Pisani, M., 1966. Gravity and magnetic measurements in the Red Sea. In: The World Rift system, Canada Geol. Survey Paper 66-14: 62-63.

Allen, J. R., 1980. Sand waves: a model of origin and internal structures. Sedimentary Geology, 26: 281-328.

Allen, J. R. & Matthews, R. K., 1982. Isotope signatures assoicated with early meteoric diagensis. Sedimentology, 29: 797-817.

Banat, K. M., 1980. Principles of clay minerals. Baghdad Univ. press, 138 p. (in Arabic).

Barnaby, R. J. & Rimstidt, J. D., 1988. Redox conditions of calcite cementation interpreted from Mn & Fe contents of authigenic calcites. Geol. Soc. Amer. Bull., 101: 795-804.

Barwis, J. H., 1978. Sedimentology of some south Carolina tidal-creek point bars, and a comparison with their fluvial counterparts. In: Fluvial sedimentology, Ed. by A. D. Miall, Mem. Can. Soc. Petrol. Geol., 5: 129-160.

Behairy, A. K. A., 1983. Marine transgression on the west coast of Saudi Arabia (Red Sea) between Mid-Pleistocene and present. Mar. Geol., 58: 25-31.

Behairy, A. K. A. & El-Sayed, M. Kh., 1984. Carbonate cements in a modern Red Sea reef, north of Jeddah, Saudi Arabia. Mar. Geol., 58: 443-450.

Ben Avraham, Z., Almagor, G. & Garfunkel, Z., 1979. Sediments and structure of the Gulf of Elat (Aqaba). Sedimentary Geol., 23: 239-267.

Berry, L., Whiteman, A. J. & Bell, S. V., 1966. Some radiocarbon dates and their geomorphological significance, emerged reef complex of the Sudan: Zeit. f. Geomorph., 10: 119-143.

Beydoun, Z. R., 1989. The hydrocarbon prospects of the Red Sea- Gulf of Aden: A review. Jour. Petrol. Geol., 12: 125-144.

Bigot, M. & Alabouvette, B., 1973. Geology and mineralization of the Tertiary Red Sea coast of northern Saudi Arabia. DGMR, 76 Jed 5, Jeddah, Kingdom of Saudi Arabia.

Boggild, G. R. & Rose, E. P. F., 1984. Mid-Tertiary echinoid biofacies as palaeoenviromental indices. Ann. Geol. Pays Hellen., Tome XXXII: 57-67.

Bokhari, M. M. A., 1981. Explanatory notes to the Recent Geological Map of the Maqna Quadrangle. Sheet 28/34D. Open file report, DGMR-OF-01-16, Jeddah. Kingdom of Saudi Arabia.

Bouma, A. H., 1962. Sedimentology of some flysch deposits: A graphic approach to facies interpretation. Elsevier, Amsterdam. 168 p.

Braithwaite, C. J. R., 1982. Patterns of accretion of reefs in the Sudanese Red Sea. Marine Geol., 46: 297-325.

Braithwaite, C. J. R., Casanova, J., Frevert, T. & Whitton, B. A., 1989. Recent stromatolites in Landlocked Pools on Aldabra, Western Indian Ocean. Palaeogeography, Palaeoclimatology & Palaeoecology, 69: 145-165.

Bramkamp, R. A., Brown, G. F., Holm, D. A. & Layne, N. M. Jr., 1962. Geologic map of the Wadi As-Sirhan quadrangle, Kingdom of Saudi Arabia. USGS, Misc. Geol. Inv. Map 1-200 A, scale 1:500,000.

Brown, G. F., 1970. Eastern margin ofthe Red Sea and the coastal strucutres in Saudi Arabia. Royal Soc. London Philos. Trans., 267: 75-87.

Burton, R. F., 1878. The gold mines of Midian and the Ruined Midianite cities. London, C. Kegan Paul, 392 p.

Clark, M. D., 1985. Geology of Al-Bad quadrangle. Sheet 28A, K. S. A., Open file report. DGMR-OF-03-20, Jeddah, Kingdom of Saudi Arabia.

Cochorn, J. R., 1983. A model for development of Red Sea. Amer. Asso. Petrol. Geol. Bull., 67: 41-69.

Cody, R. D. and Hull, A. B., 1980. Experimental growth of primary anhydrite at low temperatures and water salinities. Geology, 8: 505-509.

Coleman, R. G., Brown, G. F. & Keith, T. E. E., 1972. Layered gabbro in southwest Saudi Arabia. USGS, Prof. Paper 800-D, D143-D150.

Coleman, J. M. & Prior, D. B., 1982. Deltaic environments. In: Sandstone depositional environments. Ed. by P. A Scholle & D. Spearing, Amer. Ass. Pertrol. Geol. Mem., 31: 139-178.

Coleman, R. G., 1977. Geologic background of the Red Sea. In: Red Sea Research, Ed. by L. S. Hilpert, DGMR Bull. 22: C1-C9. Jeddah, Kingdom of Saudi Arabia.

Compton, R. R., 1985. Geology in the field. John Wiley and Sons. New York, Chichester, Brisbane, Toronto, singapore., 398 p.

Coniglio, M., James, N. P. & Aissaoui, D. M., 1988. Dolomitization of Miocene carbonate, Gulf of Suez, Egypt. Journal of Sediment. Petrol., 58: 100-119.

Darke, C. L. & Girdler, R. W., 1964. A geophysical study of the Red Sea. Geoph. Jour. Royal Astro. Soc., 8: 473-485.

Davies, F. B. & Grainger, D. J., 1985. Geolgic map of Al- Muwaylih quadrangle, sheet 27A, Kingdom of Saudi Arabia. Geoscience Map GM-82C, DGMR, Jeddah, Saudi Arabia.

Davies, P. S., Stoddart, D. R. & Sigee, D. C., 1971. Reef forms, Addu Atoll, Maldive Islands. In: Regional variation in Indian Ocean coral reefs, Ed. by D. R. Stoddart & Sir Maurice Yonge, Zool. Soc. London Symposum No. 28: 220-240, Academic Press, London.

Dubertret, L., 1970. Review of structural geology of the Red Sea and surrounding areas. Royal Soc. London Philos. Trans., A267: 9-20.

Dullo, W. C., Hotzl, H. & Jado, A. R., 1983. New stratigraphic result from Tertiary sequence of the Midyan area, NW Saudi Arabia. Newsl. Stratigr., 12: 75-83.

Dullo, W. C., 1986. Variation in diagenetic sequence: An example from Pleistocene coral reefs, Red Sea, Saudi Arabia. In: Reef Diagenesis, Ed. by J. H. Schroeder & B. H. Purser, pp. 77-90. Springer-Verlag, Berlin, Heidelberg.

Elliott, T., 1989. Siliciclastic shorelines. In: Sedimentary environments and facies, Ed. by H. G. Reading, pp. 155-189. Blackwell Science Publ., Oxford, London, Edinburgh, Boston, Melbourne.

Esteban, M. & Klappa, C. F., 1983. Subaerial exposure environment. In: Carbonate depositional environments, Ed. by P. A. Scolle, D. G. Bebout & C. H. Moore. Mem. Am. Ass. Petrol. Geol. 33: 1-54.

Etheridge, F. G. and Wescott, W. A., 1984. Tectonic setting, recognition, and hydrocarbon reservoir potential of fan delta deposits: In sedimentology of gravels and conglomerates, Eds. E. H. Koster and R. J., Steel, Mem. Con. Soc. Petrol. Geol., 10: 217-235.

Evans, G., 1970. Coastal nearshore sedimentation: a comparison of clastic and carbonate deposition. Proc. Geol. Ass., 81: 493-508.

Friedman, G. M., 1988. Histories of coexisting reefs and terrigenous sediments: The Gulf of Elat (Red Sea), Java Sea, and Neogene basin of Negev, Israel. In: Carbonate-clastic transitions, Ed. by L. J. Doyle & H. H. Roberts, pp. 77-90. Elsevier, Amsterdam, Oxford, New York, Tokyo.

Fuchtbauer, H. & Elord, J. M., 1971. Different sources contributing to beach sand, Southern Bornholm, Denmark. Sedimentology, 917: 69-79.

Gall, J. C., 1983. Ancient sedimentary environments and the Habitats of living organisms, introduction to palaeoecology. Springer-Verlag, Berlin, Heidelberg, New York, Tokyo. 219 p.

Gass, I. G. & Gibson, I. L., 1969. Structural evolution of the rift zones in the Middle East. Nature, 221: 926-930.

Gass, I. G., 1979. Evolutionary model for the Pan-African crystalline basement: Evolution and mineralization of the Arabian-Nubian shield. Inst. Appl. Geol. Bull., 1: 11-20, Jeddah, Kingdom of Saudi Arabia.

Geukens, F., 1966. Geology of the Arabian Peninsula-Yemen. USGS, Prof. Paper 560-B, 23 p.

Girdler, R. W. & Styles, P., 1974. Two stages Red Sea floor-spreading. Nature, 247: 7-11.

Grim, R. E., 1968. Clay mineralogy. 2nd ed., McGraw-Hill, New York. p. 596.

Girdler, R. W. & Southern, T. C., 1987. Structure and evolution of the northern Red Sea. Nature, 330: 716-721.

Gvirtzman, G., Buchbinder, B., Sneh, A., Nir, Y. & Friedman, G. M., 1977. Morphology of the Red Sea fringing reefs: A result of erosional pattern of the last Glacial low-stand sealevel and the following Holocene recolonisation. Sec. Symp. Coreaux recifs Coralliens fossils, Paris, Mem. Bur Recher, Geol. Mine., 89: 480-491.

Gvirtzman, G., & Friedman, G. M., 1977b. Sequence of progressive diagenesis in the coral reef. Amer. Asso. Petr. Geol., Studies in Geology, 4: 357-380.

Gvirtzman, G. & Buchbinder, B., 1978. Recent and Pleistocene coral reefs and coastal sediments of the Gulf of Aqaba. 10th. Int. Sedim. Congress, Jerusalem, Post Cong. Excursion, Y4: 163-191.

Haddad, E. A., Aissaoui, D. M. & Soliman, M. A., 1984. Mixed siliciclastic carbonate-siliciclastic sedimentation on a Miocene fault-block, Gulf of Suez, Egypt. Sediment. Geol., 37: 185-202.

Hadley, D. G., Schmidt, D. L. & Coleman, R. G., 1982. Summary of Tertiary investigations in western Saudi Arabia. Open-file Report, USGS-OF-03-5. Jeddah, Saudi Arabia.

Haq, B. V., Hardenbol, J. & Vail, P. R., 1987. Chronology of fuluctuating sealevels since the Triassic. Science, 235: 1156-1167.

Hay, W. M., Rosol, M. J., Jory, D. E. & Sloan, J. L., 1988. Plate tectonic control of the global patterns of detrital and carbonate sedimentation. In: Carbonate-clastic transitions, Ed. by L. J. Doyle & H. H. Roberts, pp. 1-35. Elsevier, Amsterdam, Oxford, New York, Tokyo.

Hendricks, R. L., Reisbick, F. B. Mahaffey, E. J., Roberts, D. B. and Peterson M. N. A., 1969. Chemical composition of sediments and interstitial brines from the

Atlantis II, Discovery and Chains Deeps. In: Hot Brines and Recent Heavy Metal Deposits in the Red Sea, Ed. by E. T. Degens & D. A. Ross, pp. 407- 440. Springer-Verlag, Berlin, Heidelberg, New York.

Hird, k. & Tucker, M. E., 1988. Contrasting diagenesis of two Carboniferous oolites from South Wales: a tale of climatic influence, Sedimentology, 35: 587-602.

Horowitz, A. S. & Potter P. E., 1971. Introductory petrography of fossils. Springer-Verlag, Berlin, Heidelberg, New York.

Howard, A. R. and Nelson, C. H., 1982. Sedimentary structures on a delta influenced shallow shelf, Norton Sound, Alaska. Geol. Mijnb., 62, pp. 29-36.

Hsu, K. J., 1972. Origin of saline giants, a critical review after the discovery of the Mediterranean evaporite. Earth Sci. Rev., 8: 371-396.

Hsu, K. J. and Montadert, I. *et al.*, 1978. Initial Reports of the Deep Sea Drilling Project, 42, USA, government Printing Office, Washington.

Ito, M. and Masuda, F., 1988. Late Cenozoic deep-sea to fan-delta sedimentation in an arc-arc collision zone, central Honshu, Japan: sedimentary response to varying plate-tectonic regime. In: Fan Deltas, sedimentology and tectonic setting, Eds. nemec, W. and Steeel, R. J., pp. 400-419. Blackie, Glasgow, and London.

Jado, A. R., Hotzl, H. & Roscher, B., 1989. Development of sedimentation along the Saudi Arabian Red Sea coast. Abstr. In 1st. Saudi Sym. On Earth Science pp.69. Jeddah, Saudi Arabia.

James, N. P. & Choquette, P. W., 1984. Diagenesis 9-Limestone. The meteoric diagnetic environment. Geosci. Canada, 11: 161-194.

Johnson & Baldwin, 1989. Shallow Siliciclastic Seas. In: Sedimentary environments and facies, Ed. by H. G. Reading, pp. 229-268. 2nd ed. Blackwell Sci. Pub., Oxford, London, Boston, Edinburgh, Melbourne.

Keller, W. D., 1970. Environmental aspect of clay minerals. Jour. Sediment. Petrol., 40: 788-813.

Kendall, A. C., 1984. Evaporites. In: Facies models, Ed. by R. G. Walker, Geoscience Canada, Reprint Series, 1: 259-297. Ainsworth Press Limit. Kitchener, Ontario.

Kerr, P. F., 1977. Optical mineralogy. 4th ed. McGraw-Hill, Inc., New York. 492 p.

Khalek, M. A., 1963. Brief notes on gypsum and dolomitic limestone deposits. DGMR, No. 194 (3/X/1524). Jeddah, Kingdom of Saudi Arabia.

Kinsman, D. J. J., 1969. Modes of formation, sedimentary association, and diagnostic features of shallow-water and supratidal evaporites. Amer. Ass. Petrol. Geol. Bull., 53: 830-840.

Kirkland, D. W. and Evans, R., 1975. Marine evaporites; origin, diagenesis and geochemistry. Benchmark papers in geology. Strousburg, Penn., Dowdon, Hutchinson and Ross, Strousburg, pp. 426.

Klug, H. P. & Alexander, L. E., 1974. Diffraction procedures for poly-crystalline and amorphous material. Wiley, New York.

Laughton, A. S. & Tramontini, C., 1970. Recent studies of the crustal structure in the Gulf of Aden. The World Rift System Tectonophysics, 8: 359-375.

Leake, B. E. Hendry, G. L., Kemp, A., Plant, A. G., Harrey, P. K., Willson, J. r, Coat, J. C., Aucott, J. W., Lunel, T. & Howart, R. J., 1969. The chemical analysis of the rock powders by automatic X-ray fluorescence. Cem. Geol., 5, pp. 7-86.

Lee, J. H., Ahn, J. O. & Peacor, D. R., 1985. Texture in layered silicates: progressive changes through diagenesis and low-temperature metamorphism. Jour. Sed. Petrol., 55: 532-540.

Leeder, D. M. Ord., D. M. and Collier, R., 1988. Development of alluvial fans and fan deltas in neotectonic extensional setting: implications for the interpretation of basin fills. In: Fan Deltas, sedimentology and tectonic setting., Eds. Nemec, W. and Steeel, R. J., pp. 173-186.

LeNindre, Y. M., 1981. The Maqna gypsum (Raghama Formation). Open-file Report, BRGM-OF-01-18. Jeddah, Saudi Arabia.

LeNindre, Y. M., Motti, E. & Vazques-Lopez, R., 1986. The Miocene of the Maqna massif: Stratigraphy and palaeogeography. Open-file Report, BRGM-OF-06-32. Jeddah, Saudi Arabia.

LePichon, X. & Francheteau, J., 1978. A plate tectonic model of the Red Sea-Gulf of Aden area. Tectonophysics, 46: 369-406.

LePichon, S., 1968. Sea floor spreading and continental drift. Jour. Geophys. Res., 73: 3661-3697.

Levell, B. K., 1980. A late Precambrian tidal shelf deposit, the lower Fjord Formation, Finnmark, north Norway. Sedimentology, 27: 539-557.;

Lindholm, R. C., 1987. A practical approach to sedimentology. Allen & Unwin, London, Boston, Sydney, Willington.

Lowe, D. R., 1965. Water escape structures in coarse-=grained sediments. Sedimentology, 22, pp. 157-204.

Lowe, D. R., 1982. Sediment gravity flows: 2, Depositional models with special references to the deposits of high-density turbidity currents. Jour. Sediment. Petrol., 52: 279-297.

Lowell, J. D. & Genik, G. J., 1972. Sea-floor spreading and structural evolution of the southern Red Sea. Amer. Ass. Petrol. Geol. Bull., 56: 247-257.

Lumsden, D. N. & Chimahusky, J. S., 1980. Relationship between dolomite non-stoichiometry and carbonate facies parameters. In: Concepts and models of dolomitization, Ed. by D. H. Zenger, J. B. Dunhum & R. L. Ethington, Soc. Econ. Paleon. Miner. Spec. Publ., 28: 123-137.

Machel, H. G. & Mountjoy, E. W., 1986. Chemistry and environments of dolomitization- a reappraisal. Earth Sci. Rev., 23: 173-222.

Mart, Y. & Ross, D. A., 1987. Post-Miocene rifting and diapirism in the northern Red Sea. Marine Geol., 74: 173-190.

Mart, Y. & Hall, J. K., 1984. Structural trends in the Northern Red Sea. Jour. Geophys. Res., 89: 352-364.

McDonald, D. A., 1979. Concepts in sandstone diagenesis. CSPG (Clastic Diagenesis Workshop), Calgary, Alberta, Canada.

McKenzie, D. P., 1970. The development of the Red Sea and the Gulf of Aden in relation to plate tectonics (summary only). Philos. Trans. Royal Soc. London, A267: 393-395.

Milliken, K., 1979. The silicified evaporite syndrome-two aspects of silicification history of former evaporite nodules from southern Kentucky and northern Tennesse. Jour. Sediment. Petrol., 49: 245-256.

Moore, R. C., Lalicker, C. G. & Fischer, A. G., 1952. Invertebrate fossils. McGraw-Hill, Inc. New York, Toronto, London. 766 p.

Motti, E., Teixido, L., Vazquez-Lopez, R. & Vial, A., 1983. Maqna massif area: Geology and mineralization. Technical Record, BRGM-TR-03-6. Jeddah, Saudi Arabia.

Motti, E., Teixido, L., Vazquez-Lopez, R. & Vial, A., 1982. Maqna massif area: Geology and mineralization. Open-file Report, BRGM-OF-02-16. Jeddah, Saudi Arabia.

Nemec, W. and Steel, R. J., 1988. What is a fan delta and how recognized it? In: Fan Deltas, sedimentology and tectonic setting., Eds. Nemec, W. and Steel, R. J., pp. 3-14. Blackie, Glasgow, and London.

Osiko, V. V. & Maksimova, G. V., 1960. Valence of the manganese activator in crystal phosphors. Optics Spectrosc., 9: 248 p.

Pettijohn, F J., Potter, P. N. & Siever, R., 1973. Sand and sandstone. Springer-Verlag, New York, Heidelberg, Berlin. 618 p.

Picard, L., 1970. On Afro-Arabian graben tectonics. Geol. Rundschau,59: 337-381.

Picard, l., 1966. Thoughts on the graben system in the Levent. In: The World Rift System, Ed. by T. T. Irvine, pp. 22-32. Canada Geol. Sur. Paper 66-14.

Piper, D. J. W., 1978. Turbidite muds and silt on deep sea fans and abyssal plain. In: Sedimentation in submarine canyons, fans and trenches, Ed. by D.J. Stanley & G. Kelling, pp. 163-175. Dowden, Hutchinson and Ross, Stroudsburg.

Plaziat, J. C., Purser, B. H. & Philobbos, E., 1990. Seismic deformation structures (seismites) in the Syn-rift sediments of the NW Red Sea (Egypt). Bull. Soc. Geol. France, 3: 419-434.

Poag, C. W., 1981. Ecologic atlas of benthic foraminifera of the Gulf of Mexico. Academic Press, New York, N. Y., 174 p.

Prinz, W. C., 1983. Geologic map of the Al-Qunfudhah quadrangle, sheet 19E, Kingdom of Saudi Arabia. Geoscience Map Gm-70C, DGMR, Jeddah, Saudi Arabia.

Purser, B. H. & Hotzl, H., 1988. The sedimentary evolution of the Red Sea rift: a comparison of the northwest (Egyptian) and northeast (Saudi Arabia) margins. Tectonophysics, 153: 193-208.

Purser, B. H. & Evans, G., 1973. Regional sedimentation along the Trucial coast, SE Persian Gulf. In: The Persian Gulf, Ed. by B. H. Purser, pp. 211-232. Springer-Verlag, Berlin.

Remond, C. & Teixido, L., 1980. Geology and mineral exploration of the sedimentary cover between Al-Bad and Al-Muwaylih. Open-file Report, BRGM-OR 80-26. Jeddah, Saudi Arabia.

Richardson, M. & Arthur, M. A., 1988. The gulf of Suez- northern Red Sea Neogene rift: a quantitative basin analysis. Jour. Mar. Petrol. Geol., London, 5: 227-248.

Richter-Bernburg, G. & Schott, W., 1954. Geological researches in western Saudi Arabia. DGMR, Open-file Report, No. 38, 69 p.

Roberts, H. H. & Murray, S. P., 1988. Gulf of northern Red Sea: depositional settings of distinct siliciclastic-carbonate interfaces. In: Carbonate-clastic transition, Ed. by L. J. Doyle & H. H. Roberts, pp. 99-143. Elsevier, Amsterdam, Oxford, New York, Tokyo.

Rochy, J. M., Bernet-Rollande, M. C., Maurin, A. F. & Monty, C., 1983. Signfication sedimentalogique et paleogeographique des divers types de carbonates bioconstruits associes aux evaporites du Miocene moyen du Gebel Esh Mellaha (Egypt). Compte. Rend. Acad. Sci., 296: 457-462.

Rosers, H. A., 1975. A detailed magnetic survey of the southern Red Sea. Geol. Jahrb. Reihe., 13: 131-153.

Ross, D. A. & Schlee, J., 1973. Shallow structure and geologic development of the southern Red Sea. Geol. Soc. America Bull., 84: 3827- 3848.

Said, R., 1962. The geology of Egypt. Elsevier Publ. Comp., Amsterdam, New York, 377 p.

Schmalz, R. F., 1969. Deep-water evaporite deposition: A genetic model. Amer. Ass. Petrol. Geol. Bull., 53: 798-823.

Schreiber, B. C., 1989. Arid shore lines and evaporites. In: Sedimentary environments and facies, Ed. by H. G. Reading, pp. 189-229. 2nd ed. Blackwell Sci. Pub., Oxford, London, Boston, Edinburgh, Melbourne.

Schreiber, B. C. & Friedman, G. M., 1976. Depositional environments of the Upper Miocene (Messinian) evaporites of Sicily as determined from analysis of intercalated carbonates. Sedimentology, 23: 255-276.

Scoffin, T. P., 1987. An introduction to carbonate sediments and rocks. Blackie, Glasgow, London. Chapman and Hall, New York. 274 p.

Sellwood, B. W. & Netherwood, R. E., 1984. Facies evolution in the Gulf of Suez area: sedimentation history as an indicator of rift initiation and development. Mod. Geol., 8: 43-69.

Shutov, V. D., Aleksandrova, A. V. & Losievskaya, S. A., 1970. Genetic interpretation of the polymorphism of the kaolinite group in sedimentary rocks. Sedimentology, 15: 69-82.

Sibley D. F. & Gregg, J. M., 1987. Classification of dolomite rock texture. Jour. Sediment. Petrol., 57: 967-975.

Skipwith, Sir P. A. D'E., 1973. The Red Sea and the coastal plain of the Kingdom of Saudi Arabia. DGMR, Tech. Rec., TR-1973-1, Jeddah, Saudi Arabia.

Spencer, C. H., 1985. Industrial potential of the Maqna massif evaporites. Open-file Report, BRGM-OF-04-32. Jeddah, Kingdom of Saudi Arabia.

Steckler, M. S. & Brink, U. S., 1986. Lithospheric strength variations as a control on new plate boundaries : example from the northern Red Sea region. Earth and Planetary Science Lett., 79: 120-132.

Stow, D. A. V., 1989. Deep clastic seas. In: Sedimentary environments and facies, Ed. by H. G. Reading, pp. 399-445. 2nd ed. Blackwell Sci. Pub., Oxford, London, Boston, Edinburgh, Melbourne.

Swartz, D. H. & Arden, D. D., 1960. Geologic history of the Red Sea. Amer. Ass. Petrol. Geol. Bull., 44: 1621-1637.

Teodorovich, G. I., 1961. Authigenetic minerals in sedimentary rocks. Consultants Bureau, New York, 120 p.

Theriault, F. & Hutcheon, I., 1987. Dolomitization and calcitization of the Devonian Grosmont Formation, north Alberta. Jour. Sediment. Petrol., 57: 955-966.

Tramontini, C. & Davies, D., 1969. A seismic refraction survey in the Red Sea. Royal Astron. Soc. Geophys. Jour., 17: 225-241.

Trent, V. A. & Johnson, R. F., 1966. Reconnaissance mineral and geologic investigation in the Maqna quadrangle, Aqaba, Saudi Arabia. USGS, Tech. Letter 51, Jeddah, Saudi Arabia.

Tucker, M. E., 1989. The field description of sedimentary rocks. Open Univer. Press Milton Keynes and Halsted Press. New York, Toronto. 112 p.

Tucker, M. E. & Wright, V. P., 1990. Carbonate sedimentology. Blackwell Sci. Publ., Oxford, London, Edinburgh, Boston, Melbourne, 482 P.

Uchupi, E. & Ross, D. A., 1986. The northern Red Sea continental rifting and salt tectonics. Geo-Mar. Lett., 5: 203-209.

Vai A. R. and Ricci-Lucchi, F., 1977. Algal crusts autochthonous and clastic gypsum in a cannbalistic evaporite basin; a case history from the Messinian of the northern Apennines. Sedimentology, 24: 211-244.

Vail, P. R. Michum, R. M. & Thompson, S., 1977. Seismic stratigraphy and global changes in sealevel. In: Stratigraphic interpretation of seimic data, Ed. C. Payton. Mem. Am. Ass. Petrol. Geol., 26: 83-97.

Van Der Ploeg, P., 1953. Egypt in the worlds oilfields, the eastern hemisphere. The science of petroleum, Vol. 6, Pt. 1, pp. 151-157. Oxford Univer. Press, London, England.

Vazquez-Lopez, R. & Motti, E., 1981. Prospecting in the sedimentary formations of the Red Sea coast between Yanbu Al-Bahr and Maqna (1968-1979), Saudi Arabia. DGMR, Tech. Rec. BRGM-TR-01-77P.

Vial, A., 1978. Rapport sur le Jabal Musayr (massif de Maqna); geologie et prospection: Bureau de Recherches Geolgiques et Minieres rapport interne (archive).

Walker, R. G., 1975a. generalized facies models for resedimented conglomerates of turbidite association. Geol. Soc. Amer., 86: 737-748.

..... 1978. Deep water sandstone facies and ancient submarine fans: models for exploration for stratigraphic traps. AAPG, 62: 232-966.

..... 1984. Shelf and Shallow marine sands. In: Facies models, Ed. by R. G. Walker, pp. 141-171. Geoscience Canada, Reprint Series 1, Ainsworth Press Limi., Kitchener, Ontario.

Walker, T. R., 1967. Formation of Red beds in Modern and Ancient deserts. Geol. Soc. Amer. Bull., 78: 353-368.

Ward, W. C. & Halley, R. B., 1985. Dolomitization in a mixing zone of near-seawater composition, Late Pleistocene, NE Yucatan Peninsula. Jour. Sediment. Petrol., 55: 407-420.

Weaver, C. E. (Ed.), 1989. Clays, Muds and Shales. Developments in sedimentology, No.44. Elsevier, Amsterdam, Oxford, New York, Tokyo, 819 p.

Wescott, W. A., 1988. A late Permian fan-delta system in the Southern Morondava Basin, Madagascar. In: Fan Deltas, sedimentology and tectonic setting., Eds. Nemec, W. and Steel, R., J., pp. 226-238. Blackie, Glasgow, and London.

Wilson, J. L., 1975. Carbonate facies in geologic history. Springer-Verlag, Berlin, 471 p.

Yousif I. A. & Beckmann, G. E. J., 1981. A palaeomagnetic study of some Tertiary and Creataceous rocks in western Saudi Arabia: evidence for movement of the Arabian Plate. Fac. Ear. Sci. Bull., 4: 89-106. Jeddah, Saudi Arabia.

Zakir, F. A. R., 1982. Preliminary study of the geology and tectonics of the Raghama Formation, Maqna area, Wadi As-Sirhan quadrangle, Kingdom of Saudi Arabia. Unpubl. Ph.D. Thesis, Rapid City, South Dakota Sch. Min. Tech., 240 p.

APPENDIX

Appendix 1-A XRD analysis results

Appendix 1-B XRF analysis results

Appendix 1-A XRD analysis results

Locality	Sample No.	Mineral Compositions															
		Quartz	Feldspar	Dolomite	Calcite	Gypsum	Anhydrite	Barite	Apatite	Celestite	Cristoba.	Hematite	Halite	Illite	Chlorite	Kaolinite	Dickite
R	1	*	*		*								*	*	*		
	2	*	*				*		*						*		
	5	*		*													
	6		*	*				*					*				
	7			*						*							
	8	*			*						*						
	1	*			*						*						
	14	*			*						*						
F	1	*	*		*	*							*	*	*		
	3	*			*						*		*				
	9	*		*							*		*				
	10		*	*		*								*		*	
D	1						*										
	2						*										
	3	*		*			*						*	*			*
	6	*	*	*									*	*			*
S	1	*	*	*		*							*	*	*		
	5	*	*	*			*						*	*	*		
N	2	*			*		*						*	*			
	25	*			*												
H	6	*		*	*												
	21			*	*												
B	2	*	*	*									*	*	*		
	6			*													
K	1	*			*												

Continued (App. 1-A)

1D	1	*	*	*										*	*		
K	1	*	*									*		*	*		
1R	7	*	*		*								*	*	*		
T	1	*			*	*							*				
	2	*			*												
Ra	3	*			*												
A	1	*	*		*												

Appendix 1-B XRF analysis results (ppm).

S-*Sharik Formation* M-*Musayr Formation* N-*Nutaysh Formation*
I-Atlantis II Deep II-Discovery Deep III-Chain Deep
*-Not measured

Ions	S-Loc.	M-Loc.		N-Loc.			Red Sea Deeps		
	K	B	N	S	F	R	I	II	III
Zr	244	136	42	536	86	425	0	800	0
Y	27	15	16	26	17	33	0	80	10
Sr	178	97	129	48	555	1203	0	4000	500
U	3	0	6	0	1	3	*	*	*
Rb	81	43	29	33	54	50	*	*	*
T	3	0	1	2	3	6	*	*	*
Pb	18	3	134	9	47	6	8	900	80
Ga	15	6	2	2	7	11	0	30	5
Zn	112	12	257	5	21	49	70	10,000	400
Cu	4	0	8	0	14	2	40	4000	300
Ni	34	6	15	3	46	20	0	40	10
Co	18	0	6	1	11	8	0	200	15
Cr	59	41	21	8	28	48	0	60	20
Ce	38	23	20	31	38	51	*	*	*
Ba	406	203	236	77	6536	248	0	20000	250
La	17	10	8	13	14	26	*	*	*